McGILL UNIVERSITY

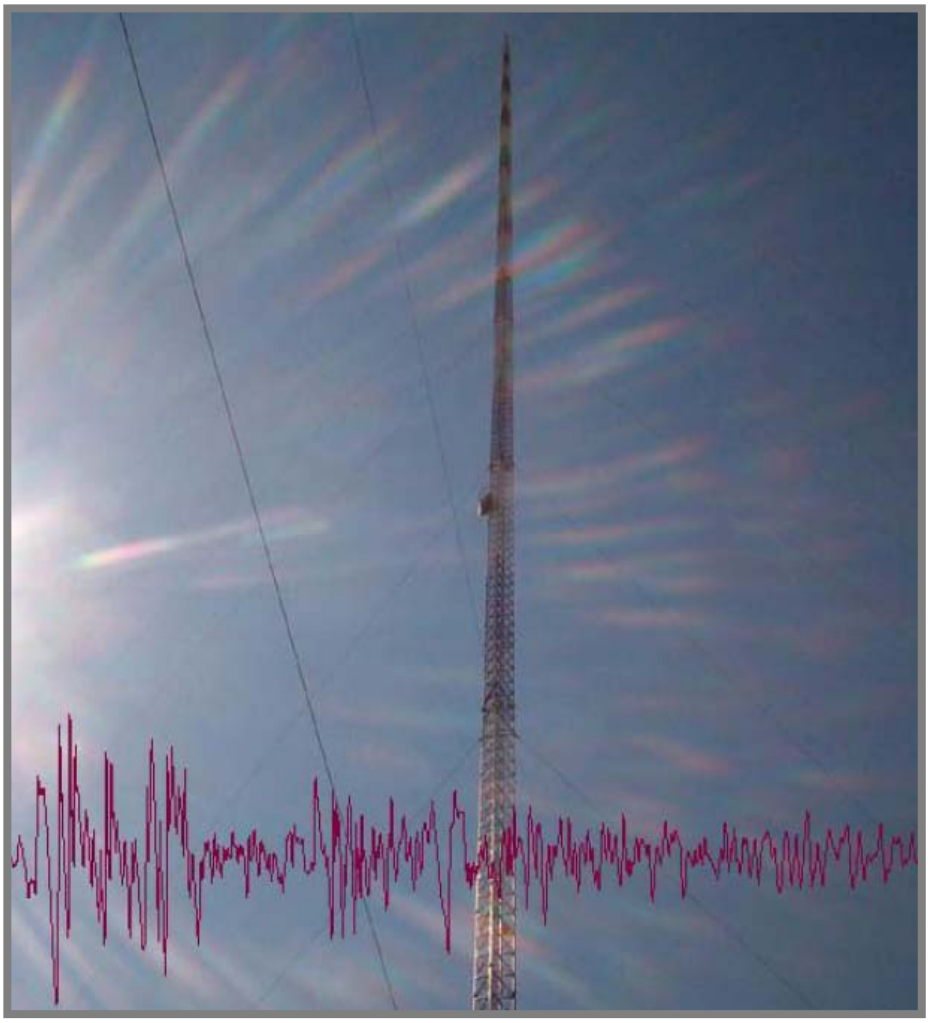

EARTHQUAKE-RESISTANT DESIGN PROCEDURES FOR TALL GUYED TELECOMMUNICATION MASTS

Seyed Ali GHAFARI OSKOEI

Department of Civil Engineering and Applied Mechanics
McGill University
Montréal, Québec, Canada. August 2010
Ph.D. Thesis

A manuscript-based thesis submitted to McGill University in partial fulfilment of the requirements of the degree of Ph.D. in Civil Engineering

EARTHQUAKE-RESISTANT DESIGN PROCEDURES FOR TALL GUYED TELECOMMUNICATION MASTS

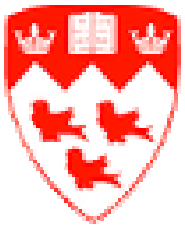

Seyed Ali GHAFARI OSKOEI

Supervisor:
PROFESSOR GHYSLAINE MCCLURE
Department of Civil Engineering and Applied Mechanics,
McGill University, Montréal, QC, Canada

Department of Civil Engineering and Applied Mechanics
McGill University
Montréal, Québec, Canada 2010
Ph.D. Thesis

Earthquake-resistant design procedures for tall guyed telecommunication masts

Seyed Ali GHAFARI OSKOEI

Ph.D. Thesis
Department of Civil Engineering and Applied Mechanics
McGill University
Room 492, Macdonald Engineering Building, 817 Sherbrooke Street West
Montréal, Québec, H3A 2K6
Canada
Tel.: 514-398-6860
Fax: 514-398-7361

Cover:
KVLY/KTHI-TV mast, the tallest existing man-made structure in the world, 628.8 m in height, USA, North Dakota, with the IMPVALL/I-ELC-180 (X) acceleration component of El Centro record

Dedicated to my parents: Dear Hamideh & Mir Ghafar
& my beloved spouse Elham

For their everlasting love and devotion

S. Ali GHAFARI OSKOEI
Department of Civil Engineering and Applied Mechanics
McGill University

ABSTRACT

Telecommunication infrastructure is a fundamental component of communication and post-disaster networks and its preservation in the case of a severe earthquake is essential. Telecommunication masts, also called guyed towers in North America, are typically tall structures whose function is to support elevated antennas for radio and television broadcasting, telecommunication, and two-way radio systems (emergency response systems such as police, fire and reinforcement/rescue troops). Therefore, immediate serviceability or even continuous function of first-aid-station infrastructure is of critically high priority in the case of a disaster.

The current research deals with the dynamic behaviour of tall guyed masts under seismic loads and builds upon the previous research done at McGill University since 1993. Engineering literature of this field reports that the design of tall guyed telecommunication masts is usually governed by serviceability criteria under severe wind conditions, typically combined with icing in cold climates. However, there is a need for seismic design checks of guyed masts constructed in zones with moderate to high seismicity. The nonlinear dynamic behaviour of tall multi-support telecommunication masts is extremely complex. Presently reliable seismic design of telecommunication masts requires nonlinear time domain analysis based on detailed finite element models. Such effort is certainly justified for especially tall and important structures located in active seismic zones. However, it may not be absolutely necessary for many tall structures whose design is likely governed by climatic load effects. The degree of complexity and sophistication of these numerical simulation procedures far exceeds common engineering practice in the trade. There exists a need for simplified procedures for earthquake-resistant design checks of tall guyed telecommunication masts; such

procedures are currently available for self-supporting lattice towers but are still lacking for guyed masts.

The first step in this research was to study the dynamic properties and characteristics of guy clusters in detail based on rational cable mechanics, with a view to develop a simplified procedure that would yield these properties for guyed telecommunication mast analysis. Detailed numerical simulations and analytical studies involving 57 guy cables from eight existing towers with varying heights of 150 to 607 m were used in this section. A mathematical frequency domain procedure was further developed to replace the nonlinear time-variant cable stiffness with an equivalent linear frequency-dependent spring/mass system, based on the response spectrum of individual guy cables and the frequency content of the input seismic excitation. The effects of substituting guy cable clusters with their equivalent linearized springs on the tower structural characteristics and their interaction with the mast stiffness were studied next. Finally, a condensed model of the guyed mast was created where the individual horizontal stiffness elements were evaluated at each cluster level and the structures' mass/stiffness matrices were developed to perform seismic analysis. The proposed procedure has been tested with nine case studies of real telecommunication masts subjected to five different seismic inputs. Another mast (located in St. Hyacinthe, Québec) has been added to the first eight considered since *in situ* measurements of natural frequencies and cable tensions are planned on this structure in the near future.

In order to further validate the proposed method, two selected telecommunication masts, a 342-m tower and a 607-m tower, were studied under the effects eighty-one recorded Californian earthquakes. A comparison of the detailed nonlinear dynamic analysis results (using commercial software ADINA) with those obtained from the proposed method confirmed the reliability of the latter as a simplified analysis procedure for seismic design checks of guyed telecommunication masts. It is to be noted that the research was originally motivated by the need to provide sound scientific background for approximate seismic design procedures of tall masts in a future revised edition of the Canadian Standards CAN/CSA-S37-01: Antennas, Towers and Antenna-Supporting Structures. Appendix M of this document is dedicated to earthquake-resistant design

procedures and does not provide any guidance for approximate analysis methods for guyed masts.

Key words: Seismic design; Telecommunication masts; Guyed towers, Dynamics of stay cables; Cable-mast dynamic interactions.

RÉSUMÉ

Les infrastructures de télécommunication sont des composants essentiels de communication dans le réseau d'installations post-critiques. Leur préservation en cas de séisme sévère est essentielle et exige une vigilance particulière dans toutes les régions sismiquement actives du monde. Les mâts de télécommunication, également appelés pylônes haubanés en Amérique du Nord, sont généralement des structures de grande taille dont la fonction est de soutenir les antennes nécessaires pour la radio et la télédiffusion, les télécommunications et les systèmes de radio bidirectionnelle (systèmes d'intervention d'urgence comme la police, les pompiers et les équipes de secours). Donc, dans le cas de structures stratégiques, la fonctionnalité complète des installations, durant ou immédiatement après le séisme, est hautement prioritaire.

Cette recherche traite du comportement dynamique des grands mâts de télécommunication sous charges sismiques et s'appuie sur des recherches antérieures menées à l'Université McGill depuis 1993. La littérature scientifique indique que la conception des mâts de télécommunication est souvent régie par des critères de fonctionnalité sous des conditions de vents violents, généralement combinés aux effets du givrage atmosphérique dans les climats froids. Cependant, il est requis de vérifier la bonne tenue parasismique des mâts de télécommunication construits dans les zones de sismicité modérée à élevée. Le comportement dynamique non-linéaire des grands pylônes de télécommunication haubanés est extrêmement complexe. À l'heure actuelle, la seule façon de vérifier la tenue parasismique de ces structures est de procéder à des analyses dynamiques non-linéaires dans le domaine temporel basées sur des modèles détaillés utilisant des éléments finis. Un tel effort est justifiable dans le cas de structures très hautes et importantes en zone d'activité sismique intense. Toutefois, pour les structures usuelles habituellement conçues en fonction des effets des charges climatiques, le degré de complexité de ces méthodes dépasse la pratique professionnelle habituelle dans ce secteur du génie. Il existe donc un besoin pratique de disposer de procédures simplifiées

pour vérifier la tenue parasismique des pylônes haubanés de télécommunication de grande taille. De telles procédures sont disponibles pour les tours de télécommunication autoportantes, mais aucune méthode rationnelle n'a été proposée à date pour les mâts haubanés.

En premier lieu, cette recherche a étudié les caractéristiques dynamiques des groupes de haubans en se basant sur les principes mécaniques connus décrivant le comportement des câbles structuraux. Des simulations numériques détaillées et des études analytiques ont été faites pour un total de 57 haubans faisant partie de huit mâts de télécommunications existants avec des hauteurs variant de 150 à 607 m. Une procédure mathématique basée sur l'analyse spectrale a été développée pour remplacer les rigidités de câbles non-linéaires variant dans le temps, par un modèle simplifié équivalent. Ce modèle est fonction de la fréquence naturelle du câble, sa masse et son élasticité, ainsi que du contenu fréquentiel de l'excitation sismique. Il tient également compte de l'interaction avec la rigidité du mât. La justification du développement de ce modèle est que chaque groupe de haubans ancrés au même niveau du mât peut ensuite être étudié à partir d'un modèle équivalent unique du type masse-ressort. Par la suite, des modèles condensés des pylônes haubanés de l'étude ont été créés où les éléments individuels de rigidité horizontale ont été introduits à chaque niveau d'attache au mât. Des matrices de masse et de rigidité équivalente des structures ont été développées à des fins d'analyse sismique et la fiabilité de l'approche simplifiée a été testée avec neuf cas réels de mâts de télécommunication soumis à cinq excitations sismiques. Une neuvième structure (située à St-Hyacinthe, Québec) s'est ajoutée aux huit premières car des mesures *in situ* de fréquences naturelles et de tensions dans les haubans sont prévues.

En guise de validation supplémentaire, la méthode développée a été vérifiée pour deux pylônes haubanés sélectionnés parmi les neuf cas, soit les mâts de 342 m et 607 m, sous l'effet de quatre-vingt-un enregistrements de tremblements de terre californiens. La comparaison des résultats d'analyse non-linéaire détaillée (avec le logiciel commercial ADINA) et ceux obtenus par la méthode proposée a confirmé la fiabilité de cette dernière comme outil pratique simplifié pour vérifier la tenue parasismique des pylônes haubanés de télécommunication de grande taille. Il est à noter que cette recherche a été élaborée

pour soutenir le développement scientifique de la norme canadienne CAN/CSA-S37 dédiée à la conception des antennes, mâts et supports d'antennes. L'appendice M qui porte sur la conception parasismique des structures de télécommunication ne comporte actuellement aucune méthode simplifiée rationnelle pour les pylônes haubanés.

Mots clés: Conception parasismique, mâts de télécommunication; pylônes haubanés, dynamique des câbles, interactions câble-mât

Statement of Original Contributions

To the author's best knowledge, the original contributions of this research include:

- The study and development of an original model to describe the horizontal static stiffness of guy cable clusters. A linearized approach is introduced which takes into account the expected maximum deformation of the mast. The new approach is straightforward and avoids nonlinear iterative solution of system of equations.

- The detailed study of the dynamic equilibrium of elastic guy cables under several excitation patterns and the development of an original model to describe the equivalent dynamic stiffness of elastic guy cables. The proposed dynamic stiffness model is frequency-dependent which makes it adjustable to the power spectrum of the excitation of the structure. The model also accounts for the effects of dynamic interactions between the mast and the guy cables. Although developed for seismic inputs, the proposed model is general and can be applied to other types of dynamic loading and other types of guyed structures.

- The development, validation and verification of a rational simplified seismic analysis method for tall guyed telecommunication masts. The proposed method is original and makes use of the new developments on guy cluster dynamics listed above. It consists of creating a condensed linearized dynamic model of the guyed mast for modal superposition analysis. Analytical expressions are also suggested to derive the horizontal stiffness matrix of the lattice mast (the shaft itself), which can replace the condensed stiffness matrix that could be derived from a detailed lattice structure model. The model validation was based on the study of nine existing guyed masts subjected to five earthquake signatures and further detailed verification involved the study of two selected masts subjected to 81 Californian earthquake records.

- The development of predictors for the maximum seismic response of guyed masts, based on the deformation of the mast predicted with the simplified linearized approach and the stiffness model of the guy clusters and lattice shaft. These

predictors include internal forces in the mast: axial compression, transverse shear force and bending moment.

Preface

This dissertation is submitted in partial fulfilment of the requirements for the degree of Doctor of Philosophy in Civil Engineering at McGill University.

I would first like to express my sincere appreciation to Professor Ghyslaine McClure at the department of Civil Engineering and Applied Mechanics of McGill University who provided me with the opportunity to conduct this research under her supervision. Her kind support, precise and regular supervision, invaluable and critical suggestions and contributions, and friendly treatment in the course of doing this study are really highly appreciated. Her vital financial support during this research is also acknowledged. I have had such a pleasant experience staying four academic years in Canada and working at McGill and I owe it to her.

This research is built upon previous work supervised by Professor McClure in relation to telecommunication structures at McGill University since 1993. The contributions of Eduardo Guevara (1993), Golamreza Ghodrati Amiri (1997), Richard Dietrich (1999), and especially my dear friend Farzad Faridafshin (2006) have enriched my knowledge of this field. I would also like to thank Mr. Brian Smith, the author of *Communication Structures,* Emeritus Professor Murty K.S. Madugula, editor of *Dynamic Response of Lattice Towers and Guyed Masts*, and the technical committee of CAN/CSA S37 whose work provided me the necessary background and knowledge to initiate this research. It is worthy to acknowledge the contribution of the IASS Working Group 4 on Masts and Towers, an animated technical working group of enthusiastic international experts of the field of Telecommunication Structures. I was privileged to attend the 23rd meeting of the IASS WG4 in Montréal on 9-13 September 2007, which provided me with a precious opportunity to get more acquainted with the challenges of this industry and a strong motivation stemming from the conviction that my doctoral research would be a useful contribution to this field of practice.

The partial financial support provided by the Natural Sciences and Engineering Research Council (NSERC) of Canada and by the telecommunication industry sponsors

of the 23rd meeting of the IASS WG4 is deeply appreciated. I am also grateful for the financial support provided by the McGill Department of Civil Engineering and Applied Mechanics in the form of several teaching assistantships.

I would also like to thank my close friend, Behrouz Shafei for his support to my studies, his kind assistance to my application for admission at McGill University, and very great time we had together in Iran during our long friendship. In addition, I would like to thank my good friends: Iman Shamim and Hamed Layssi, my closest companions in the Executive Committee of McGill Iranian Student Association (MISA), for all our pleasant moments and experience we have had together. In addition, I would like to appreciate the company from my friends Khosrow Hassani (my buddy), Ali Shirazi (my advisor for the first days), Hooman Keyhan and Farshad Habibi at McGill and in Montreal which has helped me most during the preparation of this thesis.

Last, but certainly not least, my special gratitude goes to my family, especially my beloved spouse Elham, for their endless love and support during my studies in Iran and Canada from start to finish. I would also like to take this special opportunity to express the admiration I feel for my mother and especially my father, Sir Mir Ghafar GHAFARI OSKOEI, Eng.: he is a kind and devoted father who inspires me in social and professional life. I wish them health and blessings all over their life.

Montréal, Québec, August 2010
S. Ali Ghafari Oskoei

Contents

List of figures

List of Tables

1. Introduction and Literature Review

1.1. Introduction

Billions of people daily take advantage of accessing telecommunication and broadcast services brought to their houses or work places by means of various structures supporting telecommunication antennas. Elevated antennas are electronic components designed to transmit or receive radio waves with a minimum of interference from obstacle; which in the lack of suitable building rooftops in built urban environment, they are most economically supported on self-supporting and guyed lattice towers. The communication industry has deeply influenced our modern lifestyle and both the general public and corporate world have become critically dependent on the reliability of communication systems.

Telecommunication structures are among the fundamental components of communication and post-disaster networks. Telecommunication masts, also called guyed towers in North America, are typically tall (height above 180 m) slender structures, whose particular function is to support elevated antennas for radio and television broadcasting, telecommunication including telephone, cellular, PCS, etc. and two-way radio systems (emergency response systems such as police, fire and emergency troops). Therefore, immediate serviceability or even continuous function of first-aid-station infrastructure is of critically high priority in the case of a disaster such as a strong earthquake.

The lateral resistance of tall telecommunication masts is provided by clusters of guy cables anchored to the ground at several support points. A guy-wire is a metal wire used to provide lateral stability in tall structures. The guy cables are normally pre-tensioned and in some towers are connected to stabilizers and outriggers at some stay levels to improve the global torsional stability of the structure. Due to their unique geometry and structural characteristics, telecommunication masts pose several engineering challenges associated with their highly nonlinear response to dynamic loads. Some of these

structures are among the tallest man-made constructions[1]. The tallest guyed mast ever built has been the Warsaw Radio Mast in Poland with a height of 645.4m, though it collapsed in 1991[2], leaving the KVLY/KTHI-TV mast in the USA, North Dakota, as the next tallest with 628.8 m in height. Figure 1.1 shows the KVLY guyed mast, constructed in 1963 and used by Fargo station for television broadcasting. From the economic point of view, guyed masts tend to be cheaper than self-standing towers, but because they require an extended area surrounding them to accommodate stay blocks, self-standing towers are more commonly used in cities as land is in short supply. Figure 1.2 illustrates the Nackasändaren twin masts, in Sweden, located in a rural area.

Reviewing the engineering literature on the seismic behaviour of telecommunication structures, it seems that although there have been several reports of structural failures due to extreme wind and/or ice, there have only been isolated reports in connection with earthquakes. McClure (1999) quoted a survey of the earthquake performance of communication structures which summarizes documented reports of only 16 instances of structural damage related to seven important earthquakes in the past 50 years. It should be mentioned that damage is not being systematically reported for these structures as such information is most often kept confidential by tower owners. However, quite recently, a consensus has been raised in North America to document earthquake-resistance design guidelines specifically developed for communication structures.

The seismic safety of communication structures cannot be compromised because of the dramatic consequences of communication disruptions during catastrophic earthquakes. One example was the malfunction of the communication facilities of a key station in the Kobe area of Japan immediately after the devastating 1995 earthquake[3]. This was said to have prevented local governments from knowing the level and scope of

---

[1] Burj Khalifa, known as Burj Dubai prior to its inauguration, a skyscraper in United Arab Emirates, is the tallest man-made structure ever built, at 828 m (2,717 ft). (http://en.wikipedia.org/wiki/Burj_Khalifa,)

[2] On August 8, 1991, the mast collapsed because of a human error during a construction procedure in exchanging the guys on the highest stack of the mast. (http://en.wikipedia.org/wiki/Warsaw_radio_mast,)

[3] The Great Hanshin earthquake occurred on January 17, 1995 in the southern part of Hyōgo Prefecture, Japan. It measured 6.8 on the Moment magnitude scale and caused more than 6,400 deaths.
(http://en.wikipedia.org/wiki/Great_Hanshin_earthquake, 18 June 2010)

Fig 1.1 *KVLY/KTHI-TV mast, the tallest existing guyed telecommunication mast, 628.8 m in height, North Dakota, USA. (http://en.wikipedia.org/)*

Fig 1.2 *Nackasändaren twin masts, 299 m in height, Nacka, Stockholm County, Sweden.*

the disaster and deploying appropriate rescue efforts. Some damage to communication towers was also reported to have occurred during the August 1999 earthquake in Turkey, which caused severe post-disaster communication problems, although details have not been in the public domain[4] (Smith 2007).

The ever increasing level of awareness of emergency-preparedness officials to the importance of preserving telecommunication to manage the post-seismic rescue effort has put pressure on service providers and encouraged researchers to establish simplified rational design procedures to evaluate the seismic safety of tall telecommunication structures. Several technical challenges and structural considerations are associated with

[4] The 1999 İzmit earthquake was a 7.6 magnitude event that struck north western Turkey on August 17, 1999. It killed around 40 to 45 thousand people and left approximately half a million people homeless. (http://en.wikipedia.org/wiki/1999_İzmit_earthquake)

the seismic behaviour of telecommunication masts. Most guyed masts, with height ranging typically from 180 m to 350 m, have their fundamental flexural frequencies within the sensitive high-power frequency range of past earthquake motions recorded. Seismic effects are not likely to govern mast design in areas with low to moderate seismic hazard. However, the mast/guy interaction could potentially trigger significant seismic effects. Past studies have suggested that earthquake effects on tall masts appear to be concentrated mostly in the top cantilevered section of tall masts (when such a feature is present) and in the first span near the base. They have also revealed that dynamic amplifications in the guy tensions are more likely to be significant in the top and bottom levels of multilevel guyed masts; and those relatively slack cables with initial tension below about 5% of their ultimate tensile strength are especially vulnerable (Smith 2007).

To date, to the best knowledge of the author, simplified and quasi-static models for seismic design of guyed masts have not been proposed in the literature, unlike for wind actions. In the Canadian Standards CSA-S37-01, Table M.1, it is recommended to perform a detailed dynamic analysis for all masts of height above 150 m and located in high seismicity areas and for all masts where continuous serviceability is needed in moderately active areas. Structures taller than 300 m should be subjected to a detailed analysis where there is a risk of injury or loss of life in moderately active areas, including the effect of asynchronous motion at the mast base and stay anchorages. The recommended methodology is based on the modeling of seismic input in terms of the prescribed components of ground displacements along the three orthogonal directions at each support and with appropriate lack of correlation. But the studies that form the basis of the CSA-S37 Appendix M have concluded that "detailed nonlinear seismic analyses are far more complex than response spectrum analysis and not always necessary". Nevertheless, calculation of the natural frequencies of masts in their initial configuration can help identify the seismic sensitivity of these structures and the potential interaction effects due to clustered frequencies. The purpose of this research is to establish a simplified rational procedure for seismic design of tall guyed telecommunication structures.

1.2. Dissertation outline

This thesis is organized in six chapters:

Chapter 1: "Introduction and literature review" presents an introduction to the seismic design of guyed telecommunication masts, the thesis outline and a condensed literature review.

Chapter 2: "The equivalent dynamic properties of guy clusters based on rational cable mechanics" presents: Ghafari Oskoei, S.A., McClure, G., 2009 "Simplified dynamic analysis method for telecommunication masts under seismic excitation" ASCE Structures Congress' 09, April 30 to May 2, 2009, Austin, Texas, USA, pp. 1-10.

Chapter 3: Ghafari Oskoei, S.A., McClure, G., "A novel approach to evaluate the equivalent dynamic stiffness of guy clusters in telecommunication masts under ground excitation", Journal of Engineering Structures, Manuscript ENGSTRUCT-D-10-00983 (revised version) submitted in February 2011. It presents a mathematical procedure to replace the nonlinear time-variant cable stiffness with an equivalent linear frequency-dependent spring/mass system.

Chapter 4: Ghafari Oskoei, S.A., McClure, G., "A robust linearized seismic analysis method for tall guyed telecommunication masts", ASCE Journal of Structural Engineering, Manuscript STENG-1145, (revised version) submitted in November 2010. The paper studies the effects of the replacement of detailed guy cable clusters by their equivalent linear springs and their interaction with the mast stiffness on the dynamic characteristics of the masts.

Chapter 5: Ghafari Oskoei, S.A., McClure, G., "Validation of a linearized seismic analysis method for tall guyed telecommunication masts", Technical Note S-10-00403, ASCE Journal of Structural Engineering, Manuscript STENG-1200, submitted in July 2010 (under revision). This short manuscript presents the results of a detailed verification of the proposed simplified seismic analysis procedure with the numerical study of two selected telecommunication masts under the effects of eighty-one recorded Californian earthquakes.

Chapter 6: “Conclusions and Recommendations for Further Studies” summarizes the main conclusions drawn from the current research and makes some suggestions for further studies and work necessary to implement the proposed method in engineering practice.

1.3. Literature review

1.3.1. Introduction

It is to be noted that this section is a truncated version of Ghafari Oskoei, S.A. (2008) "Simplified seismic analysis methods for guyed telecommunication masts", Structural Engineering Series Report 2008-1. Available online at: http://www.mcgill.ca/library-findinfo/escholarship/ [5].

An updated review of the related literature is also presented at the beginning of each chapter, as a part of the manuscripts submitted for publication. It is also to be noted that a historical review of the static and dynamic analysis procedures of guyed masts is summarized in Appendix A. This review summarizes older studies published prior to the mid 1990s.

1.3.2. Recent studies at McGill University

This section presents the salient features of past work on guyed masts dynamics carried out in the department of Civil Engineering and Applied Mechanics of McGill University by Guevara (1993-1994), Amiri (1993-1997), Dietrich (1999), and Faridafshin (2006), under the supervision of Professor McClure.

Guevara (1993-1994)

The first detailed finite element modeling study ever reported on the nonlinear seismic response of three guyed telecommunication towers was done by Guevara (Guevara and McClure, 1993, McClure and Guevara, 1994). It was an exploratory study which high level of modeling detail could reveal the importance of dynamic effects on guyed masts that were not apparent from previous studies. In the literature review section of his study, Guevara (1994) stated that traditional attempts at the numerical modelling of guyed

[5] URL: http://digitool.Library.McGill.CA:80/R/-?func=dbin-jump-full&object_id=20007&current_base=GEN01

towers, for instance by McCraffrey and Hartman (1972), Augusti et al. (1986), and Ekhande and Madugula (1988), were accompanied by several simplifications in the structural model. Although these simplifications are not significantly influential when studying the static response of structure, they are no longer appropriate for the dynamic analyses of masts. Recognizing these deficiencies, Guevara's work concentrated on detailed numerical simulations of three guyed telecommunication towers in the time domain, namely a 24-m tower with two stay levels, a 107-m tower with six stay levels, and a 324-m tower with seven stay levels. The towers were subjected to S00E 1940 El Centro and N65E 1966 Parkfield accelerograms, which were scaled down to match the elastic design spectra of the 1990 National Building Code of Canada for the Montréal Region. Special attention was paid to the combination of horizontal and vertical ground accelerations in the case of the tallest mast. In addition, surface wave propagation was also studied by considering asynchronous inputs at the ground support points of the guyed tower.

Guevara's study indicated that the high frequency component of the excitation affected only the shortest tower. More significant dynamic amplifications were found in the extreme guy clusters, i.e. top and bottom, for the response of the two other structures. The mast models were validated through a frequency analysis of the equilibrium configuration under the dead weight of the structure and the cable pre-tensioning force. Detailed modeling of the tallest mast was recommended, because of the large number of different member properties along the height of the mast. It was noted that correct modeling of the torsional behaviour of the tallest mast could not be achieved with an equivalent beam-column formulation. In the case of the tallest mast, multiple-support excitations caused additional dynamic effects that were not present when only synchronous ground motion was simulated. The work indicated that cable-mast interactions were dominating in the frequency range of lower axial modes of the mast. Important dynamic interactions were found between the mast and the guy wires when horizontal and vertical ground accelerations were combined as input.

Ghodrati Amiri (1997)

With the main objective of proposing some seismic sensitivity indicators for the design of tall telecommunication masts, Amiri (1997) studied eight existing structures, varying in height between 150 to 607 m. It was anticipated that assessing the sensitivity of a guyed mast to earthquake effects with simple indicators would be a first step to determine whether a detailed nonlinear dynamic study is necessary.

The shaft structures were modeled as three-dimensional trusses. Structural damping was included using an equivalent viscous damper with a value of 2% of critical in parallel with each bar element. Three different classical seismic excitations (namely El Centro, Parkfield, and Taft) were applied as an acceleration-based input. The horizontal acceleration was accompanied by a synchronous vertical component with 75% of the horizontal amplitude.

Unlike self-supporting structures, guyed masts have several closely-spaced lateral and flexural modes, with the first 15 modes frequently below 3 Hz. Their dominant mode shapes are strongly influenced by the guying configuration and the relative lateral stiffness of the various guying levels. Amiri (1997) proposed an empirical expression to evaluate the fundamental flexural period of the mast as a function of height only. However, due to lack of data for towers above 350 m, it is cautioned to limit the use of his formula to the 150-350 m range; Wahba (1999) later proposed another empirical formula compatible with Amiri's. Both formulas (obtained from curve-fitting procedures) confirmed that the total height was the most direct factor in determining the lowest natural frequency of guyed towers. However, an equation that considers the stiffness and the mass of structure to estimate the eigenproperties of guyed masts is more rational, as indicated for example in Appendix D of the Australian Standard AS 3995-1994 "Design of steel lattice towers and masts".

Following his detailed analyses and studying several response indicators - including base shear, axial force in the mast, cable tension, shear force and bending moment of the mast, and deformations, Amiri proposed some simplified models and guidelines to relate the overall seismic sensitivity of tall guyed towers to their essential structural properties.

The maximum tower base shear, the distribution of horizontal earthquake forces and the distribution of the maximum dynamic component of mast axial forces along the tower height due to combined horizontal and vertical ground accelerations were estimated using empirical equations based on the tower height.

Dietrich (1999)

Dietrich (1999) presented the detailed nonlinear dynamic analysis of an existing guyed mast with a height of 150 m previously studied by Amiri (1997). This time, the tower was subjected to realistic three-dimensional displacement-controlled ground motion of El Centro signature. Special attention was paid to the effect of the vertical ground motion and to the out-of-plane response of a horizontal input. Other points of interest were the effects of asynchronous ground motion and the presence of ancillary components.

For the particular case investigated, results indicated that all three translational components of ground motion must be included at once in the seismic analysis in order to reflect the combined vertical and horizontal effects and the resulting non-uniform biaxial bending and shear in the mast.

Faridafshin (2006)

Following the findings of Dietrich (1999), the seismic behavior of three existing masts with varying heights of 213, 313, and 607 m (taken from Amiri, 1997) was investigated again with special considerations for the realistic modeling of ground motion at the supports. The earthquake excitation was prescribed as a displacement-controlled motion providing the opportunity to consider the asynchronous shaking of the cable ground anchors and mast base. Figure 1.3 demonstrates the schematic seismic excitation at supports for the 607 m mast (Faridafshin ***et. al.***, 2008). This effect was studied by varying the shear wave velocity of the traveling wave corresponding to different degrees of soil stiffness according to NBCC 2005 and observing the general trends of selected response indicators.

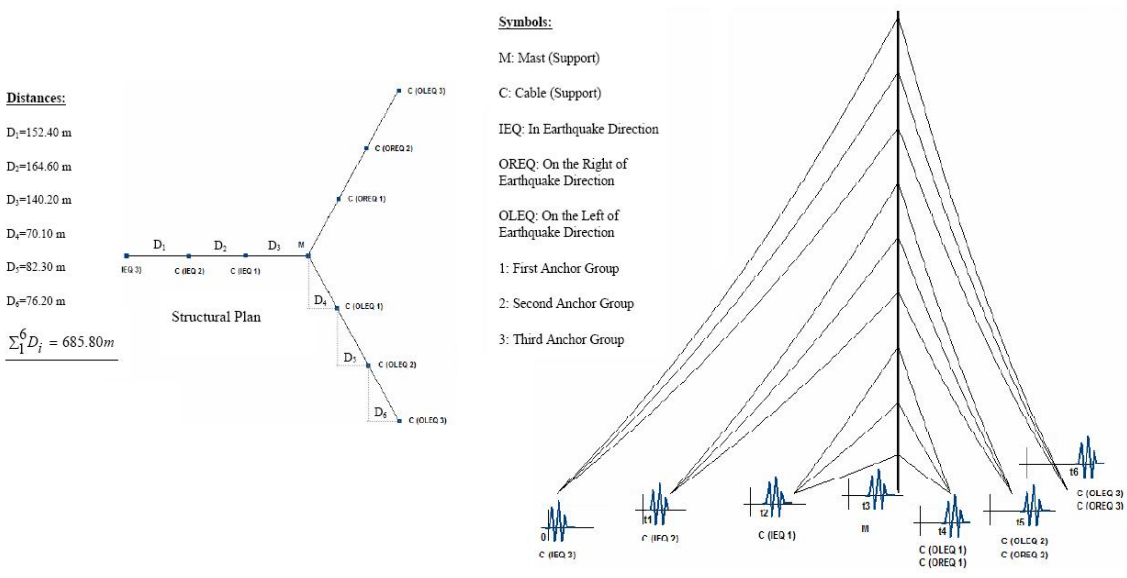

Figure 1.3 *Schematic figure illustrating the asynchronous ground motion inputs at supports for the 607 m tower. t_is represent the arrival times of the earthquake wave ($t_6>t_5>t_4>t_3>t_2>t_1$)*

The main purpose of this study was to clarify some of the previous results and attempt to identify more definite trends in the calculated response of tall masts subjected to realistic three-dimensional ground motion. Figure 1.4 is a schematic summary of the results of all the simulations for the three towers. Depending on the soil stiffness, represented by the horizontal shear wave velocity, the structures of different heights started showing sensitivity at different soil stiffness levels. The three towers showed sensitivity to asynchronous shaking of their ground supports. The taller the structure, on a stiffer soil the sensitivity to asynchronous shaking has initiated. More severe structural response was obtained for softer soil conditions, and the 607 m mast showed sensitivity even for relatively stiff soils.

Faridafshin reported that the peak response most often occurred in the very beginning of the ground shaking when one side of the tower was vibrating and the excitation had not started in the other parts. This impulsive response indicated the vulnerability of guyed masts to out-of-phase excitation. The effects of considering or excluding the structural damping and the vertical component of ground motion were also separately investigated and both factors were found to affect the response indicators significantly. In conclusion,

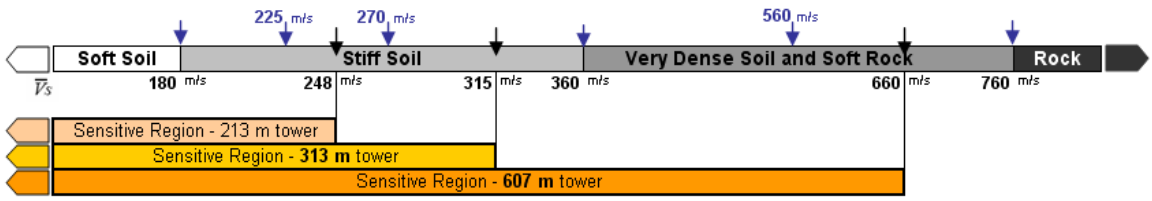

Figure 1.4 *Sensitivity to asynchronous shaking in relation to the shear wave velocity of the soil*

the study confirmed that accurate nonlinear seismic analysis of tall guyed masts must include coherent ground motion records, asynchronous shaking at multiple support points, and structural damping.

1.3.3. A review of Code developments

As mentioned earlier, the dependency of communication networks on very tall masts has made them strategic components of the system, especially in the case of post-disaster response. Under very strong shaking, it is possible that they would not remain serviceable during major strong motion; however, they must not experience important damage in order to resume their function shortly after the event. Especially in high seismicity areas, tower owners are required to assess the seismic performance of their towers. Consequently, in the last decade, there has been an increased interest in North America, as well as Europe, in establishing earthquake resistance design guidelines specifically for communication structures. The primary purpose of these design standards and guidelines is to enable tower designers to provide constructions that satisfy the local building control requirements, where general seismic design criteria for buildings would not be appropriate for communication structures.

In this section, a review of the general recommendations for the seismic analysis of guyed masts by IASS-WG4 will be presented first. Considering the recent developments of the North American Telecommunication Codes, the Canadian Code and the American Code for telecommunication towers will then be reviewed in more details.

Recommendations of IASS for the seismic analysis of guyed telecommunication masts[6]

The International Association for Shell and Spatial Structures, IASS-WG4, published very general recommendations for the analysis and design of guyed masts in 1981. This report suggested that a simplified seismic analysis of guyed towers be done using a static lateral load proportional to their weight (like in most building codes). It recommended several simplifying assumptions in order to linearize the analysis and to use modal superposition. Simple linear springs were suggested to represent the guys, which were associated with lumped masses representing the inertia effects of the cables. However, it mentioned caution in the use of this spring-mass guy cable model for tall masts, due to significant geometric nonlinearities introduced in slackening guys. Since seismic design loads represent extreme events, their combination with the dead loads only was suggested, with the assumption that earthquakes occur in still air conditions. IASS-WG4 further recommended (with no detailed guidance) using random vibration approaches in seismic load modeling and neglecting the ground surface wave propagation effects.

Canadian Standard CSA-S37-01(R2006), Antennas, Towers, and Antenna-Supporting Structures

Guidance on earthquake-resistant design and seismic analysis of communication structures is contained in Appendix M of the Canadian standard CSA-S37-01 (R2006). It is not a mandatory part of the Standard. These guidelines were first introduced in the 1994 edition (Appendix L) and then revised and augmented in 2001: the 2001 version of the standard has been reaffirmed with no change in 2006[7]. According to CAN/CSA S-37,

[6] The International Association for Shell and Spatial Structures (IASS) was founded in 1959 by a group of prominent engineers and architects involved in the design of long-span structures. Working Group No. 4 on Masts and Towers was founded in 1969 to exchange ideas and experiences in order to form recommendations for guyed masts design. This guideline document was published by IASS WG4 in 1981 and was never re-edited; however, the monograph by Smith (2007) summarizes the latest update of IASS WG4 work.

[7] Appendix M is currently under revision to reflect recent research results and the changes in Canadian seismic hazard introduced in the 2005 edition of the National Building Code. The revised edition should be published in 2012.

earthquake effects should be considered for susceptible towers of critical importance, e.g. post-disaster communication systems, in high-risk earthquake zones.

There are three main considerations which dictate the seismic design requirements of a telecommunication structure, namely: the seismic hazard at the tower site, the geotechnical aspects of the site, and the performance level required by the owner for the structure. The definition of earthquake-resistance performance levels was first introduced in the 2001 edition of the Standard to address this last consideration. The selection of an appropriate reliability level is another key design decision in structural engineering. The tower owner (telecommunication service provider) should decide on the appropriate reliability level, usually quantified in terms of appropriate partial loading factors. In general, properly designed masts should resist moderate earthquakes without significant damage and major earthquakes without collapse. However, if the structure is part of a post-disaster communication network, its damage or loss of functionality may amplify the number of fatal casualties and compromise the rescue effort. The Canadian Code uses three categories to define the safety level of the structure: prevention of injury or loss of life, interrupted serviceability, and continuous serviceability.

In the Canadian Code, it is recommended that all structures located in high seismicity areas *(Peak Ground Acceleration,* $PGA > 30\%\ g$*)* be checked to insure that no injury or loss of life may result from the collapse of the structure. Structures located in low seismicity areas, ($PGA < 15\%\ g$), need no seismic design precaution. In moderate seismicity areas, the effect of earthquake loads should be considered in design of all structures supported on buildings and of structures where continuous serviceability has to be maintained. Furthermore, a seismic design check on the structures of interrupted serviceability is recommended for unusually configured structures or in guyed masts taller than 300 m.

The coincidence between the dominant natural frequencies of the structure and the frequency content of the excitation will extensively influence the seismic sensitivity of the structure. Therefore, the first step in the assessment of the tower sensitivity to

earthquakes is the evaluation/prediction of the dominant natural frequencies of the structure.

It is worthy of note that CSA S37 recommends the dynamic analysis of self-supporting lattice structures only for the 50-m and taller towers requiring continuous serviceability in active seismic zones. In addition, special caution is recommended for irregular towers, towers supported by building, and towers mounted by excessively heavy head loads. However, in the case of guyed telecommunication towers, most masts with height ranging typically from 150 m to 300 m have their fundamental flexural frequencies within the sensitive range of the frequency content of the excitation. Nonetheless, seismic effects are not likely to govern the design (wind effects will be more critical) in areas with moderate seismic hazard. The Standard mentions that mast-guy dynamic interaction could be, potentially, an important phenomenon of response amplification. This may be worthy of investigation when the vertical ground motion is combined with the usual horizontal one, provided that there is a frequency coincidence between the input dominant frequencies and the frequencies of the dominant strongly-coupled cable and mast modes. Furthermore, the study of the earthquake effects requires modeling of the seismic input in terms of the prescribed components of the ground displacements along the three orthogonal directions at each support and with an appropriate correlation. Earthquake effects on the masts itself appear to be significant only in the top cantilevered portion (if present) of tall masts and in the first span near the base. Also, dynamic amplifications in the guy tensions are more likely to be significant in the top and the bottom levels of the multilevel guyed masts. Those relatively slack cables with initial tension below about 5% of their UTS, although rarely used in practice, are potentially more vulnerable than taut cables.

Rational simplified and quasi-static analysis models for guyed masts under seismic actions have not been proposed in the literature, unlike for wind actions[8]. Therefore, CSA-S37 recommends performing a detailed dynamic analysis for all masts of height

[8] The Patch Load Method: Sparling, B.F., Smith, B.W., Davenport, A.G., (1996): Simplified dynamic analysis methods for guyed masts in turbulent winds. Bulletin of the International Association for Shell and Spatial Structures, Vol. 37(2), pp. 89-106.

above 150 m located in high seismicity areas and for all masts where continuous serviceability is needed in moderately active areas. But all of the studies forming the research basis of Appendix M of the Canadian Standard have shown that detailed nonlinear seismic analyses are far more complex than response spectrum analysis, and not always necessary. Calculation of the natural frequencies of the initial tower configuration can help to identify the seismic sensitivity of the structure and potential interaction effects due to clustered frequencies. However, for towers with a confirmed potential for seismic sensitivity, it is clear that a rational simplified procedure for seismic design would be very useful.

American Standard ANSI/TIA/EIA-222-G on Seismic design provisions

The American Electrical and Telecommunication Industries Association – EIA/TIA (TIA/222G Telecommunication Industry Standard, 2005) has established earthquake resistance design guidelines specifically for communication structures, primarily to satisfy local building control requirements. The objective of this standard is to provide recognized literature and minimum design requirements for antenna-supporting structures and antennas for all classes of communications service, such as AM, FM, microwave, wireless, TV, etc.

According to TIA/222G, earthquake effects may be ignored for structures presenting a low hazard to human life or damage to property in the event of failure. Moreover, structures used for services that are optional or where a delay in returning the service would be acceptable, such as residential wireless, television, radio, wireless cable, amateur and CB radio communication, maybe designed without any seismic considerations. In addition, seismic design may be ignored for any structure located in a region of low seismic hazard. Furthermore, for towers without torsional, stiffness, and mass irregularities earthquake effects may be ignored when the total seismic shear force is less than 75% of the total horizontal wind load without ice. However, in the all other cases, earthquake effects must be considered in the design of telecommunication towers. It should be noted that the seismic requirements of TIA/222G are mandatory, while the Canadian guidelines are not.

TIA/222G lists four seismic analysis methods: Method 1 Equivalent static lateral force; Method 2 Equivalent modal analysis; Method 3 Modal superposition analysis; Method 4 Time history analysis.

However, Methods 2 and 3 are not strictly applicable to guyed masts who exhibit nonlinear response under strong ground shaking. The equivalent lateral force, Method 1, is deemed applicable to guyed masts with maximum height of 450 m (with maximum ground anchor distance of 300 m for guy cables) and without mass or stiffness irregularities. It should be noted that vertical seismic forces may be ignored in the first three methods. Considering the limitations and the deficiencies of Method 1, time history analysis, Method 4, is the alternative for all towers and masts with or without irregularities. In this detailed approach, vertical components of seismic excitation as well as spatial variations can be explicitly considered in the analysis.

Equivalent lateral force procedure (TIA/222G Method 1): In the equivalent lateral force procedure, the total horizontal seismic shear force is calculated and further distributed along the height of the mast. Consequently, the structure will be analyzed statically using these equivalent seismic forces as external loads.

Time history analysis (TIA/222G Method 4): The time history analysis of TIA/222G recommends that the mathematical model of the guyed mast represent the spatial distribution of the mass and the stiffness throughout the structure, including structural damping equivalent to 5% of critical viscous damping. The mathematical model should be able to consider the inertia and the damping of the cables properly.

The procedure for scaling the input ground motion is presented in details. Consequently, a time-history analysis for each input time histories in accordance with acceptable methods of structural analysis is performed. There are a couple of minimum acceptable modeling considerations for guyed masts in TIA/222G. For instance, the mast model can be an elastic three-dimensional beam-column mast, an elastic three-dimensional truss model or a three-dimensional frame-truss model. In addition, the analysis shall take into account the global $P-\Delta$ effects on the mast induced by its sway

motion. Also, for guyed telecommunication masts, the effects of out-of-phase excitation of the anchor point shall be included in the analysis.

According to TIA/222G, the mast translations (sway) and rotations (twist and tilt) under service loads shall comply with certain serviceability limits, unless otherwise required. If precise serviceability criteria are not specified by the tower owner/service provider, TIA/222G lists a few general minimum requirements.

1.3.4. Review of other works

There are not many published reports in the open scientific literature on the seismic behaviour of telecommunication towers. However, even if the number of researchers in the field is limited, several appreciable developments have been made in the more general area of dynamics, especially under wind loading.

Traditional attempts at the numerical modelling of guyed towers were accompanied by simplifications in the model, such as replacing the cables by equivalent springs or substituting the masts with equivalent Timoshenko beam-columns. Later on, however, studies by Augusti et al. (1990) and Argyris and Mlejnek (1991) revealed that although these simplifications are not significantly influential when studying the static response of structure, they are no longer appropriate for dynamic analyses of guyed masts.

One work reported by Augusti et al. (1990) included the modelling of a 200 m guyed mast with three guying levels, in which equivalent static linear springs were employed to model the guy cables and where the equivalent stiffness of the springs varied with the frequency of oscillation. However, the inertia effects of the cables were neglected. Furthermore, another numerical study by Raman et al. (1988) clearly confirmed the importance of geometric nonlinearities in the guyed tower responses under quasi-static loads.

In the 1990s, aside from the work done at McGill University, a few other studies have been completed in Canadian research centers in dynamic analysis of guyed telecommunication towers, namely research at the University of Western Ontario on simplified dynamic analysis procedure for masts subjected to turbulent wind effects (Sparling 1995 and Sparling and Davenport 1999) and at the University of Windsor on the general dynamic properties of guyed masts (Wahba 1999) and a more recent study by Meshmesha (2005) on seismic design of tall masts.

In more details, the scope of Meshmesha's research was to use a finite element model capable of predicting accurately the response of guyed towers when subjected to seismic loading, with a view to provide simplified equations to determine the fundamental natural frequencies of guyed masts as well as other response indicators, for instance the base shear, the bending moment, and the axial force in the mast and the tension in the cables. This study was very similar to Amiri's (Amiri 1997) but the seismic loading included more detailed Canadian seismicity considerations. It covered nine guyed telecommunication towers (some used by Amiri) with heights from 60m to 591m using ABAQUS software. The effect of the antenna weights on the seismic response of these towers were investigated and found to be insignificant. Finally, several empirical equations were proposed for various guyed mast response indicators in various Canadian cities. All these expressions were function of tower height and cannot be extrapolated to other design conditions than those for which they were derived.

Some tower designers have also carried out studies on seismic analysis of communication towers and masts on the West coast of the United States. Fantozzi (2006) studied the nonlinear analysis of a 2000 ft guyed tower, located in California region, with and without mass irregularities. The analysis considered both in-phase and out-of-phase base motion for comparison. The results of the nonlinear analyses were compared to those obtained using the equivalent lateral force method introduced by TIA/EIA-222-G, and the tower was found to meet the standard requirements.

Hensley (2005), at Virginia Polytechnic Institute and State University, developed a finite element model of a 120-m tall mast also using ABAQUS and studied its three-

dimensional response to two ground motion records, Northridge, and El Centro, with three orthogonal components. Hensley conducted a parametric study on the dominant structural parameters, and the results were used to characterize the trends in the structural response of guyed masts under seismic loading.

Europeans have also contributed to research on the seismic design of guyed telecommunication masts. The nonlinear dynamic response calculation method was presented by Mossavi Nejad (1996), at University of Westminster, UK, based on step-by-step response calculation in the time domain. The dynamic loading was generated as a series of cross-correlated earthquake histories defined by the base frequency envelope of typical earthquake records exciting the main frequency components of the structure.

The analysis was applied to the numerical model of a 327 meters tall guyed mast with five levels of stays and a cantilever at the top. The results obtained from nonlinear dynamic analysis were compared to conventional mass-spring system approaches. Mossavi Nejad mentioned that although the stiffness matrix constructed for the mass-spring model provided good estimation of the static deflections of the guyed mast, the results obtained from the linear dynamic analysis of the mass-spring model are not comprehensive enough to give good comparison with the results of time domain analyses, which highlights the need for more improvements on the computational models.

In Germany, Zhang and Peil (1996) have employed a cable element model in nonlinear dynamic analysis of guyed towers with a view to evaluate their stability under seismic loads. They studied the sensitivity of the calculated tower motions to small changes in the boundary and initial conditions. Their results indicated that guyed towers cannot be simply classified as chaotic systems although their motion trajectories are sensitive to the small changes in boundaries and initial conditions. Although the concept of energy increment map was developed to judge the stability behaviours of guyed towers under earthquake actions, the complexity and sophistication of detailed nonlinear dynamic analysis were remained a challenge.

2. The equivalent dynamic properties of guy clusters based on rational cable mechanics

2.1. Introduction

No complete approximate analysis method has been proposed yet for the seismic design of guyed masts. There have been some efforts included in EIA-222 for the preliminary seismic analysis of short masts or AS 3995 associated with frequency analysis and there is call for a method of general applicability in this field. The main difficulty with the quasi-static approach is to define realistic acceleration profiles that account for the localized variations of the mast lateral stiffness, the dynamic interaction between vertical and horizontal effects and the geometric nonlinearity of the response of such structures. In effect, a rational and reasonably accurate seismic method of general applicability is virtually impossible to develop. Therefore, CSA-S37 recommends performing a detailed dynamic analysis under certain conditions.

Detailed nonlinear seismic analyses are far more complex than response spectrum analysis and are not routinely performed for design. In fact, design of tall telecommunication masts is usually governed by combinations of turbulent wind and atmospheric icing effects in cold climates. As such, there is a practical need for simplified procedures to perform design checks on the seismic vulnerability of tall masts. Such procedures should be simple enough such that they are less time-consuming than nonlinear time-history analysis yet they must be accurate enough not to be misleading on the tower seismic safety nor overly conservative. If a simplified procedure indicates that seismic effects influence the final design, then a more complete detailed nonlinear seismic analysis would be necessary. Clearly, the purpose of the simplified procedure presented by the author is not to replace detailed seismic analysis when it is necessary, but rather to determine whether it is necessary.

As a first step towards the development of a simplified dynamic analysis procedure for tall guyed telecommunication masts, the equivalent dynamic properties of guy clusters are studied in detail in the following chapter. The method is based on rational cable

mechanics and is verified with results from detailed finite element analysis of selected detailed models of real guy cables. Primarily, the static equilibrium of elastic cables is studied using a new mathematical approach from which the equivalent static stiffness of elastic guy cables is evaluated. In order to develop a simplified model for the equivalent dynamic stiffness of elastic guy cables, an undamped single-degree-of-freedom (SDOF) system is considered and the nonlinear equation of motion is established. The equation of motion is solved using an approximate solution method and the results are verified with detailed finite element simulations. A few application examples are presented to illustrate the reasonable engineering accuracy of the procedure.

This first portion of the research was presented as: Ghafari Oskoei, S.A., McClure, G., 2009 "Simplified dynamic analysis method for telecommunication masts under seismic excitation" ASCE Structures Congress' 09, April 30 to May 2, 2009, Austin, Texas, USA, pp. 1-10. The paper is presented in the next section[1] and Appendix B gives more details on the application examples. ASCE has granted permission to the author to reproduce this publication as part of this doctoral dissertation[2]:

[1] A few editing modifications have been made to match the thesis referencing scheme. However, the content has been kept similar to the original submission. Permalink: http://dx.doi.org/10.1061/41031(341)113

[2] The ASCE copyright policy: http://www.asce.org/Content.aspx?id=21545

2.2. Simplified dynamic analysis methods for guyed telecommunication masts under seismic excitation

Authors:

S. Ali Ghafari Oskoei, Ph.D. Candidate, Department of Civil Engineering and Applied Mechanics, McGill University, Montréal, Québec, Canada, H3A 2K6.
ali.ghafari@mail.mcgill.ca
Ghyslaine McClure, Associate Professor, Department of Civil Engineering and Applied Mechanics, McGill University, Montréal, Québec, Canada, H3A 2K6.
ghyslaine.mcclure@mcgill.ca

2.2.1. ABSTRACT

Earthquake-resistant design of essential infrastructure is paramount in areas with high seismic hazard and risk. Such critical infrastructure includes tall telecommunication masts which are highly nonlinear structures owing to the behaviour of their multi-level guy clusters. During earthquakes, their multi-support foundation is subjected to seismic wave delays that vary with the shear wave velocity of underlying soil. Such effects can be properly described in detailed nonlinear seismic analysis models, which are mainly used to explain exceptional situations (for example, mast failures) and for research purposes. However, the degree of complexity and sophistication these models require is too high for routine engineering design, and simplified procedures are necessary to perform design checks on the seismic vulnerability of tall masts. As a first step towards a simplified dynamic analysis procedure, this paper presents a method to obtain the equivalent dynamic properties of guy clusters. The method is based on rational cable mechanics and is verified with results from detailed finite element analysis of selected detailed models of real guy cables. However, the number of towers and the frequency range studied are limited, as this paper presents an ongoing research. More case studies are necessary to validate the method before it can be used in engineering practice.

Proceedings of the 2009 Structures Congress, pp. 1020-1029

2.2.2. INTRODUCTON

Earthquake-resistant design of essential infrastructure is paramount in areas with high seismic hazard and risk. Undoubtedly, the last decade has seen important improvements in seismic design and analysis procedures for building structures and applications to other constructed facilities have benefited from these developments, including tall telecommunication masts. Telecommunication masts, also called guyed towers in North America, have vital functionality in communication networks. They are typically tall (height above 180 m), slender structures, whose lateral resistance is provided by clusters of guy cables attached at different elevations and anchored to the ground at several support points. Guyed masts are highly nonlinear structures owing to the behaviour of their multi-level guy clusters. Also, their multi-support foundation is subjected to seismic wave delays that vary with the shear wave velocity of underlying soil. Such effects can be properly described in detailed nonlinear seismic analysis models which are mainly used to explain exceptional situations (for example, mast failures) and for research purposes. However, the degree of complexity and sophistication these models require is too high for routine engineering design. To date, detailed nonlinear finite element analysis is the only rational and reliable approach for seismic analysis of guyed telecommunication towers. However, it entails analysis time, effort, and cost that are difficult to justify since earthquakes effects would typically require a design check on a configuration obtained from other environmental and operational loads. This further highlights the need for rational simplified analysis procedures in this application.

This paper presents a method to obtain the equivalent dynamic properties of guy clusters for simplified dynamic analysis. The method is based on rational taut cable mechanics and is verified with results from detailed finite element analysis of three selected detailed models which are described next. The detailed seismic analysis procedure used to verify the proposed method is described in [Faridafshin and McClure, 2008].

2.2.3. GUYED TOWER MODELS

The guyed cables selected for this study are taken from real guyed telecommunication masts studied by [Faridafshin, 2006]. The geometric characteristics of the three masts are summarized in Table 2.1 and a schematic of the 213-m mast is illustrated in Figure 2.1 to provide an example. It is noteworthy that the 607-m mast is among the tallest man-made structures and is located in Sacramento, California. Complementary information on modeling considerations can be found in [Faridafshin, 2006] and [Faridafshin and McClure, 2008].

2.2.4. ELASTIC CABLE STATIC EQUILIBRIUM

The method used by [Faridafshin, 2006] to model the guy cables in commercial finite element analysis software [ADINA R&D, 2004] was based on defining the cable elements along the chord line between the two end support points. The cable pretension forces are introduced as an initial strain in the truss elements and a static nonlinear analysis is performed to define the relaxed cable position. The restart option of ADINA is then employed to continue the analysis in the deformed initial static configuration of the structure.

The parametric solution that describes the relaxed position of an inclined elastic cable profile is introduced as follows in [Irvine, 1981]:

Height (m)	No. of stay levels	No. of anchor groups	Panel width (m)	Panel Height (m)
607.1	9	3	3	2.25
313.9	5	2	2.14	1.52
213.4	7	2	1.52	1.52

Table 2.1 *GEOMETRY OF THE THREE MASTS STUDIED [FARIDAFSHIN, 2006].*

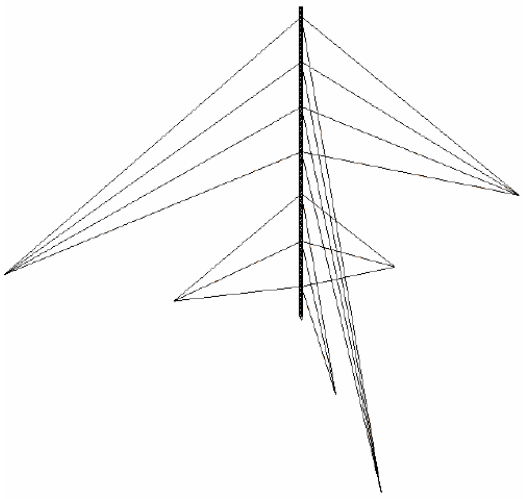

Figure 2.1 *GEOMETRIC LAYOUT OF 213-M MAST [FARIDAFSHIN, 2006].*

$$l_t = \frac{HL_0}{EA} + \frac{HL_0}{W}\left\{sinh^{-1}\left(\frac{V}{H}\right) - sinh^{-1}\left(\frac{V-W}{H}\right)\right\} \quad (2.1)$$

$$h = \frac{WL_0}{EA}\left(\frac{V}{W} - \frac{1}{2}\right) + \frac{HL_0}{W}\left\{\left\{1 + \left(\frac{V}{H}\right)^2\right\}^{1/2} - sinh^{-1}\left(\frac{V-W}{H}\right)\right\} \quad (2.2)$$

where l_t is the total cable length and h is the vertical difference in elevation between the cable ends. These two equations must be solved simultaneously to obtain the vertical reaction force at the supports V and the horizontal component of the cable tension H. EA is the axial rigidity of the elastic cable, W is the total weight, and L_0 is the unstrained cable length. This solution is easily obtained using the "fsolve" function of MATLAB. However, the objective is to introduce a simplified method which will not require the simultaneous solution of nonlinear equations.

As shown in Figure 2.2, the usual $x - z$ coordinate system is rotated such that x_* measures the distance along the chord from the left support point and z_* measures the perpendicular distance to the cable profile from the chord. Therefore, the following trigonometric relations apply: $x_* = x\ \sec\theta + z\ \sin\theta$, $z_* = z\ \cos\theta$, and $H_* = H\ \sec\theta$.

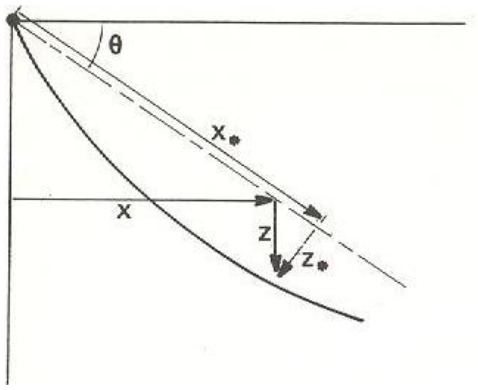

Figure 2.2 *INCLINED CABLE AXIS TRANSFORMATION*

When the cable profile is assumed parabolic, the horizontal component of cable tension is expressed as:

$$H_* = \frac{m\,(g\ cos\,\theta)\,l_t^2}{8\,d} \tag{2.3}$$

where d is the sag of the cable perpendicular to the chord line. According to [Irvine, 1981], the cable length can be estimated by the following truncated series expansion:

$$L = \int_0^{l_t} \left\{1 + \left(\frac{dz}{dx}\right)^2\right\}^{1/2} dx = l_t \left\{1 + \frac{8}{3}\left(\frac{d}{l_t}\right)^2 - \frac{32}{5}\left(\frac{d}{l_t}\right)^4 + \cdots\right\} \tag{2.4}$$

and one can approximate the elastic strain as $\varepsilon = (L - l_t)/l_t$. Subsequently, $H_* = EA\,\varepsilon + F_i$, in which F_i is the initial pretension. Considering only the first two terms of the expansion in Equation (2.4), we have:

$$H_* = EA\left\{\frac{8}{3}\left(\frac{d}{l_t}\right)^2\right\} + F_i \tag{2.5}$$

Replacing (2.3) into (2.5) yields a cubic equation in terms of d:

$$\frac{64}{3}\frac{EA}{l_t^2}\,d^3 + 8\,F_i\,d - m\,(g\,\cos\theta)\,l_t^2 = 0 \qquad (2.6)$$

The cubic equation can be rewritten in standard form as

$$A'\,d^3 + B'\,d + C' = 0 \qquad (2.7)$$

where the coefficients are

$$A' = \frac{64}{3}\frac{EA}{l_t^2} \qquad B' = 8F_i$$

$$C' = -\,m\,(g\,\cos\theta)\,l_t^2 \qquad (2.8)$$

To facilitate the solution of (2.6) in MATHEMATICA we define parameter D' as

$$D' = -9\,A'^2\,C' + 1.7321\,\sqrt{A'^3(4\,B'^3 + 27\,A'\,C'^2)} \qquad (2.9)$$

and isolate the sag d on the left-hand-side:

$$d = -0.8736\,B'D'^{\,-1/3} + 0.3816\,A'^{\,-1}\,D'^{\,1/3} \qquad (2.10)$$

Although (2.9) and (2.10) appear cumbersome in notation, (2.10) is solved directly without any iteration or numerical scheme. Table 2.2 compares the results obtained from (2.10) with the "exact" solution of (2.1) and (2.2) from MATLAB, for all the guy cables of the 213-m tower. It is seen that the maximum difference in the two sets of results is less than 5% and that the approximation underestimates the cable tension.

2.2.5. EQUIVALENT STATIC STIFFNESS OF ELASTIC GUY CABLE

The equivalent static stiffness of the guy cable is defined by considering the change in cable tension corresponding to a change in chord length, in any given static equilibrium configuration. In a telecommunication mast, this equilibrium is defined for the entire

structure and changes in cable chord lengths of the guy cables are related to mast displacements. Equation (2.10) can also be used to obtain the equivalent mean static stiffness of guy cables through monitoring the variation of the tension force in the cable versus the change in chord length. Table 2.3 compares the equivalent mean stiffness values obtained by solving Equations (2.1) and (2.2) - the reference MATLAB solution, with the results obtained from (2.10).

These results indicate that the proposed simplified model for static cable stiffness agrees with the exact theoretical model with errors less than 0.5% for all the 3 masts studied. It is worthy of note that these values also agree with detailed results obtained from numerical simulations in ADINA.

2.2.6. EQUIVALENT DYNAMIC STIFFNESS OF ELASTIC GUY CABLE

Previous studies on nonlinear seismic analysis of guyed masts such as [Faridafshin, 2006] and [Amiri, 1997] as well as the current results have indicated that the main source of the time variant nonlinear behaviour of tall telecommunication masts is the variations in the dynamic stiffness of the guy cables. In the present work, the dynamic stiffness of a guy cable is studied by imposing a harmonic displacement to one end and monitoring the variation of the instantaneous stiffness of the cable over time. In order to develop a

	Proposed		MATLAB	
Cable	d (m)	H* (N)	H* (N)	Error
1	0.4	26,703	26,899	0.73%
2	0.429	29,406	29,840	1.45%
3	0.488	38,445	39,256	2.07%
4	2.279	35,473	36,562	2.98%
5	2.459	42,623	44,257	3.69%
6	2.655	58,724	61,409	4.37%
7	2.837	78,443	82,548	4.97%

Table 2.2 *COMPARISON OF THE CABLE TENSION FROM PROPOSED METHOD AND MATLAB CODE.*

Cable	Proposed		MATLAB	Error
	H* (N)	K (N/m)	K (N/m)	
1	46,271	373,570	374,150	0.16%
2	52,346	231,747	232,390	0.28%
3	61,541	151,925	152,590	0.44%
4	51,683	96,209	96,460	0.26%
5	53,562	83,421	83,660	0.29%
6	68,439	84,730	85,010	0.33%
7	84,988	83,584	83,930	0.41%

Table 2.3 *COMPARISON OF THE EQUIVALENT STATIC STIFFNESS OF THE CABLES FROM PROPOSED METHOD AND MATLAB CODE.*

simplified model for dynamic analysis, an undamped single-degree-of-freedom (SDOF) system is considered in Figure 2.3.

The quadratic function derived in Equation (2.5) from the series expansion in Equation (2.4) is suitable only for taut cables with small kinematics and deformations. As sags increase when cables slacken, the series approximation must include more terms to approximate the hyperbolic functions of the theoretical solution.

As such, the deformed cable profile, $z(x)$, is assumed to be in symmetric 4th order form:

$$z = (-d/l^4)\,(x-l)^4 + (2d/l^2)\,(x-l)^2 - d\ , \quad 0 \le x \le 2l \tag{2.11}$$

The length of the cable, L, and the corresponding elongation, e, are:

$$L = \int_0^{l_t} \left\{1 + \left(\frac{dz}{dx}\right)^2\right\}^{1/2} dx = l_t \left\{1 + \frac{8}{3}\left(\frac{d}{l_t}\right)^2 - \frac{8192}{5}\left(\frac{d}{l_t}\right)^4 + \cdots\right\} \tag{2.12}$$

$$e = \frac{2\,d^2}{3l} - \frac{512\,d^4}{5l^3} \tag{2.13}$$

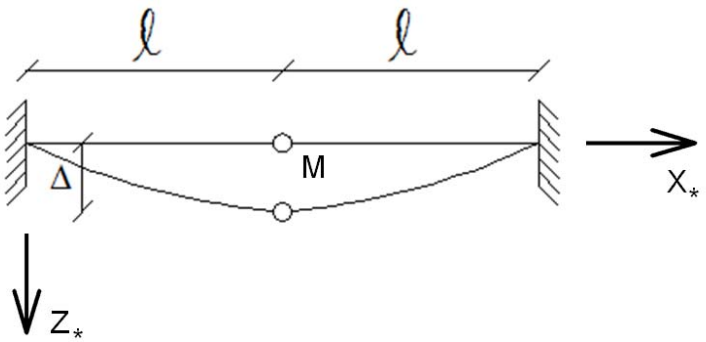

Figure 2.3 *EQUIVALENT SDOF SYSTEM FOR CABLE DYNAMICS*

where d is the sag of the cable. Our numerical investigations suggest that these approximations are valid for taut cables with $d/l_t \leq 0.02$, and the elastic strain energy stored in the cable can be calculated using the above assumptions.

The total energy, U, of the equivalent SDOF dynamic system at any time t is expressed in (2.14) and comprises the elastic strain energy stored in the cable and the kinetic and potential energy of the equivalent mass M (weight w):

$$U = \frac{4}{3} P_0 \frac{\Delta^2}{l} + \frac{4}{9} \frac{EA}{l} \frac{\Delta^4}{l^2} + \frac{1}{2} M \dot{\Delta}^2 - w\Delta \qquad (2.14)$$

where Δ is the vertical displacement of the middle point of the cable at the position of the equivalent mass M. Following parametric studies on this model, it was concluded that an equivalent mass M equal to $2/3$ of the total mass (weight) of the cable provides the optimal representation of the complete cable response[3]. The axial tension, P_0, is harmonic

$$P_0 = P_i + \delta EA/2l \, \sin(2\pi f \, t) \qquad (2.15)$$

where P_i is the initial pretension of the cable and δ is the magnitude of the harmonic displacement exerted at the cable end with forcing frequency $\Omega = 2\pi f$.

[3] This value is the generalized mass of a SDOF system assuming a half-sine mode shape (single loop vibration).

The equation of dynamic equilibrium for the equivalent SDOF system is obtained by minimizing the total energy of the cable:

$$M\ddot{\Delta} + \frac{8P_0}{3l}\Delta + \frac{16EA}{9l^3}\Delta^3 = w \qquad (2.16)$$

Replacing (2.15) in (2.16), the equation of dynamic equilibrium takes the form:

$$M\ddot{\Delta} + \left(\frac{8}{3l}P_i\right)\Delta + \left(\frac{8}{3l}\frac{\delta EA}{2l}\sin(2\pi f\, t)\right)(\Delta - \Delta_s) + \frac{16EA}{9l^3}\Delta^3 = w \qquad (2.17)$$

where Δ_s is the maximum displacement of the middle point of the cable, at mass M, in the static configuration. Equation (2.17) is highly nonlinear. Moving the harmonic forcing function on the right-hand-side and rewriting the total sag as the sum of its static and time-varying components, $\Delta = \Delta_s + x$, we obtain:

$$M\ddot{x} + \frac{8\,P_i}{3l}(x + \Delta_s) + \frac{16EA}{9l^3}(x + \Delta_s)^3 = w - \frac{4\delta EA}{3l^2}\, x\, \sin(2\pi f\, t) \qquad (2.18)$$

The cable elongation, e, is written as:

$$e = \frac{2}{3l}\left((\Delta_s - x)^2 - {\Delta_s}^2\right) - \frac{512}{5l^3}\left((\Delta_s - x)^4 - {\Delta_s}^4\right) \qquad (2.19)$$

Expanding the left-hand-side of (2.18) yields:

$$M\ddot{x} + \frac{8\,P_i}{3l}\,x + \frac{8\,P_i}{3l}\Delta_s + \frac{16EA}{9l^3}x^3 + \frac{16EA}{9l^3}\,\Delta_s^3 + \frac{16EA}{3l^3}x\Delta_s^2 + \frac{16EA}{3l^3}\,x^2\Delta_s$$

$$= w - harmonic\ term \qquad (2.20)$$

It is seen that the 3rd and 5th terms will be cancelled by the weight w in the static equilibrium condition and (2.20) can be reduced to:

$$M\ddot{x} + \left(\frac{8\,P_i}{3l} + \frac{16EA}{3l^3}\Delta_s^2\right)x + \frac{16EA}{3l^3}\,\Delta_s\,x^2 + \frac{16EA}{9l^3}x^3 \qquad (2.21)$$

$$= -\frac{4\delta EA}{3l^2}\,x\,\sin(2\pi f\,t)$$

Equation (2.21) represents the dynamic motion of the proposed simplified cable model and will be solved next to establish the equivalent dynamic stiffness of the guy cable.

2.2.7. SOLVING NONLINEAR EQUATION MOTION

Equation (2.21) is highly nonlinear for relatively large imposed displacements. We first investigate the effect the amplitude of the cable motion on its fundamental frequency, ω_0. Further, we find a simplified solution to (2.21) based on linearization and some averaging techniques.

2.2.8. Perturbation Method

There are two nonlinear terms in the left-hand side of (2.21) (quadratic and cubic) that can be considered separately. We discuss next the effect of the cubic term only while the quadratic term could be treated in the same manner.

We rewrite (2.21) in terms of the linear frequency ω_0 of the oscillator and consider the cubic term on the right-hand side to obtain the non homogeneous form:

$$\ddot{x} + \omega_0^2\,x = -\varepsilon\,x^3 \qquad (2.22)$$

where

$$\omega_0^2 = \frac{8\,P_i}{3l\,M} + \frac{16\,EA\,\Delta_s^2}{3l^3\,M} \qquad (2.23)$$

$$\varepsilon = \frac{16EA\Delta_s}{9l^3\,M} \tag{2.24}$$

The expansion of the perturbation term ε up to its 2nd order in (2.22) yields:

$$(\ddot{x}_0 + \varepsilon\,\ddot{x}_1 + \varepsilon^2\ddot{x}_2) + (\omega^2 - \varepsilon\,\alpha_1 - \varepsilon^2\alpha_2)\,(x_0 + \varepsilon\,x_1 + \varepsilon^2 x_2)$$

$$= -\varepsilon\,(x_0 + \varepsilon\,x_1 + \varepsilon^2 x_2)^3 \tag{2.25}$$

where

$$\alpha_1 = \frac{3A_0^2}{4\,\omega^2}, \quad \alpha_2 = \frac{21A_0^4}{128\omega^6} \tag{2.26}$$

Finally, the effect of the cubic term in (2.21) on the cable natural frequency of the linear system is included in the following implicit equation:

$$\omega^2 = \omega_0^2 + \varepsilon\frac{3A_0^2}{4\,\omega^2} + \varepsilon^2\,\frac{21A_0^4}{128\omega^6} \tag{2.27}$$

Similarly, the influence of the quadratic term in (2.21) can be obtained and be superimposed to the expression in (2.27) – see (2.29) for the combined result.

It is useful to treat differently cables that will undergo resonance (i.e. small oscillations) and those that will (with large amplitudes of motion) to get more accuracy in the proposed method. For cables with small kinematics,

$$\omega = \eta\,\omega_0, \quad \eta = \sqrt{0.5\left(1 + \sqrt{1 + 3\varepsilon A_0^2/\omega_0^4}\right)} \tag{2.28}$$

with $A_0 = \omega x_{max}$. Since A_0 is also a function of ω, iterations are necessary to solve (2.28) for a given x_{max}. In the same manner, for cables with large oscillations, the frequency at iteration i is given by:

$$\omega_i^2 = \omega_0^2 + \varepsilon \frac{3A_0^2}{4\,\omega_{i-1}^2} + \varepsilon^2 \left(\frac{21A_0^4}{128\omega_{i-1}^6} - \frac{15A_0^2}{2\omega_{i-1}^4} \right) \quad , i = 1, 2, 3, \ldots \tag{2.29}$$

2.2.9. APPROXIMATE SOLUTION

The objective is to solve (2.21) to obtain the equivalent dynamic cable stiffness, represented by the coefficient of the linear term in x. We introduce $\overline{x} = \frac{2}{3} x_{max}$ and replace x^2 by $\overline{x}\,x$ and x^3 by $\overline{x}^2\,x$. Further, the right-hand-side of (2.21) represents the force exerted on the system. For this term we replace x by some average parameter $x_{max} Q_1(\Omega)$:

$$\frac{4\delta EAx}{3l^2} = \frac{8\delta EAx_{max}\,Q_1(\Omega)}{3l^2} \tag{2.30}$$

The expression for $Q_1(\Omega)$ in (2.31) is based on curve fitting of detailed numerical simulation results.

$$Q_1(\Omega) = \frac{\lambda^2 \left(1/\left(1-\beta^2\right)\right) \left((\omega/2\pi)^2 - b\right)}{0.095\,\gamma^2 - 1.02\,\gamma + 2.74} \tag{2.31}$$

where the parameter λ^2 is defined in [Irvine, 1981] as:

$$\lambda^2 = (mg\cos\theta\, l_t/H_*)^2 (l_t EA/(H_* L_e)) \tag{2.32}$$

$\gamma = \Omega/\omega_1$, in which ω_1 is the frequency of the longest cables, $b = 0.4\,\gamma - 0.3$ if $0 \le \gamma \le 2$ and $b = 0.5$ if $2 \le \gamma \le 5$.

Enforcing all the above expressions in (2.21), the following form is obtained for the equation of motion and the coefficient of *x* represents the equivalent dynamic stiffness:

$$M\ddot{x} + \left(\frac{8\,P_i}{3l} + \frac{16EA}{3l^3}\Delta_s^2 + \frac{16EA}{3l^3}\,\Delta_s\bar{x} + \frac{16EA}{9l^3}\bar{x}^2\right)x = -\frac{8\delta EAx_{max}\,Q_1(\Omega)}{3l^2}\;\sin(2\pi f\,t) \tag{2.33}$$

The response of the system described by (2.33) with zero initial conditions $\dot{x}(0) = x(0) = 0$ takes the classical form:

$$x = \frac{P_0}{k}\,\frac{1}{1-\beta^2}\,(\sin(\Omega t) - \beta\sin(\omega t)) \tag{2.34}$$

where Ω is the frequency of loading and β is the frequency ratio $\beta = \Omega/\omega$.

$$\omega = \sqrt{\left(\frac{8\,P_i}{3l} + \frac{16EA}{3l^3}\Delta_s^2 + \frac{16EA}{3l^3}\,\Delta_s\bar{x} + \frac{16EA}{9l^3}\bar{x}^2\right)/M} \tag{2.35}$$

$$P_0 = \frac{8\delta EAx_{max}\,Q_1(\Omega)}{3l^2} \tag{2.36}$$

The method is iterative due to the dependency of many terms on x_{max}. The convergence of this iterative scheme is established by:

$$(x_{max})_i = Q_2(\Omega)\,(x_{max})_{i-1} \tag{2.37}$$

$$Q_2(\Omega) = \frac{\lambda\left((\omega/2\pi)^2 - c\right)}{0.24\,\gamma^2 - 1.75\,\gamma + 3.25} \tag{2.38}$$

with $c = 0.75\,\gamma - 1.5$ if $0 \le \gamma \le 2$, and $c = 0$ if $2 \le \gamma \le 5$. All the above calculations can be efficiently programmed in a short code or Excel Sheet.

Before numerical applications are shown next, it is important to mention that the proposed method was derived for tall telecommunication masts in the range of 200 to 400 m in height with guy cables with minimum pretension corresponding to approximately 10% of their ultimate strain. These guys have their fundamental frequency in the range of 0.5 to 0.15 Hz. Considering that typical earthquakes have their strong motion in the range of 0.3 to 3 Hz, the choice of γ in the range of 1 to 5 covers all important frequencies of the response spectra.

2.2.10. APPLICATION EXAMPLES

Figure 2.4 and Figure 2.5 present two application examples and compare the horizontal dynamic cable tension obtained by detailed finite element analysis with ADINA (left plot) and the approximation of the proposed equivalent SDOF model (right plot). The results indicate good agreement between the two proposed approaches. Also, the static results shown in superposition to the dynamic results of the SDOF model indicate the importance of the dynamic amplifications of the response, especially for the longer cable in Figure 2.4.

2.2.11. CONCLUSION

An approximate method has been proposed to evaluate the equivalent static and dynamic stiffness of guy cables used in telecommunication masts. The method was shown to agree with detailed finite element analysis results. The next step is to perform dynamic analysis on a complete mast using the equivalent dynamic stiffness of each guy cluster. The effects of cable damping will also be considered at a later stage of the research.

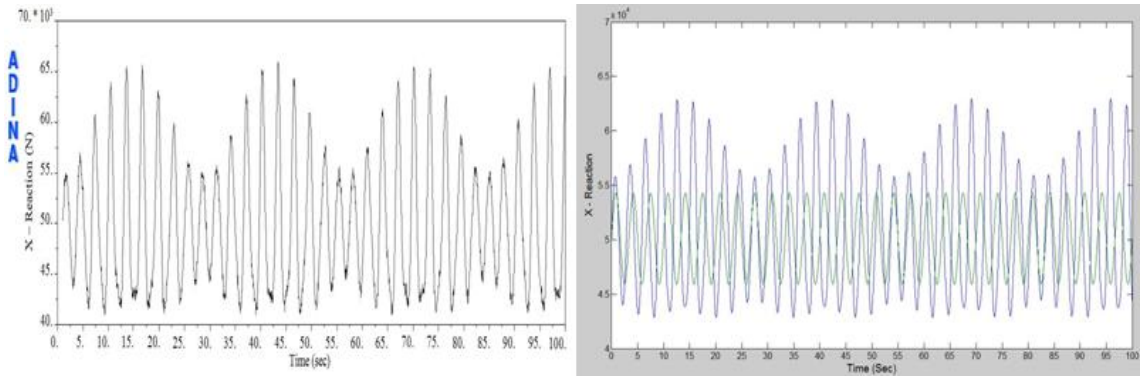

Figure 2.4 *HORIZONTAL TENSION RESPONSE OF THE 7TH (LONGEST) CABLE, 213-M MAST TO HARMONIC LOADING WITH FREQUENCY OF 0.3 HZ. LEFT: DETAILED NONLINEAR ANALYSIS. RIGHT: STATIC AND DYNAMIC RESPONSE USING THE PROPOSED SDOF METHOD.*

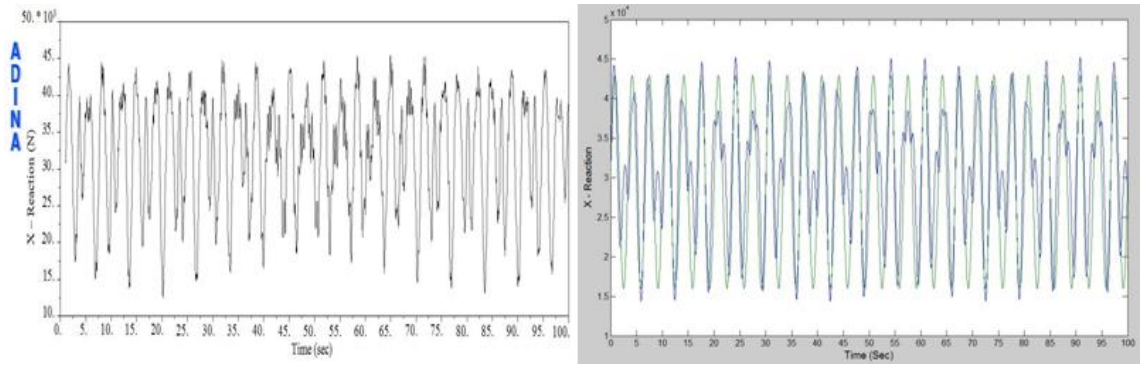

Figure 2.5 *HORIZONTAL TENSION RESPONSE OF THE 4TH CABLE, 213-M MAST TO HARMONIC LOADING WITH FREQUENCY OF 0.3 HZ. LEFT: DETAILED NONLINEAR ANALYSIS. RIGTH: STATIC AND DYNAMIC RESPONSE USING THE PROPOSED SDOF METHOD.*

REFERENCES

Please see the last section.

3. A novel approach to evaluate the equivalent dynamic stiffness of guy clusters in telecommunication masts under ground excitation

3.1. Introduction

A study of the equivalent dynamic properties of individual guy cables such as those used in tall telecommunication masts was presented in Chapter 2 based on rational cable mechanics and nonlinear static and dynamic analysis of elastic cables under harmonic excitation patterns.

In this chapter, the study of individual guy cables is extended to cover their geometric nonlinear response as part of a cluster of guy cables attached to telecommunication masts under seismic excitations. A novel frequency domain algorithm is presented to evaluate the dynamic performance of guy cables under seismic excitations. This algorithm will later be used in the global proposed approach (in Chapter 4) to perform seismic design checks on tall masts. Detailed numerical simulations involving 57 guy cables from eight existing towers with varying heights of 150 to 607 m were used in the study. The research initially concentrates on the determination of the frequency-variant stiffness of guy cables. Individual inclined cable models were extracted from the complete finite element models of the structures and were tested upon parametric harmonic displacement exerted to one end along the horizontal x-coordinate. The Guy stiffness Dynamic Amplification Factors ($GDAF$) is derived to describe the dynamic stiffness of the cables under certain excitation patterns.

Several approaches are examined to develop $GDAF$ graphs associated with the response spectrum of individual cables to harmonic excitation. A mathematical procedure was later developed to evaluate the dynamic stiffness of individual cables under specific earthquake signature and to replace the guy cables clusters with an equivalent linear frequency-dependent spring/mass system. Comparison of the main response indicators of these models and the detailed finite element analysis results confirmed the reasonable and consistent engineering accuracy of the proposed method, which is far less demanding

than full nonlinear dynamic analysis. The equivalent dynamic guy stiffness model will contribute efficiently towards the development of a new robust rational model of general applicability for seismic design of tall guyed telecommunication masts.

This research was summarised into a manuscript: Ghafari Oskoei, S. A., and McClure, G. "A novel approach to evaluate the equivalent dynamic stiffness of guy clusters in telecommunication masts under ground excitation." *Journal of Structural Engineering, (revised version) submitted in February 2011.* The following section presents the manuscript with minor changes to fit into the general format of the thesis and Appendix C gives more details on the application examples.

3.2. A novel approach to evaluate the equivalent dynamic stiffness of guy clusters in telecommunication masts under ground excitation

Authors:

S. Ali GHAFARI OSKOEI[1], Ghyslaine McCLURE[1,*]

[1] Department of Civil Engineering and Applied Mechanics, McGill University, 817 Sherbrooke St. West, Montréal, Québec, Canada, H3A 2K6.

[*] Corresponding author: Phone: +1 514 3986677, Fax: +1 514 3987361. ghyslaine.mcclure@mcgill.ca

3.2.1. Abstract

Telecommunication structures are essential components of communication and post-disaster networks and critically important facilities require reliable earthquake-resistant design procedures in seismically active regions. Calculation of the nonlinear seismic response of tall guyed masts using detailed time-step finite element methods is far more complex than linear response spectrum analysis that is routinely used in structural engineering practice. It is recognized that detailed computational procedures are not always necessary, in particular when the goal of the analysis is to provide a global earthquake-resistant design check on a regular structure with predictable response: this is when rational simplified methods are called upon to calculate the seismic demand. However, up to now, no such method exists for tall guyed masts that can account for the dynamic cable-mast interactions which dominate seismic effects in these structures. In the study reported here, the writers explore the dynamic behavior of guy cables under harmonic and seismic support ground motion through detailed computational modeling and propose a novel frequency-dependent method to evaluate the equivalent dynamic stiffness of guy clusters. This development will contribute efficiently towards a new

robust rational model of general applicability for simplified seismic analysis of tall guyed telecommunication masts.

Detailed numerical simulations involving 57 guy cables from eight existing towers with varying heights of 150 to 607 m were used in the study. A mathematical procedure was developed to replace the nonlinear time-variant cable stiffness with an equivalent linear frequency-dependent spring/mass system, based on the response spectrum of individual guy cables and the frequency content of the seismic excitation. Comparison of the main response indicators of these equivalent models and the detailed nonlinear finite element analysis results confirmed the reasonable and consistent engineering accuracy of the proposed simplified method with considerable savings in analysis effort.

Key words: Cable dynamics; Stay cables; Seismic analysis; Telecommunication towers; Guyed masts.

3.2.2. Introduction

Guyed telecommunication masts are tall structures whose function is to support elevated antennas for radio and television broadcasting, telecommunication, and two-way radio systems. This infrastructure is vital to emergency response in important disasters and its immediate serviceability or even continuous functionality is of critically high priority in the event of strong magnitude earthquakes.

It is generally recognized that, in latticed guyed telecommunication towers, wind effects and combinations of wind and atmospheric icing effects are more likely to govern the structural design (stability, strength, and serviceability) than are earthquake effects, especially in cold climates. Although we have some reports of tower failures due to extreme wind and/or ice, there are no such reports in connection with earthquakes in Canada and very few in the United States. A 1999 survey of the earthquake performance of communication towers [1] summarizes documented reports of only 16 instances of

tower damage (including damage on self-supporting lattice towers as well as masts) related to seven important earthquakes that occurred after 1950. Smith [2] also reported some damage to communication towers during the devastating August 1999 earthquake in Turkey, although details have not been published. It should be mentioned that seismic damage is not being systematically reported for these structures as such information is most often kept confidential by tower owners.

Since the late 1990s, and largely due to the publication of documented damages for the January 1995 Kobe earthquake [3], there has been an increased interest in North America in establishing earthquake-resistant design guidelines specifically for communication towers. The US Federal Emergency Management Administration has intensified the effort of its National Earthquake Hazard Reduction Program on the risk reduction for lifeline structures [4,5]. This increased awareness of seismic risk has, in turn, encouraged the Telecommunication Industries Association (TIA) to formulate mandatory seismic provisions for the first time in the 2005 edition (Revision G) of its ANSI/TIA 222 Standard [6]. In Canada, the 1994 edition of the Canadian Standards Association CSA S37 on Antennas, Towers, and Antenna-Supporting Structures [7] had already introduced an appendix devoted to seismic analysis of towers, which was expanded in the 2001 edition (*Annex M Earthquake-resistant design of towers*) and is currently under revision. It is noteworthy that no rational simplified seismic analysis procedure is available yet in these standards for tall nonlinear masts, a knowledge gap that has motivated the present work in view of the upcoming 2012 edition of the CSA S37 standard.

Dynamic analysis of tall guyed masts, like of other cable-stayed structures, is a persistent challenge for structural engineers. The generally accepted approach, although rarely applied in actual design practice, is to predict the response using nonlinear finite element analysis in the time domain. As summarized in [2,8], there is extensive literature on detailed computational modeling of tall guyed communication masts subjected to dynamic loads of various sources. Of main relevance here are the computational studies on real-scale towers subjected to turbulent wind effects [9,10,11]; sudden ice shedding or guy wire breakage [12]; and earthquakes [13,14,15,16] and more recently [17,18]. Only a

few published studies have focused on the development of simplified dynamic analysis procedures for tall masts under wind effects. Sparling and Davenport [11] proposed a static patch load method to estimate the turbulent response of telecommunication masts to gusty wind using linearized frequency-domain analysis. Taking advantage of modal decomposition introduced by Irvine [19] for taut cables, Desai and Punde [20] proposed a nine-degree-of-freedom cable model generally applicable to cable-stayed structures under wind loading. Finally, Ghodrati Amiri [16] and Meshmesha *et al.* [21] have developed empirical formulas to estimate the maximum values of selected seismic response indicators of tall masts, usually in connection with a specific earthquake design spectrum or for localized seismic data, which limits the applicability of their work whenever seismic hazard data is adjusted.

Typical guyed telecommunication masts used in North America have regular geometry and mass distribution, with heights ranging from 150 to 350 m. These structures have their lowest fundamental frequencies within the sensitive range of past earthquake records, i.e. 0.1-10 Hz with concentrated effects in the 0.3-3 Hz range for horizontal ground motion [22], and may therefore require earthquake-resistant design procedures when erected in high seismic hazard areas. Detailed finite element analyses conducted during this research have confirmed that potentially important seismic effects in guyed masts are induced by the dynamic response of guy clusters and cable-mast interactions.

Tower height (m)	No. of stay levels	No. of anchor groups	Panel width (m)	Panel height (m)	Location
607.1	9	3	3	2.25	USA, California, Sacramento
342.2	7	2	2	1.52	Canada
313.9	5	2	2.14	1.52	Canada
213.4	7	2	1.52	1.52	Canada
200	8	3	1.8	1	Argentina, Buenos Aires
198.1	6	2	2.13	1.52	Canada, Prince Edward Island
152.4	8	2	0.84	0.61	Canada, Alberta, Elk River
150	7	2	1.3	1	Canada, Alberta, Little Buffalo

Table 3.1 Geometry of Latticed Masts Analyzed

The scope of the work presented here is to propose a new approach to evaluate the linearized dynamic stiffness of guy wires which will account for these cable-mast interactions. This new procedure is a milestone contribution towards the development of a new model of general applicability for simplified seismic analysis to perform design checks on tall guyed telecommunication masts [23].

The study is based on data from eight real lattice masts: it is not possible to present all their structural details but more information can be found in [16,18] that have also used these same structures. General information on the masts is summarized in Table 3.1, and Fig. 3.1 depicts the geometric layout of a 342-m mast as a typical example. The numerical tools for the study were the commercial nonlinear finite element analysis software ADINA [24] and MATLAB [25]. Cables were modeled with elastic tension-only 3-node truss elements. Each cable element has been supplemented by a parallel longitudinal dashpot with viscous damping constant equivalent to 1.2% critical to account

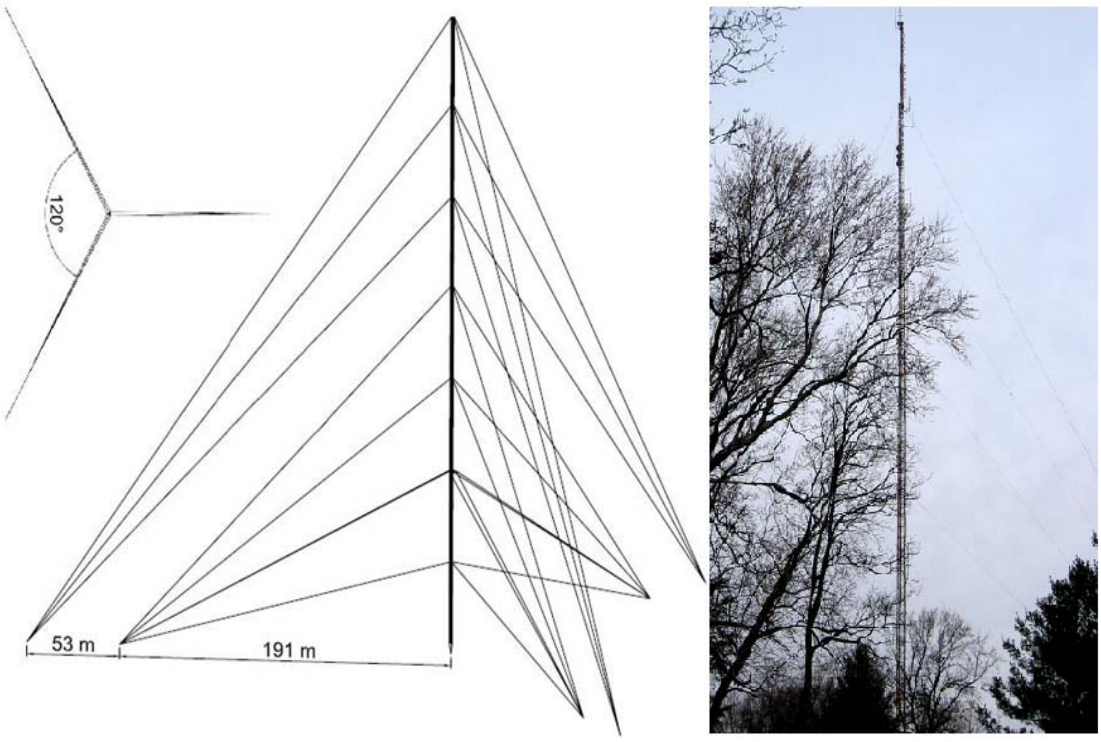

Figure 3.1 *Geometric layout and plan view of a 342-m mast*

for structural damping and the fact that aerodynamic damping is not explicitly modeled. Each cable mesh comprises 10 parabolic elements, i.e. 20 numerical integration points are provided along the cable length. The steel latticed masts have their leg members and horizontal frames idealized as frame elements and the diagonal members are truss elements. Each physical member of the mast is represented by a single two-node element between joints, and the material is Hookean. A similar damping model as for the cables is introduced.

3.2.3. Dynamic behavior of tall guyed masts

The structural behavior of tall guyed masts is complex. This complexity mainly arises from significant geometric nonlinear response of the guy cables and the interaction between the cables and the mast. The slenderness of the mast itself (beam-column effects) may also amplify the nonlinear response in sway motion. The random nature of most dynamic loads (shocks, wind and earthquake excitations) and realistic three-dimensional modeling considerations bring additional challenges. In seismic analysis in particular, the effect of the spatial variation of the excitation at multiple ground support points and the effect of the vertical component of ground motion should be considered to assure realistic and conservative simulation results [18]. In the present research, these nonlinearities were all duly considered in detailed numerical models and their relative contributions to overall nonlinear dynamic response to random loading were assessed. To determine the frequency-dependence of the effective guy wire lateral stiffness, a series of simulations involved the guy cable and mast response to harmonic sway displacement of varied amplitude and frequency, prescribed at different guying levels. The results indicated that the mast response was almost linear in terms of the amplitude of the prescribed harmonic displacements. However, the guy cluster stiffness coefficients varied significantly with high nonlinearity in terms of the forcing frequency. This investigation also highlighted the dominant contribution of the cable dynamic stiffness and indicated that other sources of nonlinearity, like mast slenderness and cable sag, were of secondary

importance. These findings prompted more numerical tests on 57 individual guy cables (all typical cables from the eight guyed masts identified in Table 3.1) for forcing motion frequencies varying between 0.1 to 3.0 Hz. This frequency range was selected to match the dominant frequency content of common earthquakes and the natural frequencies of the stay cables. The results of these numerical simulations were used to characterize the dependency of guy cable stiffness on forcing frequency.

3.2.4. Frequency-variant stiffness of guy cables

Individual inclined cable models were extracted from the complete finite element models of the guyed masts and were subjected to an in-plane harmonic horizontal displacement prescribed at their top end, as illustrated schematically in Fig. 3.2. All modeling considerations were kept exactly the same as in [18]. The only difference was to reduce viscous damping to 1% of critical to model the effects of structural damping, and to add

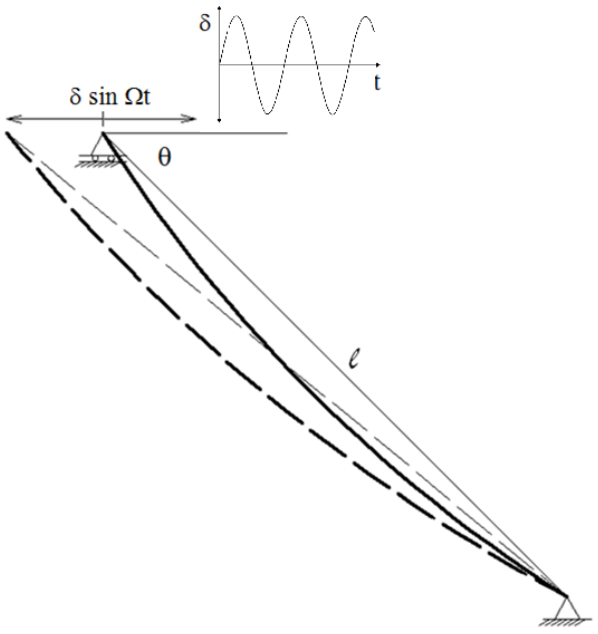

Figure 3.2 *In-plane harmonic horizontal displacement prescribed at the top end of an inclined elastic cable.*

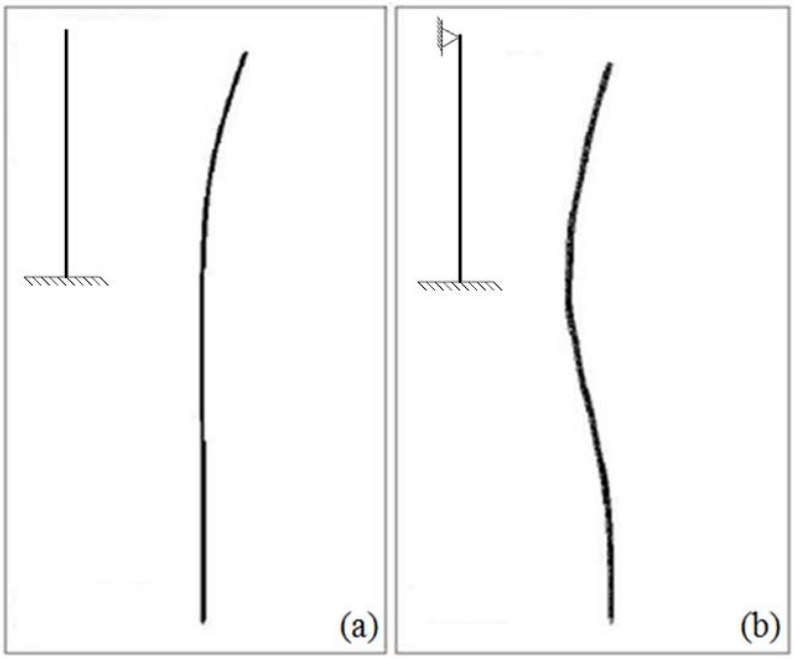

Figure 3.3 *Fundamental sway mode shapes typical of tall telecommunication masts: (a) 607-m high with 9 stay levels and (b) 213-m high with 7 stay level.*

numerical damping to assure convergence of the iterations and filter the high frequency noise induced by the finite element discretization; this was especially critical for short taut cables subjected to high frequency excitations.

The effect of the amplitude of the mast's lateral displacement at guying level, δ, on the cable dynamic stiffness has also been studied. Previous work by Ghodrati Amiri [16] indicated that there are two main forms of fundamental mode shape for tall masts: the cantilever sway mode associated with very tall masts equipped with long upper guy cables (Fig. 3.3a) and the fixed-pinned beam transverse mode (Fig. 3.3b) for shorter masts with stiff upper guy clusters. These patterns were considered when selecting the appropriate amplitude, δ, of the forced harmonic motion for the individual guy cables depending on their cluster elevation in the mast.

Figure 3.4 illustrates the typical vertical displacement response (along global z-coordinate) of two guy cables from the 213-m mast subjected to harmonic excitation. Fig.

3.4a shows a response near resonance with a clear beating pattern [26], while Fig. 3.4b shows a case far from resonance with a decay pattern after the initial transient response [27]. The time history plots start at time t = 1 sec from the static equilibrium position. Figure 3.4c is the normalized amplitude of the Discrete Fourier Transform (DFT) of the $z(t)$ response in Fig. 3.4b.

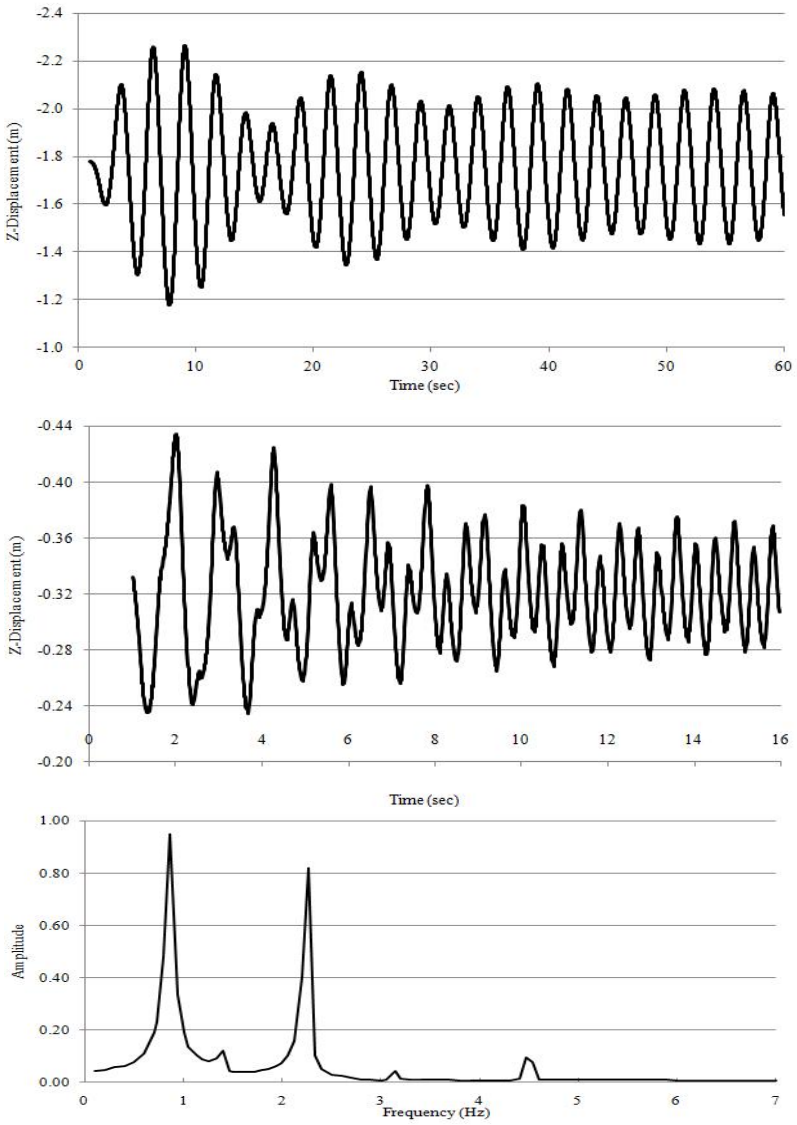

Figure 3.4 *Time history of z-displacement at midpoint of guy cable of the 213-m mast to forced harmonic horizontal displacement (a) Top cluster cable at 0.4 Hz, (b) Second cluster from base at 2.25 Hz, and (c) Normalized amplitude Fourier transform of (b)*

For all the studied cables, the frequency content graphs of the displacement response to periodic excitation clearly show the dominance of the fundamental transverse mode of the cable. For example, in Fig. 3.4c, the dominant peak response is obtained at the cable natural frequency (0.85 Hz) while the second peak corresponds to the forcing frequency. This observation was also reported in [20], and forms a valid basis for simplified models for dynamic analysis of cable-stayed structures excited in a frequency range well separated from their natural frequencies.

The secant (or total) dynamic stiffness of the cable (to be related to the forcing frequency Ω) is defined as the maximum horizontal component of the cable tension, max $H(t)$, obtained under harmonic excitation, divided by the amplitude δ of the imposed horizontal displacement at the top support (guy-mast attachment point), as shown on Fig 3.2. In order to facilitate highlighting cable dynamic effects in this study, the writers define the Guy stiffness Dynamic Amplification Factor ($GDAF$) as the ratio of the secant dynamic stiffness and its corresponding static value. The equivalent static stiffness of a guy cable is defined by the change in cable tension corresponding to a change in chord length. In [28], the writers proposed Equation (1) to calculate the static sag d measured perpendicular to the chord at mid length. The expression appears cumbersome but it was obtained directly, with symbolic mathematical manipulations, from the exact solution of the cubic static equilibrium equation of a linear elastic cable with parabolic profile. Equation (1) is very useful because it provides the explicit form of the static sag d in terms of the guy cable geometry, pretension force and axial rigidity.

$$d = -0.8736\, B' D'^{\,-1/3} + 0.3816\, A'^{\,-1}\, D'^{\,1/3} \tag{1}$$

where the coefficients are

$$A' = \frac{64}{3}\frac{EA}{l^2} \tag{2a}$$

$$B' = 8F_i \tag{2b}$$

$$C' = -\,m\,(g\ \cos\theta)\,l^2 \tag{2c}$$

$$D' = -9\,A'^2\,C' + 1.7321\,\sqrt{A'^3(4\,B'^3 + 27\,A'\,C'^2)} \tag{2d}$$

$$H = \frac{m\,(g\ \cos\theta)\,l^2}{8\,d} \tag{3}$$

In these equations, EA is the axial stiffness of the cable, l is the chord length, F_i is the initial pretension force, m is the mass per unit length (mg is the weight) and θ is the inclination angle of the chord in the initial configuration. All the variables used in these equations have compatible SI units. Equations (1) and (3) can be used simultaneously to calculate the static cable sag and the corresponding cable tension and hence determine the static horizontal stiffness of the guy cable. Let H_1 the horizontal tension associated with initial sag d_1. A new value of static tension H_2 (associated with sag d_2) can be calculated for a displaced cable configuration defined as $l_2 = l_1 + \Delta l$ and the equivalent static stiffness is $(H_2 - H_1)/\Delta l$.

Except when the excitation corresponds to a resonant sway frequency of the mast, the maximum cable response typically occurs during the initial transient phase comprising the first few cycles of oscillations, as illustrated in the time history plots of Fig. 3.4. Considering the relatively short duration of strong shaking during earthquakes, usually less than one minute, these initial transient maximum values would likely dominate the seismic response of the structure, and they are deemed an appropriate and conservative representation of the maximum dynamic effects in the guy cables.

3.2.5. GDAF spectra

Figure 3.5 presents two typical examples of graphs showing the variation of GDAF versus the forcing frequency of the harmonic sway motion (GDAF response spectrum), for two different guy cables of the study. These graphs were constructed from the results

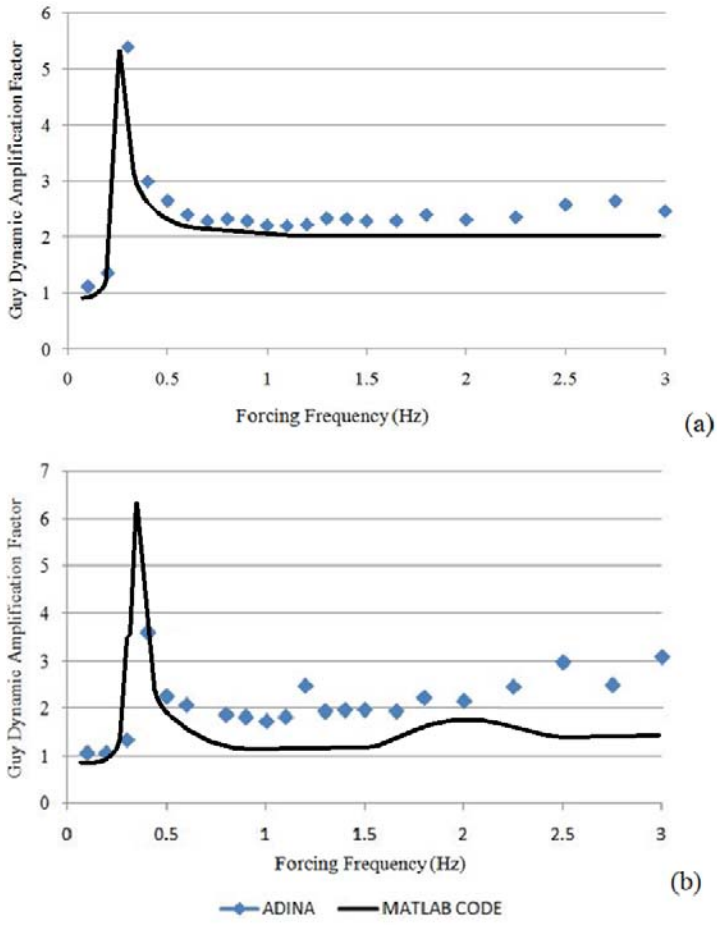

Figure 3.5 *Cable GDAF vs. forcing frequency of harmonic horizontal displacement (a) $\delta = 0.30\ m$ at top end of a 377-m cable (2nd cluster from top) in the 342-m mast, (b) $\delta = 0.20\ m$ at top end of a 233-m cable (top cluster) in the 198-m mast.*

obtained by detailed nonlinear finite element analysis models in ADINA, as represented by each discrete data point. The continuous lines shown in Fig. 3.5 were obtained with a MATLAB predictive model that will be introduced later.

In general, each graph consists of three distinct parts defined according to the forcing frequency range. The first segment with a GDAF close to unity is observed for forcing frequencies lower than the first transverse in-plane natural frequency of the guy cable, indicating negligible dynamic effects. The second part is the resonance peak occurring at the cable lowest transverse mode frequency. Finally, the third portion of the graph at the

right of the resonance peak represents the dynamic effects due to wave propagation and reflection in the guy cable, with GDAF values typically varying between 1.5 and 2.5.

Equation (4) was developed in [28] to predict the fundamental in-plane transverse mode frequency of the taut parabolic linear elastic cable:

$$f = \frac{1}{2\pi}\sqrt{\left(\frac{16\,F_i}{3l} + \frac{128EA}{3l^3}\left(\Delta_s^2 + \Delta_s\bar{x} + \frac{\bar{x}^2}{3}\right)\right)/M} \qquad (4)$$

where Δ_s is the static cable sag at rest (reference configuration) and $\bar{x}$ is the static sag obtained after enforcing a horizontal cable end displacement equal to the amplitude δ of the forced harmonic motion. $\bar{x}$ can be evaluated directly using Equation (1). M is taken as $2/3$ of the total mass of the cable and represents the equivalent lumped reactive mass of the guy cable at mid length.

A complex vibration phenomenon which was observed in some GDAF spectra is related to fundamental frequency mode transfers, a cable dynamics phenomenon that was first studied in [29]. When a cable with fundamental transverse frequency f_1 is excited at multiple frequencies $2f_1$, $3f_1$, etc., it progressively develops oscillations according to its fundamental mode shape. This vibrational mode transfer can cause large oscillations as local resonances are developing at multiple frequencies, and local peaks will appear on the GDAF spectrum. This is illustrated in Fig. 3.6a showing the time history sag response of a cable of the 4th cluster from the base of the 213-m mast subjected to harmonic end motion at 0.80 Hz ($2f_1$). It is seen that the displacement amplitude is growing due to progressive mode transfer, and the steady-state is reached after approximately 8 sec of sustained excitation. The corresponding frequency content (Normalized DFT amplitude spectrum) is shown in Fig. 3.6b where the largest peak corresponds to the fundamental transverse frequency of the cable at 0.39 Hz.

However, in most of the studied cases, it takes a considerable amount of time (in the order of 10 sec) for the sustained harmonic excitation to cause such mode transfer to build up. It is therefore reasonable to consider that these phenomena will not likely occur in guy cables during an earthquake since the strong shaking episodes are of short duration and do not contain a pure sustained harmonic (random rather than tonal).

The geometrically nonlinear behavior of guy cables highlights the importance of studying the effect of the amplitude of the forced harmonic motion on the GDAF spectrum. In this part of the study, the horizontal displacement amplitudes (δ values) were selected based on the maximum probable sway displacement response of the masts

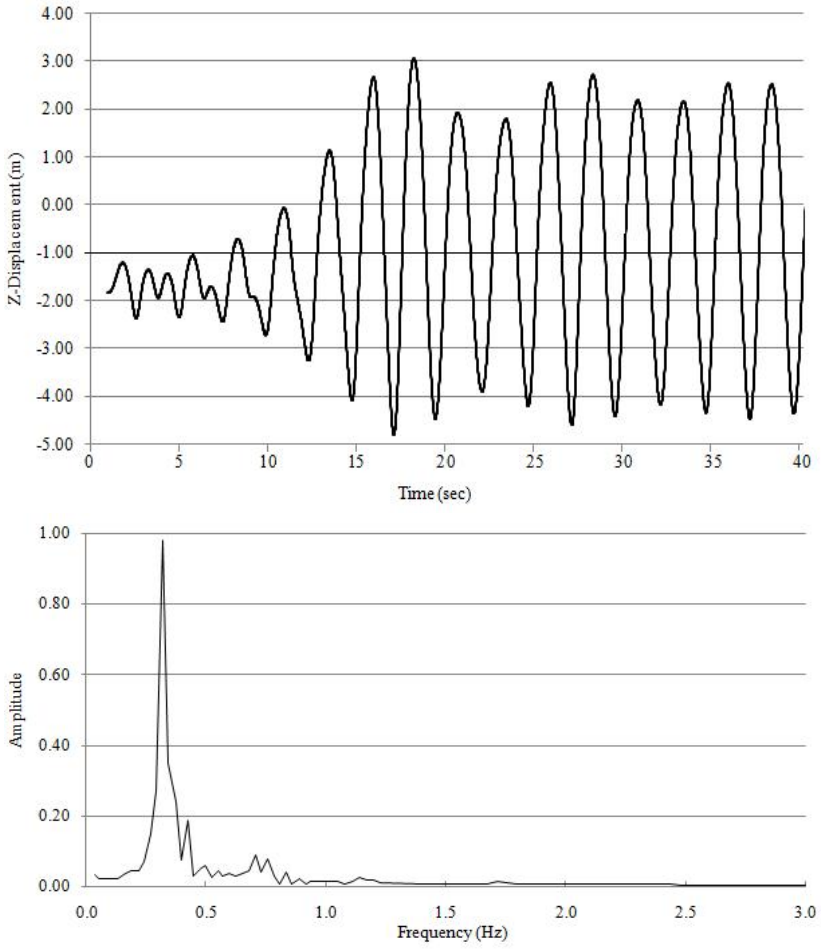

Figure 3.6 *Cable GDAF versus. forcing frequency of harmonic horizontal displacement (a) 0.30 m at top end of a 377-m cable (2nd cluster from top) in the 342-m mast, (b) 0.20 m at top end of a 233-m cable (top cluster) in the 198-m mast*

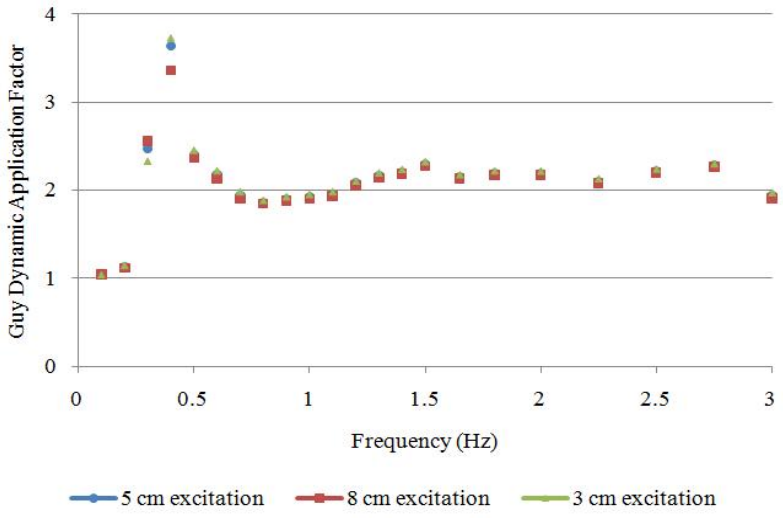

Figure 3.7 *Cable GDAF versus forcing frequency of harmonic excitation with amplitude of 3, 5 and 8 cm for the top cluster cable of the 213-m mast*

at cluster attachment levels, under selected earthquakes. Further, a variability of approximately $\pm 50\%$ was considered on these amplitudes and the corresponding stiffness values were compared to assess the consistency of any trend in the results. Not surprisingly, the results indicated low sensitivity of the GDAF spectra to the amplitude of the excitation outside resonance because the guy cables remained taut and mainly responded by elastic deformation rather than by changing their profile. This is illustrated in Fig. 3.7 showing an example of GDAF spectra with horizontal motion amplitudes δ of 3, 5 and 8 cm for the top cluster cable of the 213-m mast. At resonance, however, GDAF values clearly depend on the amplitude of the motion, and smaller motion tends to trigger higher GDAF values.

3.2.6. Predictive model for GDAF spectra

Only a few typical GDAF response spectra of guy cables under harmonic horizontal excitations have been illustrated in Fig. 3.5 and Fig. 3.7. Constructing these diagrams from detailed nonlinear finite element simulations is a tedious task and the writers have proposed in [28] a simplified mathematical algorithm (implemented in MATLAB) which approximates the maximum dynamic response of stay cables under harmonic excitation using a single degree-of-freedom model to construct GDAF spectra such as the example shown in solid line on Fig 3.5. This analytical model considers the nonlinear equation of motion of a guy cable under harmonic excitation assuming a single-loop sinusoidal shape function (fundamental symmetric mode). The dynamic response of the equivalent SDOF system was expanded around the static nonlinear equilibrium position resulting from self weight, initial strains, and imposed support translation. This response was linearized using a perturbation method and an iterative averaging scheme.

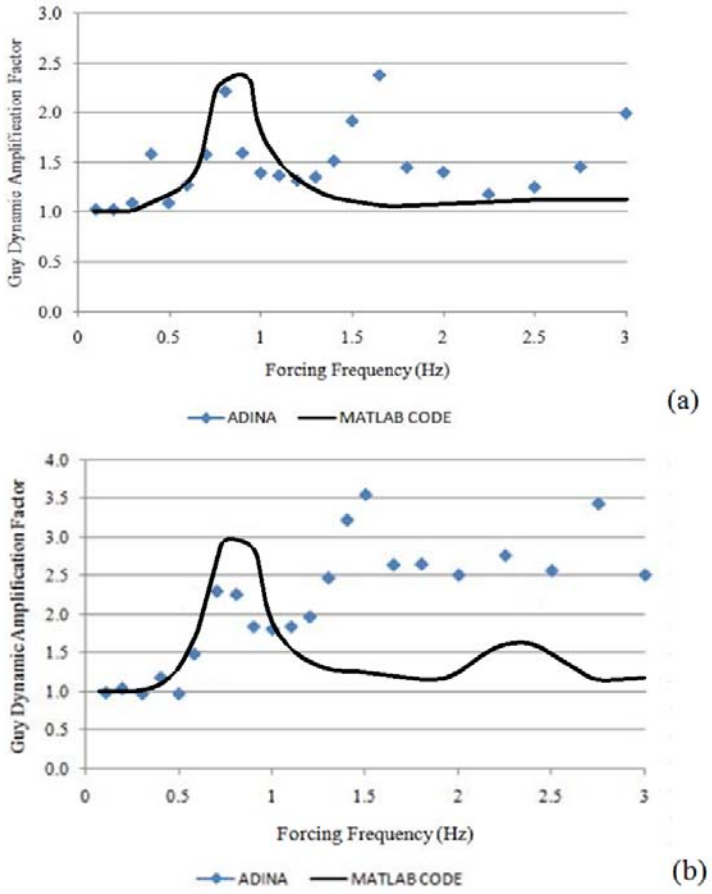

Figure 3.8 *GDAF spectra $\delta = 0.016\ m$: (a) 2nd cable from the base of 198-m mast ($f_1 = 0.70\ Hz$ and $l = 102\ m$); (b) 3rd cable from the base of 152-m mast ($f_1 = 0.60\ Hz$ and $l = 106\ m$).*

The lower clusters of guyed masts comprise short and taut cables characterised by higher natural frequencies than that of longer cables used in the upper clusters. The response of short guy cables to support excitation typically involves a large number of harmonics and is difficult to represent using a simplified nonlinear SDOF model. The approximate model implemented in MATLAB code was developed to represent the response of the longer guy cables that would strongly interact with the mast if large sway motions are induced. The optimum accuracy is for cable lengths in the range of 150 to 500 m, providing lateral support to guyed telecommunication masts in the height range of 150 to 350 m. Therefore some important differences are expected between the detailed nonlinear

dynamic calculations obtained with ADINA and the simplified nonlinear SDOF model results from the MATLAB code: such differences are illustrated in Fig. 3.8 for relatively short cables.

Based on the analysis of all the simulation results generated in the study, it was possible to identify a general trend in the GDAF spectra, represented in Fig. 3.9 by an idealized GDAF response spectrum plot divided in three portions: the static response range, the resonant range with very large response, and the dynamic response range.

The static branch covers forcing frequencies lower than the fundamental transverse in-plane natural frequency of the cable, f_1, and is associated with GDAF = 1. The resonance portion is determined by three important parameters: the value of f_1, the resonance bandwidth and the maximum value of GDAF . As mentioned earlier, Equation (4) can provide a reasonably accurate estimate of f_1. Using the analogy with the classical linear viscously damped SDOF at resonance, the maximum dynamic amplification factor of $1/2\xi$ is assumed to apply also to the linearized response of the equivalent SDOF derived in [18] for the guy cable. Recalling that the GDAF is defined as the maximum force $H(t)$

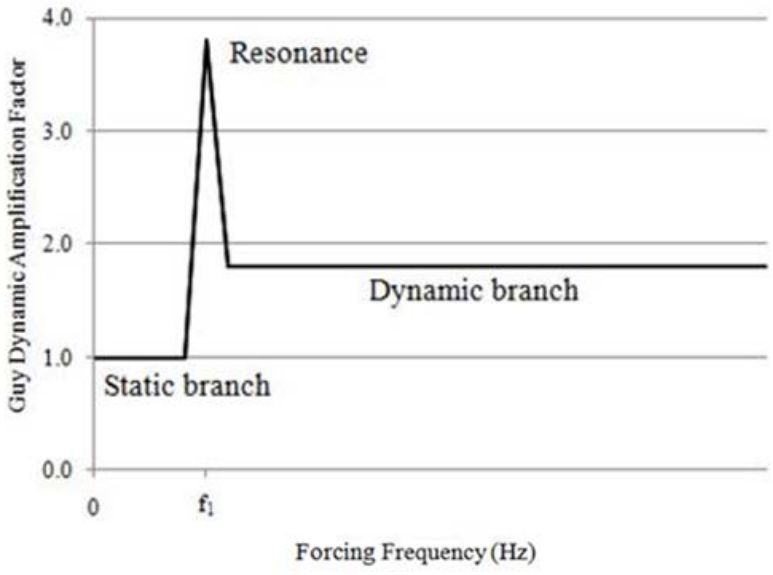

Figure 3.9 *Idealized GDAF response spectrum of long stay cables subjected to harmonic sway motion at mast attachment point.*

developed in the guy cable divided by the forced motion amplitude, δ, while the static stiffness value used as reference is also derived for a displaced configuration of δ, then the peak value of GDAF at resonance can be taken as $1/2\xi$ where ξ is the equivalent viscous damping ratio of the guy cable. However, this simplification proves overly conservative in the light of the detailed simulation results. Seismic guy displacements are typically resulting from the lower frequency sway modes of the mast, characterized by large vibrations of the guys of the upper clusters, combined to the ground motion directly induced at the anchor points. Such large motion can generate aerodynamic damping in the order of 6-7% critical, which adds up to the effects of internal structural damping of about 1% critical [8]. In this study a constant value of 5% of critical viscous damping is used for all cables. The half-power bandwidth can be approximated by $0.10\, f_1$, which corresponds to the half power bandwidth $(2\xi f_1)$ of a linear SDOF system with 5% of critical viscous

The dynamic branch of the spectrum is mainly related to the higher dynamic stiffness of the guy cables. Maximum values of GDAF for this part were found to vary from 1.2 to 3.0. In an attempt to find a simple, yet rational estimate for the GDAF in the dynamic branch, the correlation between the GDAF values and the cable parameter λ^2 introduced by Irvine [19] was examined. λ^2 is an indicator of the relative tautness of a suspended elastic cable, relating its elastic stiffness to its geometric or gravitational stiffness. Cables with parameter λ^2 of the order of 20 or less have a dynamic behavior similar to that of taut strings as most of their variations in chord length results from elastic effects. For relatively taut cables with d/l inferior to $1/8$, the expression is:

$$\lambda^2 = \left(\frac{mg\, l\, \cos\theta}{\bar{T}}\right)^2 \frac{\left(\frac{EAL}{\bar{T}}\right)}{l\left(1+8\left(\frac{d}{l}\right)^2\right)} \tag{5}$$

where $\bar{T}$ is the average cable tension. The linear regression of Equation (6) was established from the results of approximately 600 numerical simulations carried out for

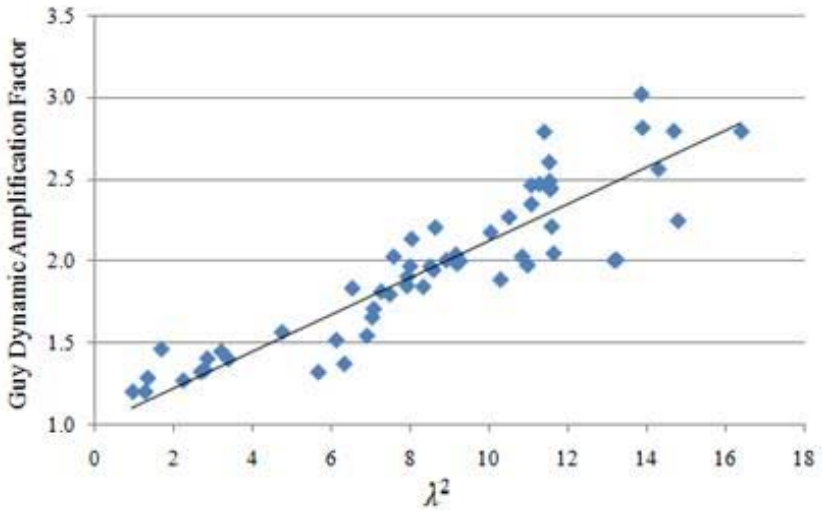

Figure 3.10 *Guy Dynamic Amplification Factor vs.* λ^2.

all the studied towers. The corresponding graph is shown in Fig. 3.10 where each data point is an arithmetical average over the results on the individual dynamic branches.

$$GDAF = 0.113\,\lambda^2 + 1 \tag{6}$$

The value of the coefficient of correlation R-square associated with the fitted line in Fig. 3.10 is equal to 0.805. However, the investigation of the data points indicated that Equation (6) is more reliable when applied to top cluster cables of masts in the height range of 200 m to 350 m. The 200-m mast is the exception with guy cables installed at very low initial pre-tension compared to the other mast designs used in the study. Another valid alternative to using Equation (6) is to calculate the GDAF value of the dynamic branch based on the average of three (or more) GDAF values associated with post-resonance frequencies obtained from separate simulations.

Figure 3.11 illustrates a sample cable response spectrum developed by means of the proposed approach with Equation (6), for the 2nd cable from the base of the 150-m tower, with $\lambda^2 = 1.47$ and modal viscous damping of 5% critical. On this figure, the idealized

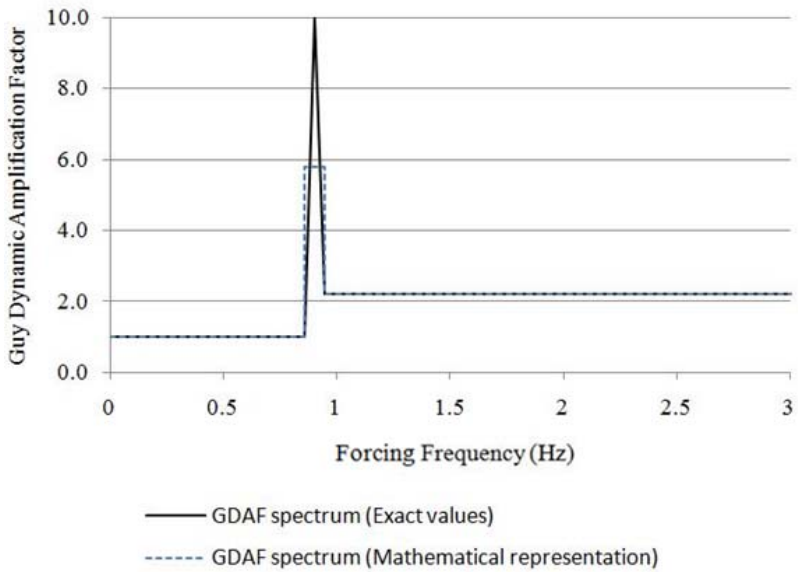

Figure 3.11 *Proposed GDAF spectrum for the 2nd cable from the base of the150-m mast ($f_1 = 0.91\ Hz$ and $l = 73\ m$).*

resonant peak (with GDAF = 10) is replaced with the narrow rectangular peak of width $0.10f_1$ (in dashed line) of equivalent energy content.

3.2.6. Equivalent dynamic cable stiffness under seismic loading

With a view to develop a rational simplified seismic analysis method for tall guyed masts, a novel concept of equivalent dynamic cable stiffness is proposed to determine the response of individual guy cables to harmonic end motion in their post-resonance range, using the GDAF values estimated with Equation (6). A detailed numerical study involving three series of seismic analyses was conducted on the guy cables of the data base to validate the proposed equivalent dynamic stiffness model. In this study, three classical earthquake records (Table 3.2) representing a variety of frequency contents and strong motion durations have been considered for the purpose of developing the maximum values of the cable dynamic response listed in Table 3.3. Strong motion data have been taken from [30]. This selection was made to allow for comparison of the

results with those of previous studies [16,18]. These signatures are deemed appropriate to represent the essential characteristics of probable seismic input excitations and should suffice at this stage to validate the proposed approach.

Using the power spectrum of a selected earthquake ($S_{excitation}$) and the GDAF response spectrum (S_{GDAF}) generated for a specific guy cable subjected to harmonic support motion, the writers propose Equation (7) to estimate a single value of the maximum dynamic amplification of the cable response, DAF_{EQ}, for this selected earthquake.

$$DAF_{EQ} = \frac{\int S_{GDAF}(f) S_{excitation}(f) df}{\int S_{excitation}(f) df} \tag{7}$$

Equation (7) is a weighted average over a reasonable range of frequencies and requires caution in the selection of the integration boundaries. Madugula Ed. [8] suggested that a frequency range of 0.3 to 3 Hz matched the dominant frequency content of most horizontal earthquake ground motions observed. In this study the upper cut-off frequency of 10 Hz was used instead.

Table 3.3 summarizes the results obtained for nine of the 57 guy cables studied, which are representative of the complete set. The entries of the table are the individual seismic DAF values, DAF_{EQ}, obtained for the three seismic records and using the following three analysis methods: detailed nonlinear finite element analysis using ADINA, the equivalent nonlinear SDOF analysis approach implemented in MATLAB code and the GDAF response spectrum approach.

Earthquake	Magnitude (M)	Station	Site condition (USGS)
Imperial Valley (El Centro)	7.00	117 El Centro Array #9	(C)
Kern County (Taft)	7.40	1095 Taft Lincoln School	(B)
Parkfield	6.10	1014.00 Cholame #5	(C)

Table 3.2 Selected Classical Earthquake Records

TOWER		607 m	607 m	313 m	213 m	200 m	198 m	152 m	150 m	150 m
GUY CLUSTER NUM FROM BASE		9th	3rd	2nd	1st	6th	2nd	4th	5th	7th
	ELC	2.9213	1.8280	2.3052	1.3710	2.8508	1.4877	1.9115	1.9672	1.7346
ADINA	PARKF	2.9380	1.9617	2.2690	1.3324	2.5155	1.3449	1.7385	1.8159	1.6495
SIMULATIONS	TAF	2.9452	1.8758	2.1822	1.3283	2.6577	1.3851	1.8549	1.9196	1.6992
	ELC	2.8144	1.6603	1.9976	1.1651	2.0826	1.1972	1.3613	1.4082	1.6103
SDOF SYSTEM	PARKF	3.1189	1.7450	1.5795	1.1490	1.9929	1.1856	1.3501	1.4091	1.6718
RESULTS	TAF	2.9470	1.6638	1.8162	1.1181	2.0193	1.2433	1.3714	1.3950	1.5958
	ELC	2.6573	1.7988	1.9634	1.2800	2.5933	1.4228	1.8508	1.7897	1.6396
SIMPLIFIED	PARKF	2.6541	1.7997	1.9586	1.2546	2.5899	1.3882	1.8416	1.7925	1.6581
RESPONSE SPEC	TAF	2.6539	1.7989	1.9607	1.2572	2.5614	1.4056	1.8851	1.7263	1.6114

Table 3.3 Seismic Dynamic Amplification Factors for Selected Cables

A first general observation is that all the cables appear to respond in their post-resonance range with DAF_{EQ} values in the range of 1.1 to 3.1. The results obtained for individual cables are very similar for the three ground motion records considered, which confirms that no significant local resonance was triggered. Using the detailed finite element simulation results as a reference, it is seen that the results obtained from the simplified procedures are reasonably accurate. A global comparison of all database results indicates that the single loop nonlinear SDOF model results are generally 16% less than those of the detailed ADINA simulations and the simplified GDAF response spectrum results are 10% less. The good accuracy of the response spectrum method is very interesting for practical design checks because of its simplicity. Also, the ADINA results are expected to yield higher seismic displacement response values than those obtained from the simplified models since the latter represent filtered responses. This filtering is a clear

advantage over the detailed nonlinear dynamic simulations that may bring numerical difficulties associated with spurious high frequencies. Real seismic cable response is also expected to be lower than predicted by ADINA finite element models due to several simplifications about aerodynamic damping and other energy dissipation mechanisms at the cable ends, as well as spurious high frequency noise inherent to finite element discretization.

3.2.7. Validation of the simplified response spectrum method

A more detailed validation of the accuracy of the proposed DAF_{EQ} response spectrum method (RS) is presented, which includes all the simulations carried out with all the studied cables. A secondary concern was to verify whether gravity effects played any significant role in the dynamic response of an inclined guy cable and whether differences in maximum cable response were obtained when the cable excitation was assumed at the top or bottom end attachment point. Irvine [19] stated that the cable inclination has only small influence on the cable dynamic properties: this was verified for a few cases with detailed nonlinear finite element analysis and no noticeable differences in the results were obtained for the prescribed motion at either end.

In the proposed RS procedure, the value of DAF_{EQ} obtained in Equation (7) is used to calculate the dynamic cable stiffness at maximum amplitude, K_{dyn}, and the corresponding dynamic cable tension, F_{dyn}:

$$K_{dyn} = DAF_{EQ} * K_{st} \tag{8}$$

where it is recalled that the static guy cable stiffness K_{st} is determined in the displaced cable configuration at maximum amplitude of the top end motion. The dynamic cable tension is therefore determined in that configuration by:

$$F_{dyn} = K_{dyn} * d_{max} \tag{9}$$

where d_{max} is the maximum horizontal displacement induced at the cable top endpoint (attachment point to the mast). The total cable tension is simply

$$F_{tot} = F_{dyn} + F_i \quad (10)$$

where F_i is the initial static cable tension.

Table 3.4 presents selected results from the ADINA simulations and simplified RS calculations for three guyed masts. Globally, these results confirm that the proposed RS procedure is conservative and reasonably accurate at predicting cable tensions in the top clusters with differences below 10% between the simplified RS procedure and detailed seismic analyses when the total cable tensions are compared. It is seen that the dynamic component of the cable tension, F_{dyn}, is systematically overestimated by the RS method with very large differences (up to 100%) for some of the lower clusters. These differences stem from the simplifying assumptions made in deriving the GDAF spectra and the fact that absolute maximum values of the response are used in the proposed RS method. Although the earthquake response spectra of the selected signatures confirm the contribution of a wide range of frequencies, a sustained tonal input is necessary for the cables to fully develop their maximum response. This was observed earlier when discussing cable response to harmonic excitation. Experience with detailed finite element simulations of the seismic response of tall masts has shown that the maximum response usually develops about one fundamental tower period after the peak strong motion [18]. Another important consideration relates to cable-mast interactions which are expected to increase the internal forces in the guy cables and in the masts. The writers have investigated these relevant aspects in another stage of their research targeting the development of a robust rational simplified procedure for seismic analysis of tall guyed telecommunication masts [23].

3.2.8. Conclusions

In this study, a novel frequency domain algorithm was presented to calculate the dynamic amplification of the response of inclined guy cables when subjected to seismically-induced horizontal displacements at their top attachment point to a mast structure. In this work, the dynamic mast-cable interactions are not yet considered. A mathematical procedure was developed to replace the nonlinear time-variant guy cable stiffness with an equivalent linear frequency-dependent spring/mass system, based on the GDAF response spectrum of individual guy cables subjected to harmonic top end motion and specific earthquake response or design spectra. Comparison of the total cable response predicted with the proposed models and the detailed finite element analysis results confirmed that the proposed approach is generally conservative and reasonably accurate for the purpose of rapid engineering design checks for guy cables with lengths in the range of 150-500 m (providing lateral support to guyed telecommunication masts in the height range of 150 to 350 m). The proposed spectral approach can be easily implemented in a MATLAB code [23], and is far less demanding than full nonlinear dynamic analysis. The writers believe that this approach could be extended to other applications involving weakly nonlinear structures such as guyed masts, cable roof networks and cable stayed bridges subjected to earthquakes and dynamic wind effects. However, the derivation assumptions would need to be carefully examined in terms of the amplitude and frequency of the guy attachment motion and the guy cable properties. The proposed model considered harmonic excitation of maximum amplitude in the range of 25 cm and frequency of 0.1 to 5 Hz, and moderately taut guy cables with λ^2 (defined in [19]) in the range of 2 to 12.

The equivalent dynamic guy stiffness model developed in this study will contribute efficiently towards the development of a new robust rational model of general applicability for seismic design of tall guyed telecommunication masts.

3.2.9. Acknowledgments

This work was funded in part by the Natural Sciences and Engineering Research Council (NSERC) of Canada under the Discovery Grant program and by the telecommunication industry sponsors of the 23rd meeting of the International Association for Shell and Spatial Structures Working Group 4 on Masts and Towers (IASS WG4), held in Montréal, Canada on 9-13 September 2007. The technical committee members of CSA S37 have also contributed detailed data for several of the telecommunication masts of the study.

Abbreviations and symbols

d: Static sag of the guy cable, in m

DAF_{EQ}: Equivalent Dynamic Amplification Factor of guy cable under specific seismic input

EA : Axial rigidity of the guy cable, in N

f: Frequency in Hz (generic)

f_i: The ith frequency of the structure/cable, in Hz

F_{dyn}: Dynamic cable tension force at maximum amplitude, in N

F_i: Initial cable pretension force, in N

$GDAF$: Guy stiffness Dynamic Amplification Factor, as the ratio of the secant dynamic stiffness and its corresponding static value, when subjected to a forced harmonic support motion $\delta \, sin \, \Omega t$

H: Horizontal cable tension, in N

K_{dyn} : Dynamic cable stiffness at maximum amplitude δ, in N/m

l: Cable chord length, in m

m: Cable mass per unit length (mg is the weight per unit length)

M: Equivalent lumped mass of the SDOF model at mid length, taken as 2/3 of the total cable mass, in kg

$S_{excitation}$: Power spectrum of a selected earthquake

$\bar{T}$: Average cable tension used in Equation (5), in m

$\bar{x}$: Static cable sag obtained after enforcing a horizontal cable end displacement equal to the amplitude δ of the forced harmonic motion, in m

δ: Lateral displacement of the mast at guying level, in m

Δ_s: is the static cable sag at rest (reference configuration), in m

λ^2: Cable parameter defined in Equation 5

θ: Chord inclination angle in the initial guy cable configuration

ξ: is the equivalent viscous damping ratio of the guy cable

Ω: forcing frequency of harmonic motion, in rad/s

Cable Cluster Num	Initial Pretension	Total Cable Tension F_{max} (KN)			Dynamic Cable Tension (KN)	
(from the base)	Fi (KN)	ADINA results	Response Spec	Difference	ADINA results	Response Spec
9	248,400	267,900	272,500	1.7%	19,500	24,100
8	418,500	452,900	464,200	2.4%	34,400	45,700
7	217,600	237,500	245,300	3.2%	19,900	27,700
6	300,900	338,300	354,900	4.7%	37,400	53,900
5	214,900	248,300	262,800	5.5%	33,400	47,900
4	176,900	211,800	226,900	6.7%	34,900	50,000
3	171,800	229,500	267,000	14.0%	57,700	95,200
2	165,300	266,700	343,200	22.3%	101,400	177,900
1	111,300	200,700	272,600	26.4%	89,400	161,300

Cable Cluster Num	Initial Pretension	Total Cable Tension F_{max} (KN)			Dynamic Cable Tension (KN)	
(from the base)	Fi (KN)	ADINA results	Response Spec	Difference	ADINA results	Response Spec
7	79,700	85,200	85,500	0.3%	5,500	5,800
6	87,700	94,400	96,400	2.1%	6,700	8,700
5	79,900	89,300	89,400	0.1%	9,400	9,500
4	62,000	73,900	73,200	0.9%	11,900	11,200
3	47,900	60,100	60,200	0.1%	12,200	12,300
2	32,400	44,300	43,400	1.9%	11,900	11,000
1	44,200	60,700	61,600	1.4%	16,500	17,300

Cable Cluster Num	Initial Pretension	Total Cable Tension F_{max} (KN)			Dynamic Cable Tension (KN)	
(from the base)	Fi (KN)	ADINA results	Response Spec	Difference	ADINA results	Response Spec
7	49,800	55,800	57,700	3.4%	6,000	8,000
6	40,700	47,800	48,400	1.2%	7,100	7,700
5	32,300	37,500	39,600	5.3%	5,200	7,300
4	29,300	36,700	44,000	16.6%	7,400	14,700
3	24,800	34,000	48,700	30.1%	9,200	23,900
2	23,600	38,600	57,300	32.7%	15,000	33,700
1	25,400	49,700	78,600	36.7%	24,400	53,200

Table 3.4 *(a) Cable Tensions in the 607-m Mast under IMPVALL/I-ELC Ground Motion, (b) Cable Tensions in the 342-m Mast under PARKF Ground Motion, (c) Cable Tensions in the 213-m Mast under KERN/TAF Ground Motion*

References

[1] McClure G. Earthquake-resistant design of towers. Meeting of International Association for Shell and Spatial Structures, Working Group 4: Towers and masts (IASS-WG4). Krakow, Poland, 12-16 September 1999.
[2] Smith BW. Communication structures. London: Thomas Telford; 2007.

[3] American Society of Civil Engineers. Hyogoken-Nanbu (Kobe) earthquake of January 17, 1995, lifeline performance. In: Technical Council on Lifeline Earthquake Engineering (TCLEE). Schiff AJ, Editor. Reston, Virginia. ASCE/TCLEE Monograph No. 14; 1998.

[4] Federal Emergency Management Administration. Recommended provisions for seismic regulations for new buildings and other structures. In: Building Seismic Safety Council, NEHRP. Part 1: Provisions (FEMA 302) and Part 2: Commentary (FEMA 303); 1998.

[5] Federal Emergency Management Administration. Telecommunication towers. In: NEHRP TS13 proposal 13-4, Section A14.5; 2000.

[6] American National Standards Institute. Structural Standard for Antenna Supporting Structures and Antennas. In: Telecommunication Industries Association, ANSI/TIA 222-G; 2005.

[7] Canadian Standards Association. Antennas, Towers, and Antenna-Supporting Structures, Annex M: Earthquake-Resistant Design of Towers. CSA Standard S37-01, pp. 106-113; 2001, R2006.

[8] Madugula MKS (Editor). Dynamic response of lattice towers and guyed masts. In: American Society of Civil Engineers Task Committee on the Dynamic Response of Lattice Towers. Reston, Virginia: ASCE Press; 2002.

[9] Iannuzzi A, Spinelli P. Response of a guyed mast to real and simulated wind. Journal of the International Association for Shell and Spatial Structures. 1989;30-1:38-45.

[10] Peil U, Nolle H, Wang ZH. Dynamic behaviour of guys under turbulent wind load. Journal of Wind Engineering and Industrial Aerodynamics. 1996;65:43-54.

[11] Sparling BF, Davenport AG. Three-dimensional dynamic response of guyed towers to wind turbulence. Canadian Journal of Civil Engineering. 1998;25:512-25.

[12] McClure G, Lin N. Transient response of guyed telecommunication towers subjected to cable ice-shedding. Atlanta, GA, USA: Proceedings of the IASS-ASCE International Symposium 1994, Publ by ASCE; 24-28 April 1994. p. 801-9.

[13] Guevara E, McClure G. Nonlinear seismic response of antenna-supporting structures. Computers and Structures. 1993;47:711-24.

[14] Kahla NB. Dynamic analysis of guyed towers. Engineering Structures. 1994;16:293-301.

[15] Moossavi Nejad SE. Dynamic response of guyed masts to strong motion earthquake. In: Proceedings of the 11th world conference on earthquake engineering, Paper No. 289. 1996.

[16] Ghodrati Amiri G. Seismic sensitivity indicators for tall guyed telecommunication towers. Computers and Structures. 2002;80:349-64.

[17] Hensley GM, Plaut RH. Three-dimensional analysis of the seismic response of guyed masts. Engineering Structures. 2007;29:2254-61.

[18] Faridafshin F, McClure G. Seismic response of tall guyed masts to asynchronous multiple-support and vertical ground motions. Journal of Structural Engineering. 2008;134:1374-82.

[19] Irvine HM. Cable structures. Cambridge, Mass.: MIT Press; 1981.

[20] Desai YM, Punde S. Simple model for dynamic analysis of cable supported structures. Engineering Structures. 2001;23:271-9.

[21] Meshmesha H, Sennah K, Kennedy JB. Simple method for static and dynamic analyses of guyed towers. Structural Engineering and Mechanics. 2006;23:635-49.

[22] Chopra AK. Dynamics of structures : theory and applications to earthquake engineering. Englewood Cliffs, N.J.: Prentice Hall; 1995.

[23] Ghafari Oskoei SA. Earthquake-resistant design procedures for tall guyed telecommunication towers. PhD thesis. Department of Civil Engineering and Applied Mechanics, McGill University; Canada: 2010.

[24] ADINA R&D, Inc. Theory and Modeling Guide, vol. I: ADINA. Watertown, Ma: Rep. ARD 04-7; 2004.

[25] MathWorks, Inc. MATLAB User's Guide, Natick, Ma: MathWorks; 2006.

[26] Georgakis CT, Taylor CA. Nonlinear dynamics of cable stays. Part 1: sinusoidal cable support excitation. Journal of Sound and Vibration. 2005;281:537-64.

[27] Xu X, He Z, Zhi-cheng Z. Nonlinear dynamic response of stay cables under axial harmonic excitation. Journal of Zhejiang University Science A. 2008;9:1193-200.

[28] Ghafari Oskoei SA, McClure G. Simplified dynamic analysis methods for guyed telecommunication masts under seismic excitation. Austin, TX, United states: ASCE SEI Structures Congress 2009, American Society of Civil Engineers; 30 April – 2 May 2009. p. 1020-9.

[29] Lilien JL, Pinto Da Costa A. Vibration amplitudes caused by parametric excitation of cable stayed structures. Journal of Sound and Vibration. 1994;174:69-90.

[30] Pacific Earthquake Engineering Research Center (PEER). PEER strong motion database. Berkeley, Calif.: http://peer.berkeley.edu/smcat/index.html (Sept. 10 2005).

4. Cable mast interaction models and seismic analysis of guyed telecommunication masts

4.1. Introduction

The geometric nonlinear response of the guy cables arranged in clusters has been comprehensively addressed in the former chapter by replacing equivalent frequency-dependent linear springs scaled based on the response spectrum of individual guy cables and specific earthquake frequency content. However, the characterization of the cable-mast interactions and the effects of the replacement of the linear equivalent springs on the dynamic characteristics of the mast still remain to be done.

In this chapter, the approximate procedure to represent the guy clusters developed in Chapter 3 is used to study the cable-mast dynamic interaction in the context of the behaviour of whole guyed telecommunication masts under seismic excitations. Simplified dynamic analysis models for earthquake-resistant design of guyed telecommunication masts will be presented next. Detailed numerical simulations involving nine existing guyed masts with varying heights of 110 to 607 m under the effects of five signatures were investigated in this study and results will be compared to the proposed simplified method.

Dynamic response of the simplified finite element models in which nonlinear guyed cables were replaced with linearized horizontal springs was studied at the first step. Comparison of these results with detailed numerical models confirmed the reliability of the introduced linear spring elements under earthquake excitations. At the next step, the stiffness and mass matrices of tower condensed models were studied and simplified seismic analysis of guyed masts was developed based on analytical approaches. As mentioned before, the aim of the method is to replace more elaborate modelling procedures as a preliminary check during the design stage; it is not meant to replace a full nonlinear analysis in instances when seismic effects indeed govern the design. It can also be used as a rapid investigation of the seismic vulnerability of existing masts. The

proposed method yields a conservative (i.e. safe) and relatively accurate (i.e. not too overly conservative) prediction of the maximum lateral seismic displacements of the mast at the various stay levels. The method is validated with several detailed analyses while a more elaborate verification is presented in Chapter 5.

This research was summarised into a manuscript: Ghafari Oskoei, S. A., and McClure, G. "A robust linearized seismic analysis method for guyed telecommunication masts." *Journal of Structural Engineering, Manuscript STENG-1145, (revised version) submitted in November 2010.* The following section presents the manuscript with minor changes in order to fit into the general format of the thesis and Appendix D gives more details on the application examples. According to ASCE publication copyright policy, the author has permission to republish the manuscript content in his doctoral thesis.

4.2. A new robust linearized seismic analysis method for tall guyed telecommunication masts

S. Ali Ghafari Oskoei[1] and Ghyslaine McClure[2]

4.2.1. Abstract

Design of tall telecommunication masts is usually governed by serviceability criteria under high wind conditions, typically combined with icing in cold climates. However, there is a need for seismic design checks for guyed masts constructed in zones with moderate to high seismicity, as is routinely prescribed for buildings in modern codes. There have been few efforts towards proposing a robust simplified method of general applicability for the seismic analysis of tall masts. These structures can be represented by the simple concept of a continuous beam-column (the lattice mast) on nonlinear elastic supports (the guy cable clusters at various stay levels). In this study, the guy cables are replaced by equivalent linear lumped parameters (stiffness, mass and viscous damping) and the effects of their interaction with the mast stiffness and inertia on the structural characteristics are discussed. The approach has been tested with nine case studies of real telecommunication masts subjected to five different seismic inputs and further validated with more analysis for two selected masts under the effects of 81 recorded Californian earthquakes.

---

[1] PhD Candidate, Dept. of Civil Engineering and Applied Mechanics, McGill Univ., 817 Sherbrooke St. West, Montréal, QC, Canada, H3A 2K6. Email: ali.ghafari@mail.mcgill.ca

[2] M. ASCE, Associate Professor, Dept. of Civil Engineering and Applied Mechanics, McGill Univ., 817 Sherbrooke St. West, Montréal, QC, Canada, H3A 2K6. Email: ghyslaine.mcclure@mcgill.ca

Key words: Seismic design; Guyed towers; Cable-mast interactions; Matrix methods; Frequency response.

4.2.2. Introduction

The structural dynamic behaviour of tall guyed masts is complex. A brief overview of the engineering literature on the seismic analysis of guyed telecommunication masts was presented in Ghafari Oskoei (2010). The complexity in the structural behaviour of guyed masts mainly arises from the significant geometric nonlinear response of the guy cables and the dynamic interaction between the cables and the mast. The first source of complexity has been comprehensively addressed in Ghafari Oskoei and McClure (2009), by replacing the guy cables with equivalent frequency-dependent linear springs. These spring properties were derived based on the response spectrum of individual guy cables and specific earthquake frequency content. Detailed numerical simulations involving 57 guy cables from eight existing towers with varying heights of 110 m to 607 m were investigated and the comparison of the main response indicators of the simplified linear frequency-dependent spring/mass system and the detailed finite element analysis results confirmed the reasonable and consistent engineering accuracy of the proposed method. However, the ultimate goal of the authors' research is to propose a robust simplified analytical approach for the seismic analysis of guyed telecommunication masts. As such, the proposed linearized dynamic stiffness models for guy clusters were an important milestone contribution towards the development of a robust method of general applicability. However, the characterization of cable-mast interactions always present in seismic analysis, still remains to be addressed. In this study, the guy cables are replaced by their equivalent lumped parameters (stiffness, mass and viscous damping) and the effects of their interaction with the mast stiffness on the structural characteristics are discussed. A condensed model of the guyed mast is created where the individual horizontal stiffness elements of the global structure were evaluated at each stay level in order to perform a simplified seismic analysis of the structure. An approximate structural

modeling approach is proposed to evaluate the stiffness terms of the condensed dynamic model without the need for elaborate mathematical formulation and time-consuming computational effort: the approach makes use of the geometric and elastic properties of the mast idealized as an elastic beam on flexible supports.

It is noteworthy that other parameters like the slenderness of the mast (beam-column effects) and the whipping effect of the top cantilevered portion of the mast (if present) may also amplify the nonlinear response of the structure in sway motion. However, these effects are duly addressed in design with various other load combinations and, for the sake of simplicity they are not considered in the proposed seismic analysis method. The approach has been tested and calibrated by comparing its results with those obtained from nonlinear dynamic analysis using realistic three-dimensional models of both the guyed mast and the seismic loading of nine case studies of real telecommunication masts subjected to five different seismic inputs. It was further validated with more analysis for two selected masts under the effects of 81 recorded Californian earthquakes. Based on the prediction of maximum mast displacements at guying levels, maximum cable reaction forces at their attachment point and maximum cable tension forces are estimated. The reference used for model validation is the complete set of results obtained from detailed nonlinear finite element dynamic simulations.

4.2.3. Case studies and earthquake input

In this research, the data base comprising eight real lattice guyed masts previously studied in detail at McGill University by Amiri (1997), Faridafshin (2006) and Ghafari Oskoei and McClure (2009) was enriched by a 111.2-m guyed telecommunication mast owned by Hydro-Québec and located in St. Hyacinthe, Québec. This tower, illustrated in Fig. 4.1, consists of six stay levels arranged at two anchor groups with outriggers located at the fourth and the sixth stay levels from the bottom. The panel width and the height of the mast are 1.116 m and 1.02 m, respectively. All numerical assumptions were kept the

Figure 4.1 111.2 m guyed telecommunication tower located in St. Hyacinthe, Québec, Canada.

same as in previous studies except for the time stepping increment which had to be reduced for stability and accuracy. Specific structural details of the other masts will not be repeated here and can be found in the works cited above. The numerical tools were the commercial finite element analysis software ADINA (ADINA R&D 2004) and MATrix LABoratory MATLAB (2006).

The three classical earthquake records used in previous studies are supplemented with two more records to cover a wider range of excitations. The first three records (El Centro, Parkfield and Taft) have been taken from Pacific Earthquake Engineering Research Center (PEER, 2005) strong motion database. The other records are a synthetic time history generated by the autoregressive method based on the power spectra recommended by the National Building Code of Canada (NBCC) (NRC, 2005) and a recorded time

history for the Montreal region. All records are scaled to fit inasmuch as possible the elastic uniform hazard design spectrum of NBCC 2005 for the region of Victoria, British Columbia. This region has one of the highest seismicity levels in Canada with prescribed peak horizontal ground acceleration (PGA) of 0.34 g on stiff soil. It is understood that none of the towers studied is actually located in Victoria, but the scaling allows the comparison of the response of the towers for different accelerograms. A final series of more complete simulations on two selected towers made use of 81 recorded Californian earthquakes scaled to a PGA of 0.30 g (Ghafari Oskoei, 2010).

4.2.4. Dynamic response of the simplified finite element models

Linearized horizontal cable model

The first step towards the robust simplified seismic analysis method for guyed masts was to replace the guy cables with a linearized single-degree-of-freedom system in the horizontal direction based on the developments presented in Ghafari Oskoei (2010). The equivalent cable stiffness values associated with El Centro, Parkfield and Taft earthquakes for the 342-m tower are reported in Table 4.1 as an example. The left column shows the static cable stiffness obtained in the horizontal direction at the upper

STAY LEVEL	STATIC STIFFNESS	SIMPLIFIED RESPONSE-SPECTRUM METHOD			ADINA SIMULATIONS BASED METHOD		
	(KN/m)	ELCENTRO	PARK	TAFT	ELCENTRO	PARK	TAFT
7	59,380	117,130	117,190	117,710	92,450	111,430	97,050
6	82,560	175,980	175,910	175,920	124,540	135,770	166,470
5	94,840	192,690	192,670	192,470	141,180	190,440	167,640
4	111,730	230,360	227,730	226,450	171,310	241,440	119,110
3	113,430	250,740	248,250	248,730	177,840	246,690	115,310
2	97,860	218,630	223,230	218,100	162,440	240,260	129,340
1	155,460	347,270	351,140	348,090	207,420	333,430	185,500

Table 4.1 *Equivalent cable stiffness values in kN/m for the 342 m tower (Stay levels are numbered from the base).*

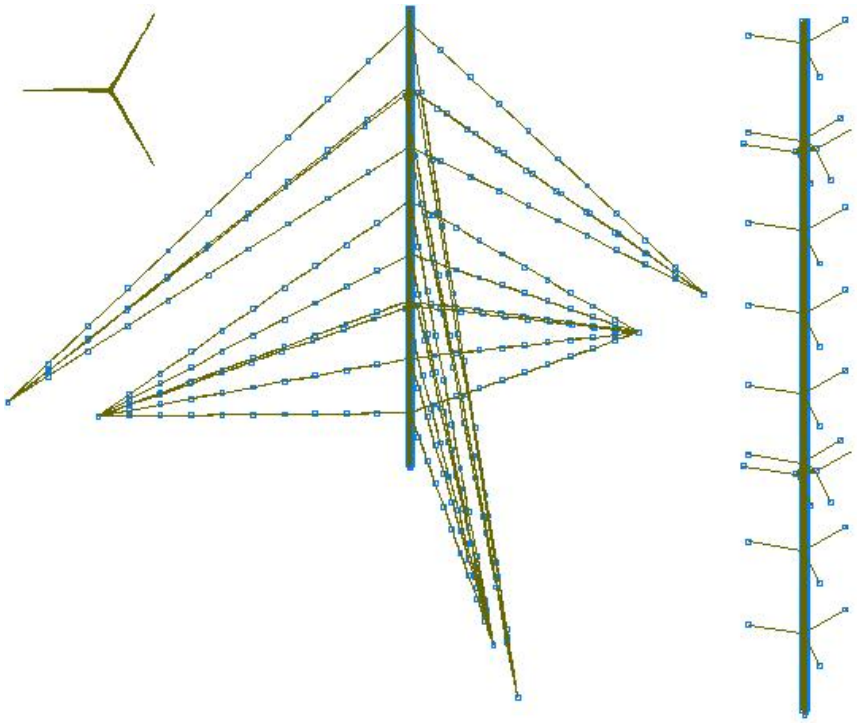

Figure 4.2 *The detailed (left) and simplified (right) geometric layouts of the 152 m mast models .*

attachment point. The other results represent the equivalent dynamic stiffness obtained using a response spectrum approach and detailed nonlinear dynamic simulations in the time domain. The results presented in Table 4.1 are representative of the different cases studied and serve to indicate the order of magnitude of the dynamic effects on the equivalent cable stiffness as the methods of analysis and the earthquake signatures are varied. These results confirm that dynamic effects are always important with the equivalent dynamic cable stiffness in the range of 1.5 to 2.2 times the static cable stiffness; these effects vary significantly for different earthquakes. It is seen that the results from the "simplified response spectrum" method are generally higher than the results from "ADINA simulations based" method, which means that the simplified models will overestimate the dynamic force response in the guyed masts; this is also a desirable feature for an approximate design check.

The viscous damping constant used in the cable dashpot model is 1.2% critical as in previous studies, assuming still air conditions and negligible aerodynamic damping (IASS, 1981; Smith 2007). Another important decision in the modeling procedure is the selection of the appropriate reactive lumped mass to assign at the stay levels. Different values were tested in detailed simulations and a parametric study confirmed that a value in the range of 5% to 25% of the total cable mass can mimic properly the inertia of the cables that contributes to generate dynamic interactions between the stay cables and the mast. The participating mass of a given cable will depend on its relative degree of slackness, as represented by the well known λ^2 parameter defined by Irvine (1981). It is recommended to use 5% to 10% for the top clusters and 20% to 20% for the bottom ones. The boundary conditions of the spring/dashpot system were set fixed in all degrees of freedom except for the horizontal translation within the cable plane. Adequate joint constraints were used to allow for the vertical deformations due to self weight and operation loads to occur. Fig. 4.2 depicts the detailed and the simplified numerical models of the 152-m mast, where the lattice mast representation is the same in the two models and each guy cable is replaced by its equivalent linearized horizontal spring/dashpot/mass system at the mast attachment point.

Fig. 4.3 indicates the orientation of the horizontal ground displacements that induces maximum response in the structure; all simulations used this same input orientation.

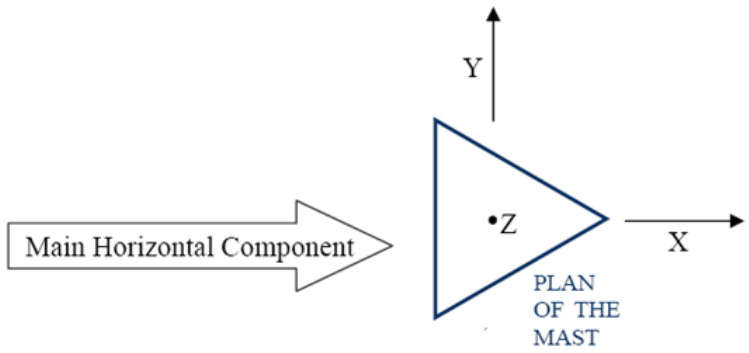

Figure 4.3 *The typical triangular cross-section of the masts and the orientation of the ground motions used in the simulations (along the X direction).*

Detailed nonlinear analysis simulations confirmed that in all the cases studied (with maximum ground acceleration levels limited to $0.34g$) none of the cables had become completely slack. This is an important observation which guarantees the safe seismic performance of the masts and the contribution of all guy cables to the lateral stiffness of the structure. The structures then keep their rotational symmetry under extreme loading conditions and are not sensitive to the orientation of the earthquake motion as the lateral stiffness is constant in all guying plane directions. Considering that all masts of the study have a triangular cross section with guy cables arranged at 120° in plan, the total horizontal stiffness of each guy cluster in any horizontal direction is equal to 1.5 times the individual guy cable stiffness.

Results and discussion

The results from the simplified and detailed mast models as illustrated in Fig. 4.2 are compared next. The horizontal displacement of the mast at the cluster attachment levels along the direction of the main horizontal earthquake component (X direction) and the cable tensions were the selected response indicators for the comparison.

Fig, 4.4 shows the time history of the horizontal displacement of the 198-m mast tower at the 5th cluster level under the Parkfield earthquake for the detailed numerical model and the simplified models. Small differences in the range of ±6% to ±8% were observed in this case. The maximum error observed in all cases was less than ±10%. Also the results based on the linearized spring method were usually overestimating the main response indicators of the structure. These linearized springs can only give a rough estimate of the nonlinear behaviour of the cables during larger displacements, as they are calibrated on values of end displacement induced by the sway motion of the mast. Moreover, the detailed seismic analysis of guyed masts involving slack cables requires a nonlinear dynamic analysis scheme with implicit time integration, while the most important limitation of the proposed method is that guy wires do not become slack (with zero tension) during the strong base motion. However, when this limitation is satisfied,

the simplified linearized spring duly considers the nonlinear behaviour of slackening cables and there is no more need for full nonlinear analysis. The computational demand of the simplified simulations is greatly reduced without much significant effects on the accuracy of the results in the context of an approximate seismic design check.

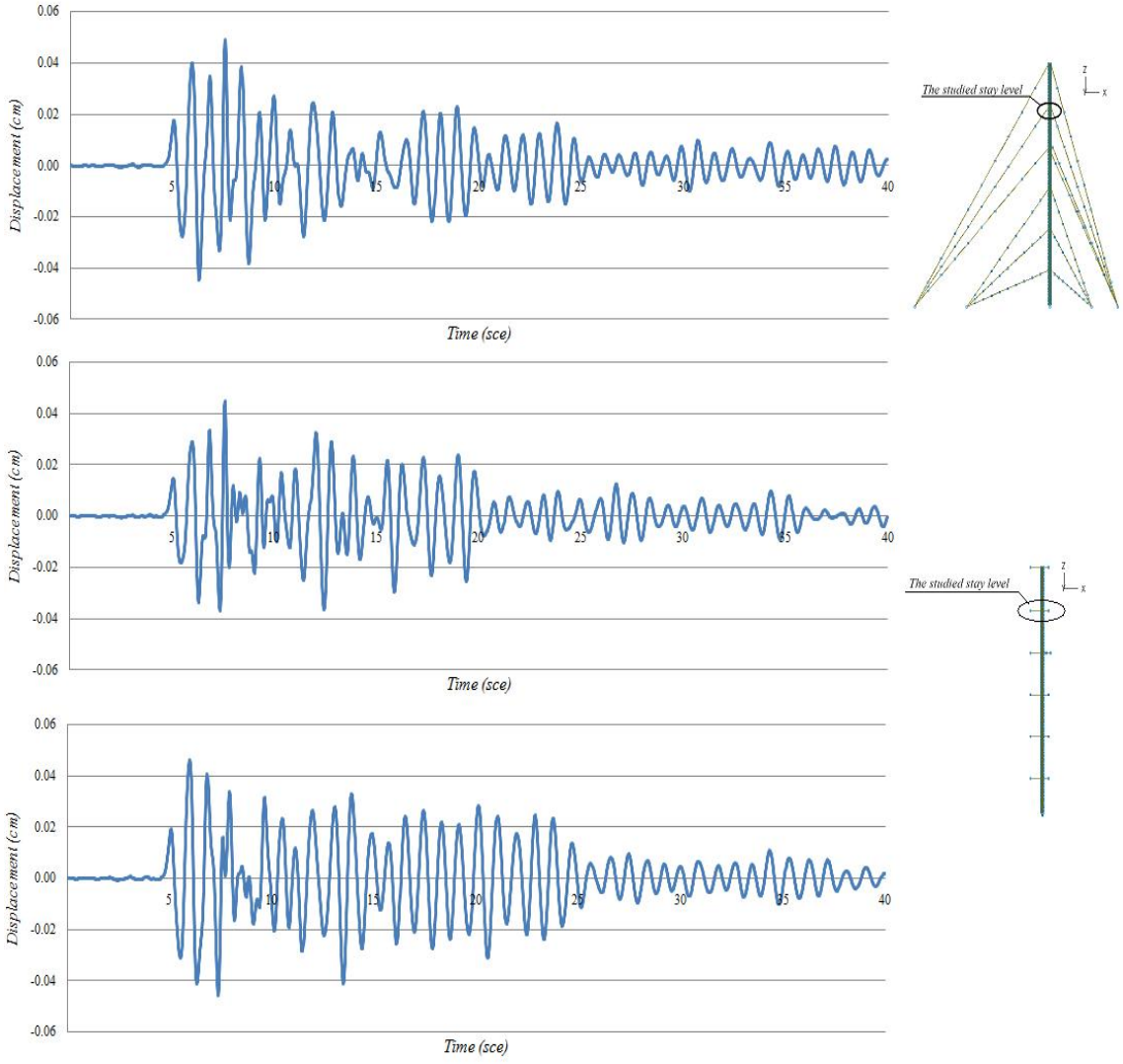

Figure 4.4 *Horizontal displacement of the 198 m mast at the 5th cluster level under Parkfield earthquake, (a) detailed nonlinear model, (b) simplified model based on the spring linearized stiffness obtained from ADINA simulations, (c) simplified model based on the spring linearized stiffness obtained from the proposed response spectral method.*

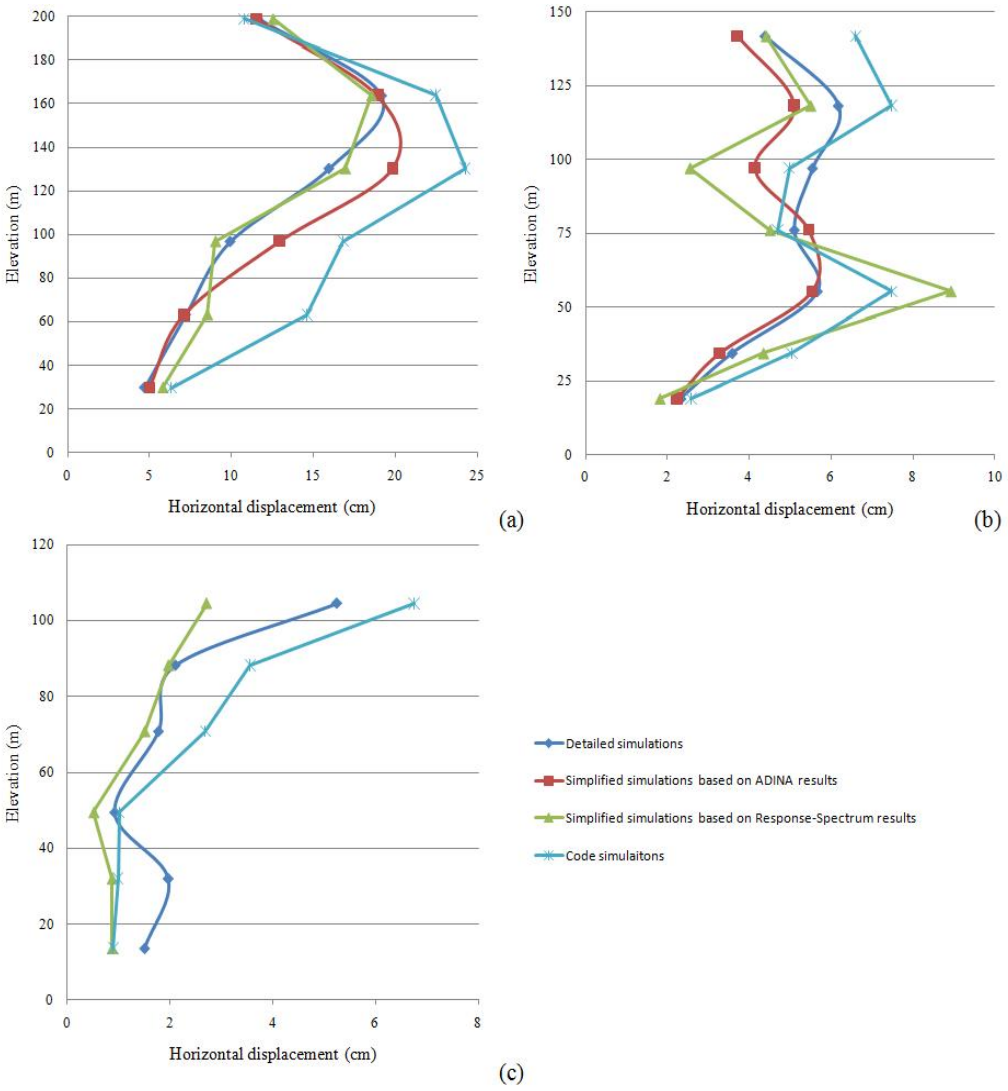

Figure 4.5 *Maximum horizontal mast displacement of (a) the 198 m tower under El Centro record, (b) the 152 m tower under Parkfield record, and (c) the 111 m tower under Taft record.*

For easier comparison, plots such as those in Fig. 4.5 were prepared showing the maximum horizontal deflection of the masts at different stay levels under different earthquake inputs. A representative sampling of the results was selected: the 198-m and the 152-m towers under El Centro and Parkfield earthquakes, respectively. Similar graphs associated with other towers and records confirmed the reliability and consistency of the results obtained throughout with the simplified linearized cable stiffness method.

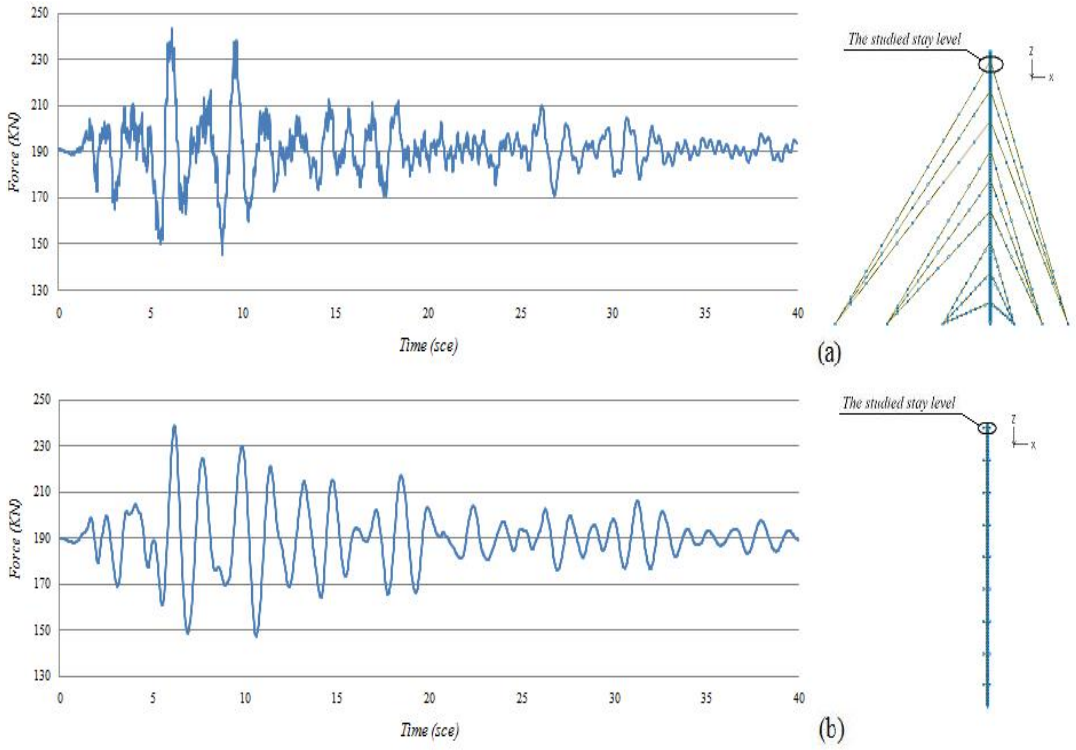

Figure 4.6 *Total tension force in the top cluster cable of the 607 m tower under El Centro earthquake for (a) detailed nonlinear model, (b) simplified model based on the spring linearized stiffness obtained from ADINA simulations.*

The other response indicator to be examined here is the tension force developed in the guy cables under the excitation. Both the total cable tension and the dynamic component of the cable tension excluding the pretension force have been used in the comparisons. Fig. 4.6 presents the time history of the total tension force of the 607-m tower at the highest cluster level under El Centro earthquake for the detailed numerical model and the simplified model based on the linearized cable spring stiffness obtained from ADINA simulations as one of the most extreme cases. It is observed that although some high frequency oscillations are filtered in the simplified model due to cable meshing simplifications, the magnitudes of the maximum peaks and the frequency contents are in general agreement.

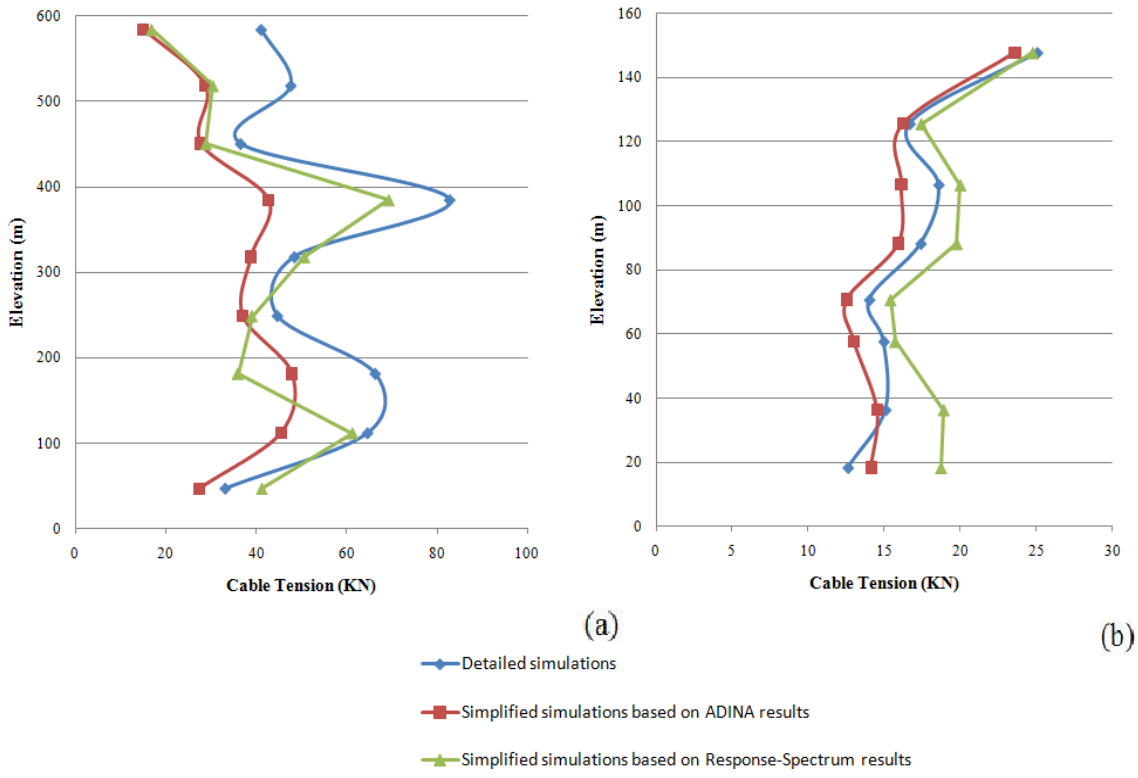

Figure 4.7 *(a) The total average cable tensions of the 607 m tower under Taft earthquake, (b) the dynamic component of the average cable tensions of the 152 m tower under Parkfield record.*

The graphs in Fig. 4.7 show the maximum cable tension associated with different earthquakes: Fig. 4.7(a) depicts the total average cable tensions of the 607-m tower under Taft earthquake and Fig. 4.7(b) depicts the dynamic component of the average cable tensions of the 152-m tower under Parkfield record. It is seen that the general trends of the results obtained from the simplified response spectrum model are in general agreement with those of the detailed nonlinear simulations. Analysis of the variability of the computed cable tensions for all cases indicated maximum relative errors of +33% on dynamic cable tension, which reduce to +14% when total cable tension is considered. One of the important findings was the effect of the frequency content of the earthquake input on the average error observed. For instance, Parkfield earthquake represents an earthquake with single pulse loading with dominant lower frequencies. In such cases, the

introduced average dynamic stiffness method works poorly in comparison to the Taft earthquake with high frequency content over a wider range. Another important observation was the accumulation of the error on the response of the short (and taut) bottom cluster guy cables which comprised a larger number of participating cable modes. The proposed method is accurate for the long cables of the top clusters, with an average error of +6.5% only.

4.2.5. Eigenvalue analysis

In order to further verify the accuracy of the proposed simplified cable models, the lowest frequencies and corresponding mode shapes of the structures under gravity loads were also compared to those obtained from detailed simulations. The modeling considerations for the frequency analysis are kept the same as in Faridafshin (2006). Since most of the lowest natural frequencies and mode shapes of the detailed models are associated with guy oscillations only, these cannot be represented by the proposed simplified model that replaces the guy cables with their equivalent spring-dashpot-mass elements. For a relevant comparison, the coupled cable-mast modes of the detailed structural model should be identified. To illustrate this, Fig. 4.8 (a) shows the mode shape associated with the 48^{th} mode (0.6 Hz) of the 152-m mast (associated with the second mode shape of the longest cables with no mast participation), while Fig. 4.8 (b) compares the first two coupled mast-cable modes of the detailed model with the simplified model developed based on the maximum deflected shape obtained with the El Centro earthquake input.

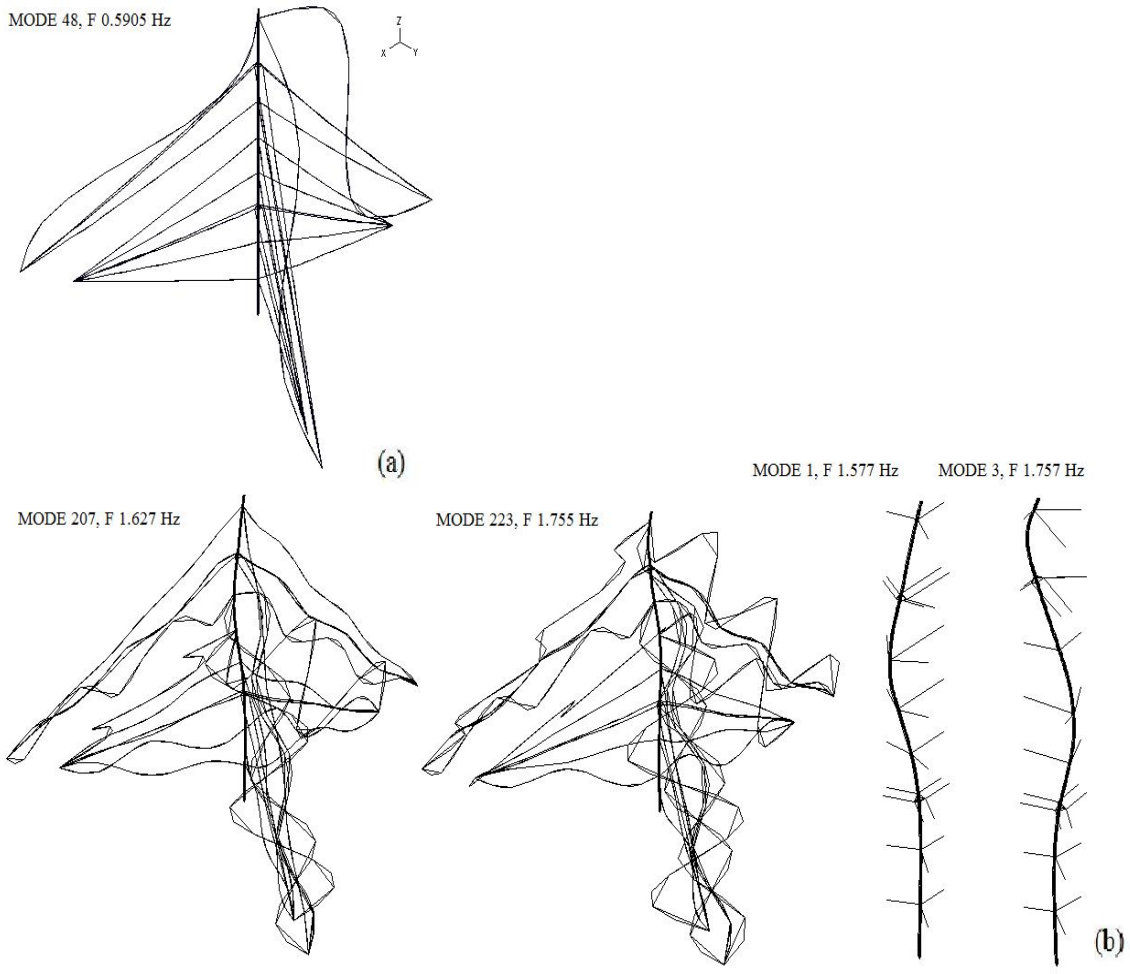

Figure 4.8 *Mode shapes and frequencies of the 152-m mast. (a) The 48th mode shape with $f = 0.59\,Hz$ associated with cable oscillations only, (b) (Left) The first two coupled mast-cable modes of the detailed model with $f_1 = 1.63\,Hz$ and $f_2 = 1.76\,Hz$, and (Right) the first two modes of the simplified model developed for the maximum displaced configuration under El Centro earthquake, with $f_1 = 1.58\,Hz$ and $f_2 = 1.76\,Hz$.*

4.2.6. Tower condensed stiffness matrix

As illustrated above, the proposed model of linearized equivalent springs to represent the guy cable clusters makes it possible to perform linear dynamic analysis of condensed models of guyed masts with very few degrees of freedom, defined along the mast axis at the different cluster attachment levels. For example, Fig. 4.9 (a) shows the eight defined

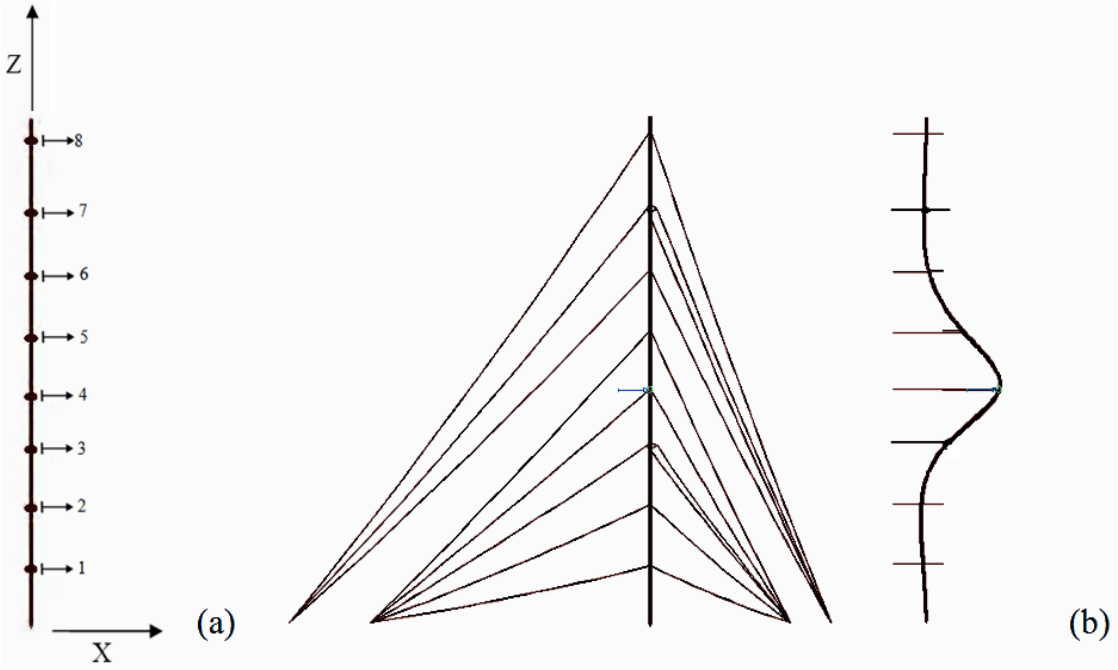

Figure 4.9 *(a) Mast degrees-of-freedom for the 152-m tower, (b) Unit load method to obtain the flexibility coefficients* f_{i4}.

degrees of freedom along the Z coordinate for the 152-m tower. The condensed stiffness matrix of the mast can be obtained by inverting the flexibility matrix derived using the unit load method. The procedure is illustrated in Fig. 4.9 (b) where the horizontal displacement response of the mast due to a unit load applied at cluster level 4 will yield the fourth column (f_{i4}) of the flexibility matrix. The structure of the flexibility matrix can be approximated by a tri-diagonal form: terms outside this bandwidth have values of the order of 5% or less than the values of the main bandwidth and are neglected in the simplified procedure. The narrow bandwidth of the flexibility matrix is also reflected in the deformation patterns of the masts, as illustrated for example in Fig. 4.10 showing the mast deformation patterns associated with the derivation of flexibility coefficients of the 152-m mast at various cluster levels.

The other important property of the condensed flexibility matrices of the masts is their asymmetry. Although the geometric nonlinearities due to the guy clusters have been eliminated by replacing their effect with equivalent linearized springs, other sources of

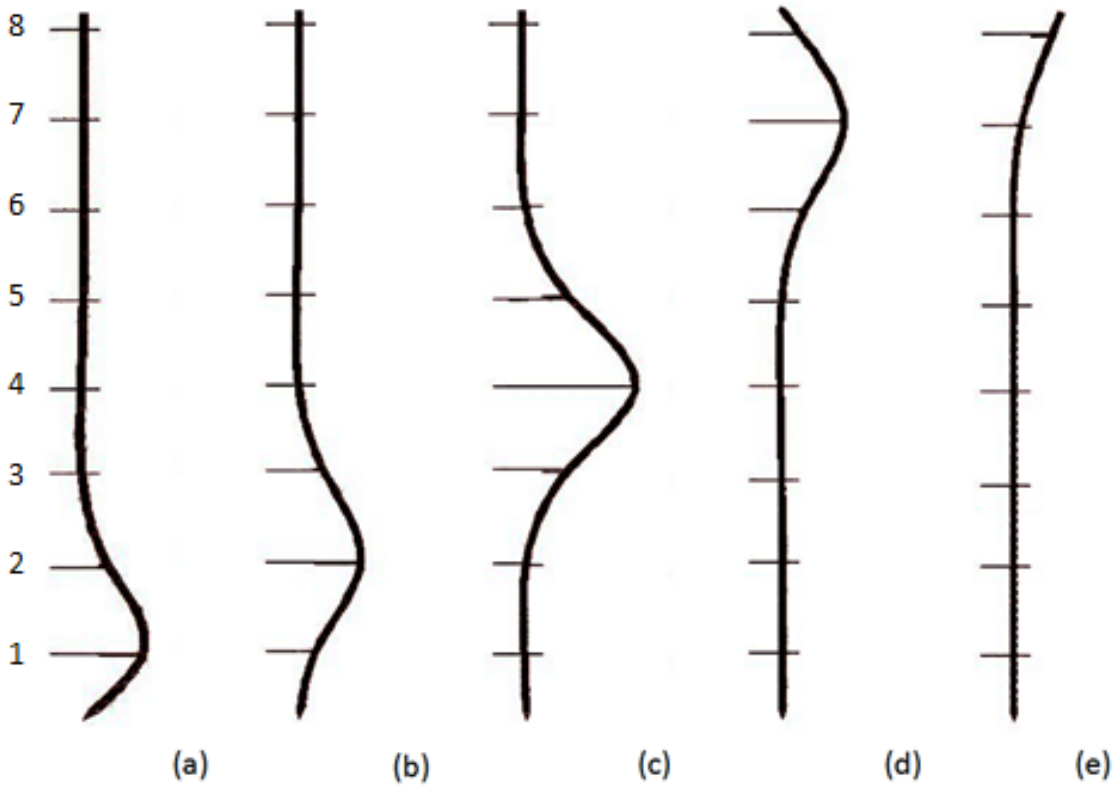

Figure 4.10 *Five typical deformation patterns associated with the 152-m tower, (a) the lowest cable cluster, (b) the second lowest cable cluster, (c) a typical intermediate cable cluster, (d) one before the top cable cluster, and (e) the top cable cluster.*

geometric nonlinearities still remain such as the geometric nonlinear behaviour of the mast itself, including P-Delta effects and the effects of large kinematics. As a result the flexibility matrices are still slightly asymmetric, and may not always be positive definite. In order to avoid possible numerical difficulties, the authors further propose to average the off-diagonal terms of the tri-diagonal flexibility matrices.

4.2.7. Cable-mast interaction model

As shown with the influence lines presented in Fig. 4.10, the unit load method is useful to study the deformation patterns for different parts of a typical guyed mast. According to Fig. 4.11, five typical deformation patterns are identified which will serve to generate the

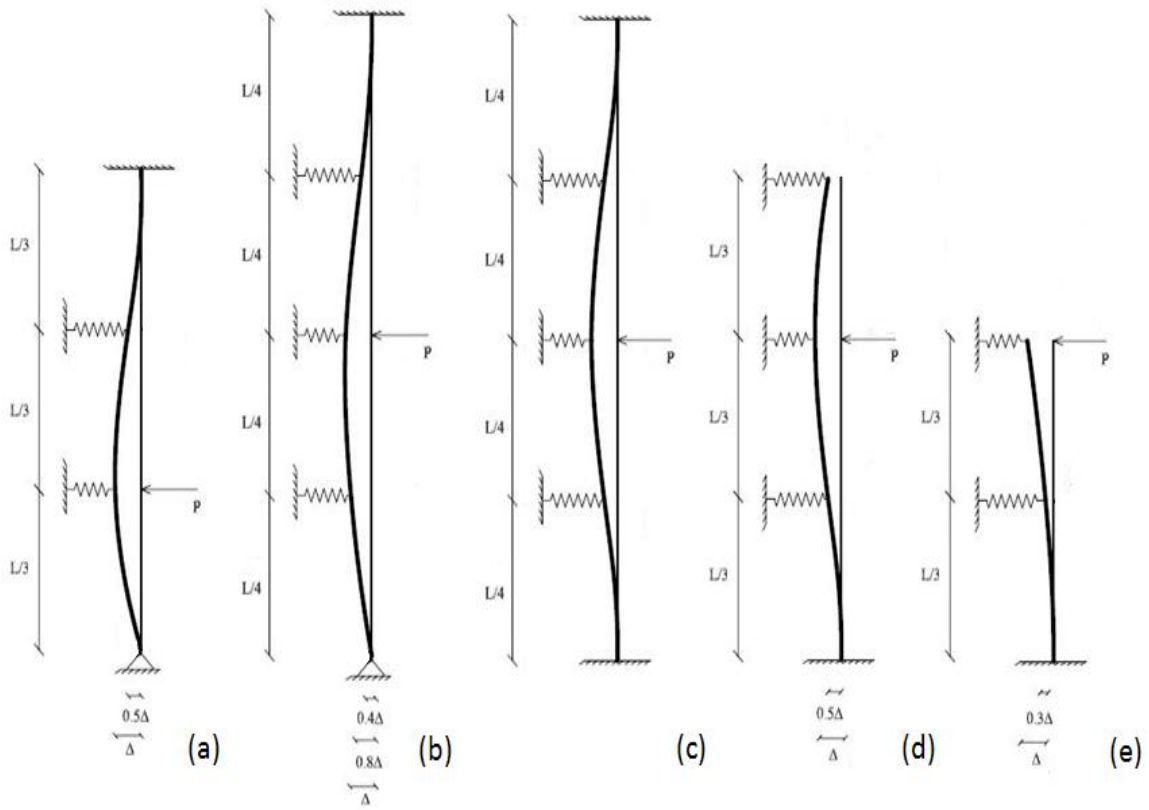

Figure 4.11 *Five typical analytical models to evaluate the flexibility terms of a typical guyed mast (a) the bottom degree of freedom is loaded with unit load P to yield f_{k1} coefficients; (b) the second degree of freedom is loaded with unit load P yield f_{k2} coefficients; (c) the intermediate degree of freedom i is loaded with unit load P yield f_{ki} coefficients; (d) the $(n-1)^{th}$ degree of freedom is loaded with unit load P to yield the $f_{k(n-1)}$ coefficients; (e) and the top degree of freedom n^{th} is loaded with unit load P to yield the f_{kn} coefficients.*

linearized stiffness of the cable-mast model. In this figure, the span lengths between the adjacent cluster levels are taken as equal and the bending rigidity of the mast is assumed constant throughout.

Fig. 4.10 (a) shows the typical deformation pattern when a unit load is applied at the lowest stay level of the mast. In the proposed simplified model, it is assumed that the mast section influenced by the load comprises the lowest three spans only and the deformed mast configuration matches a pinned boundary condition at the base and a fixed end (rotational restraint) at the top end of the deflected section. The other simplifying

assumption for the construction of the simplified model shown in Fig. 4.11 (a) relates to the form of the deflected shape: the horizontal deflection of the mast at the second stay level is taken as half of the deflection at the first stay level in order to estimate the contribution of the adjacent cable cluster. This approximation is based on the deformation patterns observed for the actual masts of the data base which have variations in span lengths and bending rigidity. An approximate model is further proposed to combine the contributions of the bending stiffness of the mast, the horizontal dynamic stiffness of the cable clusters and the cable-mast interactions, as follows. The flexibility terms associated with the unit load applied at the first degree of freedom (the bottom cluster) are obtained from Eq. (1).

$$f_{11} = \frac{1}{1.3\,K_{c1} + K_{mast-1}} \tag{1a}$$

$$f_{21} = \frac{0.5}{1.3\,K_{c1} + K_{mast-1}} \tag{1b}$$

in which, K_{c1} is the stiffness of the cable cluster at the first level (the stiffness of the cluster is equal to 1.5 times the individual cable stiffness). K_{mast-1} is the lateral stiffness of the mast calculated at the bottom stay level, assuming the simple pinned-fixed beam shown in Fig. 4.11(a). The analytical solution of the deflected shape of the elastic beam at level 1 due to a unit force yields a value of $20\,{L_1}^3/(2187\,EI)$ where L_1 is the total length of the continuous beam section of interest up to the third cluster attachment point from the base, $L_1 = l_1 + l_2 + l_3$. l_i is the i^{th} span length.

Fig. 4.10(b) illustrates the typical deformation pattern associated with the lateral unit load applied at the second cable cluster from the base. In this case, the influenced section comprises the four lowest spans. Further studies illustrated that this model can be replaced by the typical deformation pattern of an intermediate section, located at least two clusters away from the bottom and the top, as shown in Figs. 4.10(c) and 4.11(c). In this case, the load is applied at cluster level i and the mid span deflection due to a unit force is $L_i^3/\,192\,EI$ for a prismatic beam of total span L_i with fixed ends on flexible supports, where L_i here is equal to $L_i = l_{i-1} + l_i + l_{i+1} + l_{i+2}$. The corresponding

flexibility coefficients are defined in Eq. (2) where $f_{(i-1,i)}$ and $f_{(i+1,i)}$ are taken as 50% of f_{ii} and all other flexibility coefficients are zero.

$$f_{i\,i} = \frac{1}{1.5\,K_{ci} + K_{mast-i}} \tag{2a}$$

$$f_{(i-1)\,i} = f_{(i+1)\,i} = \frac{0.5}{1.5\,K_{ci} + K_{mast-i}} \tag{2b}$$

in which, K_{ci} is the stiffness of the cable cluster at i^{th} level (the stiffness of the cluster is equal to 1.5 times the individual cable stiffness). Finally, based on the deformation patterns of the two top clusters illustrated on Figs. 4.10 (d) and (e) and their corresponding analytical models depicted in Fig. 4.11(d) and (e), the flexibility terms are suggested in Eqs. (3) and (4) where n indicates the top cluster level.

$$f_{(n-1)(n-1)} = \frac{1}{1.33\,K_{c(n-1)} + K_{mast-(n-1)}} \tag{3a}$$

$$f_{(n-2)(n-1)} = f_{n\,(n-1)} = \frac{0.55}{1.33\,K_{c(n-1)} + K_{mast-(n-1)}} \tag{3b}$$

in which, $K_{c(n-1)}$ is the stiffness of the cable cluster at the $(n-1)^{th}$ level and $K_{mast-(n-1)}$ is the stiffness of the assumed mast beam on flexible supports equal to $K_{mast-(n-1)} = 81EI/L_{(n-1)}^3$, and $L_{(n-1)}$ is equal to $L_{(n-1)} = l_{(n-2)} + l_{(n-1)} + l_n$.

$$f_{nn} = \frac{1}{1.1\,K_{cn} + K_{mast-n}} \tag{4a}$$

$$f_{(n-1)\,n} = \frac{0.33}{1.1\,K_{cn} + K_{mast-n}} \tag{4b}$$

in which, $K_{c\,n}$ is the stiffness of the cable cluster at the n^{th} (tower top) cluster level, K_{mast-n} is the stiffness of the assumed mast beam equal to $K_{mast-n} = 3EI/L_n^3$, and $L_n = l_{(n-1)} + l_n$. These results are presented in the tri-diagonal matrix form of Table 4.2. The inverse of this tri-diagonal flexibility matrix yields a fully populated stiffness matrix.

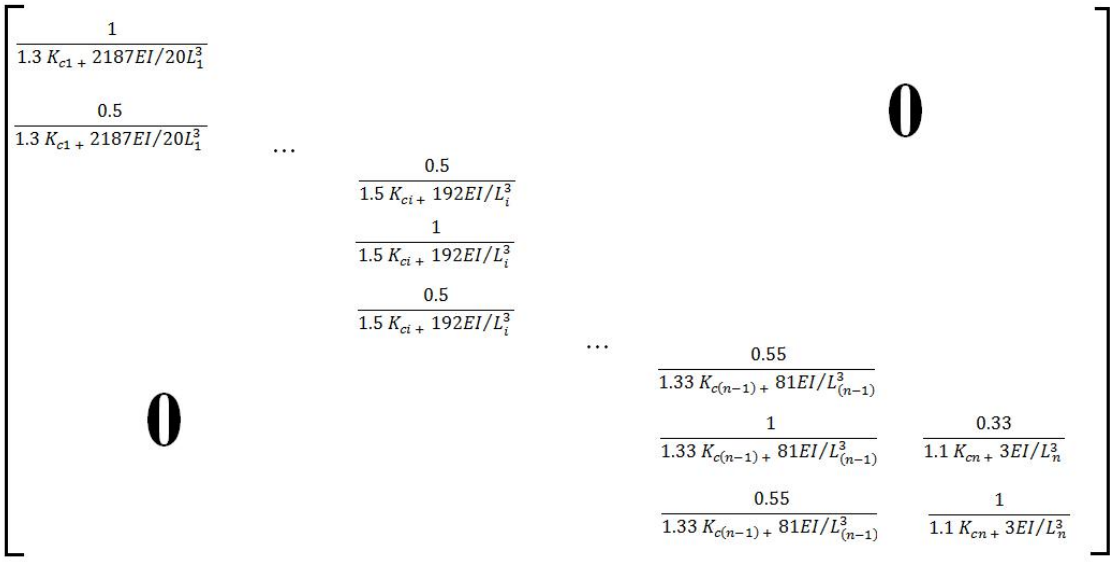

Table 4.2 The typical flexibility matrix for n-cluster guyed telecommunication mast.

A short code was written in MATLAB to perform the linear dynamic analysis of the simplified condensed models based on the calculated matrices, and some typical results are compared next to those of the detailed nonlinear finite element model simulations.

4.2.8. Results and discussion

A simplified condensed model as described above was created for 45 cases (9 towers times 5 input base motion records). Some typical MATLAB code results are shown in Figs. 4.5 and 4.12 together with the results obtained with the more elaborated models. Comparison of these results with the detailed numerical simulations confirmed that the simplified condensed dynamic models are generally more flexible and consistently overestimate the deformation of the structure with a reasonable engineering tolerance (about 15% on average). This is important to ensure safe tower serviceability checks.

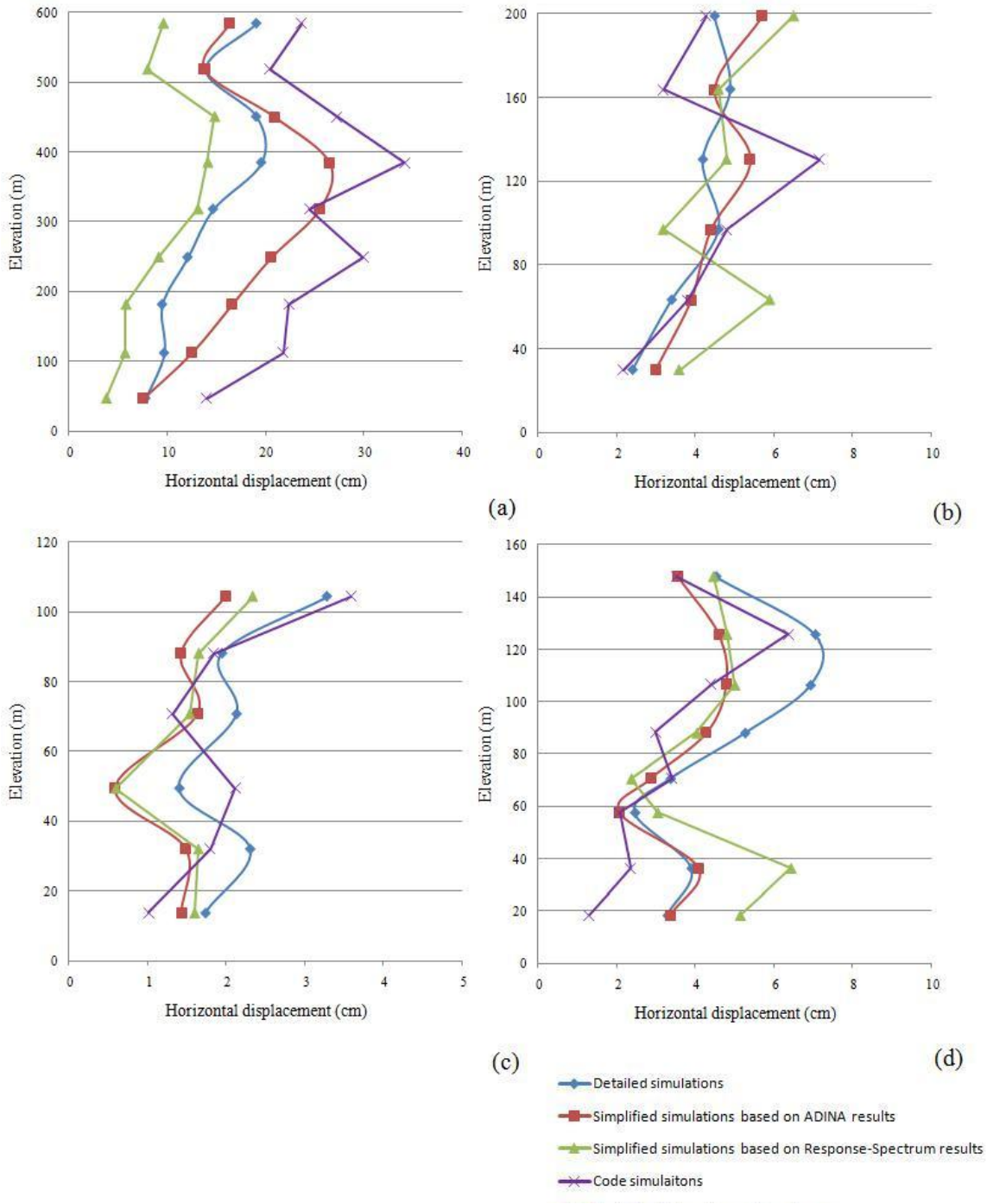

Figure 4.12 *The maximum horizontal displacement in X direction of (a) the 607 m tower under El Centro record, (b) the 198 m tower under Parkfield record, (c) the 111 m tower under the selected record of Montreal region, and (d) the 152 m tower under the generated synthetic earthquake.*

In order to further verify the sensitivity of the proposed simplified method to the signature of the earthquake input, two selected towers, the 342-m and the 607-m masts, were studied under the effects of 81 recorded Californian earthquakes scaled to a peak ground acceleration of 0.30 g (Ghafari Oskoei, 2010). Fig. 4.13 plots the envelope curves of the average displacements simulated for the 342-m tower under the 81 earthquake records. Inserts in this figure represent the statistical distribution of the results obtained using the condensed analytical method with symmetric stiffness matrix. Fig. 4.14 shows the envelope curves of the average cable tension forces simulated for this tower under the 81 earthquake records. In this figure, results referred to as "Analytical Method" were derived based on the forces induced in the linearized springs under the deformation patterns illustrated in Fig. 4.11.

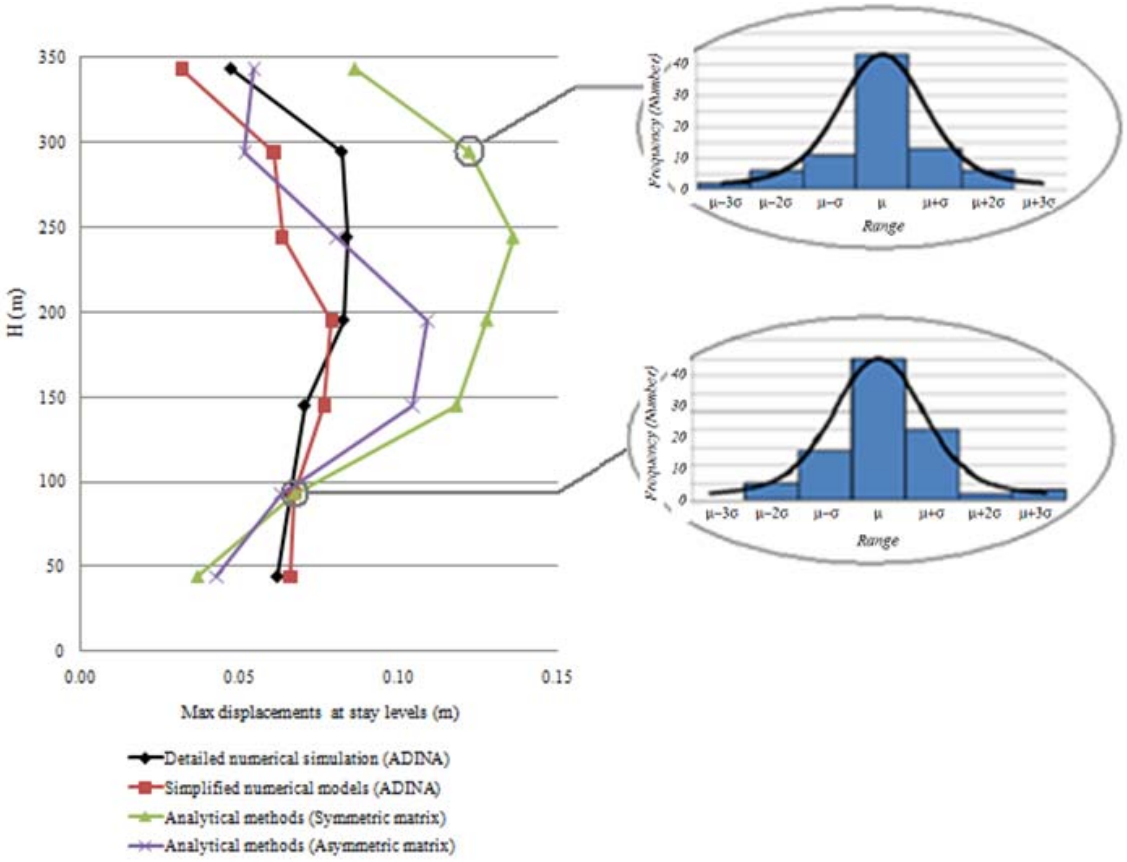

Figure 4.13 *Maximum horizontal displacements of the 342-m mast - average response under the effects of 81 earthquake records scaled to* $PGA = 0.3\ g$.

The purpose of the condensed method is to provide a conservative (over prediction) of the mast displacements at stay levels for approximate design checks. This is clearly achieved at all guy cluster attachment levels (except for the displacements at the bottom one) in Figs. 4.13 and 4.14 when considering the method based on the condensed symmetric stiffness matrix of the mast. The non symmetric method provides less conservative (and more accurate) estimates but it tends to underestimate the maximum response at the top clusters (see Fig. 4.13) which is unconservative.

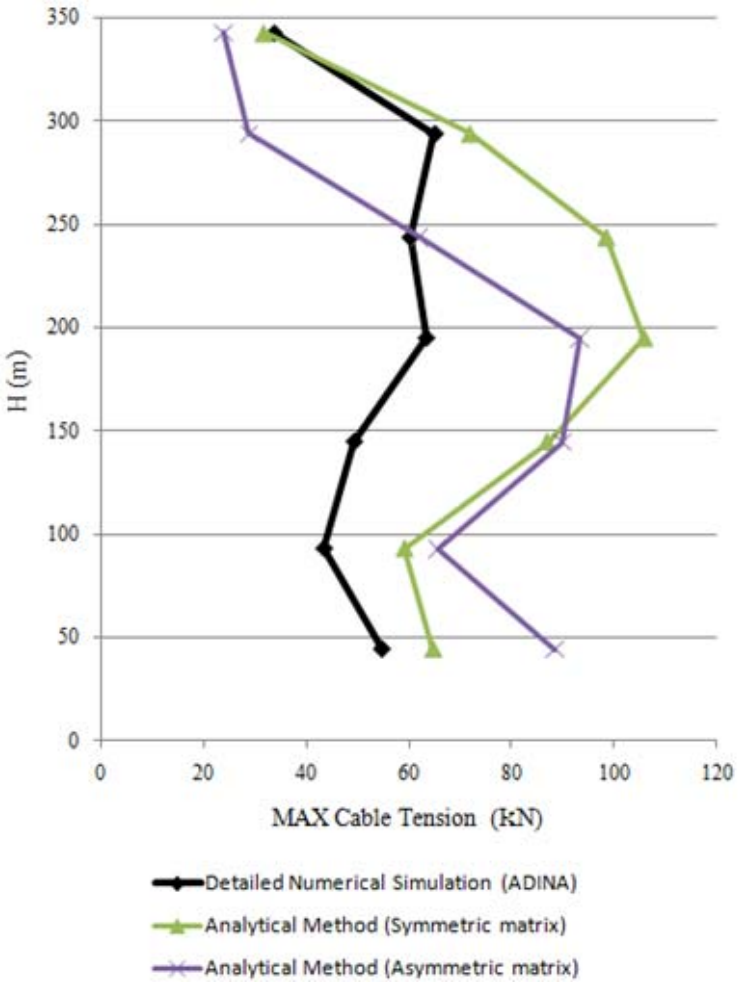

Figure 4.14 Maximum cable tension forces of the 342-m mast - average response

The statistical distribution of the results shown in Fig 4.13 for two selected points, illustrates the variability of the average values predicted. In particular, the narrow distribution of the results at the top cluster confirms that the average value provides a reliable estimate of the maximum probable response of the structure.

Although the proposed condensed method is restricted to tower heights not exceeding 350 m, a global comparison of the different methods was done for the 607-m mast (Ghafari Oskoei, 2010), which further confirmed that the condensed analytical method with symmetric stiffness matrix provides conservative results under synchronous earthquakes on stiff ground. Finally, the approximate symmetric stiffness matrix is the method recommended for design check applications because it provides a safe overestimation of the mast displacements and cable tension forces.

4.2.9. Conclusions

A new robust linearized seismic analysis method for guyed telecommunication masts was presented in detail and illustrated with numerical examples. The aim of the method is to replace more elaborate modelling procedures as a preliminary check during the design stage. It can also be used as a rapid investigation of the seismic vulnerability of existing masts. Of course, if the method indicates a marginal seismic response for a given mast, a more detailed investigation will be necessary. As such, this method is an interesting reference to be included in National Codes. However, the authors would recommend limiting the application of the method to masts not taller than 350 m, due to the lack of sufficient verification data for taller masts.

Notation

The following symbols are used in this paper:

EI Bending rigidity of the mast (assumed constant)

f_{ij} Flexibility coefficient of the guyed mast

$K_{c\,i}$ Horizontal stiffness of the cable cluster attached to the mast at the i^{th} stay level

K_{mast-i} Horizontal stiffness of the mast calculated at the i^{th} stay level

l_i Vertical distance between guy cluster elevation at level i and $i-1$

L_i Span of the continuous beam section (as defined in Fig. 4.11)

References

Please see the last section.

5. Verification of the proposed method for seismic analysis method for guyed masts

5.1. Introduction

The structural dynamic behaviour of tall guyed telecommunication masts under earthquake excitation is complex. This complexity mainly arises from the significant geometric nonlinear response of the guy cables and the interaction between the cables and the mast. The first source has been comprehensively addressed in the context of Chapters 2 and 3, where a model of equivalent frequency-dependent linear springs is developed to represent the behaviour of guy cables. The effects of the replacing guy cables with linear springs on cable-mast dynamic interactions were studied in Chapter 4 in which simplified condensed seismic analysis models for tall guyed telecommunication masts were introduced. The proposed approach was found safe and reasonably accurate for design check purposes, with the understanding that earthquake-sensitive masts would require a complete finite element analysis to obtain more accurate response.

This chapter presents a more comprehensive verification of the proposed method with the study of two guyed telecommunication masts under the effects of eighty-one recorded Californian earthquakes. All data have been taken from PEER (Pacific Earthquake Engineering Research Center) Strong Motion Database while the original data have been collected from different sources[1]. The masts selected are a 342-m tower, representative of the height range of applicability of the proposed method (intended for towers of 180 to

[1] California Department of Water Recourses (CDWR). (2009). "The Strong Motion Program." CDWR, Sacramento, Calif., < http://www.oandm.water.ca.gov/earthquake/ >

California Geological Survey, formerly known as California Division of Mines & Geology (CDMG). (2009). "Center for Engineering Strong Motion." CESMD, Sacramento, California, < http://www.conservation.ca.gov/cgs/ >

Southern California Earthquake Center (SCEC). (2009). "Southern California Earthquake Center Databases and Resources." Los Angeles, Calif., < http://www.data.scec.org >

US National Earthquake Information Center (USGS). (2009). "Earthquake Hazards Program." Pasadena, Southern Calif., < http://earthquake.usgs.gov/regional/neic/ >

350 m), and a 607-m tower, representative of an extreme height case that should always be treated with detailed nonlinear dynamic analysis. Several response indicators were studied. At the first step and based on the maximum mast displacements at guying levels obtained from the condensed seismic analysis method, estimates are found for the maximum resultant cable reaction forces at their mast attachment point and the maximum individual guy tension forces. For mast design checks, estimates are also found for the maximum seismic force response in the mast, namely axial compression, shear force and bending moment.

The main results of this part of the research have been summarised into a technical note: Ghafari Oskoei, S. A., and McClure, G. "Validation of a linearized seismic analysis method for tall guyed telecommunication masts." *Journal of Structural Engineering, Manuscript No. S-10-00403, submitted in July 2010* (under major revision). A technical report was also prepared as a Structural Engineering series report of the Department of Civil Engineering and Applied Mechanics, McGill University, which includes several detailed simulation results: Ghafari Oskoei, S. A. (2010). "Validation of a linearized seismic analysis method for tall guyed telecommunication masts." eScholarship@McGill, Montréal, Canada, <http://www.mcgill.ca/library-findinfo/escholarship/>[2]. The following section presents the manuscript with minor changes to fit into the general format of the thesis. Finally, a section has been devoted to the derivation of the mast seismic force response indicators: axial compression, shear force and bending moment.

[2] URL of this record:

http://digitool.Library.McGill.CA:80/R/-?func=dbin-jump-full&object_id=92850&current_base=GEN01

5.2. Validation of a linearized seismic analysis method for tall guyed telecommunication masts

Authors:

S. Ali Ghafari Oskoei, Ph.D. Candidate, Department of Civil Engineering and Applied Mechanics, McGill University, Montréal, Québec, Canada, H3A 2K6.

ali.ghafari@mail.mcgill.ca

Ghyslaine McClure, Associate Professor, Department of Civil Engineering and Applied Mechanics, McGill University, Montréal, Québec, Canada, H3A 2K6.

ghyslaine.mcclure@mcgill.ca

5.2.1. Abstract:

A new robust linearized seismic analysis method for guyed telecommunication masts has been developed by the authors for design check purposes (Ghafari and McClure 2009, STENG-742 and STENG-1145). This method yields a conservative prediction of the maximum lateral seismic displacements of the mast at the various stay levels. Its analytical development addressed the geometric nonlinear response of the guy cables and the cable-mast dynamic interactions. The method was calibrated using detailed nonlinear dynamic analysis of nine real guyed masts subjected to a few earthquake signatures. This technical note presents a more extensive validation of the method and discusses some trends observed in the results for two selected guyed telecommunication masts under the effects of eighty-one recorded Californian earthquakes. Based on the prediction of maximum mast displacements at guying levels, maximum resultant cable reaction forces at their attachment point and maximum cable tension forces are estimated. A comparison of the detailed analysis results with those obtained from the linearized simplified method confirms the reliable performance of the simplified method.

Key words: Seismic design; Telecommunication masts; Guyed towers

5.2.2. Introduction

A new robust linearized seismic analysis method for guyed telecommunication masts was presented in Ghafari and McClure (STENG-1145). Following the study of the geometric nonlinear dynamic response of its individual guy cables (Ghafari and McClure, 2009 and STENG-742), a condensed dynamic model of the mast is created that captures its horizontal response. The condensed stiffness and mass matrices of nine real telecommunication masts were determined and their seismic response calculated for five different earthquake signatures. The results indicated good and safe predictive performance of the proposed method in view of approximate design checks.

This technical note presents a more extensive validation of the proposed method with the study of two guyed telecommunication masts under the effects of eighty-one recorded Californian earthquakes. The masts selected are a 342-m tower, representative of the height range of applicability of the proposed method (180 to 350 m), and a 607-m tower, representative of an extreme height case that should be treated with detailed nonlinear dynamic analysis. Based on the maximum mast displacements at guying levels obtained from the condensed seismic analysis method, maximum resultant cable reaction forces at their mast attachment point and maximum cable tension forces are also estimated.

5.2.3. Mast case studies

The two masts selected have been previously studied in detail by Amiri (1997), Faridafshin and McClure (2008) and Ghafari and McClure (2009, STENG-742, STENG-1145). The 342.2-m mast model, shown in Figure 5.1a, comprises seven guying stay levels arranged in two ground anchor groups for a total of 24 guy wires. The dimensions of the mast panel width and height are 2.00 and 1.54 m, respectively, and there is a torsional stabilizer (outrigger) at the second stay level from the base. The tower is located in Canada.

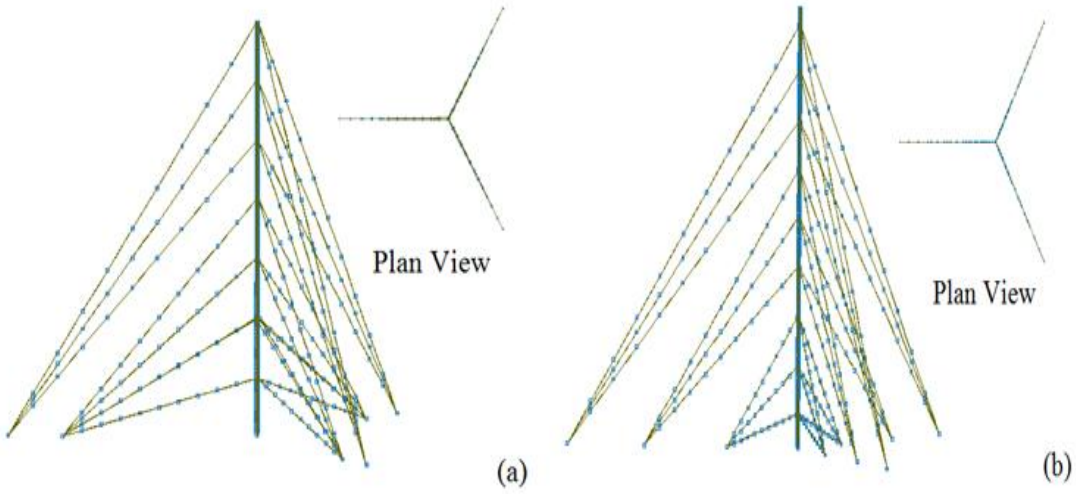

Figure 5.1 *Geometric layout of (a) the 342-m mast, Canada and (b) the 607-m mast, Sacramento, California.*

The second tower is 607.1-m tall and comprises nine guying stay levels arranged in three ground anchor groups (See Figure 5.1b) for a total of 27 guy wires. The dimensions of the mast panel width and height are 3.00 and 2.25 m, respectively.

5.2.4. Seismic loading

Eighty-one measured Californian earthquake records of horizontal accelerations, starting from the Humbolt Bay earthquake in 1937 to the Northridge earthquake in 1994 and representing different frequency contents and strong motion durations have been considered in this study. All data have been taken from PEER (Pacific Earthquake Engineering Research Center) Strong Motion Database[3]. Detailed information on the selected earthquake records and the corresponding analysis results are presented in Ghafari (2010).

[3] http://peer.berkeley.edu/smcat/search.html

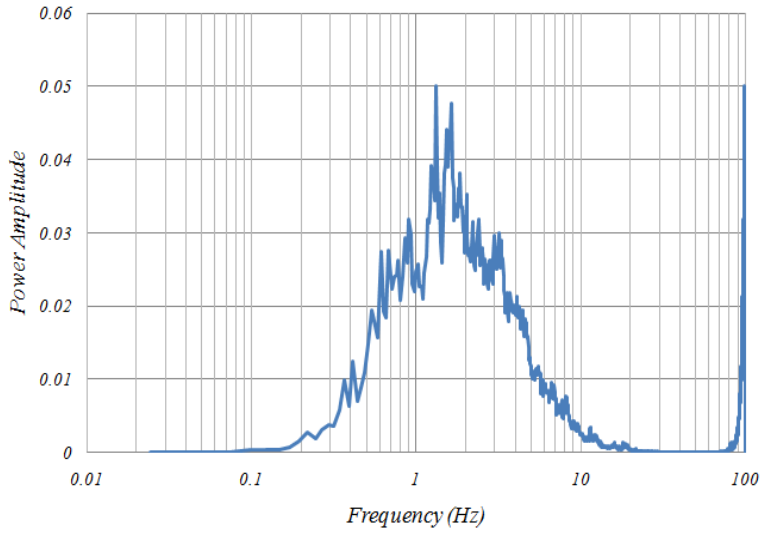

Figure 5.2 The average frequency content of 81 Californian selected earthquakes.

Since most earthquake records of the PEER database are available for several seismological stations, the record with the maximum peak ground acceleration (PGA) has been selected for analysis. Baseline correction was performed using SeismoSignal software (Seismosoft 2010) and all selected records were scaled to have the same peak horizontal ground acceleration value of $PGA = 0.3\,g$. This simple scaling corresponds to the PGA value compatible with the uniform hazard elastic design spectrum of the Canadian National Building Code (NRC 2005) for Victoria (British Columbia), specified for stiff ground and a probability of exceedance of 2% in 50 years. The scaling facilitates the comparison of the results obtained from all the records analysed.

The frequency content and the power spectra of the individual records were studied. Typical high-energy frequency content of world earthquakes is known to lie in the $0.1 - 10\,Hz$ range[4]. The average frequency content of the 81 horizontal earthquake records selected for the study is presented in Figure 5.2, showing peak energy in the

[4] With a concentration in the $0.1 - 10\,Hz$ range for horizontal motion while vertical motion involves the higher frequency band: CSA Standard S37-01 (2001): Antennas, Towers, and Antenna-Supporting Structures, Appendix M: Earthquake-Resistant Design of Towers, Canadian Standards Association, Canada, pp. 106-113.

$0.5 - 4.0\,Hz$ range. Bracketed durations of recorded strong motion (above $0.05\,g$) typically vary between $15\,s$ and $30\,s$. In this research $40\,s$ is conservatively taken as the reference duration for most cases. Other modeling considerations are kept the same as in Ghafari and McClure (STENG-742 and STENG-1145).

5.2.5 Results

The detailed numerical models of the two structures were analyzed in ADINA (2004) under the effects of the 81 earthquake signatures prescribed as synchronous horizontal displacements at the ground support points. Time history plots of the horizontal deformations at the middle point of each guy cable and cable tension forces at the middle point were prepared. Profiles of the maximum horizontal displacements at cable stay

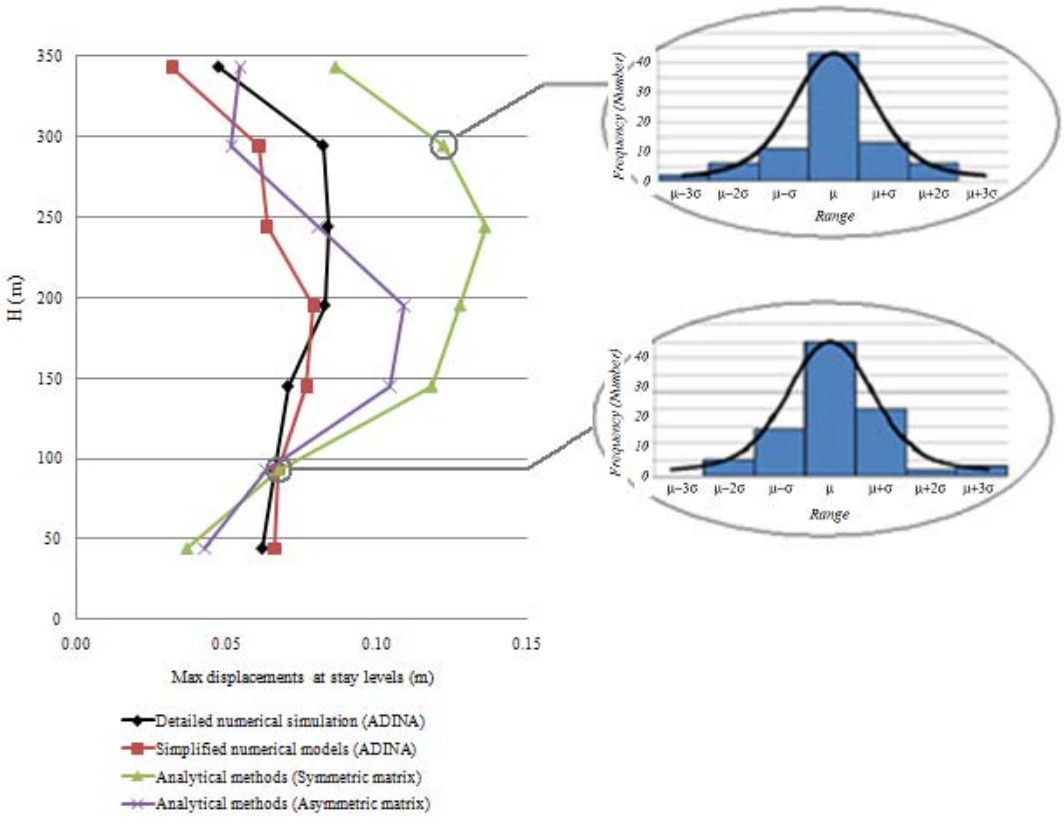

Figure 5.3 *Maximum horizontal displacements of the 342-m mast - average response under the effects of 81 earthquake records scaled to PGA = 0.3 g..*

levels along the height of the masts were also extracted from the detailed finite element analysis results for comparison with the results obtained from the condensed seismic analysis method, as discussed next and illustrated in Figure 5.3 to Figure 5.5. Detailed results of the complete study can be found in Ghafari (2010).

Results labelled as "Simplified numerical models (ADINA)" in the figures were those obtained by replacing the detailed finite element models of the guy cables by linearized springs while the mast structure retained its detailed lattice configuration. The two other curves were obtained from the condensed dynamic analysis models, based on the procedure introduced in Table 4.2 of Ghafari and McClure (STENG-1145) for each earthquake record. In this procedure, the condensed asymmetric flexibility matrix of the structure is assembled and its inverse is non symmetric; the analysis results are labelled

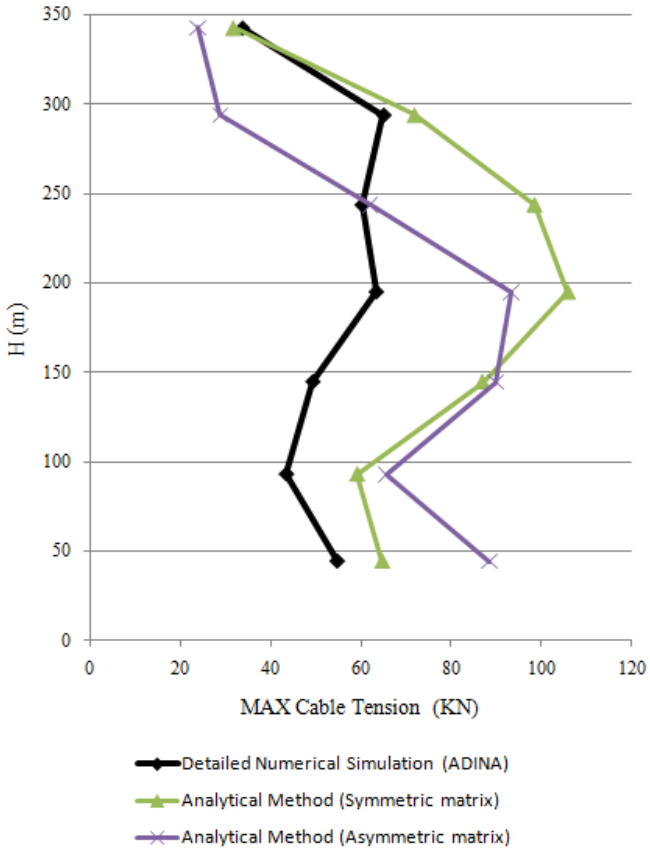

Figure 5.4 Maximum cable tension forces of the 342-m mast - average response.

as “Analytical methods (Asymmetric matrix)”. A last simplification is introduced where the resulting non symmetric matrix is made symmetric by averaging its off-diagonal terms, and these results are labelled as “Analytical models (Symmetric matrix)”. The objective of this comparison is to illustrate whether the symmetric condensed stiffness approach is satisfactory for approximate design checks.

Figure 5.3 plots the envelope curves of the average displacements simulated for the 342-m tower under the 81 earthquake records. Inserts in this figure represent the statistical distribution of the results obtained using the condensed analytical method with symmetric stiffness matrix. Figure 5.4 shows the envelope curves of the average cable tension forces simulated for this tower under the 81 earthquake records. In this figure, results referred as “Analytical Method” were derived based on the developed forces in the linearized springs under the deformation patterns illustrated in Figure 5.3.

The purpose of the condensed method is to provide a conservative (over prediction) of the mast displacements at stay levels for approximate design checks. This is clearly achieved at all guy cluster attachment levels (except for the displacements at the bottom one) in Figure 5.3 and Figure 5.4 when considering the method based on the condensed symmetric stiffness matrix of the mast. The non symmetric method provides less conservative (and more accurate) estimates but it tends to underestimate the maximum response at the top clusters (see Figure 5.3) which is unconservative.

The statistical distribution of the results shown in Figure 5.3 for two selected points, illustrates the variability of the average values predicted. In particular, the narrow distribution of the results at the top cluster confirms that the average value provides a reliable estimate of the maximum probable response of the structure.

Although the proposed condensed method is restricted to tower heights not exceeding 350 m, a global comparison of the different methods is done in Figure 5.5 for the 607-m mast. These results further confirm that the condensed analytical method with symmetric stiffness matrix provides conservative results under synchronous earthquakes on stiff ground.

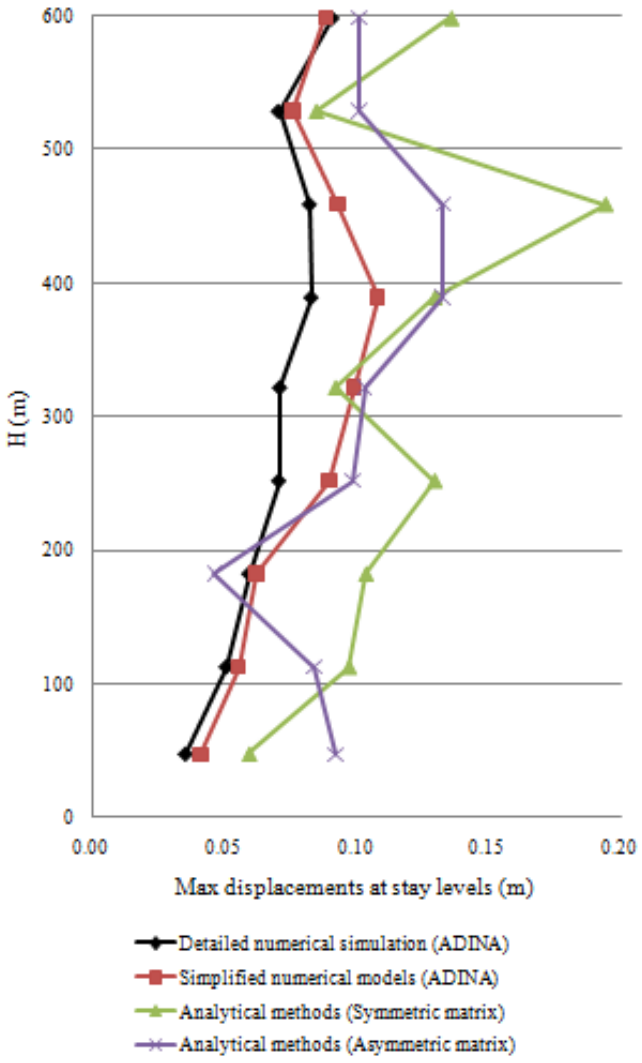

Figure 5.5 *Horizontal displacements of the 607-m mast - average response under the effects of 81 earthquake records scaled to PGA = 0.3 g.*

Overall, the results presented in this note indicate that a more accurate prediction of the mast displacements and cable tension forces is obtained using the condensed model with asymmetric stiffness matrix. However, the approximate symmetric stiffness matrix is more appropriate because it provides a safe overestimation of the mast displacements and cable tension forces. This is the method recommended for design applications.

5.2.5 Conclusions

This technical note confirms the good performance of the robust linearized analysis method presented by the authors for approximate seismic analysis of tall guyed telecommunication masts. The results presented were obtained from four analysis models of two masts subjected to 81 earthquake records scaled at a peak horizontal ground acceleration value of 0.30 g. The simplified method with condensed symmetric stiffness matrix provides a reliable and conservative estimate of the maximum displacements and cable tension forces of the mast at guy cluster attachment levels. The method is intended for approximate design checks of tall masts in the 150 – 350 m; taller masts located in moderate to high seismic areas should be analysed with complete nonlinear seismic analysis models.

References

Please see the last section.

5.3. Predicting maximum seismic force response in the mast: axial compression, shear force and bending moment

In addition to serviceability checks on the deformation profile, telecommunication mast design requires strength verifications for the guy cable tension forces (and ground anchors) and other mast response indicators such as the axial compressive force, the maximum shear force at the cluster attachment levels and the maximum bending moment along the mast. The maximum value of the cable resultant force can be approximated using the predicted value of the maximum horizontal displacements in the mast, Δ and the equivalent dynamic stiffness of the guy cables introduce in Equation (3.12). As such, the horizontal cable resultant force, N_h, can be approximated by Equation (5.1) and the vertical component of the cable resultant force, N_v, can be obtained by Equation (5.2).

$$N_h = 1.5\, K_{dynamic} * \Delta \qquad (5.1)$$

$$N_v = N_h * \tan\theta \qquad (5.2)$$

in which, θ is the guy cable angle with horizon. Based on the simplified models proposed to develop the condensed flexibility matrix of guyed masts and illustrated on Figure 4.11 of Ghafari and McClure (STENG-1145), simple analytical equations are introduced: Equation (5.3) estimates the maximum bending moment in each span of the mast below the cluster, and Equation (5.4) estimates the maximum shear force at each cluster level, assuming guy wires are arranged symmetrically in groups of three.

$$M_{max} = \frac{5}{32}\ N_h\ L \qquad (5.3)$$

$$V_{max} = \frac{2}{3}\ N_h \qquad (5.4)$$

where M_{max} is the maximum bending moment in the intermediate part of each span, V_{max} is the maximum shear force in the mast at each cluster attachment elevation, and L is the corresponding span length.

The maximum axial compression in the mast can be estimated through superimposing the components due to dead loads and the vertical cable tension components obtained at each cluster level, N_v. Recognising that the maximum values of these vertical resultant forces are not synchronous, it is recommended to take their root mean square value to provide a more realistic estimate. No simplified expression is provided for twisting moments as detailed numerical studies have shown that they are only of secondary importance under earthquake effects (Faridafshin, 2006).

6. Conclusions and recommendations for future studies

6.1. Summary and main conclusions

The doctoral research presented in this dissertation has achieved its main goal: to develop a robust and rational approximate method for seismic analysis of tall guyed telecommunication masts.

The method was designed to replace the current complex numerical simulation procedures for the nonlinear seismic analysis of telecommunication towers and provides the engineers of the field with an enhanced design tool to perform simplified seismic design checks for guyed masts. Such procedures are currently available for self-supporting lattice towers but are still lacking for guyed masts; the research was planned to provide the necessary background studies for National Code developments and a simplified method of potential widescale engineering use.

The study focused on enriching the understanding of the complex dynamic behaviour of tall guyed masts under seismic loading. The complexity mainly arises from significant geometric nonlinear response of the guy cables and the interaction between the cables and the mast. In the first part, the research concentrated on the study of the dynamic behaviour and characteristics of guy cables under periodic excitations and equivalent dynamic guy stiffness/mass models were introduced to replace guy cables. The next step was devoted to characterizing cable-mast interactions and the developing simplified condensed dynamic analysis models of the whole mast. The comparison of the results from the simplified method and detailed simulations confirmed the reliability and accuracy of the proposed method.

The validation of the proposed method was carried out by comparing numerical simulation results involving two selected guyed telecommunication masts under the effects of eighty-one Californian earthquake records. It was concluded that the simplified method with condensed symmetric stiffness matrix provided a reliable and conservative

estimate of the maximum displacements and cable tension forces of the mast at guy cluster attachment levels. The method is intended for approximate design checks of tall masts in the 150 – 350 m; taller masts located in moderate to high seismic areas should be analysed with complete nonlinear seismic analysis models.

6.2. Research limitations and recommendations for future work

The research limitations are summarized into two main topics which are discussed in the following: software/computational restrictions and experimental tests. The research was essentially numerical and required extensive simulation work as the detailed nonlinear finite element analysis results served as the reference for the development of the simplified models. Also, the author is fully aware that although detailed numerical models may appear accurate because of their high sophistication, they may overlook some important elements of reality and that such numerical models should, inasmuch as possible, be verified by means of sample field tests and measurements. Computational considerations appear easier to accommodate than physical testing issues. Some field tests have been conducted by utilities and tower' owners, but results are most often kept confidential and not available for public research.

The research was initially planned to take advantage of CLUMEQ Supercomputer Center with supercomputing platforms at two sites, namely Montréal (at McGill University) and Québec City (Université Laval). However, the problem was raised when in practice the efficiency of the parallel computation was not considerable because of the limitations set on the particular academic version of the ADINA license: we could only use a maximum of 4 CPUs (one node) on each job. Moreover, the nature of most numerical simulation throughout this research was time-marching and not so compatible with the substructure scheme of ADINA in parallel computation. As a consequence, most numerical simulations had to be carried out on the slower computing platform available on the departmental graduate computer laboratory. This issue has been solved only recently so other researchers will benefit from tremendous improvement of the computing speed on CLUMEQ.

Another important limitation was related to the field tests and measurement that were originally planned to verify the results of some computer simulations of this research. In summer 2009, there was an initial plan to conduct experimental validation tests of the guy system model with ambient vibration measurements and operational modal analysis on

the 111-m tower located in St. Hyacinthe, Québec, illustrated in Figure 4.1 and E.1. The tower is owned and operated by Hydro Québec and is used for control of its power transmission network. Although considerable time and effort was devoted to design this test plan, the measurements have not been carried out yet (end of summer 2010). Several reasons have explained the delays which were out of control of the research group; however, the measurements should be made in the upcoming year and will therefore be the subject of future studies. Appendix E presents some of the test planning considerations for the St-Hyacinthe mast.

6.3. Application of the proposed method in engineering practice

As discussed in Chapter 1, guidance on earthquake-resistant design and seismic analysis of communication structures is contained in Appendix M of the Canadian Standard CSA-S37-01(R2006) which is not a mandatory part of the Standard. This means that currently seismic design of telecommunication towers is not mandatory, and only very few exceptional mast designs in Canada have actually been verified with a rational seismic analysis approach. With the advent of performance-based design of structures, however, the practice will have to evolve to at least simplified seismic check procedures for masts that are most at risk, as already recommended in Appendix M.

The author believes that the method proposed in this research can be implemented as a special module in specialized mast design software used in industry with due consideration of the Canadian seismicity requirements detailed in the National Building Code of Canada. Finally, it is to be emphasized that the method is intended for design checks of tall masts in the 150 – 350 m range only; taller masts located in moderate to high seismic areas should be analysed with complete nonlinear seismic analysis models. Figure 6.1 illustrates the flow chart indicating how the full procedure looks like in the context of a design office and common engineering practice.

Special attention should be paid to the limitations and the scope of the proposed method for a safe reliable engineering use. The method is originally designed for the masts of 150 to 350 m height with regular distribution of mass and stiffness. Heavy and especial accessories and instruments should be considered properly in the mass matrix. In terms of the distribution of geometry and stiffness, the regular arrangement of guy clusters and proper cable pretension force is of high importance. Frequency analysis is highly recommended to find out suspicious mode shapes and frequencies within the sensitive range of common earthquakes. For the cases of doubtful results, detailed finite element analysis is suggested.

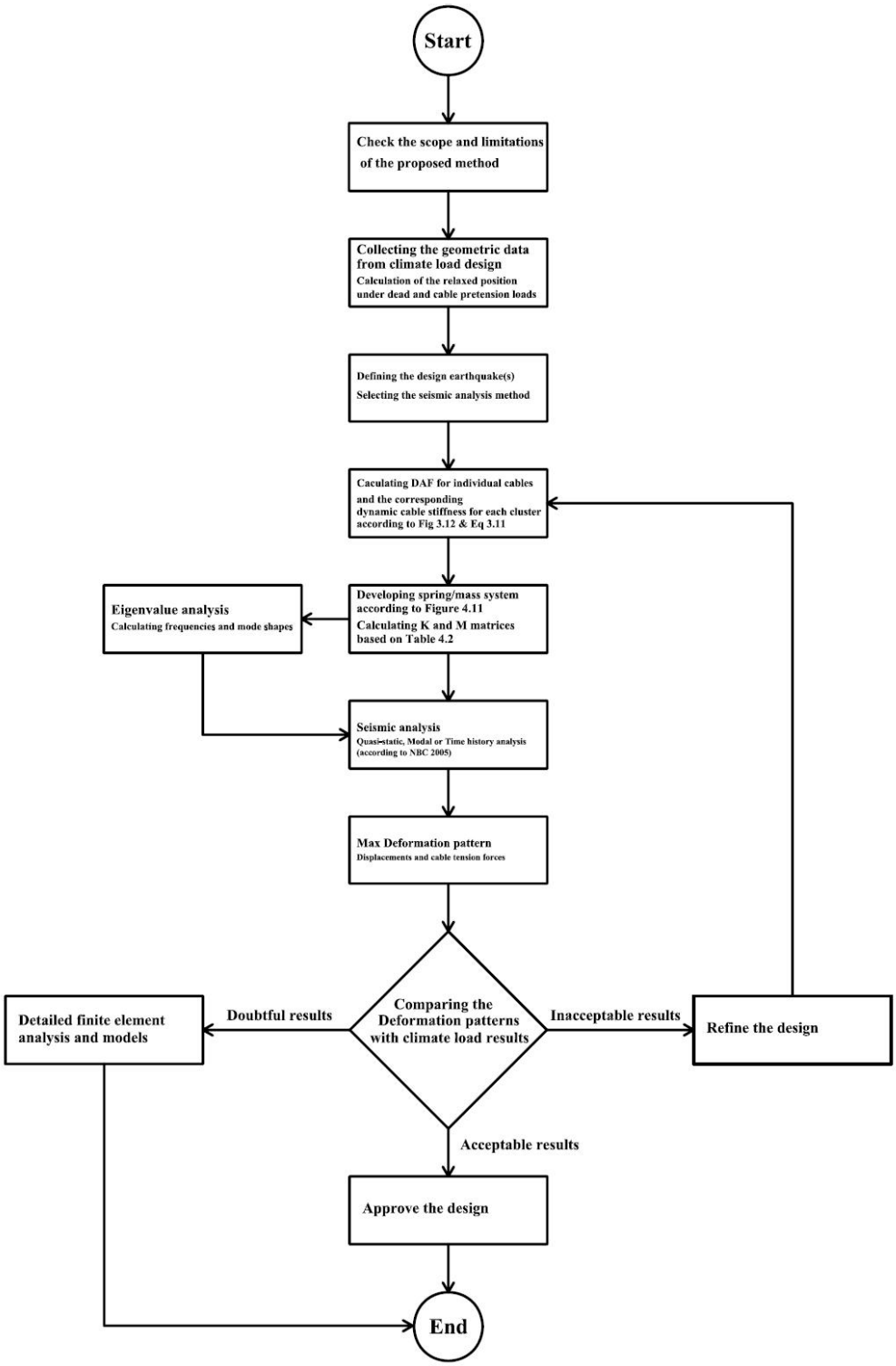

Figure 6.1 *Flow chart showing the steps for siesmic design ckecks of guyed telecommunication masts according to the introduced method.*

Appendix A: History of the static and dynamic analysis of guyed masts

Static analysis

Cohen and Perrin (1957), Hull (1962), Poskitt and Livesley (1963), and Goldberg and Meyers (1965)

Early investigators of the static behaviour of guyed masts have considered the mast as a continuous beam-column resting on nonlinear elastic supports where the spring constants are provided by the lateral stiffness of the guys attached to the shaft.

Shears and Clough (1968)

Considered a finite element idealization for an integrated guyed tower analysis in which parabolic elements were used for the guys and beam-column elements for the mast.

Goldberg and Gaunt (1973)

Studied the stability of guyed towers using linearized slope-deflection equations to analyze a multi-level guyed tower. They considered the secondary effects due to bending and changes in the axial thrust in the mast based on the small deflection theory.

Chajes and Chen (1979), and Chajes and Ling (1981)

Investigated mainly the stability behaviour of short guyed towers with one or two stay levels.

Schrefler, Odorizzi and Wood (1983)

Proposed a method of analysis for combined beam and cable structures using a unified formulation for the geometrically nonlinear analysis of two-dimensional beam and line elements using a total Lagrangian approach.

Fiesenheiser (1957), Odley (1966), Williamson and Margolin (1966), Reichelt, Brown and Melin (1971), Rosenthal and Skop (1980, 1982), and McClure (1984)

These researchers also presented various approaches for static analysis of short guyed masts.

Raman, Surya Kuman and Sreedhara Rao (1988)

Considered static analysis using sub-structuring and finite element techniques for large displacement analysis of guyed towers. Two-node 3-D beam-column elements and two-node 3-D truss elements are employed in the finite element model to discretize the mast and the cables, respectively.

Ekhande and Maduguala (1988)

Studied modelling aspects of geometrically nonlinear effects. They presented a three-dimensional nonlinear static analysis of guyed towers consisting of cable, truss and beam member combinations.

Issa and Avent (1991)

Used a discrete field analysis approach to develop a solution procedure for the analysis of guyed towers. The assumptions of small kinematics and linear elastic behaviour were used for modelling of the tower. The effects of nonlinear cable/tower interaction were also included.

Ben Kahla (1993 and 1995)

Proposed a method for static analysis of guyed towers under wind effects. An assembly of truss and catenary cable elements was considered for the guy cables and the mast was represented by an equivalent beam-column model.

Fahleson (1995)

The effect of wind and ice loads on guyed masts was studied. Measurements were made on a 323-m guyed TV and radio mast in Northern Sweden, equipped with an extensive

data collection system in the winter 1988-89, following the collapse of another mast due to ice overload.

Dynamic Analysis

Davenport (1959)

Developed a linear model to describe the vibration of guy cables under wind loads, assuming that the static deflected shape of the guy is parabolic.

McCaffrey and Hartman (1972)

Proposed a mathematical model to predict the dynamic tower response under wind. They analyzed a 302-m tower with fixed base and five guying levels, using truncated modal superposition (the structure was assumed to oscillate linearly about its static equilibrium position). The mast was modelled as an equivalent beam-column with a lumped mass idealization.

Irvine (1981)

Investigated the dynamic behaviour of guyed towers, with emphasis on analytical expressions for linearized cable vibrations.

Gerstoft and Davenport (1986)

Established a simplified procedure to analyze nonlinear guyed towers under wind loading. The guyed mast itself was modelled as a beam on elastic supports.

Augusti, Borri, Marradi and Spinelli (1986)

Modelled a 200-m mast with three guying stay levels using equivalent linear elastic springs for the guy cables. The inertia effects of the cables were ignored, and the mast was modelled as a space truss with seven lumped masses along its height.

Buchholdt, Moosavinejad and Iannuzzi (1986)

Studied time domain methods and compared them with linear frequency domain methods for structures subjected to wind loads and guy ruptures.

Augusti, Borri and Gusella (1990)

Reported the results of the detailed geometrically nonlinear analyses of two guyed towers (130-m and 275-m) under wind loading.

Argyris and Mlejnek (1991)

Analyzed a 152.5-m transmitter tower with two guying stay levels subjected to an idealized sinusoidal earthquake loading (as a rough simulation of an earthquake).

Lin (1994)

Studied the transient response of guyed telecommunication towers subjected to sudden cable ice-shedding using detailed nonlinear time-domain numerical simulations.

Appendix B: Partial results on periodic excitation studies

This appendix presents some detailed results of the time histories of the vertical displacements and the cable tension forces at the middle of the cables of the studied masts to harmonic loading with different frequencies. Different approaches are compared throughout these graphs in order to validate the proposed simplified methods in chapter 2.

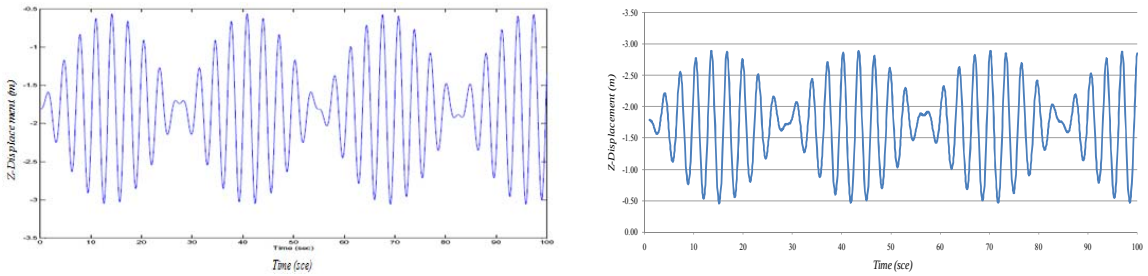

Figure B.1. Vertical Displacement of the middle point of 7th cable, 213-m mast to harmonic loading with frequency of 0.3 Hz: Detailed Nonlinear (Right) vs. Proposed SDOF Method (Left).

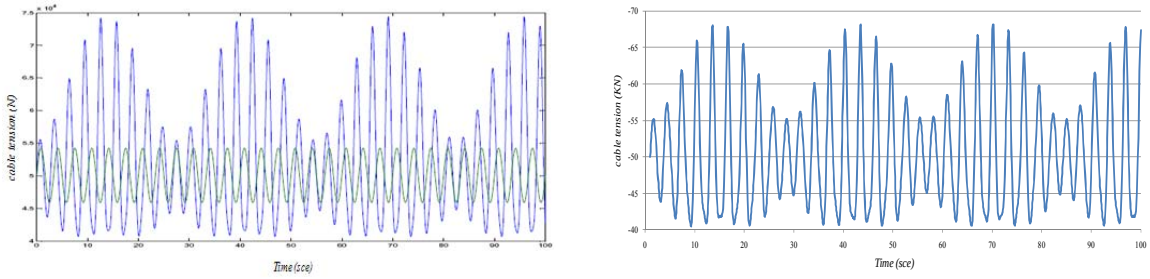

Figure B.2. Cable Tension force at the middle point of 7th cable, 213-m mast to harmonic loading with frequency of 0.3 Hz: Detailed Nonlinear (Right) vs. Proposed SDOF Method (Left).

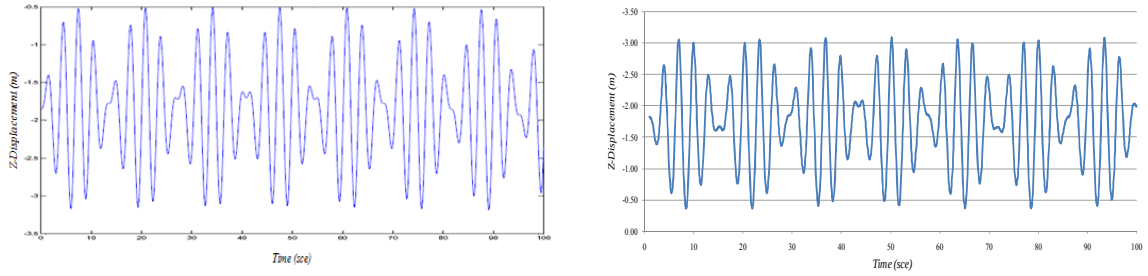

Figure B.3. Vertical Displacement of the middle point of 6th cable, 213-m mast to harmonic loading with frequency of 0.3 Hz: Detailed Nonlinear (Right) vs. Proposed SDOF Method (Left).

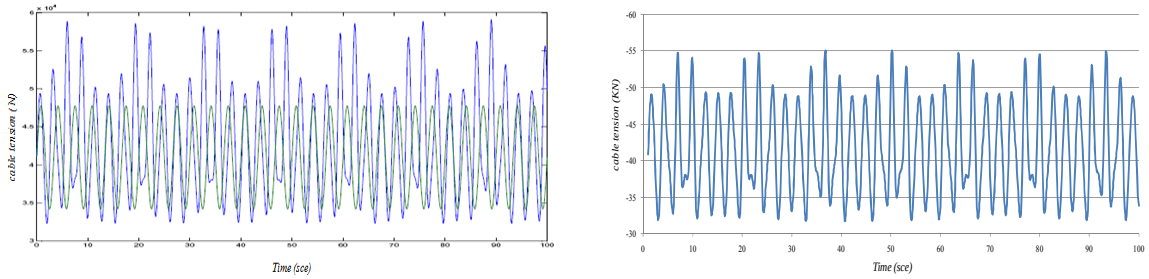

Figure B.4. Cable Tension force at the middle point of 6th cable, 213-m mast to harmonic loading with frequency of 0.3 Hz: Detailed Nonlinear (Right) vs. Proposed SDOF Method (Left).

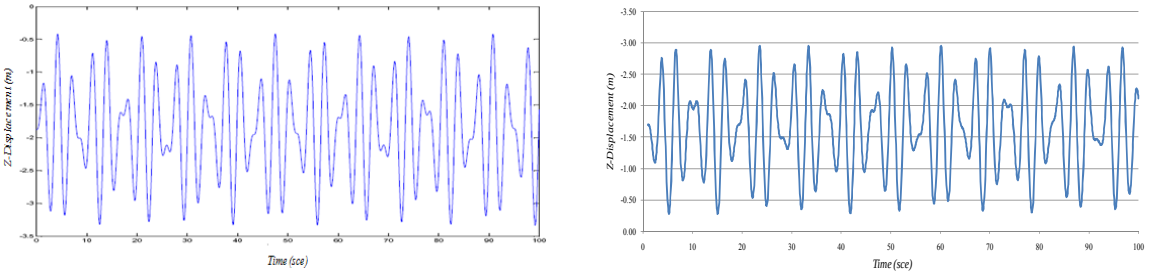

Figure B.5. Vertical Displacement of the middle point of 5th cable, 213-m mast to harmonic loading with frequency of 0.3 Hz: Detailed Nonlinear (Right) vs. Proposed SDOF Method (Left).

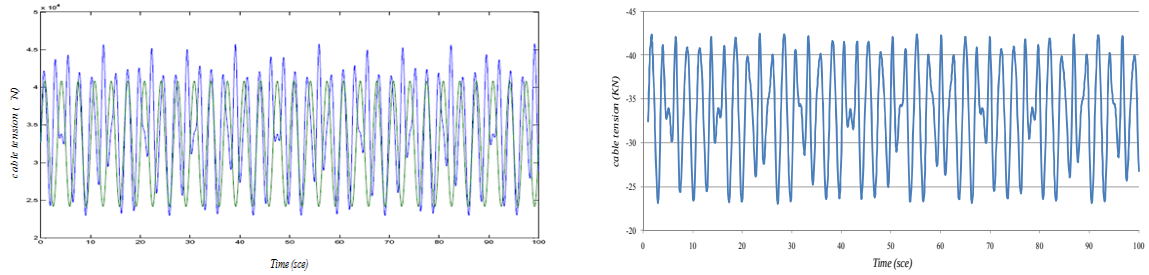

Figure B.6. Cable Tension force at the middle point of 5th cable, 213-m mast to harmonic loading with frequency of 0.3 Hz: Detailed Nonlinear (Right) vs. Proposed SDOF Method (Left).

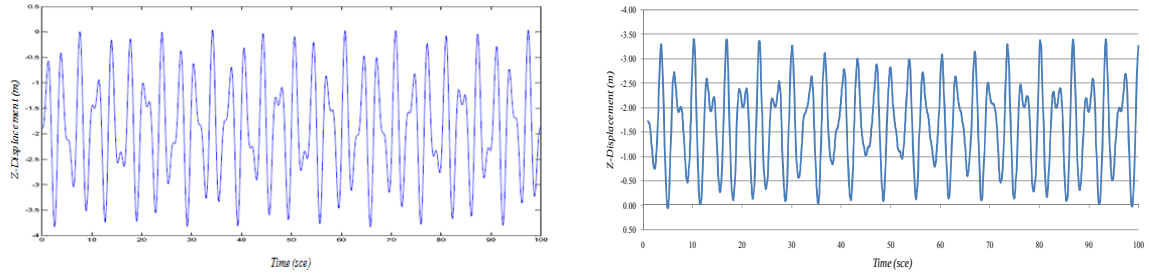

Figure B.7. Vertical Displacement of the middle point of 4th cable, 213-m mast to harmonic loading with frequency of 0.3 Hz: Detailed Nonlinear (Right) vs. Proposed SDOF Method (Left).

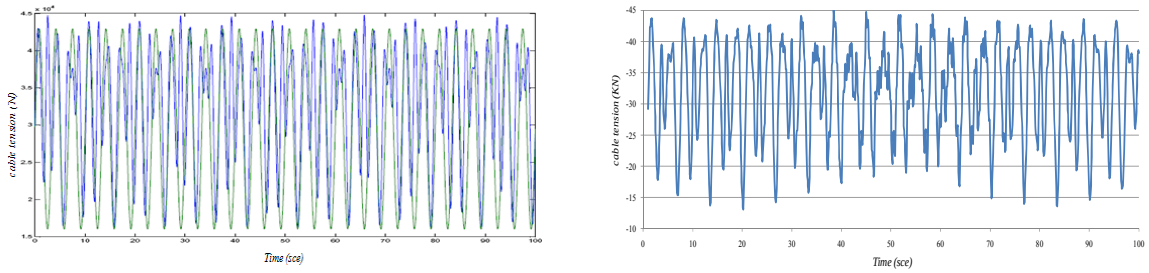

Figure B.8. Cable Tension force at the middle point of 4th cable, 213-m mast to harmonic loading with frequency of 0.3 Hz: Detailed Nonlinear (Right) vs. Proposed SDOF Method (Left).

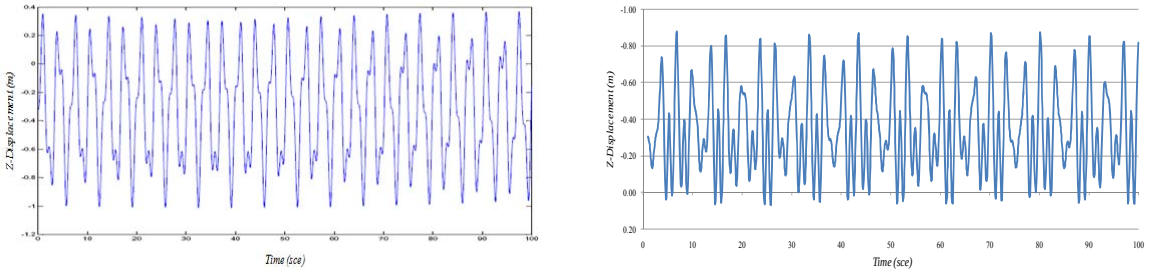

Figure B.9. Vertical Displacement of the middle point of 3rd cable, 213-m mast to harmonic loading with frequency of 0.3 Hz: Detailed Nonlinear (Right) vs. Proposed SDOF Method (Left).

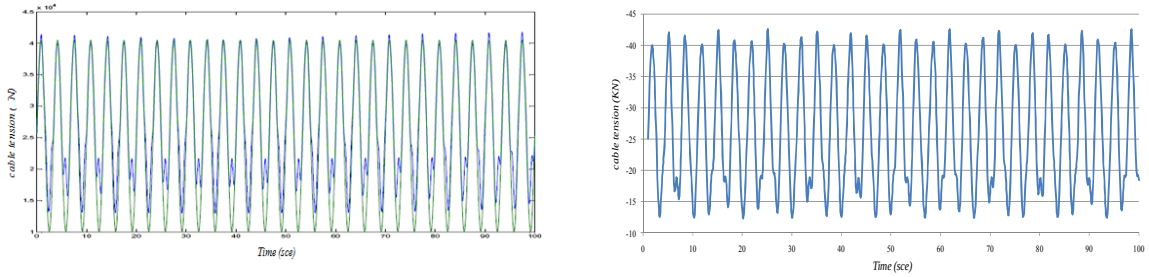

Figure B.10. Cable Tension force at the middle point of 3rd cable, 213-m mast to harmonic loading with frequency of 0.3 Hz: Detailed Nonlinear (Right) vs. Proposed SDOF Method (Left).

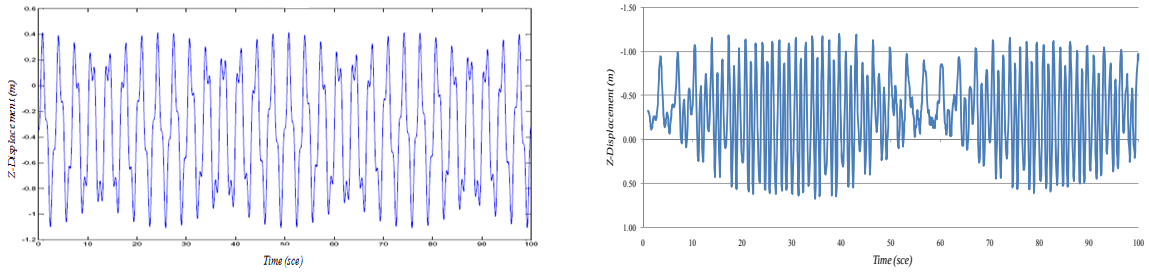

Figure B.11. Vertical Displacement of the middle point of 2nd cable, 213-m mast to harmonic loading with frequency of 0.3 Hz: Detailed Nonlinear (Right) vs. Proposed SDOF Method (Left).

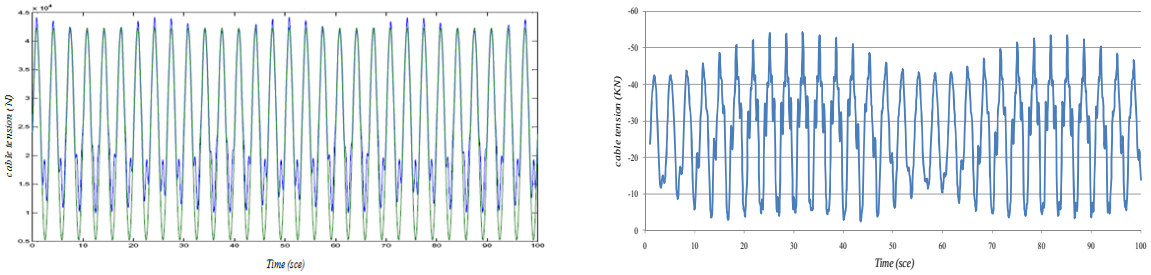

Figure B.12. Cable Tension force at the middle point of 2nd cable, 213-m mast to harmonic loading with frequency of 0.3 Hz: Detailed Nonlinear (Right) vs. Proposed SDOF Method (Left).

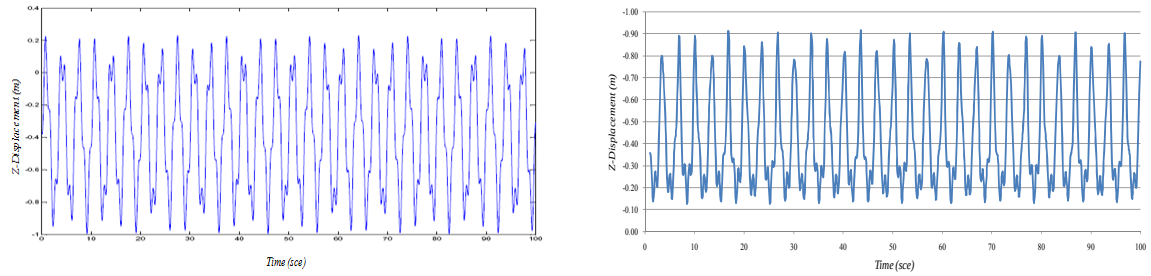

Figure B.13. Vertical Displacement of the middle point of 1st cable, 213-m mast to harmonic loading with frequency of 0.3 Hz: Detailed Nonlinear (Right) vs. Proposed SDOF Method (Left).

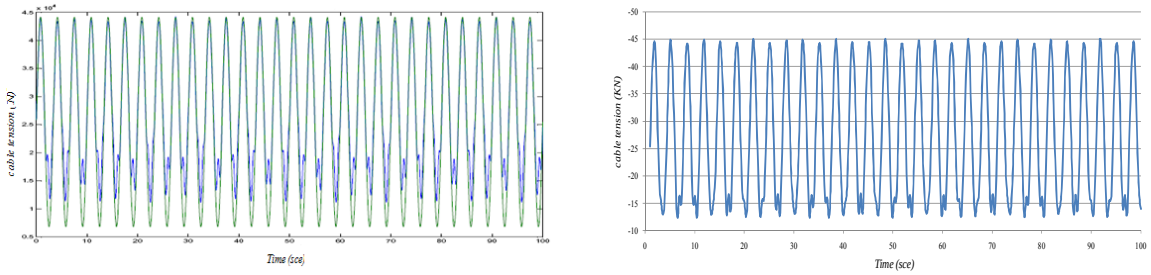

Figure B.14. Cable Tension force at the middle point of 1st cable, 213-m mast to harmonic loading with frequency of 0.3 Hz: Detailed Nonlinear (Right) vs. Proposed SDOF Method (Left).

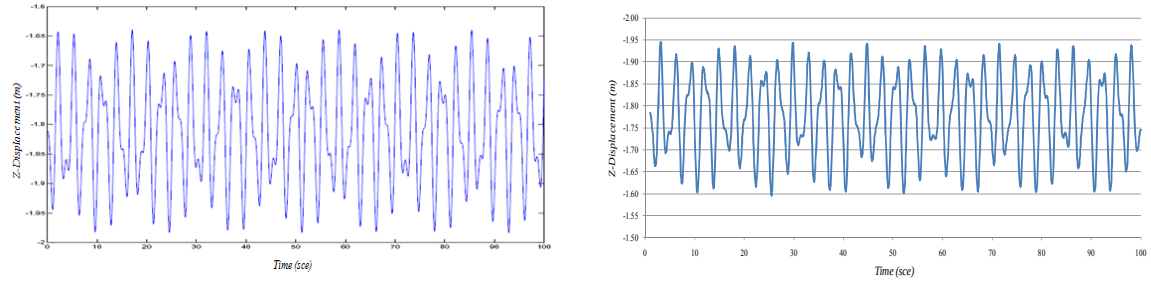

Figure B.15. Vertical Displacement of the middle point of 7th cable, 213-m mast to harmonic loading with frequency of 0.6 Hz: Detailed Nonlinear (Right) vs. Proposed SDOF Method (Left).

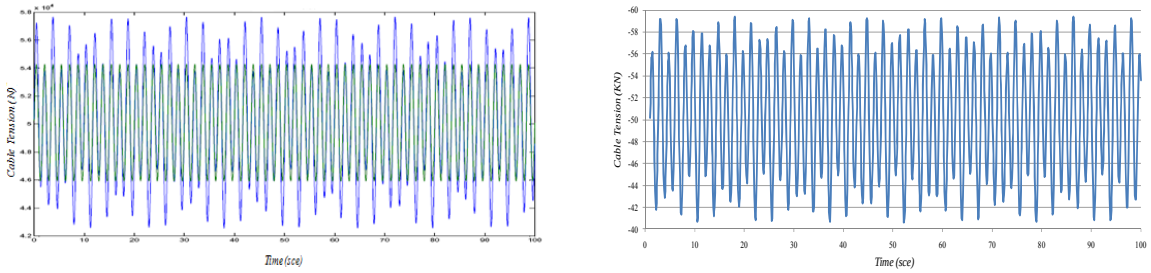

Figure B.16. Cable Tension force at the middle point of 7th cable, 213-m mast to harmonic loading with frequency of 0.6 Hz: Detailed Nonlinear (Right) vs. Proposed SDOF Method (Left).

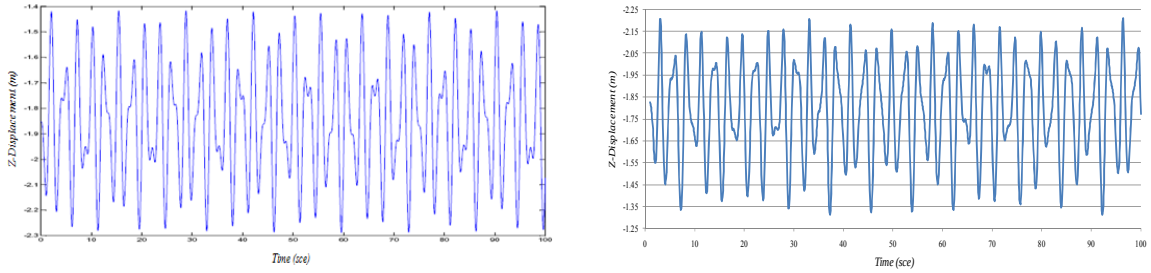

Figure B.17. Vertical Displacement of the middle point of 6th cable, 213-m mast to harmonic loading with frequency of 0.6 Hz: Detailed Nonlinear (Right) vs. Proposed SDOF Method (Left).

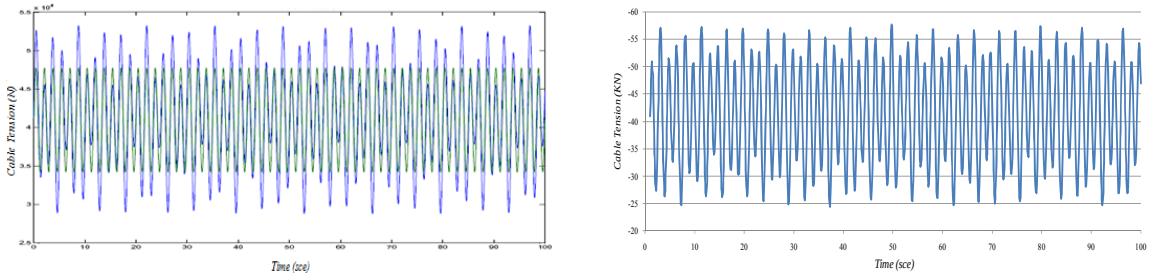

Figure B.18. Cable Tension force at the middle point of 6th cable, 213-m mast to harmonic loading with frequency of 0.6 Hz: Detailed Nonlinear (Right) vs. Proposed SDOF Method (Left).

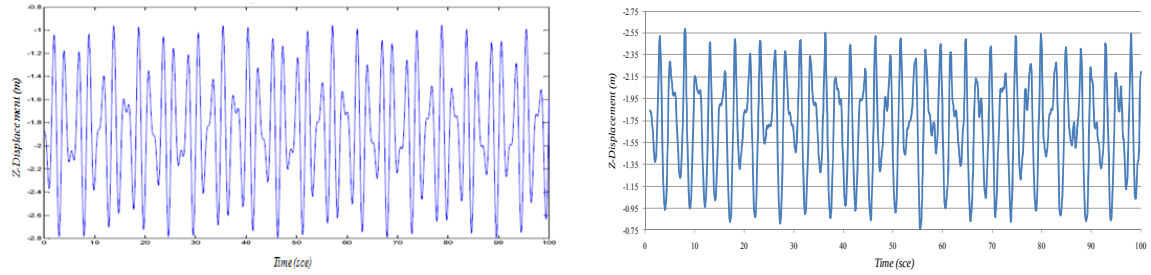

Figure B.19. Vertical Displacement of the middle point of 5th cable, 213-m mast to harmonic loading with frequency of 0.6 Hz: Detailed Nonlinear (Right) vs. Proposed SDOF Method (Left).

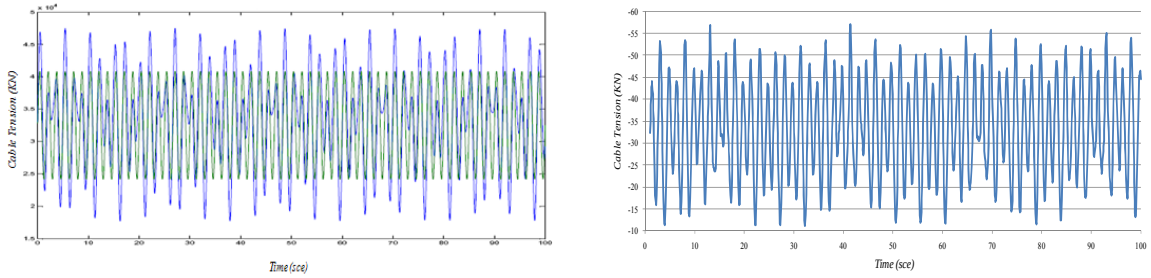

Figure B.20. Cable Tension force at the middle point of 5th cable, 213-m mast to harmonic loading with frequency of 0.6 Hz: Detailed Nonlinear (Right) vs. Proposed SDOF Method (Left).

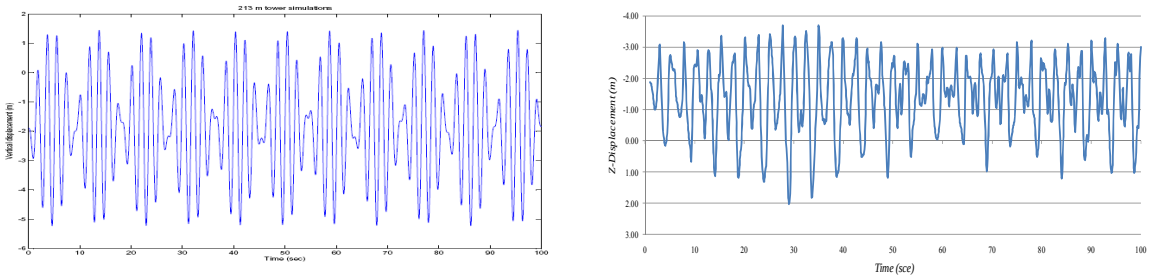

Figure B.21. Vertical Displacement of the middle point of 4th cable, 213-m mast to harmonic loading with frequency of 0.6 Hz: Detailed Nonlinear (Right) vs. Proposed SDOF Method (Left).

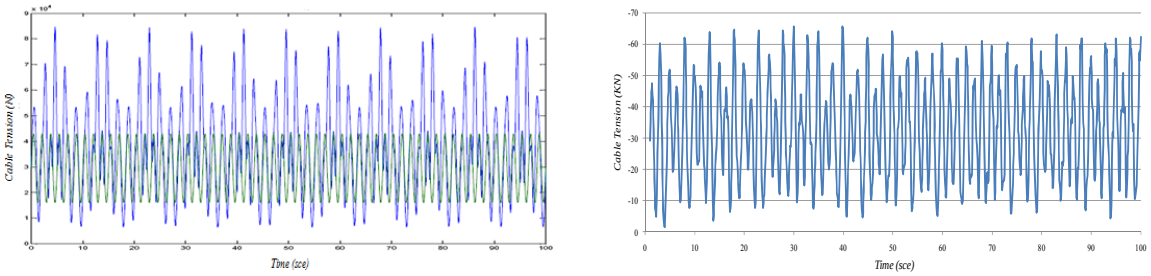

Figure B.22. Cable Tension force at the middle point of 4th cable, 213-m mast to harmonic loading with frequency of 0.6 Hz: Detailed Nonlinear (Right) vs. Proposed SDOF Method (Left).

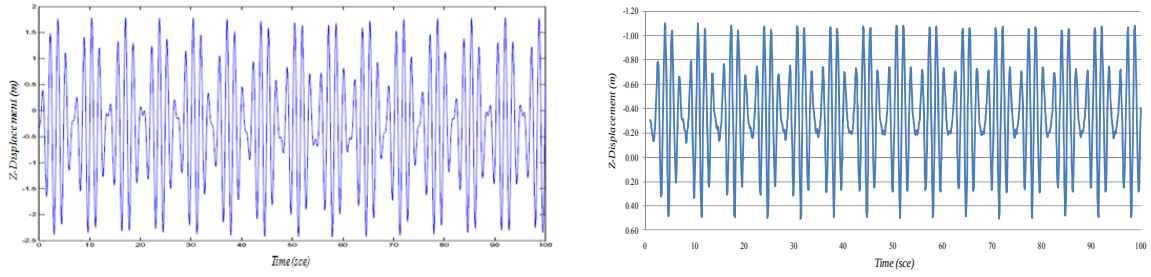

Figure B.23. Vertical Displacement of the middle point of 3rd cable, 213-m mast to harmonic loading with frequency of 0.6 Hz: Detailed Nonlinear (Right) vs. Proposed SDOF Method (Left).

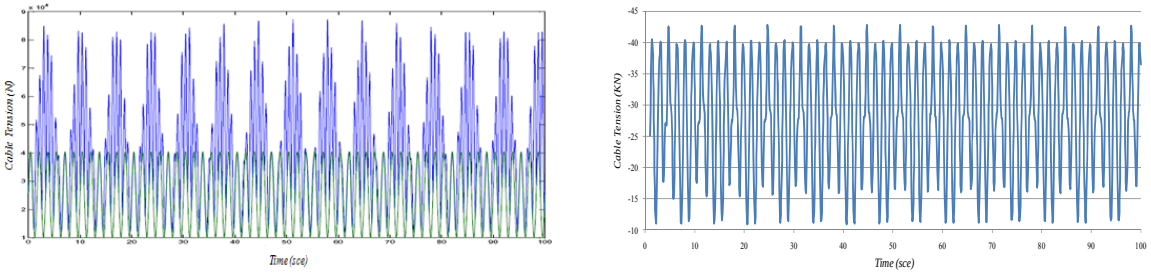

Figure B.24. Cable Tension force at the middle point of 3rd cable, 213-m mast to harmonic loading with frequency of 0.6 Hz: Detailed Nonlinear (Right) vs. Proposed SDOF Method (Left).

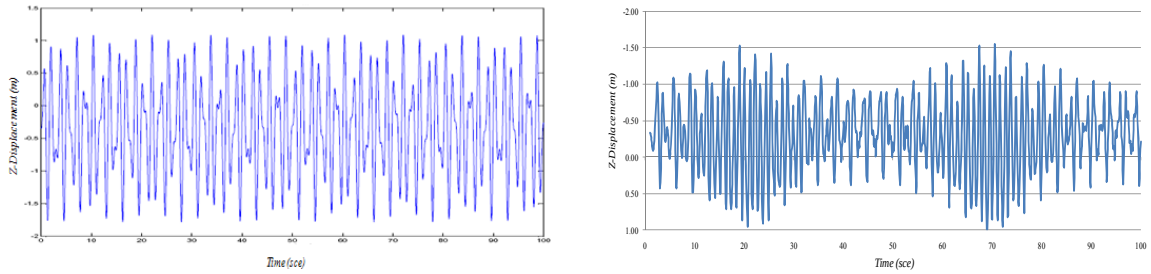

Figure B.25. Vertical Displacement of the middle point of 2nd cable, 213-m mast to harmonic loading with frequency of 0.6 Hz: Detailed Nonlinear (Right) vs. Proposed SDOF Method (Left).

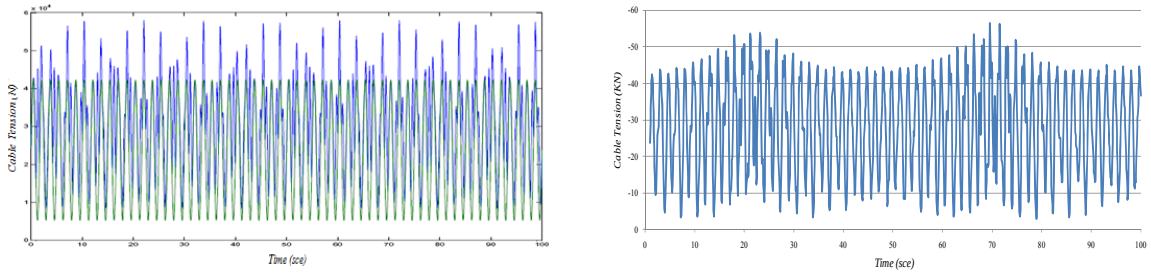

Figure B.26. Cable Tension force at the middle point of 2nd cable, 213-m mast to harmonic loading with frequency of 0.6 Hz: Detailed Nonlinear (Right) vs. Proposed SDOF Method (Left).

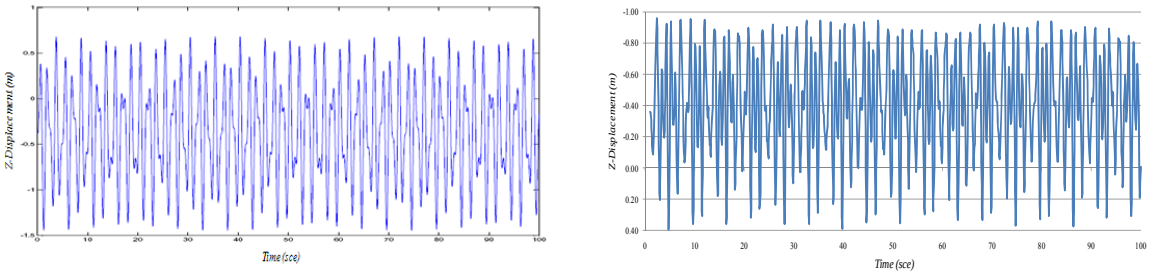

Figure B.27. Vertical Displacement of the middle point of 1st cable, 213-m mast to harmonic loading with frequency of 0.6 Hz: Detailed Nonlinear (Right) vs. Proposed SDOF Method (Left).

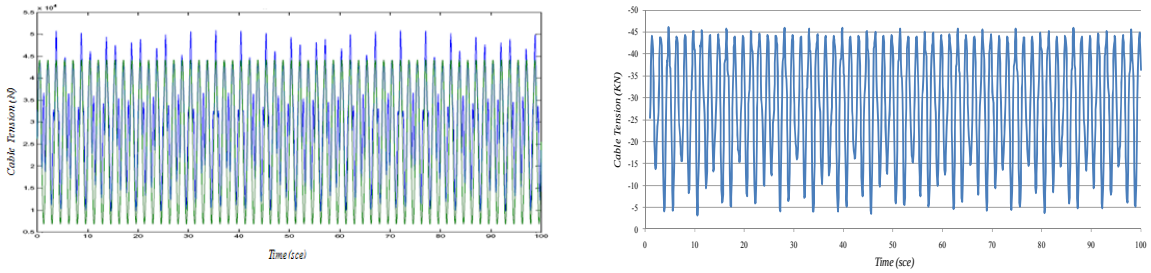

Figure B.28. Cable Tension force at the middle point of 1st cable, 213-m mast to harmonic loading with frequency of 0.6 Hz: Detailed Nonlinear (Right) vs. Proposed SDOF Method (Left).

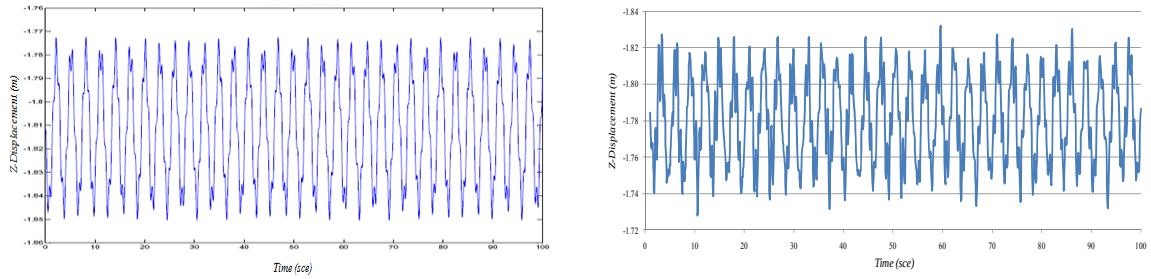

Figure B.29. Vertical Displacement of the middle point of 7th cable, 213-m mast to harmonic loading with frequency of 1.5 Hz: Detailed Nonlinear (Right) vs. Proposed SDOF Method (Left).

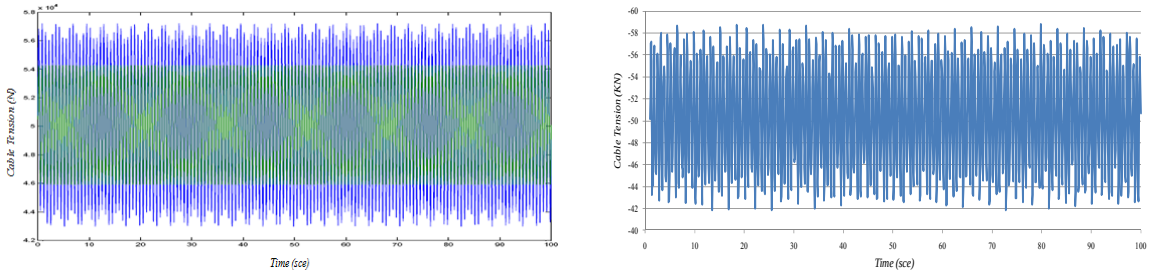

Figure B.30. Cable Tension force at the middle point of 7th cable, 213-m mast to harmonic loading with frequency of 1.5 Hz: Detailed Nonlinear (Right) vs. Proposed SDOF Method (Left).

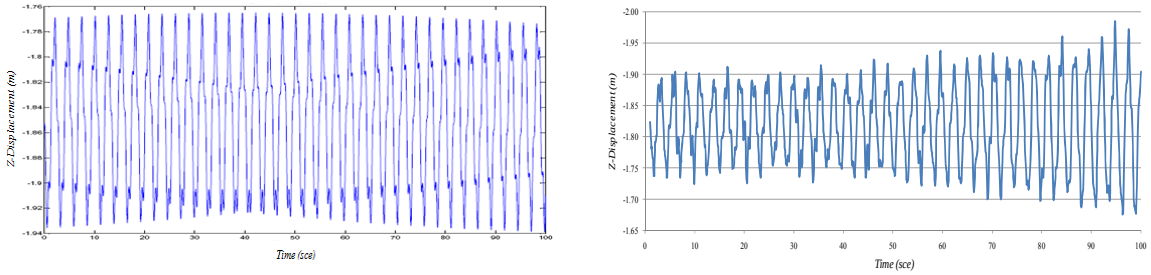

Figure B.31. Vertical Displacement of the middle point of 6th cable, 213-m mast to harmonic loading with frequency of 1.5 Hz: Detailed Nonlinear (Right) vs. Proposed SDOF Method (Left).

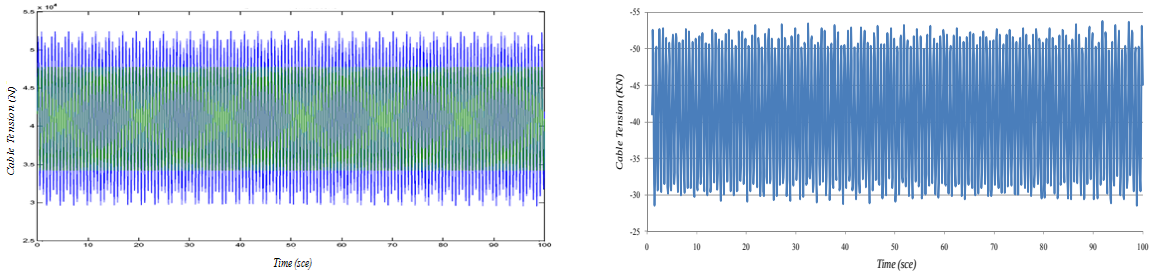

Figure B.32. Cable Tension force at the middle point of 6th cable, 213-m mast to harmonic loading with frequency of 1.5 Hz: Detailed Nonlinear (Right) vs. Proposed SDOF Method (Left).

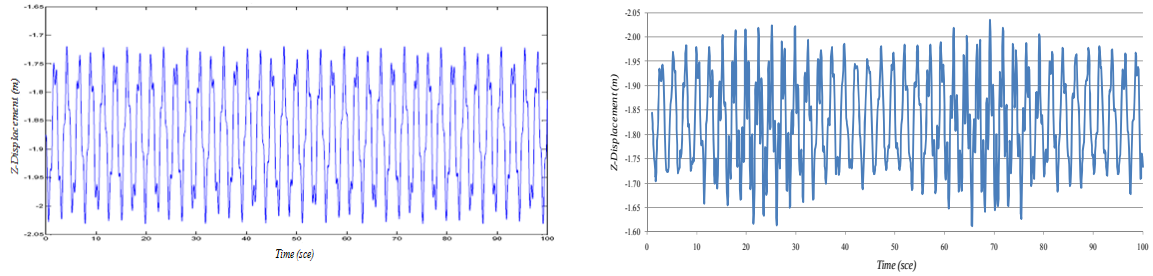

Figure B.33. Vertical Displacement of the middle point of 5th cable, 213-m mast to harmonic loading with frequency of 1.5 Hz: Detailed Nonlinear (Right) vs. Proposed SDOF Method (Left).

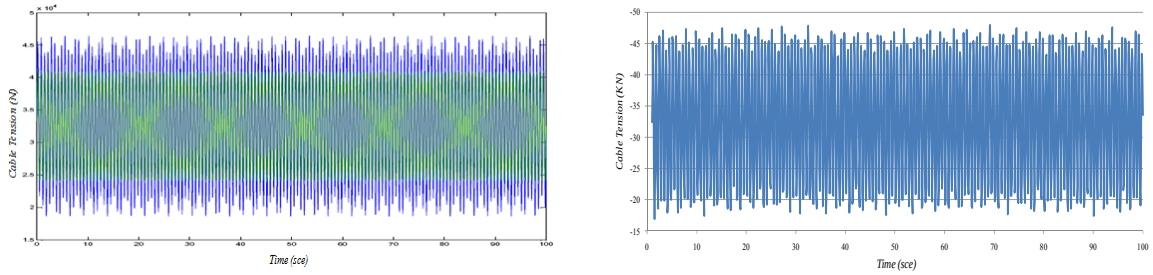

Figure B.34. Cable Tension force at the middle point of 5th cable, 213-m mast to harmonic loading with frequency of 1.5 Hz: Detailed Nonlinear (Right) vs. Proposed SDOF Method (Left).

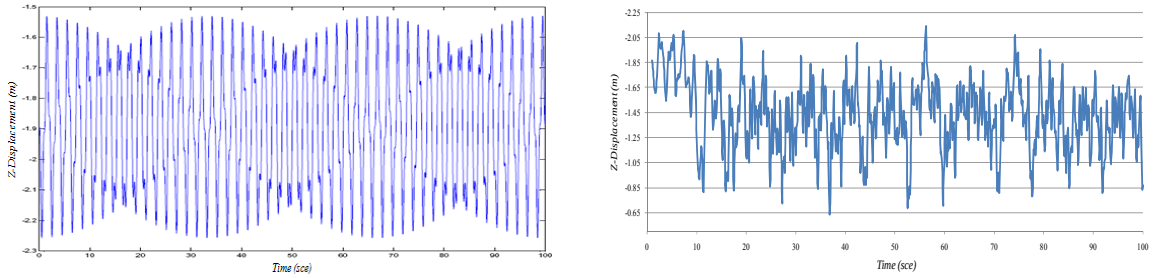

Figure B.35. Vertical Displacement of the middle point of 4th cable, 213-m mast to harmonic loading with frequency of 1.5 Hz: Detailed Nonlinear (Right) vs. Proposed SDOF Method (Left).

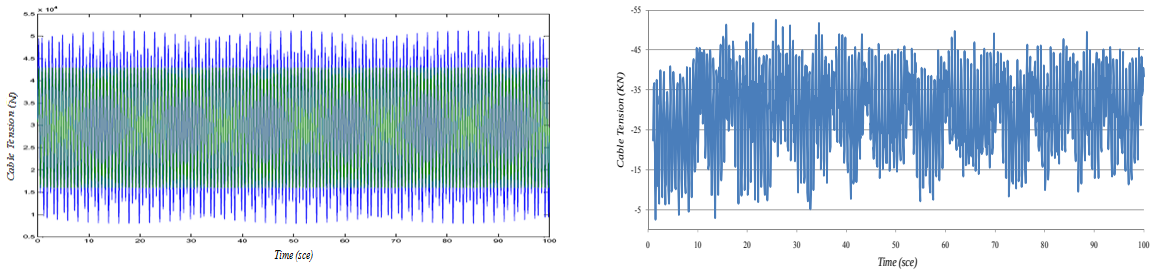

Figure B.36. Cable Tension force at the middle point of 4th cable, 213-m mast to harmonic loading with frequency of 1.5 Hz: Detailed Nonlinear (Right) vs. Proposed SDOF Method (Left).

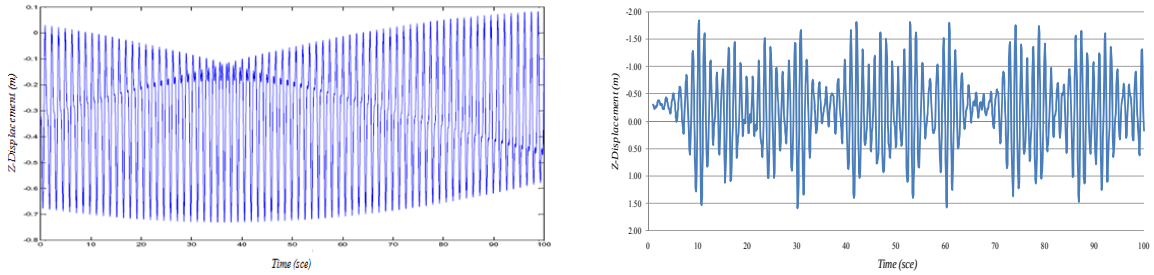

Figure B.37. Vertical Displacement of the middle point of 3rd cable, 213-m mast to harmonic loading with frequency of 1.5 Hz: Detailed Nonlinear (Right) vs. Proposed SDOF Method (Left).

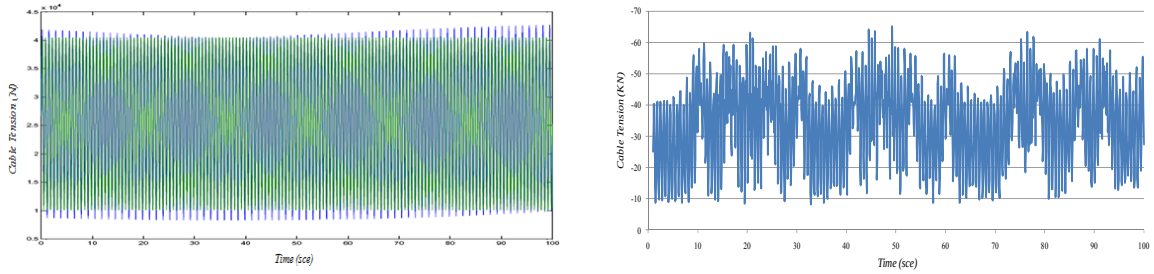

Figure B.38. Cable Tension force at the middle point of 3rd cable, 213-m mast to harmonic loading with frequency of 1.5 Hz: Detailed Nonlinear (Right) vs. Proposed SDOF Method (Left).

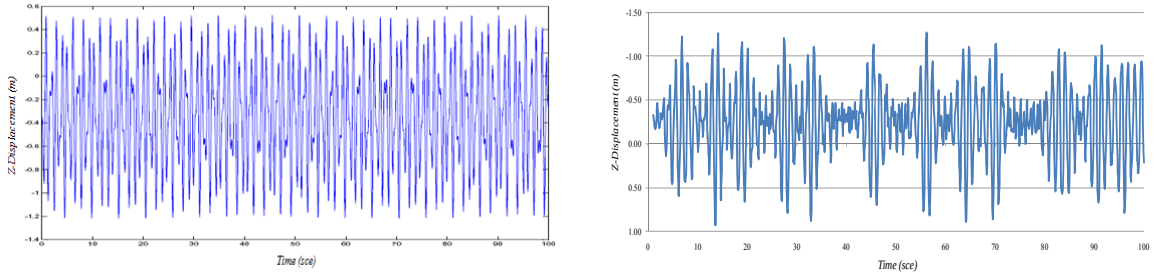

Figure B.39. Vertical Displacement of the middle point of 2nd cable, 213-m mast to harmonic loading with frequency of 1.5 Hz: Detailed Nonlinear (Right) vs. Proposed SDOF Method (Left).

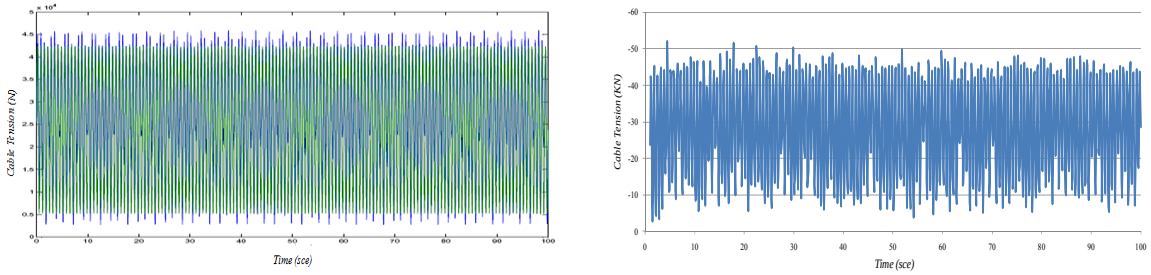

Figure B.40. Cable Tension force at the middle point of 2nd cable, 213-m mast to harmonic loading with frequency of 1.5 Hz: Detailed Nonlinear (Right) vs. Proposed SDOF Method (Left).

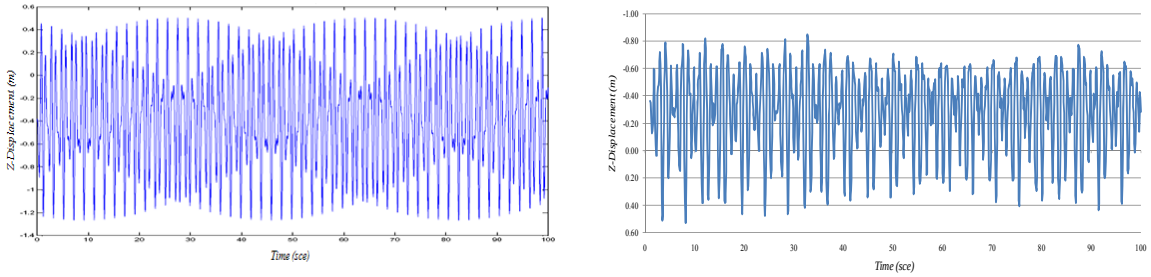

Figure B.41. Cable Tension force at the middle point of 1st cable, 213-m mast to harmonic loading with frequency of 1.5 Hz: Detailed Nonlinear (Right) vs. Proposed SDOF Method (Left).

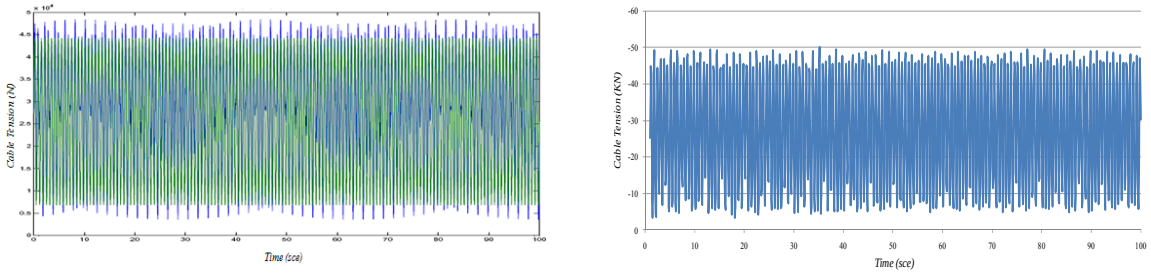

Figure B.42. Cable Tension force at the middle point of 1st cable, 213-m mast to harmonic loading with frequency of 1.5 Hz: Detailed Nonlinear (Right) vs. Proposed SDOF Method (Left).

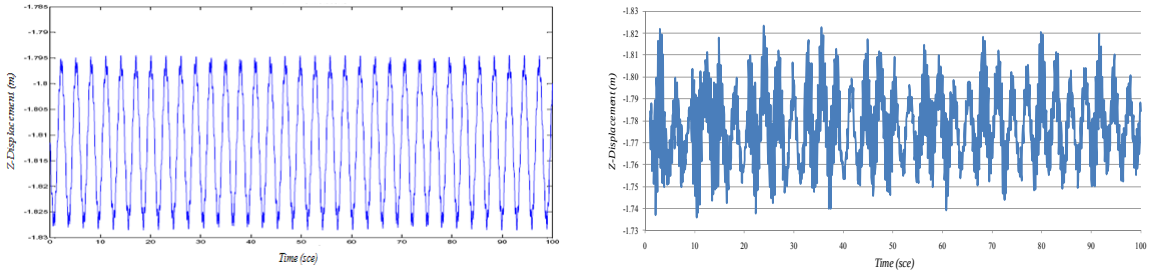

Figure B.43. Cable Tension force at the middle point of 7th cable, 213-m mast to harmonic loading with frequency of 3.0 Hz: Detailed Nonlinear (Right) vs. Proposed SDOF Method (Left).

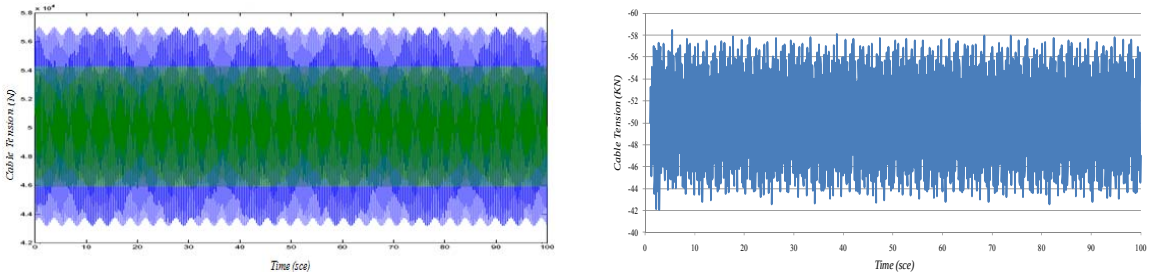

Figure B.44. Cable Tension force at the middle point of 7th cable, 213-m mast to harmonic loading with frequency of 3.0 Hz: Detailed Nonlinear (Right) vs. Proposed SDOF Method (Left).

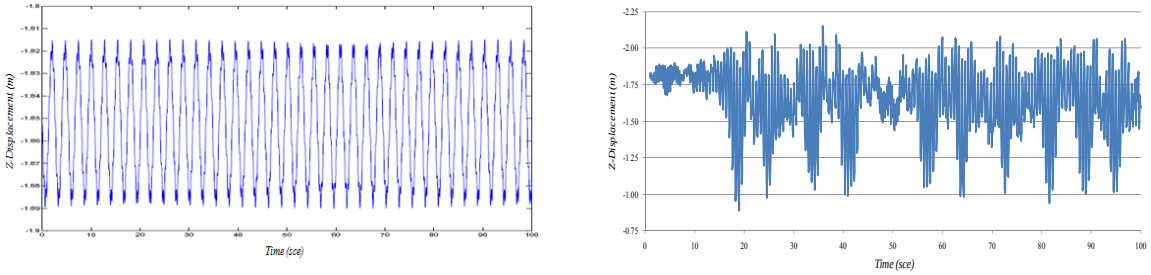

Figure B.45. Cable Tension force at the middle point of 6th cable, 213-m mast to harmonic loading with frequency of 3.0 Hz: Detailed Nonlinear (Right) vs. Proposed SDOF Method (Left).

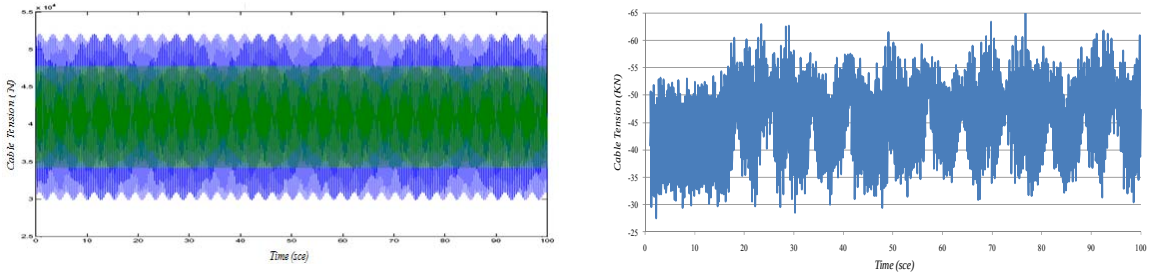

Figure B.46. Cable Tension force at the middle point of 6th cable, 213-m mast to harmonic loading with frequency of 3.0 Hz: Detailed Nonlinear (Right) vs. Proposed SDOF Method (Left).

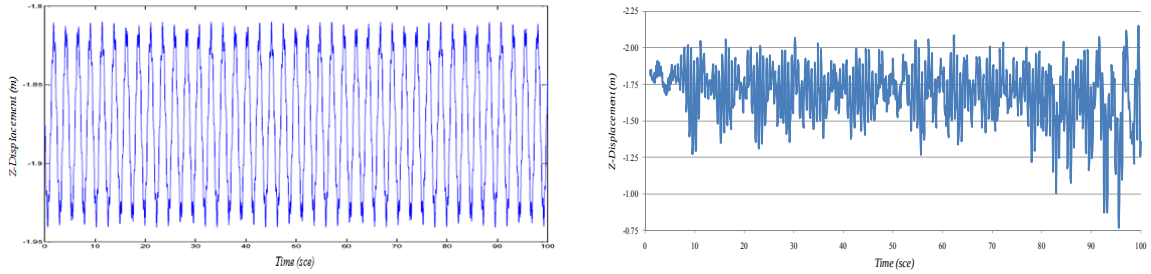

Figure B.47. Cable Tension force at the middle point of 5th cable, 213-m mast to harmonic loading with frequency of 3.0 Hz: Detailed Nonlinear (Right) vs. Proposed SDOF Method (Left).

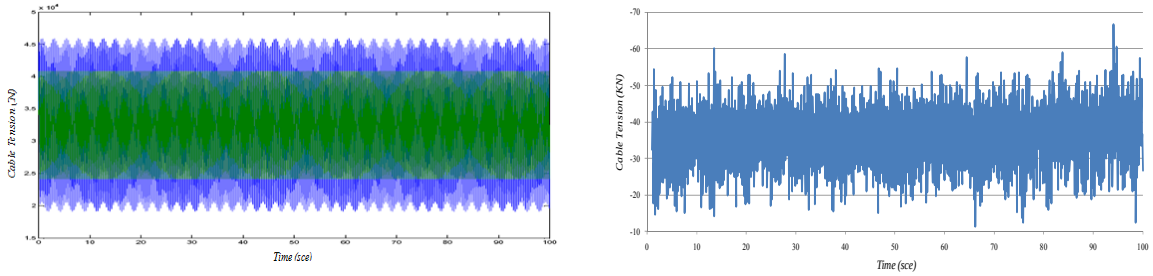

Figure B.48. Cable Tension force at the middle point of 5th cable, 213-m mast to harmonic loading with frequency of 3.0 Hz: Detailed Nonlinear (Right) vs. Proposed SDOF Method (Left).

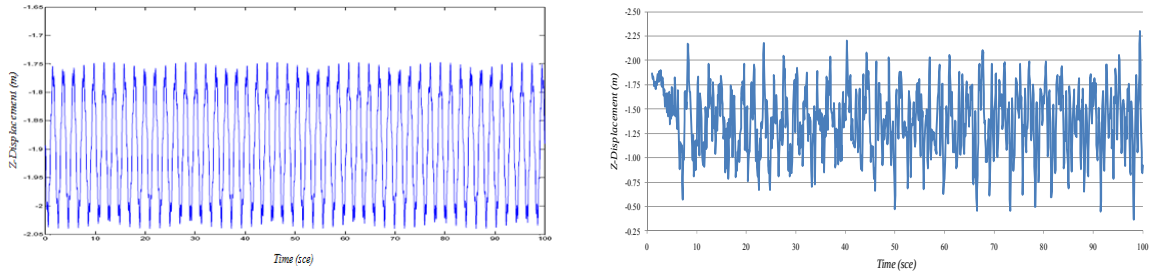

Figure B.49. Cable Tension force at the middle point of 4th cable, 213-m mast to harmonic loading with frequency of 3.0 Hz: Detailed Nonlinear (Right) vs. Proposed SDOF Method (Left).

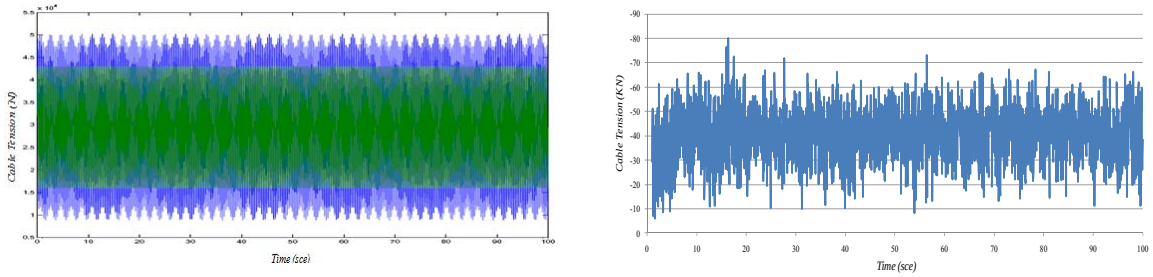

Figure B.50. Cable Tension force at the middle point of 4th cable, 213-m mast to harmonic loading with frequency of 3.0 Hz: Detailed Nonlinear (Right) vs. Proposed SDOF Method (Left).

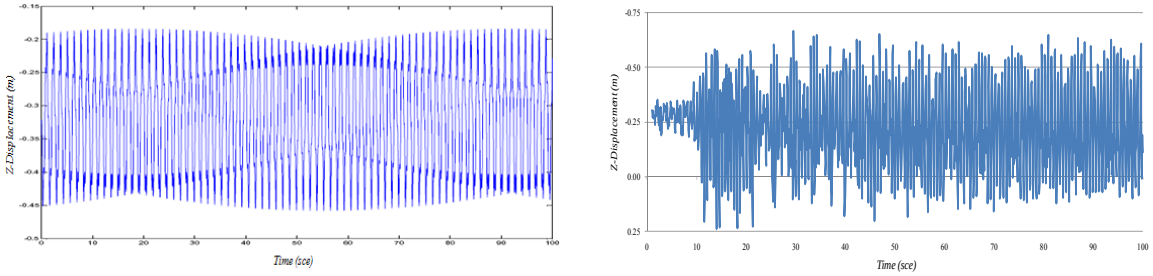

Figure B.51. Cable Tension force at the middle point of 3rd cable, 213-m mast to harmonic loading with frequency of 3.0 Hz: Detailed Nonlinear (Right) vs. Proposed SDOF Method (Left).

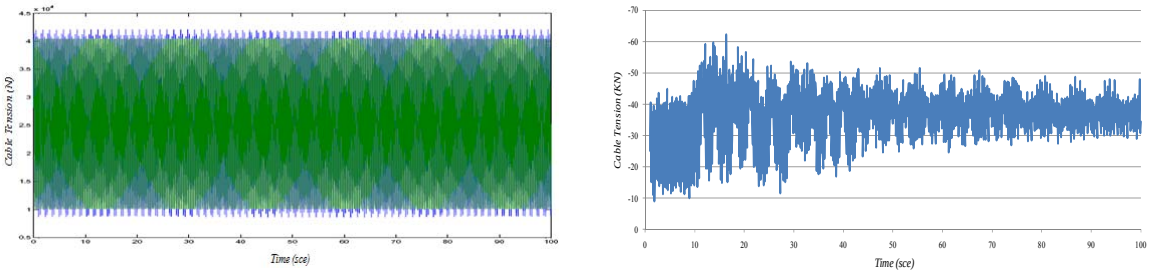

Figure B.52. Cable Tension force at the middle point of 3rd cable, 213-m mast to harmonic loading with frequency of 3.0 Hz: Detailed Nonlinear (Right) vs. Proposed SDOF Method (Left).

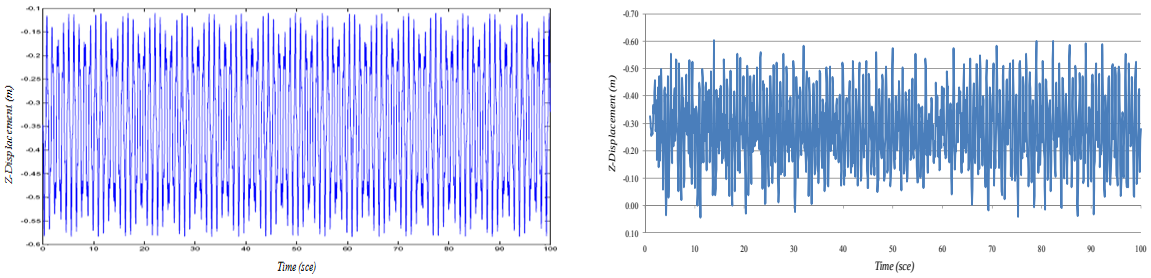

Figure B.53. Cable Tension force at the middle point of 2nd cable, 213-m mast to harmonic loading with frequency of 3.0 Hz: Detailed Nonlinear (Right) vs. Proposed SDOF Method (Left).

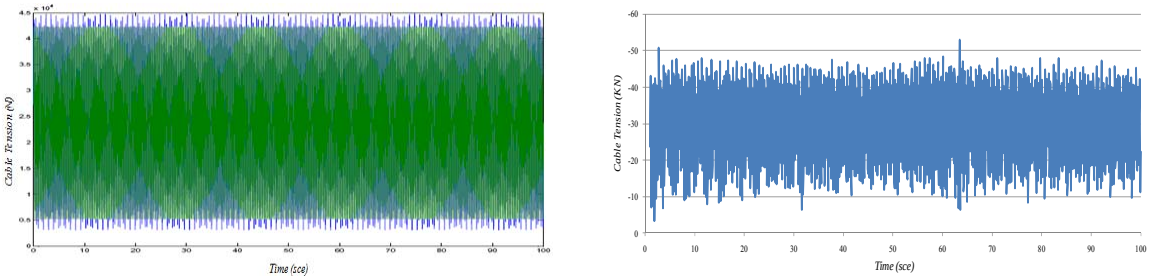

Figure B.54. Cable Tension force at the middle point of 2nd cable, 213-m mast to harmonic loading with frequency of 3.0 Hz: Detailed Nonlinear (Right) vs. Proposed SDOF Method (Left).

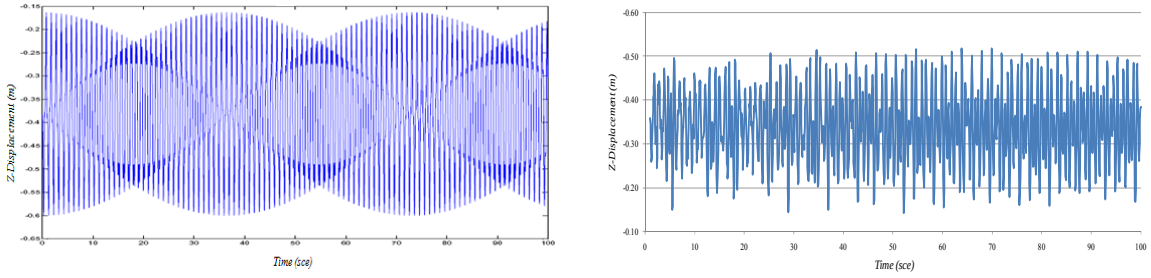

Figure B.55. Cable Tension force at the middle point of 1st cable, 213-m mast to harmonic loading with frequency of 3.0 Hz: Detailed Nonlinear (Right) vs. Proposed SDOF Method (Left).

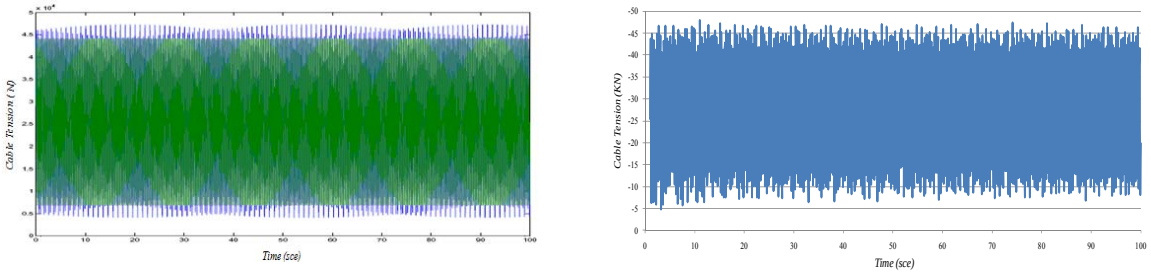

Figure B.56. Cable Tension force at the middle point of 1st cable, 213-m mast to harmonic loading with frequency of 3.0 Hz: Detailed Nonlinear (Right) vs. Proposed SDOF Method (Left).

Appendix C: Study of guy cables under seismic excitation

This appendix presents some detailed results of the time histories of the cable resultant force of the studied masts to selected earthquakes. These graphs will be used to support the theories presented in chapter 3.

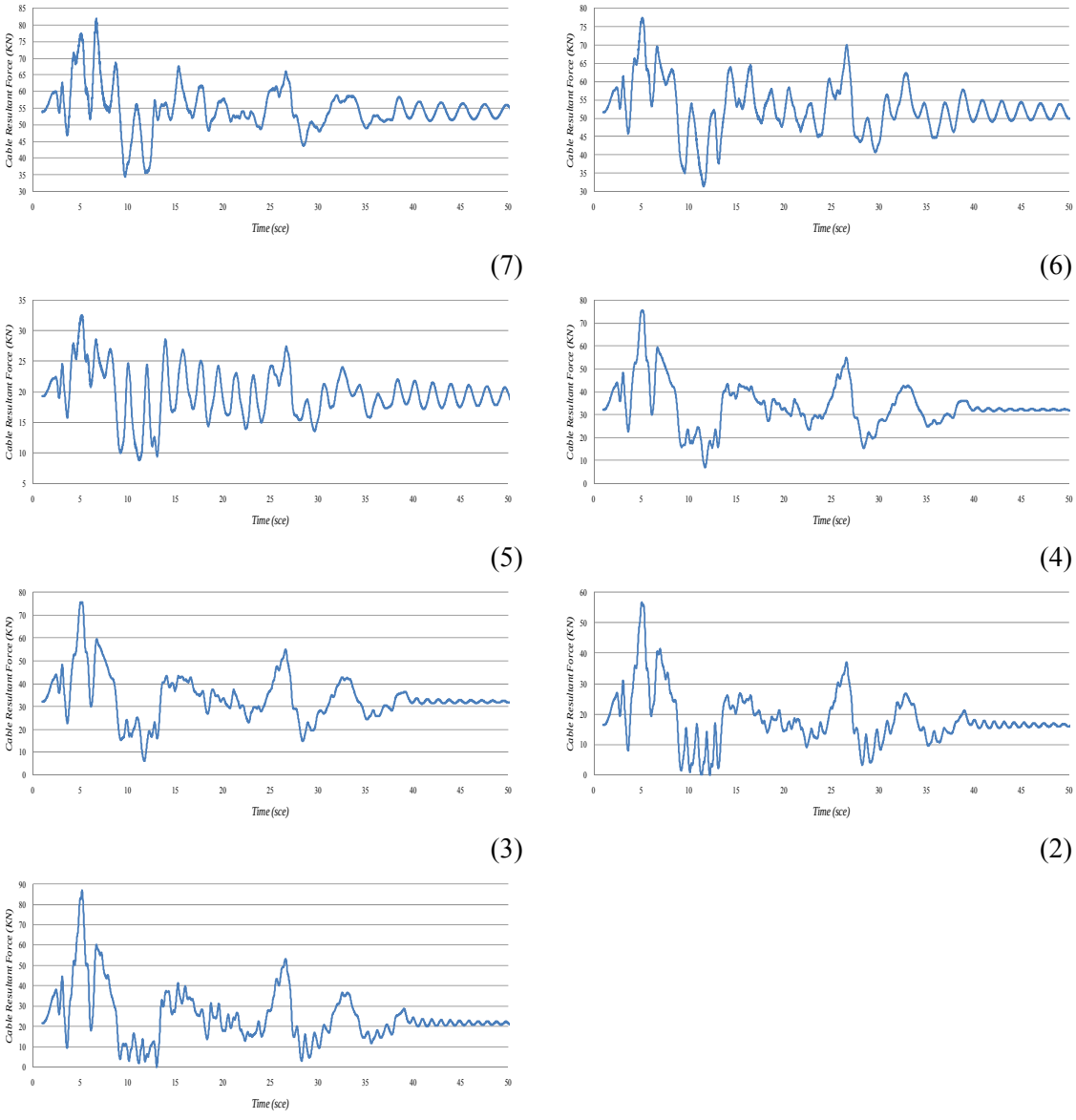

Figure C.1. The cable resultant force of the guy cables of 150-m mast to ElCentro earthquake: (7) the longest and (1) the shortest cable.

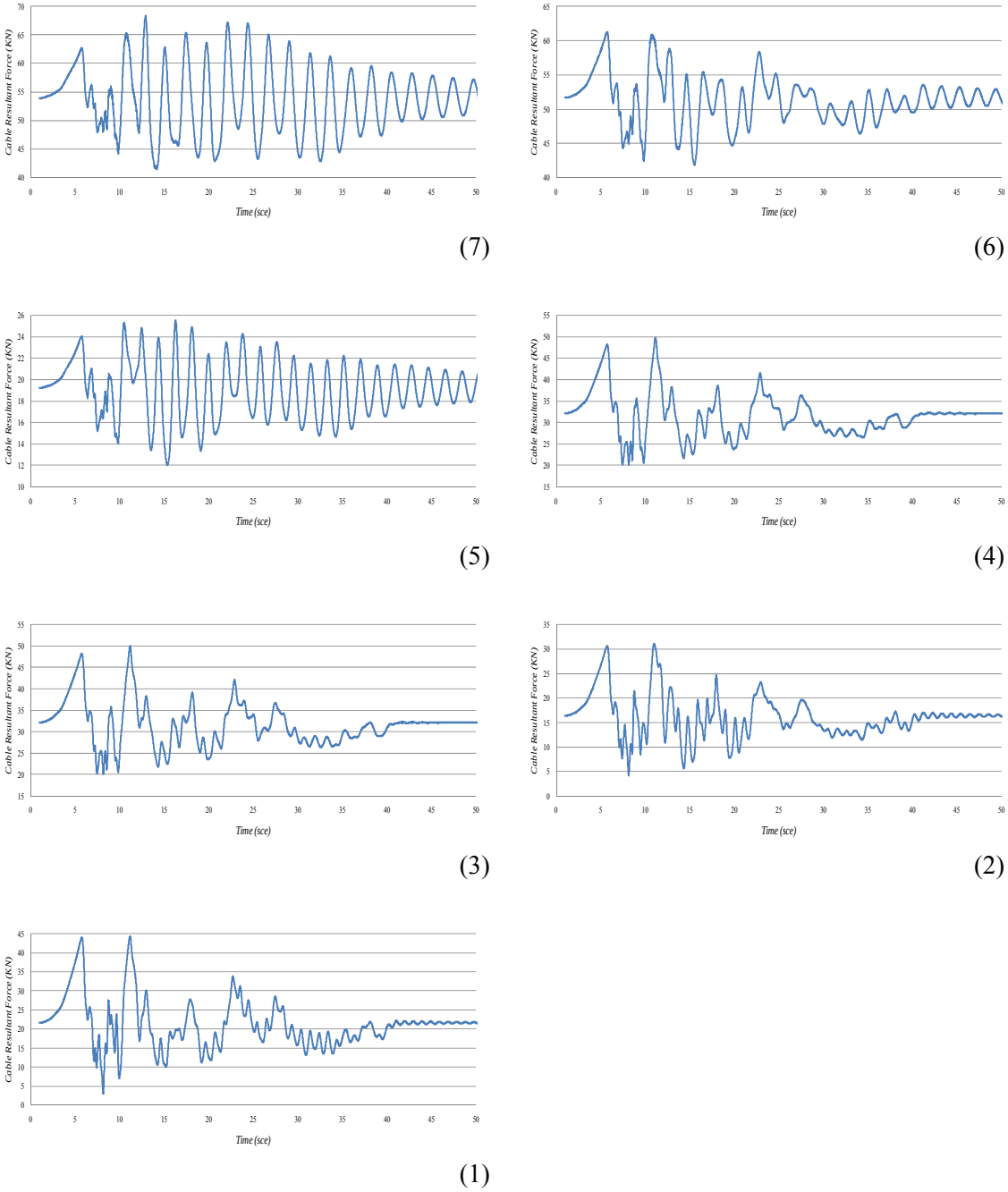

Figure C.2. The cable resultant force of the guy cables of 150-m mast to Parkfield earthquake: (7) the longest and (1) the shortest cable.

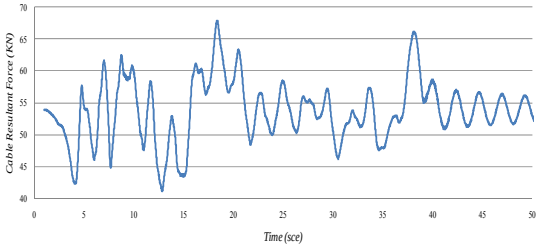

(7)

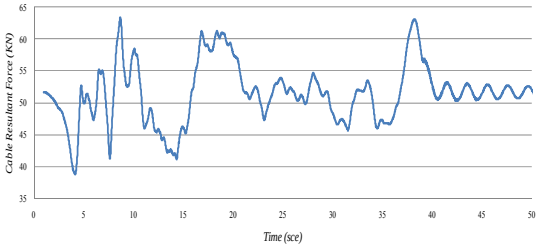

(6)

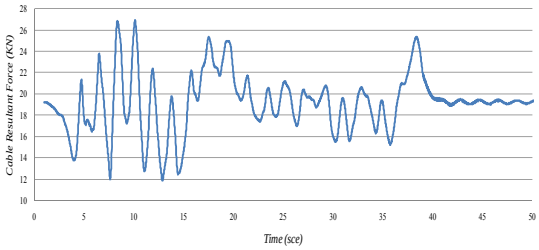

(5)

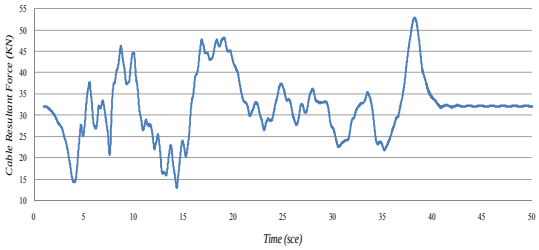

(4)

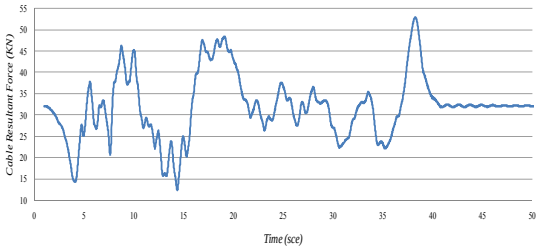

(3)

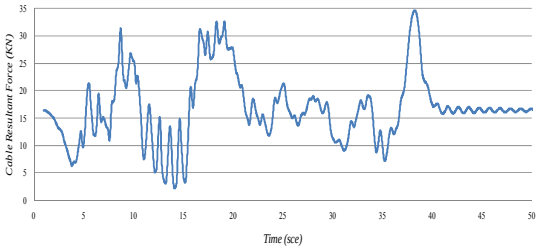

(2)

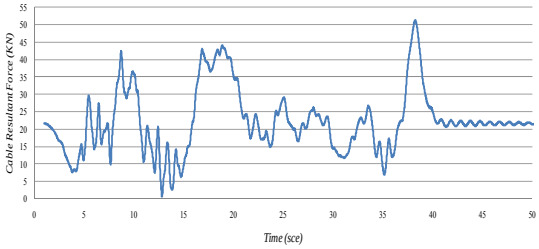

(1)

Figure C.3. The cable resultant force of the guy cables of 150-m mast to Taft earthquake: (7) the longest and (1) the shortest cable.

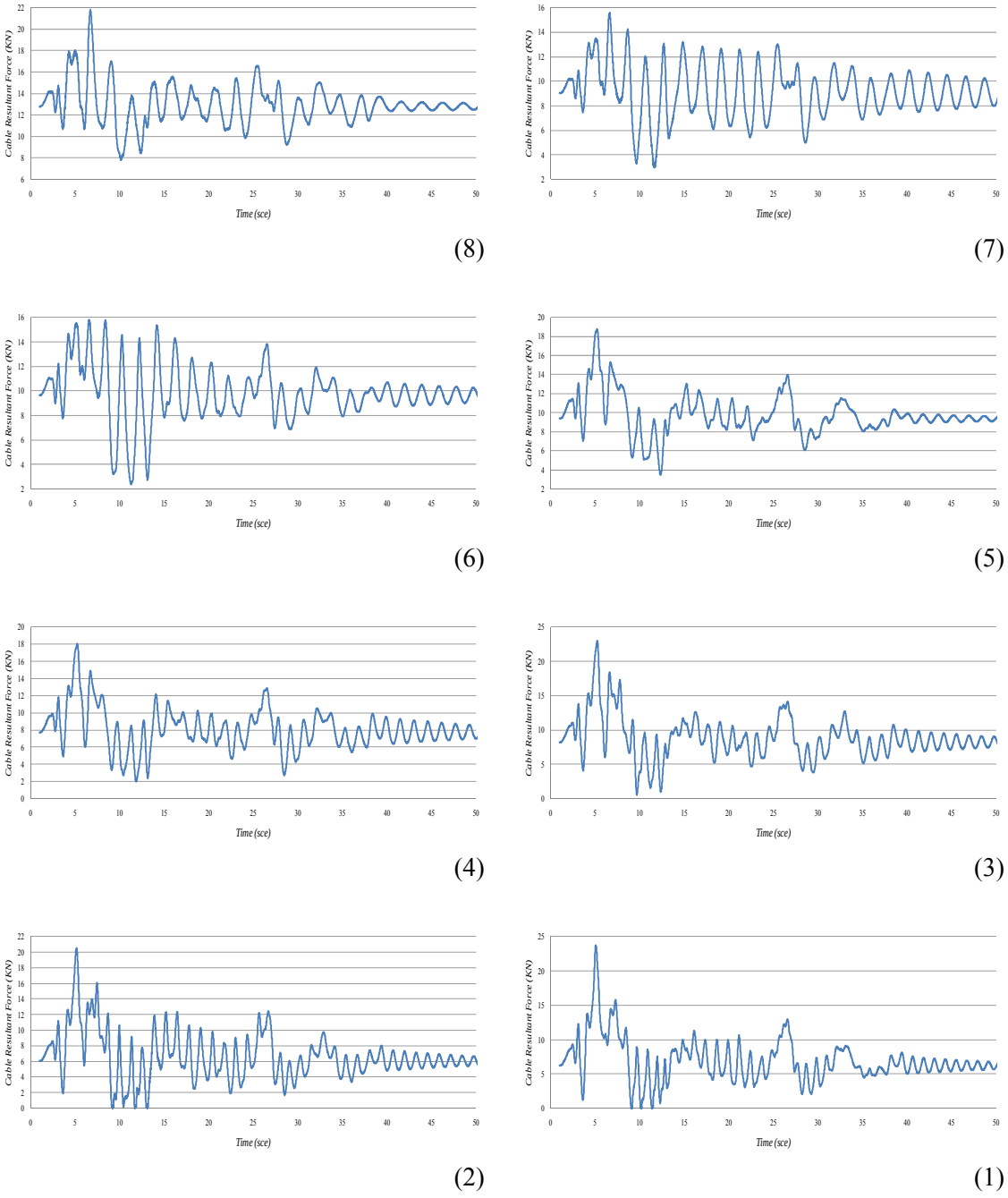

Figure C.4. The cable resultant force of the guy cables of 152-m mast to ElCentro earthquake: (8) the longest and (1) the shortest cable.

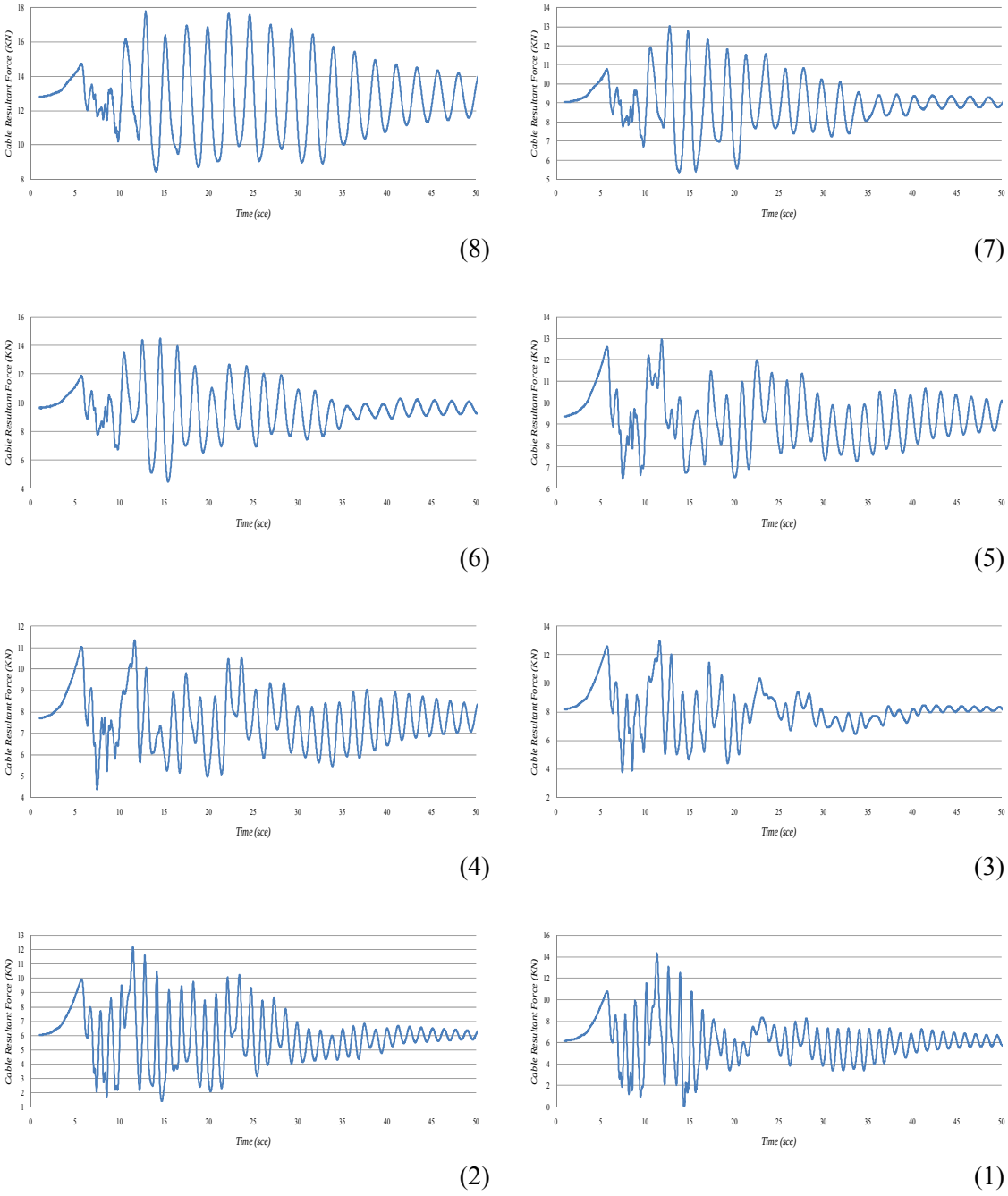

Figure C.5. The cable resultant force of the guy cables of 152-m mast to Parkfield earthquake: (8) the longest and (1) the shortest cable.

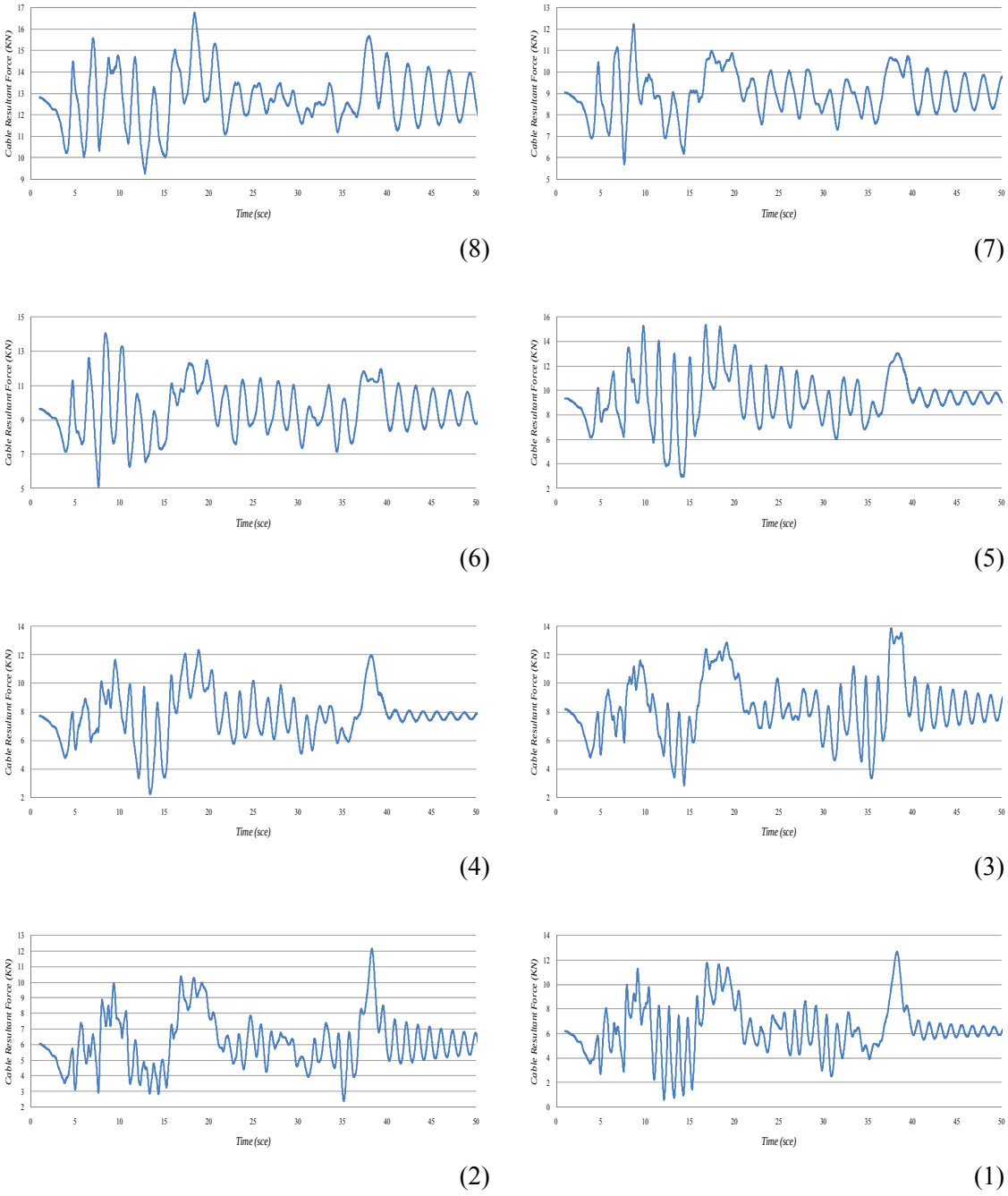

Figure C.6. The cable resultant force of the guy cables of 152-m mast to Taft earthquake: (8) the longest and (1) the shortest cable.

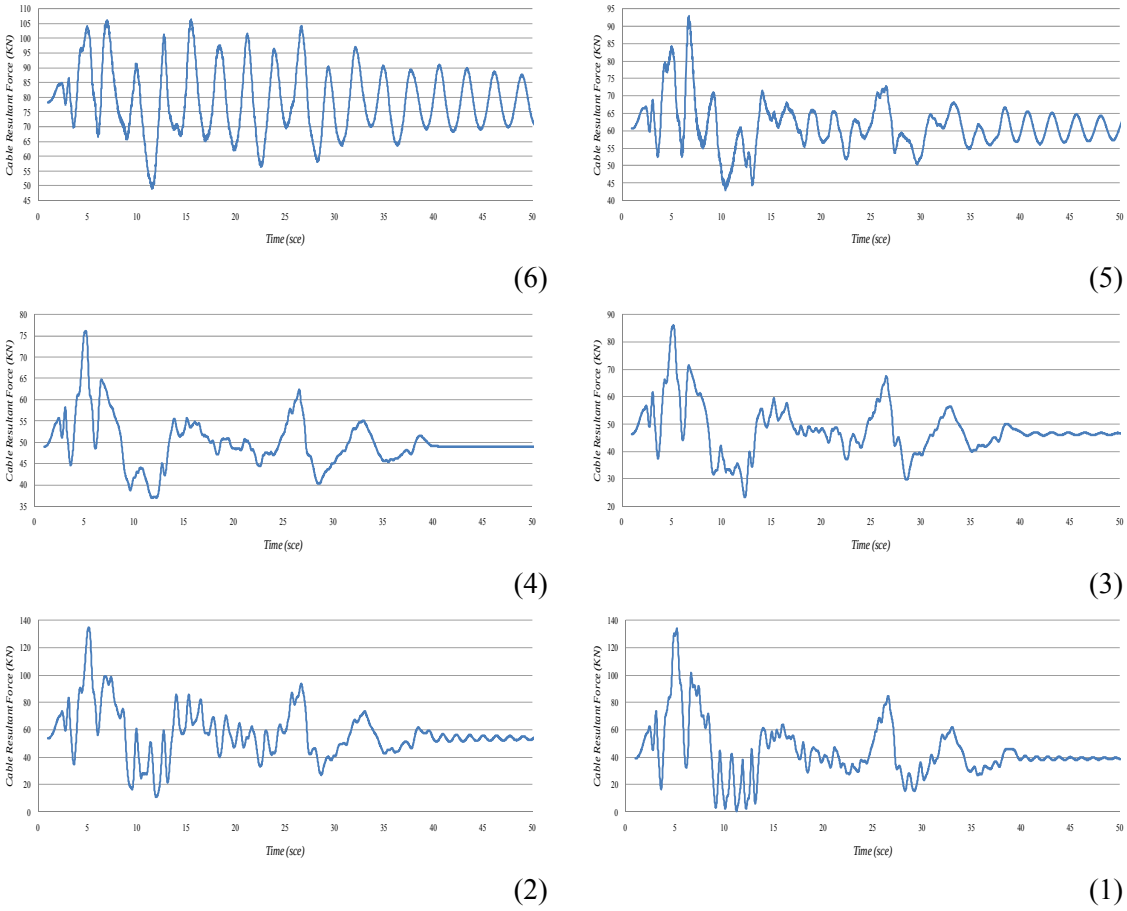

Figure C.7. The cable resultant force of the guy cables of 198-m mast to ElCentro earthquake: (6) the longest and (1) the shortest cable.

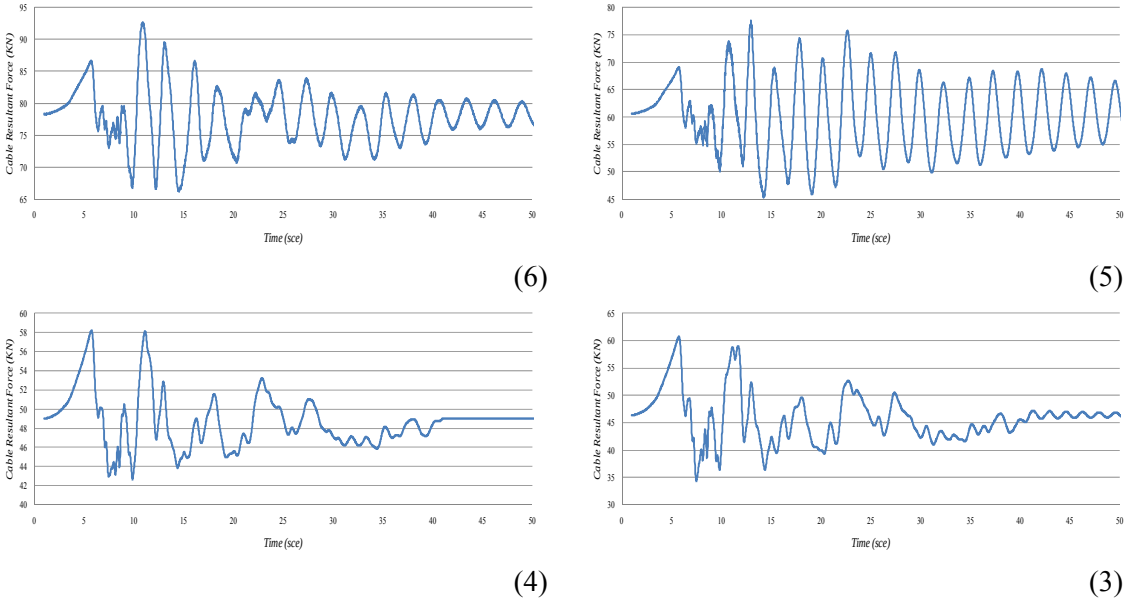

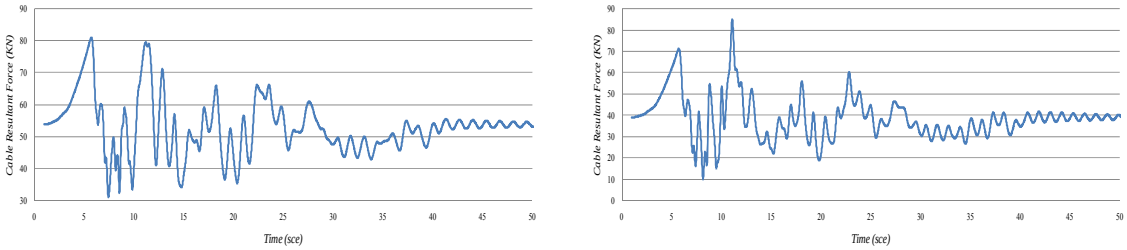

(2) (1)

Figure C.8. The cable resultant force of the guy cables of 198-m mast to Parkfield earthquake: (6) the longest and (1) the shortest cable.

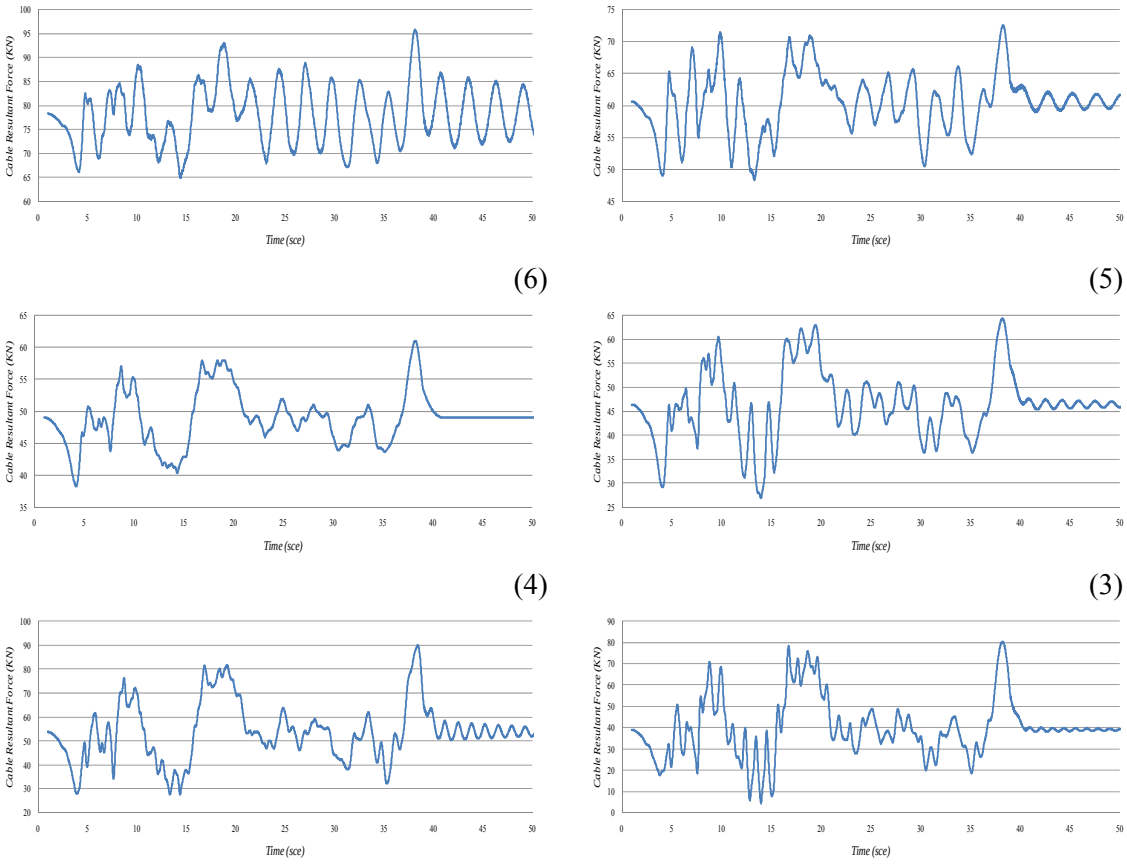

(6) (5)

(4) (3)

(2) (1)

Figure C.9. The cable resultant force of the guy cables of 198-m mast to Taft earthquake: (6) the longest and (1) the shortest cable.

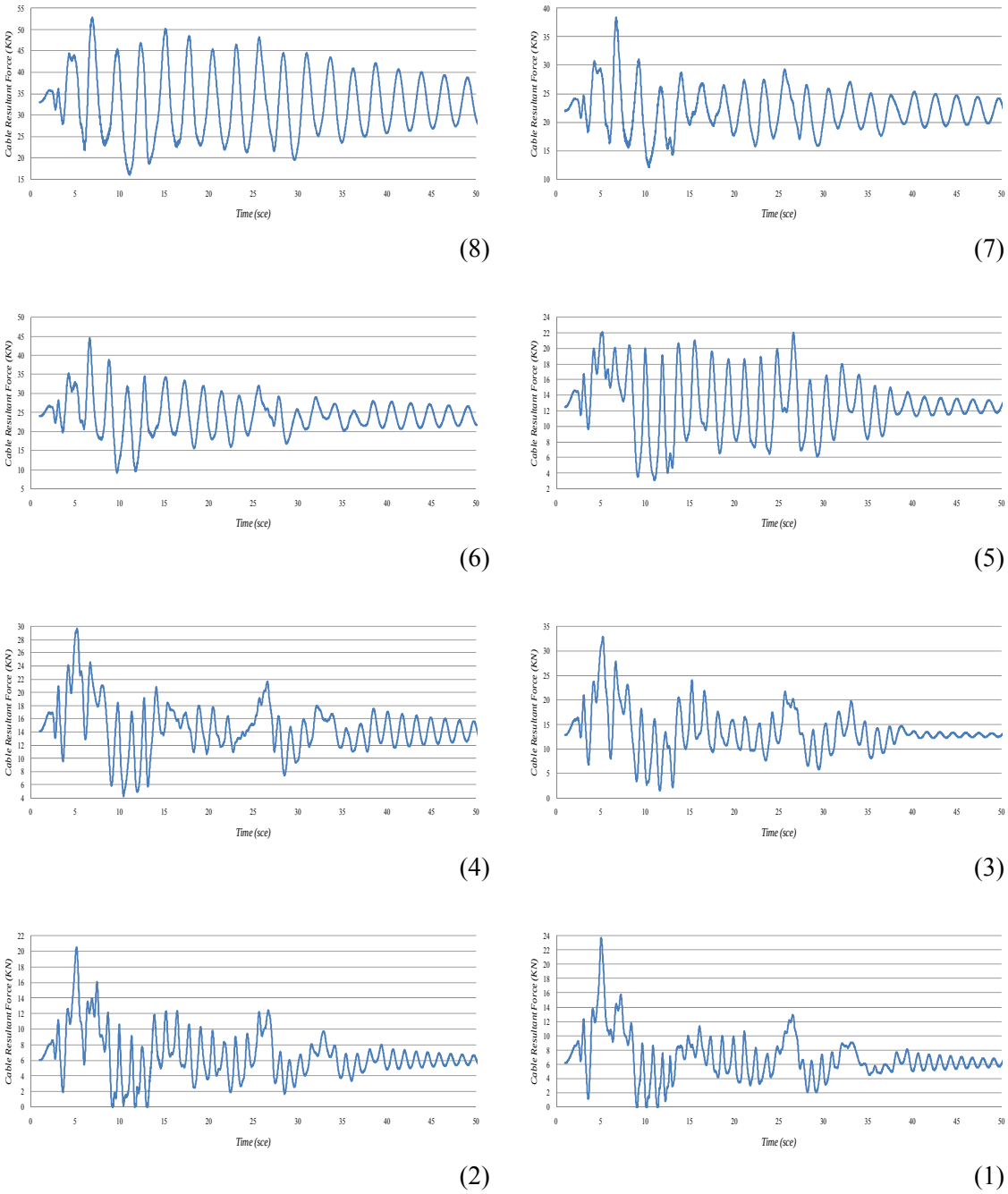

Figure C.10. The cable resultant force of the guy cables of 200-m mast to ElCentro earthquake: (8) the longest and (1) the shortest cable.

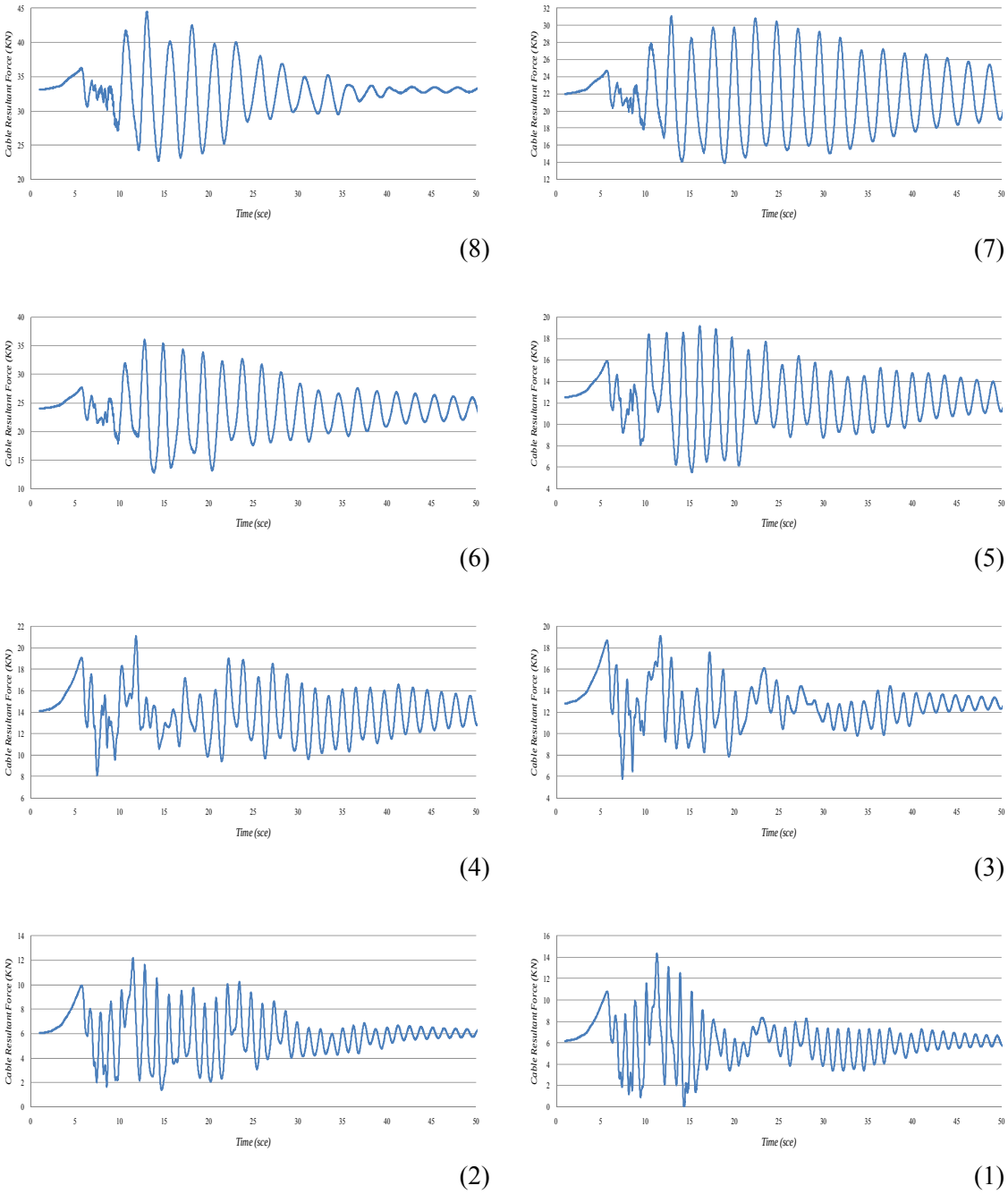

Figure C.11. The cable resultant force of the guy cables of 200-m mast to Parkfield earthquake: (8) the longest and (1) the shortest cable.

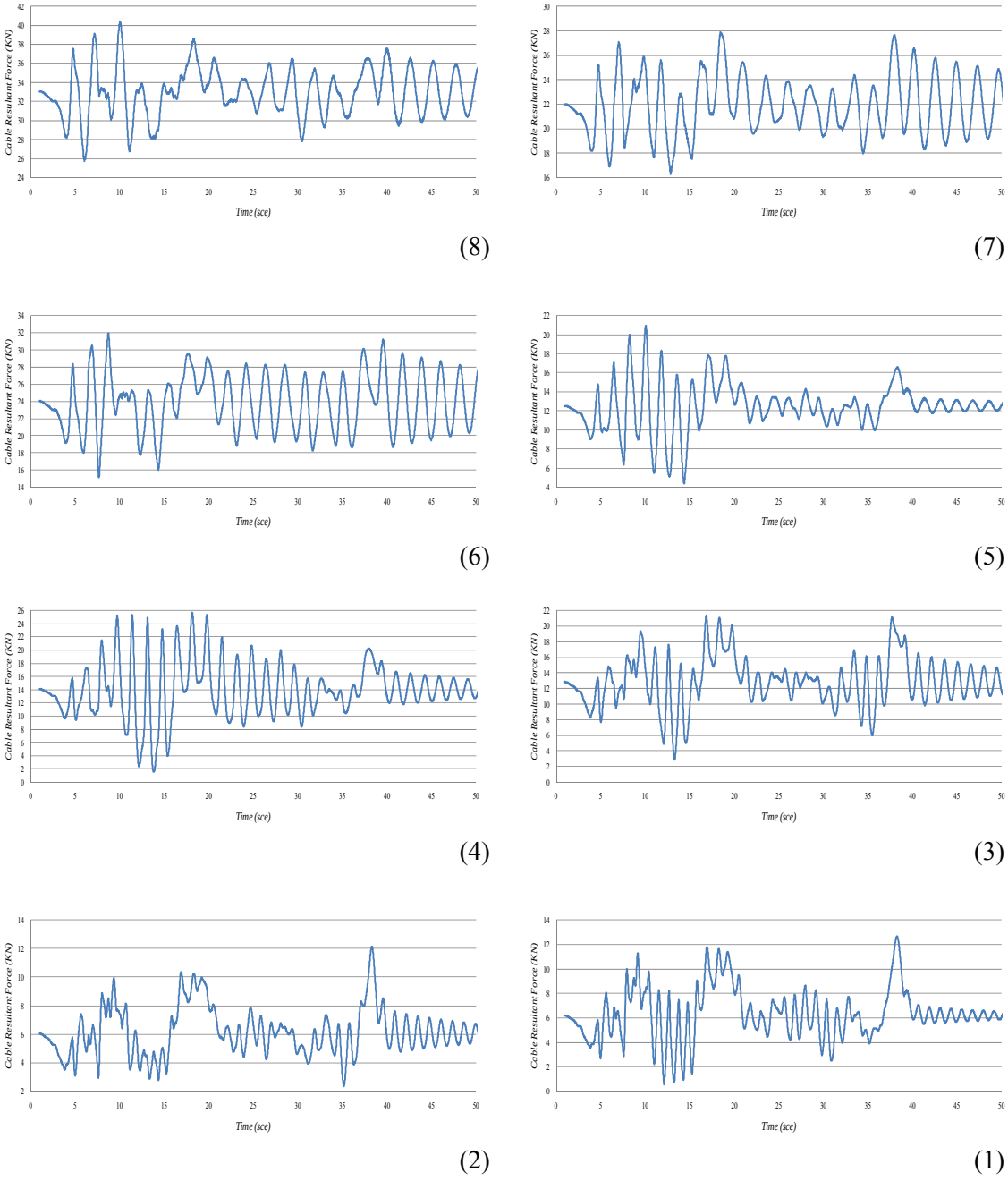

Figure C.12. The cable resultant force of the guy cables of 200-m mast to Taft earthquake: (8) the longest and (1) the shortest cable.

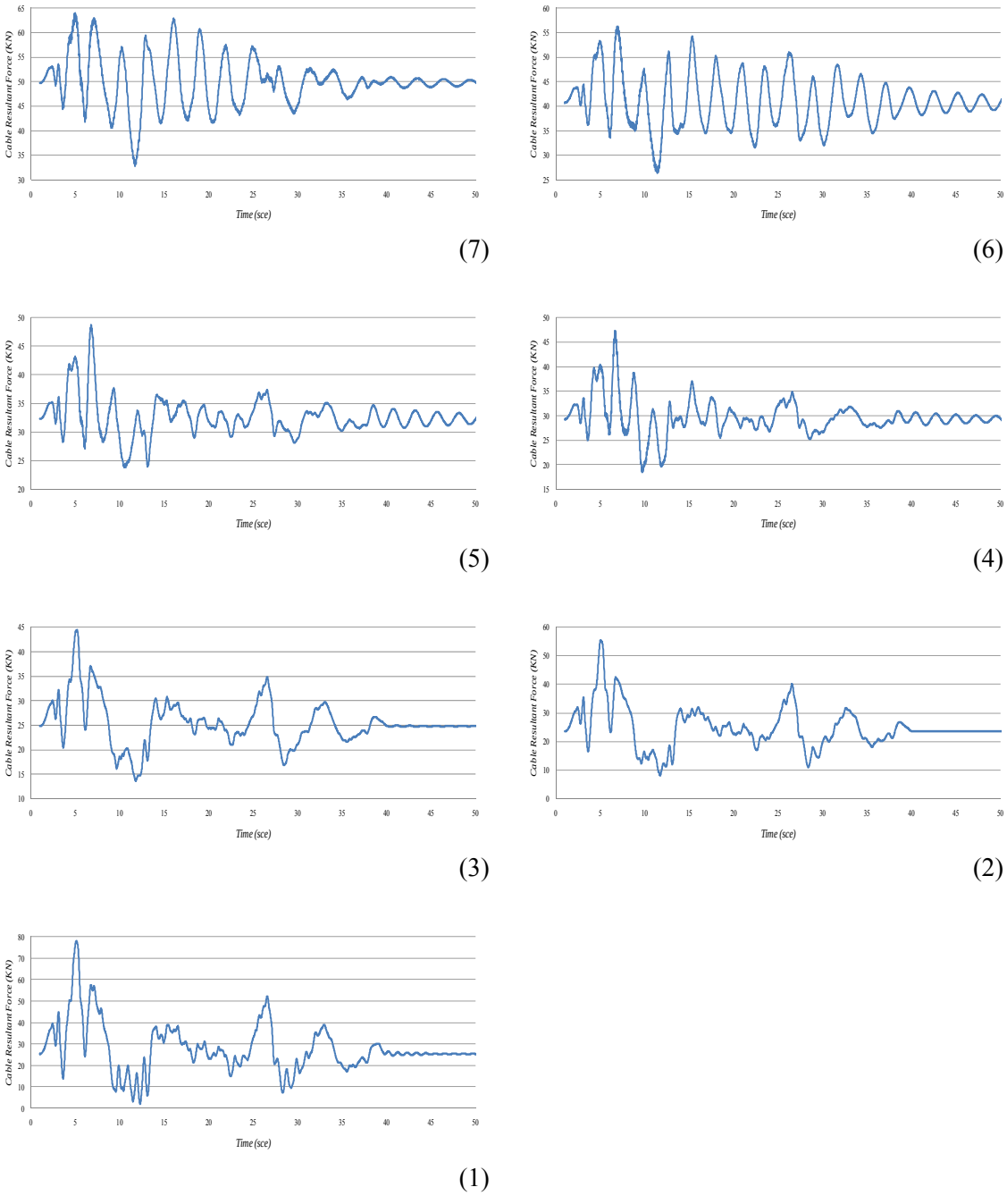

Figure C.13. The cable resultant force of the guy cables of 213-m mast to ElCentro earthquake: (7) the longest and (1) the shortest cable.

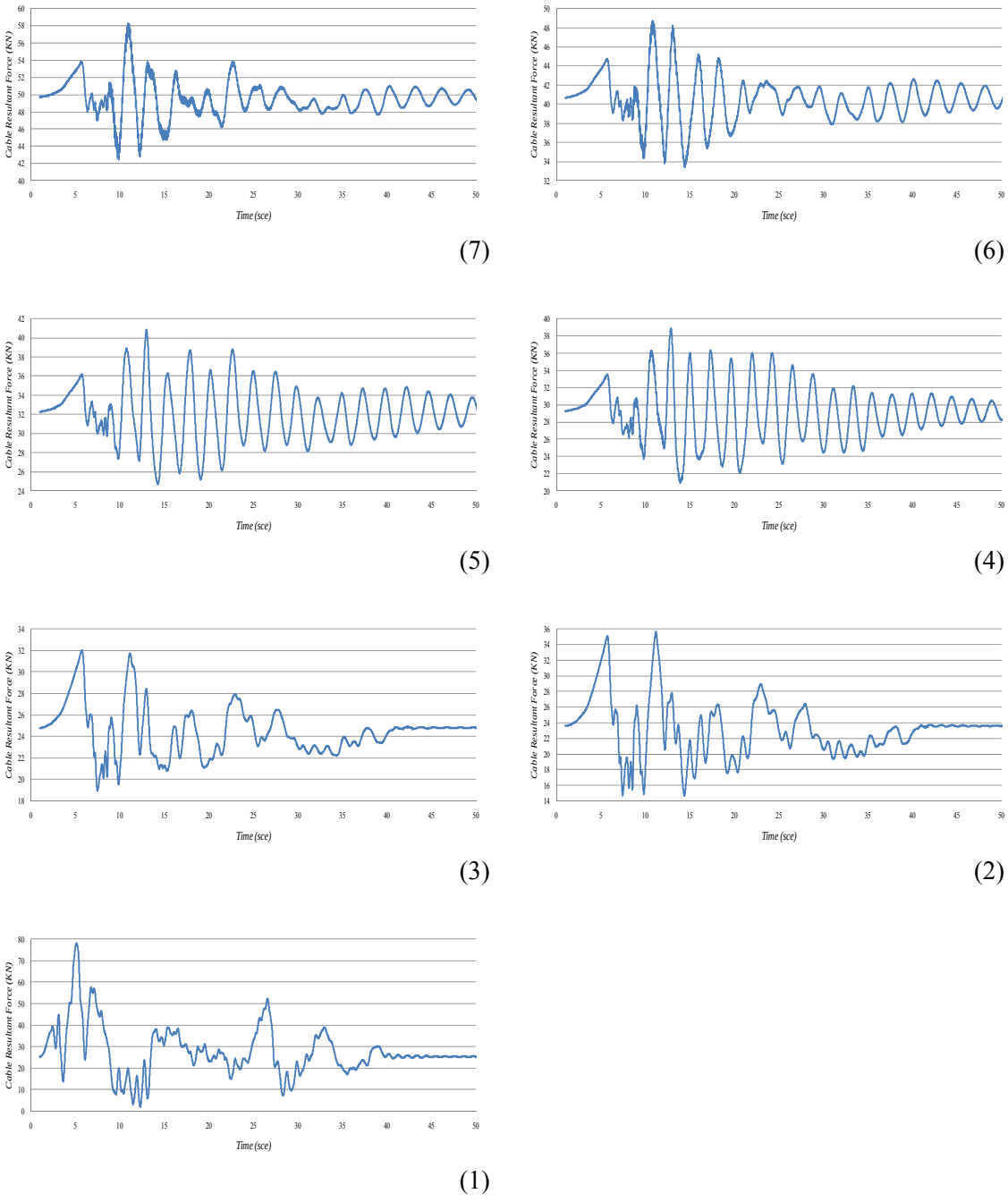

Figure C.14. The cable resultant force of the guy cables of 213-m mast to Parkfield earthquake: (7) the longest and (1) the shortest cable.

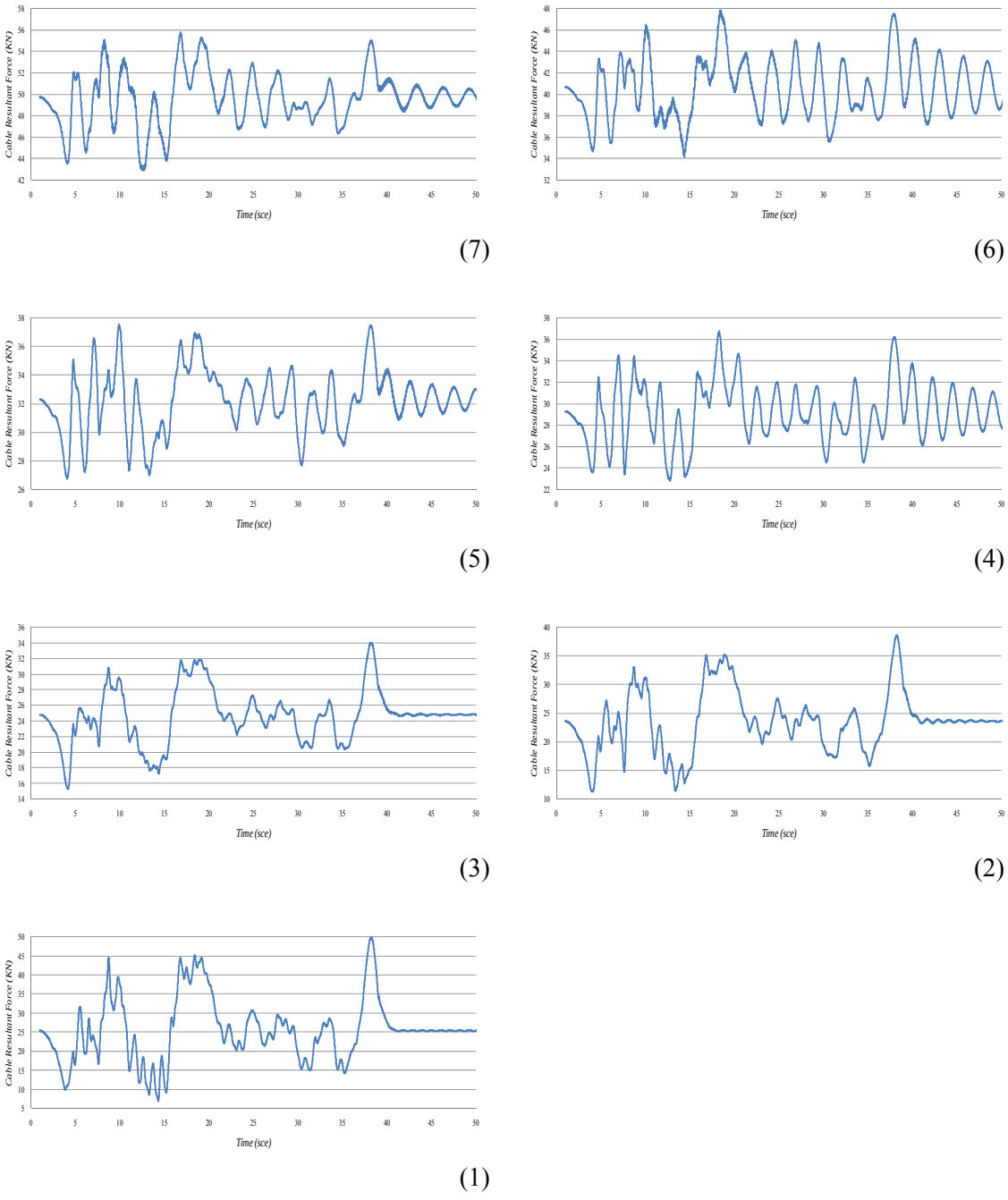

Figure C.15. The cable resultant force of the guy cables of 213-m mast to Taft earthquake: (7) the longest and (1) the shortest cable.

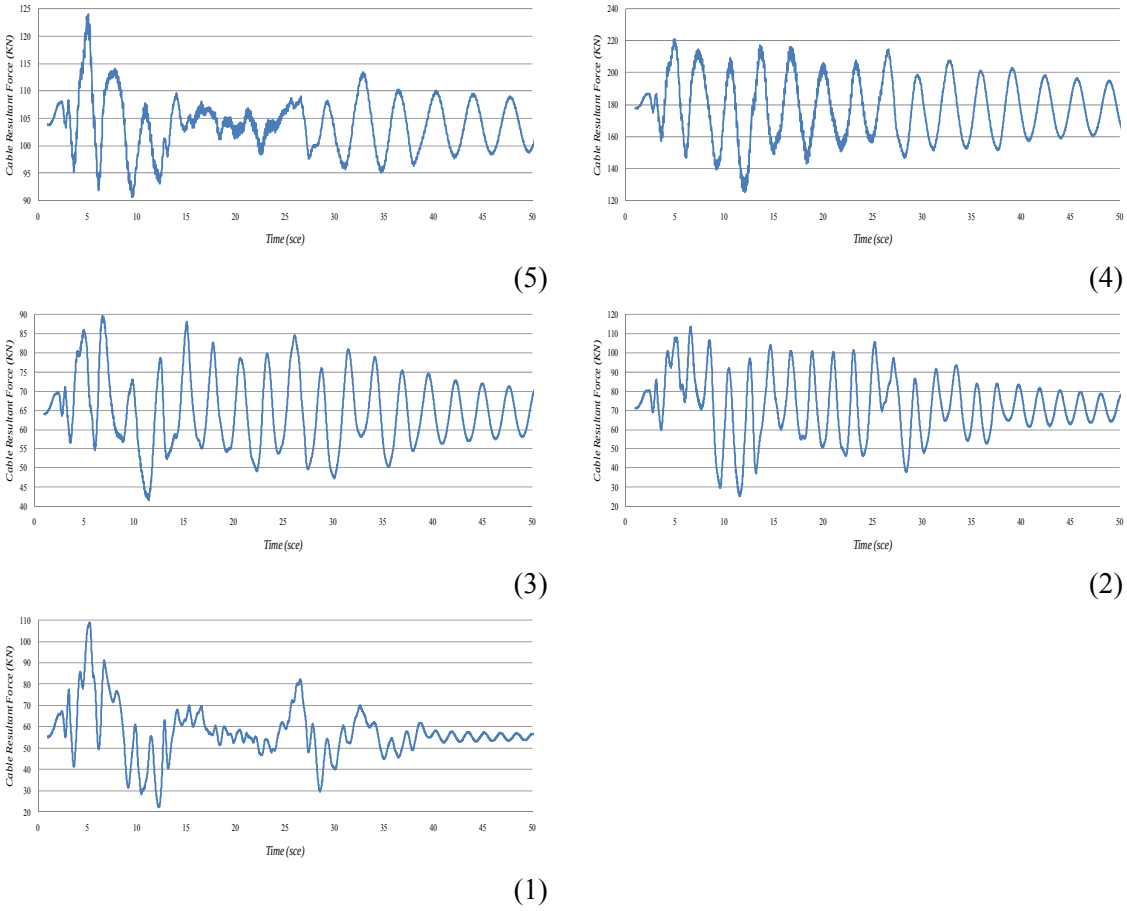

Figure C.16. The cable resultant force of the guy cables of 313-m mast to ElCentro earthquake: (5) the longest and (1) the shortest cable.

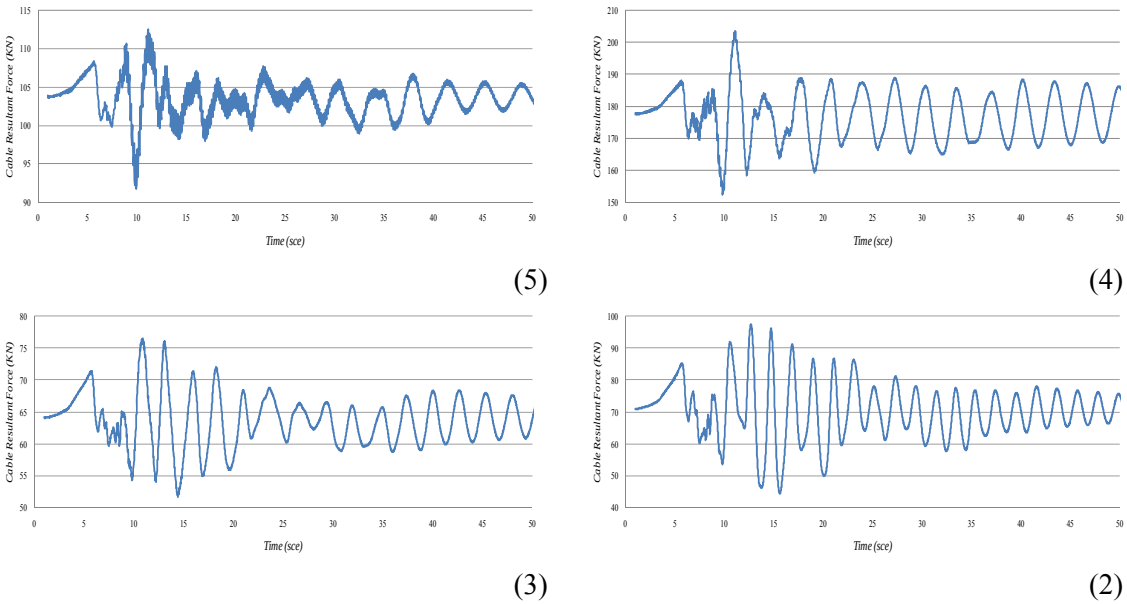

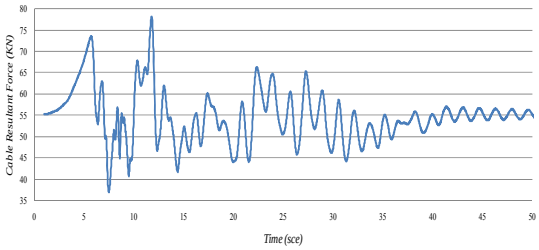

(1)

Figure C.17. The cable resultant force of the guy cables of 313-m mast to Parkfield earthquake: (5) the longest and (1) the shortest cable.

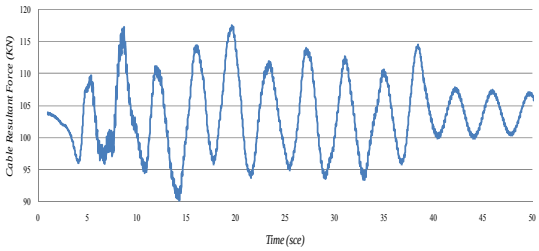

(5)

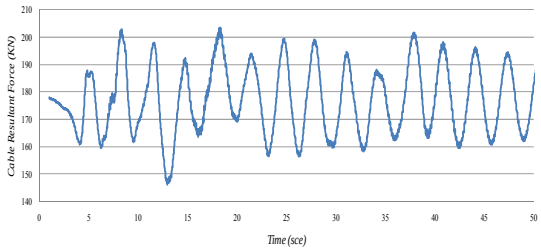

(4)

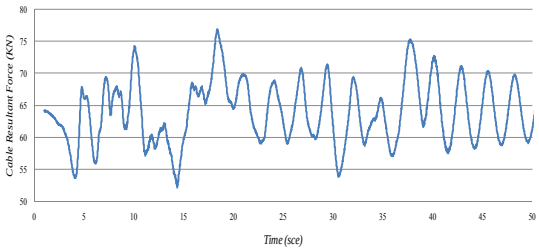

(3)

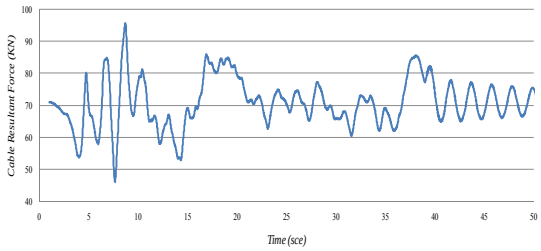

(2)

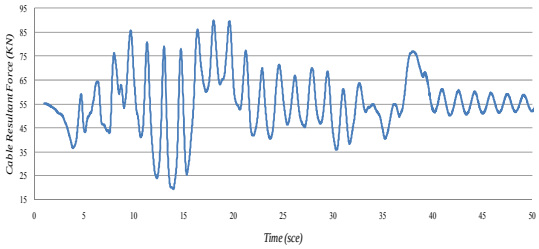

(1)

Figure C.18. The cable resultant force of the guy cables of 313-m mast to Taft earthquake: (5) the longest and (1) the shortest cable.

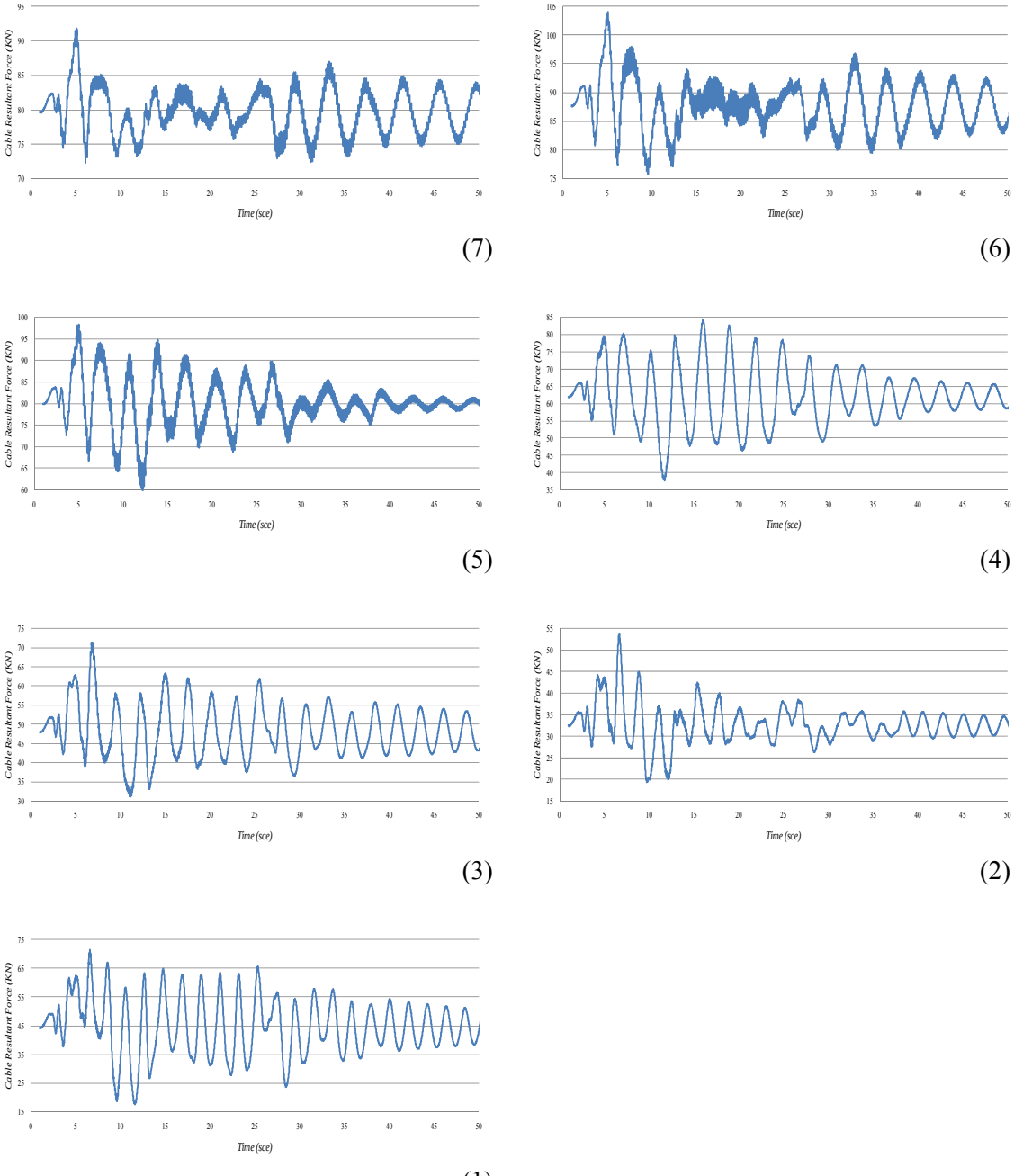

Figure C.19. The cable resultant force of the guy cables of 342-m mast to ElCentro earthquake: (7) the longest and (1) the shortest cable.

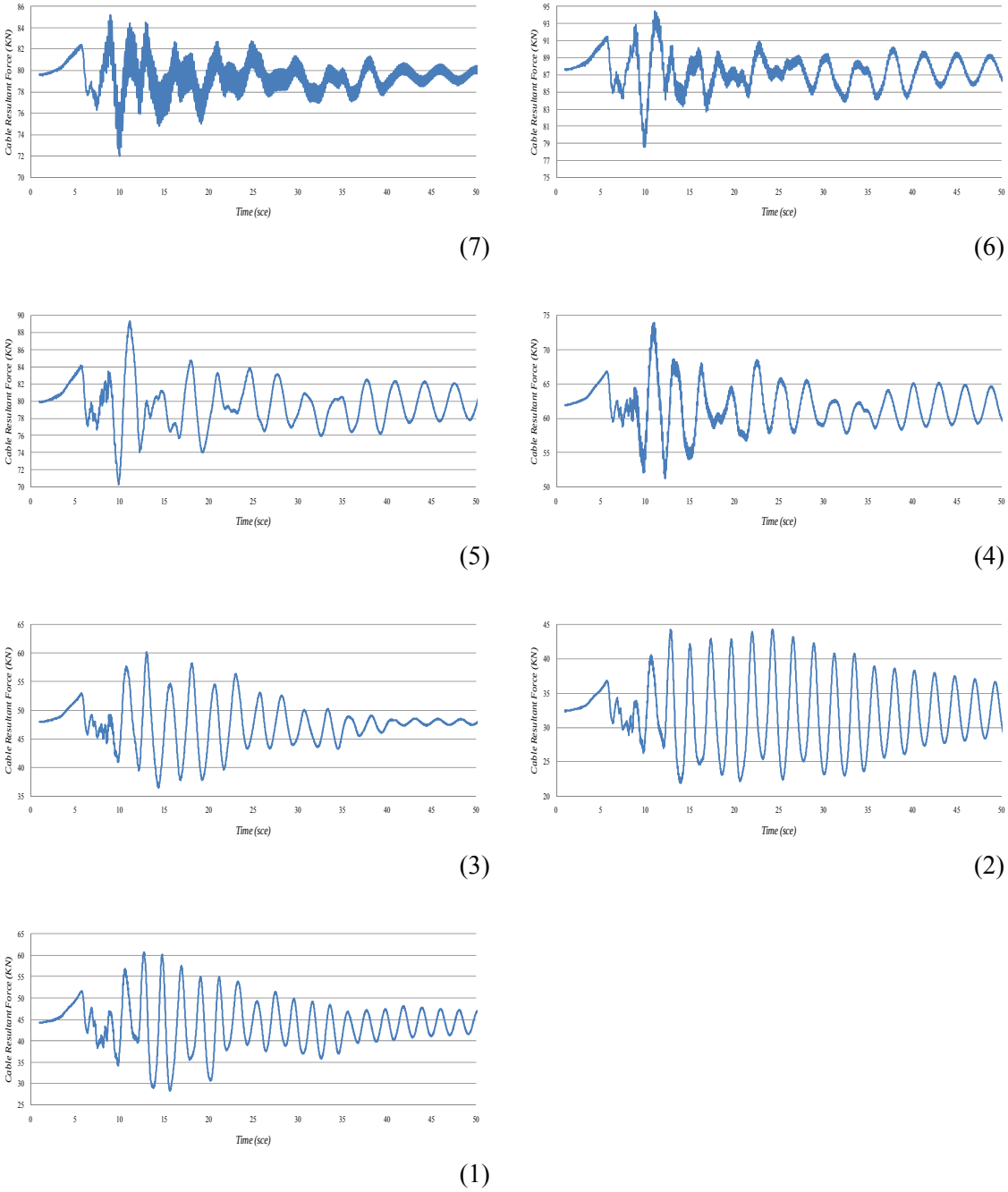

Figure C.20. The cable resultant force of the guy cables of 342-m mast to Parkfield earthquake: (7) the longest and (1) the shortest cable.

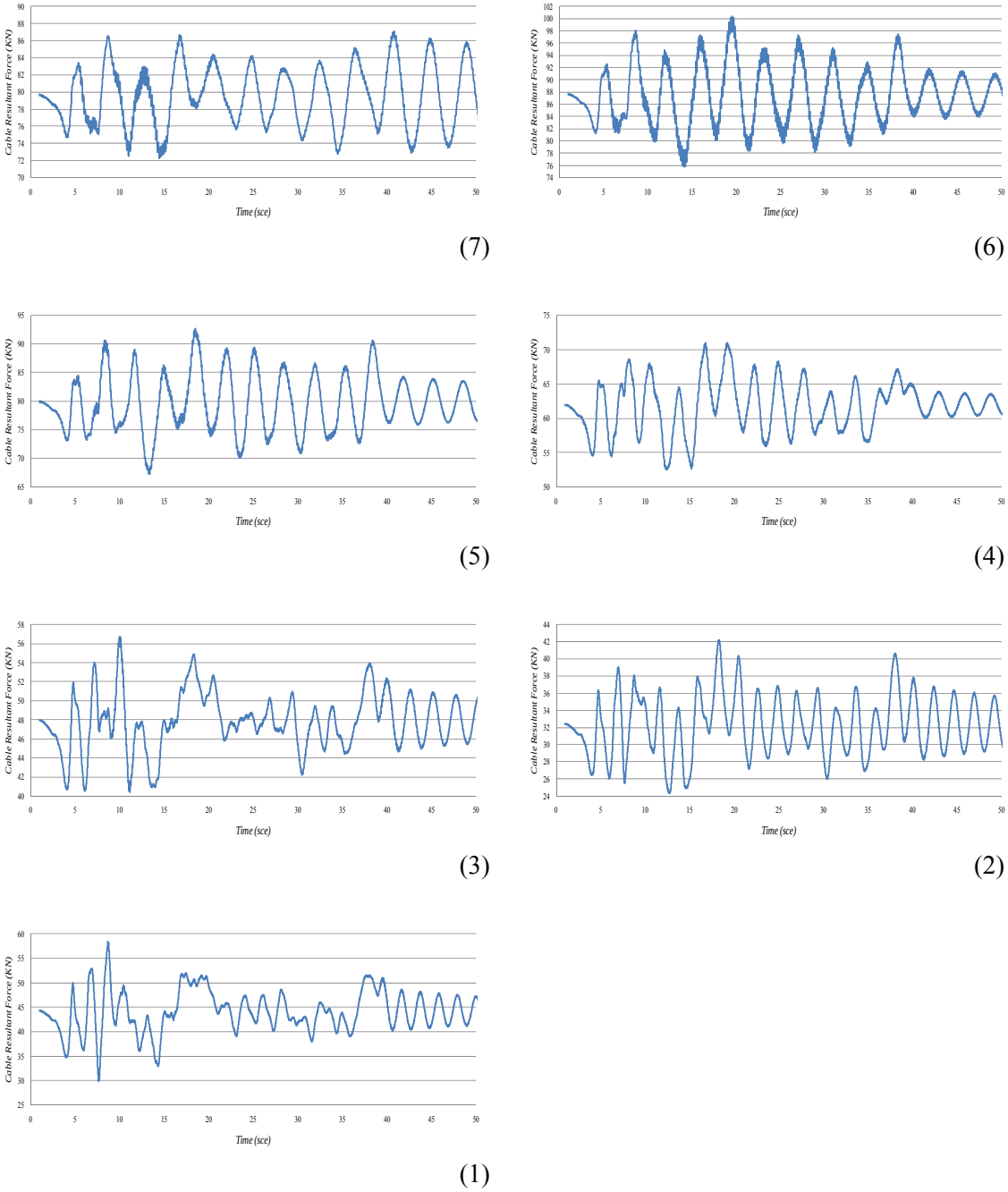

Figure C.21. The cable resultant force of the guy cables of 342-m mast to Taft earthquake: (7) the longest and (1) the shortest cable.

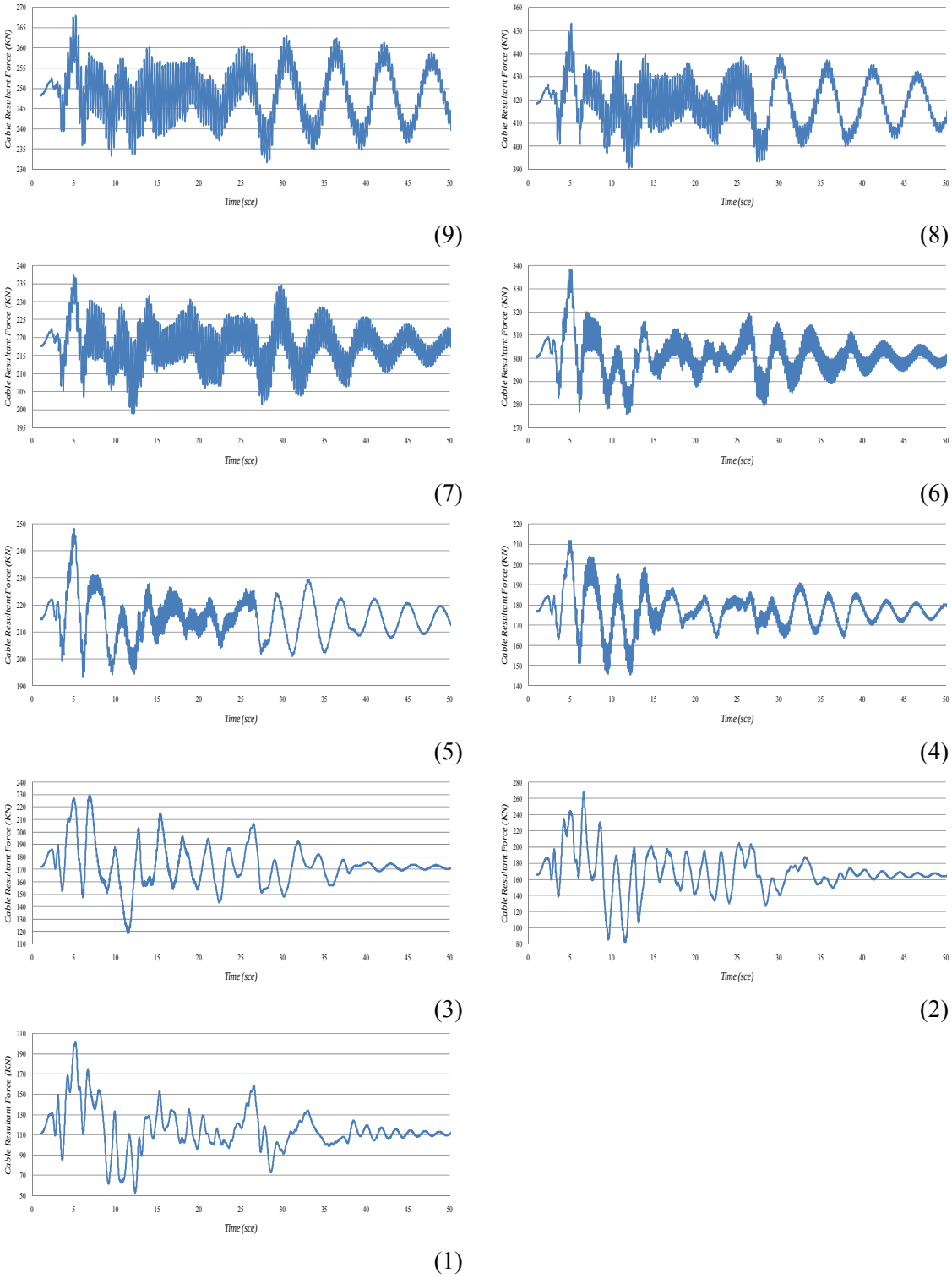

Figure C.22. The cable resultant force of the guy cables of 607-m mast to ElCentro earthquake: (9) the longest and (1) the shortest cable.

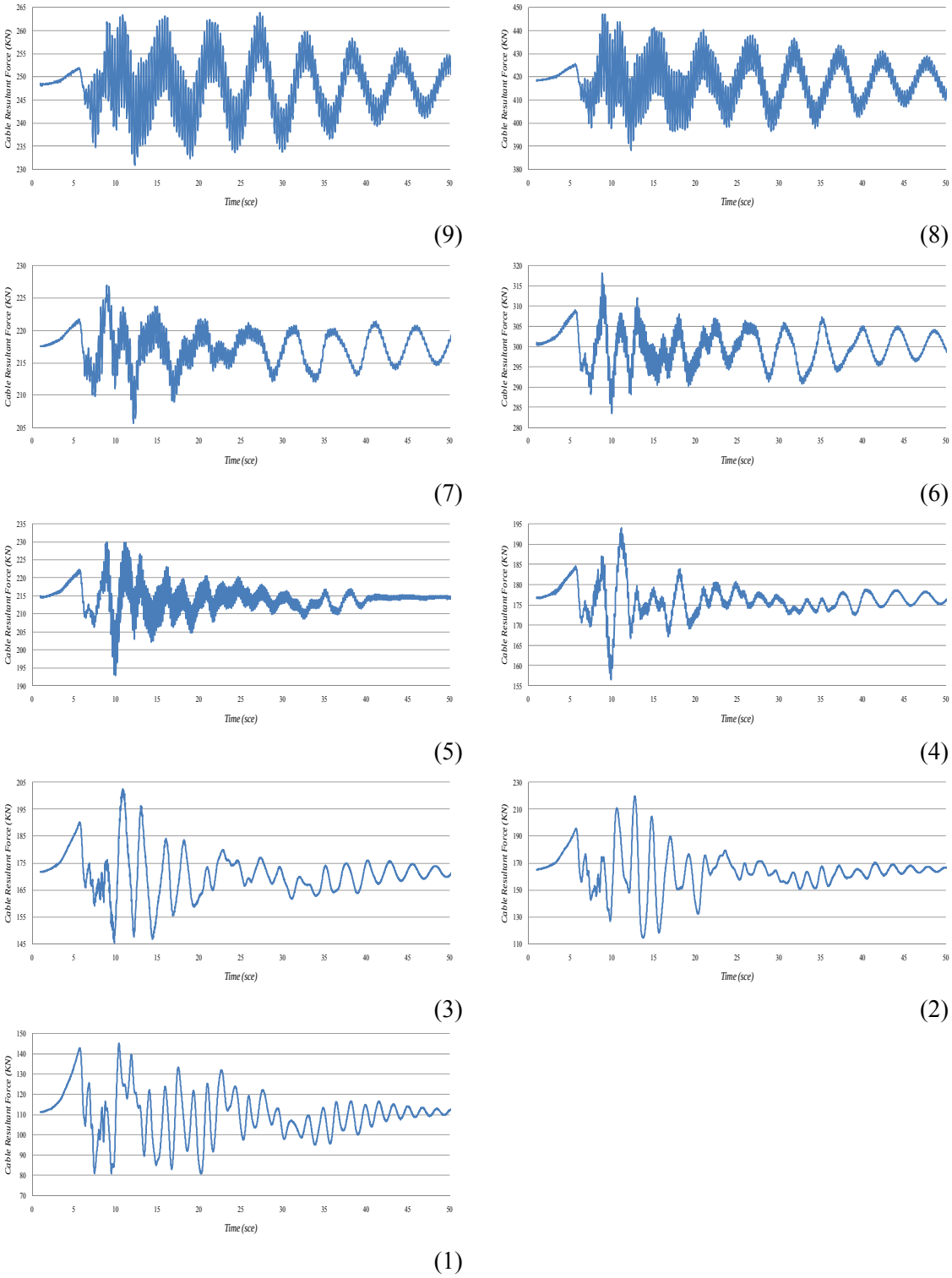

Figure C.23. The cable resultant force of the guy cables of 607-m mast to Parkfield earthquake: (9) the longest and (1) the shortest cable.

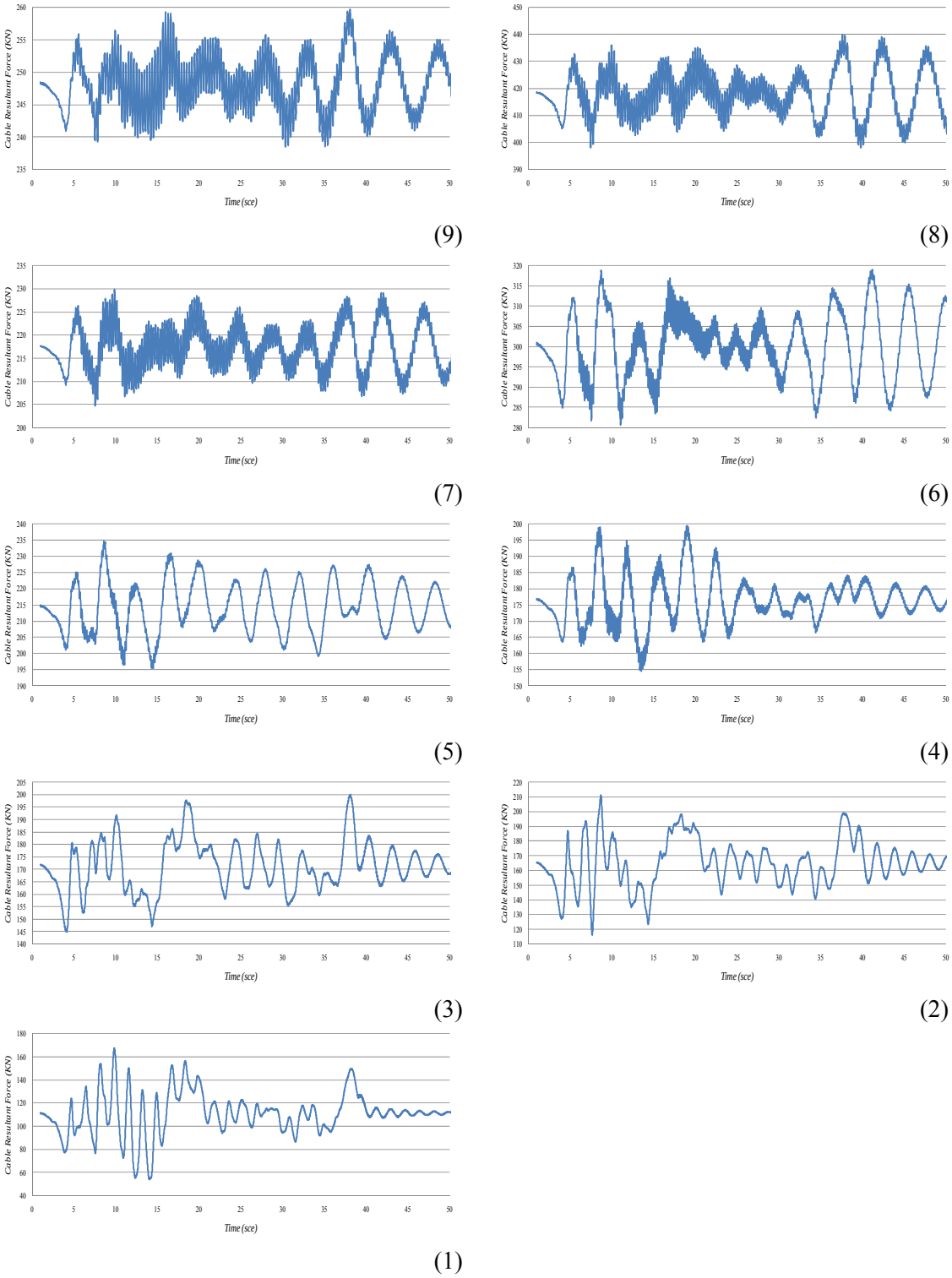

Figure C.24. The cable resultant force of the guy cables of 607-m mast to Taft earthquake: (9) the longest and (1) the shortest cable.

Appendix D: Presentation of partial results using the proposed simplified approach

This appendix presents some detailed results of the maximum horizontal displacements and cable tension forces of the studied masts under the effects of the selected earthquakes. Different approaches are compared throughout these graphs in order to validate the accuracy and the reliability of the proposed simplified methods in chapter 4.

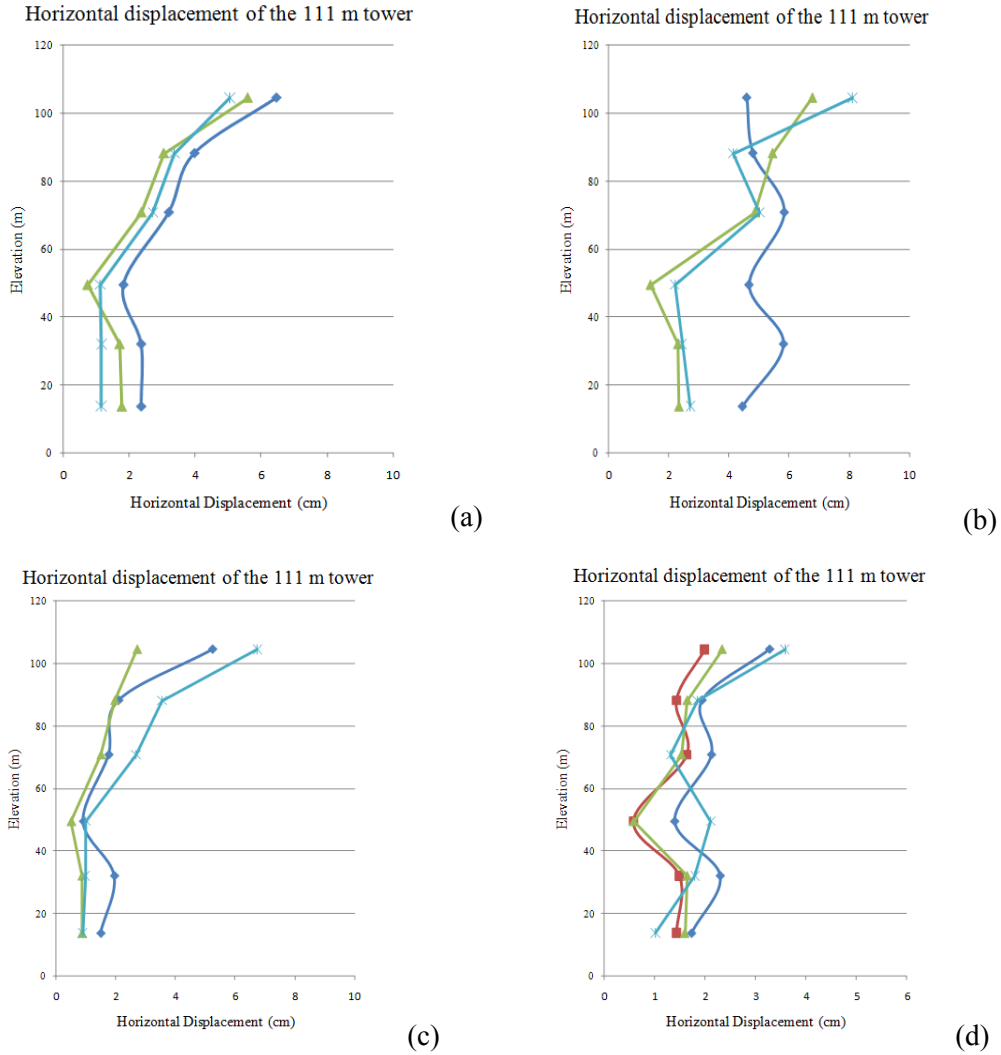

Figure D.1. Maximum horizontal mast displacement of the 111 m tower under different earthquakes: (a) ElCentro, (b) Parkfield, (c) Taft and (d) Montreal Region Earthquakes.

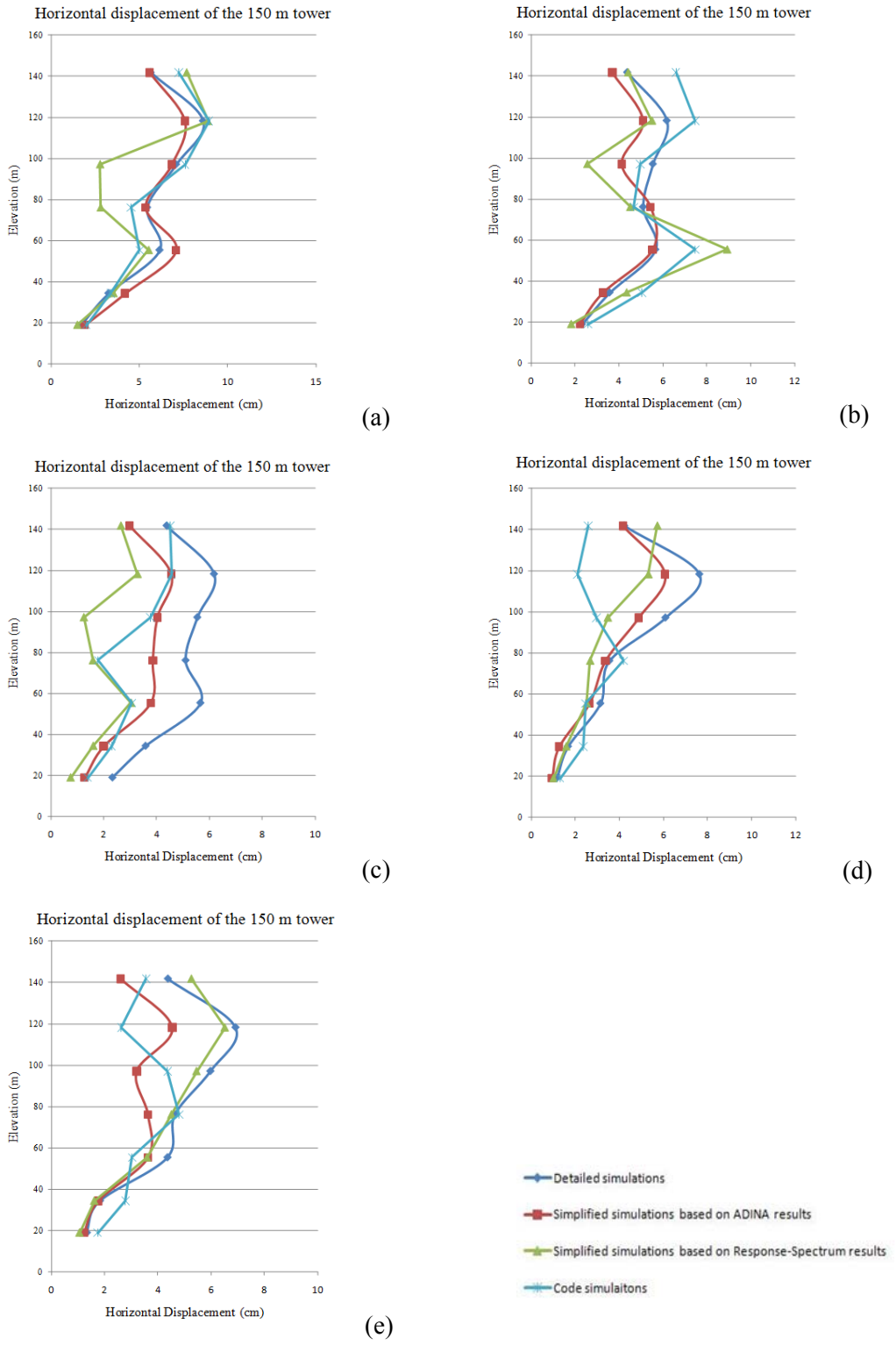

Figure D.2. Maximum horizontal mast displacement of the 150 m tower under different earthquakes: (a) ElCentro, (b) Parkfield, (c) Taft, (d) Montreal and (e) Synthetic Earthquakes.

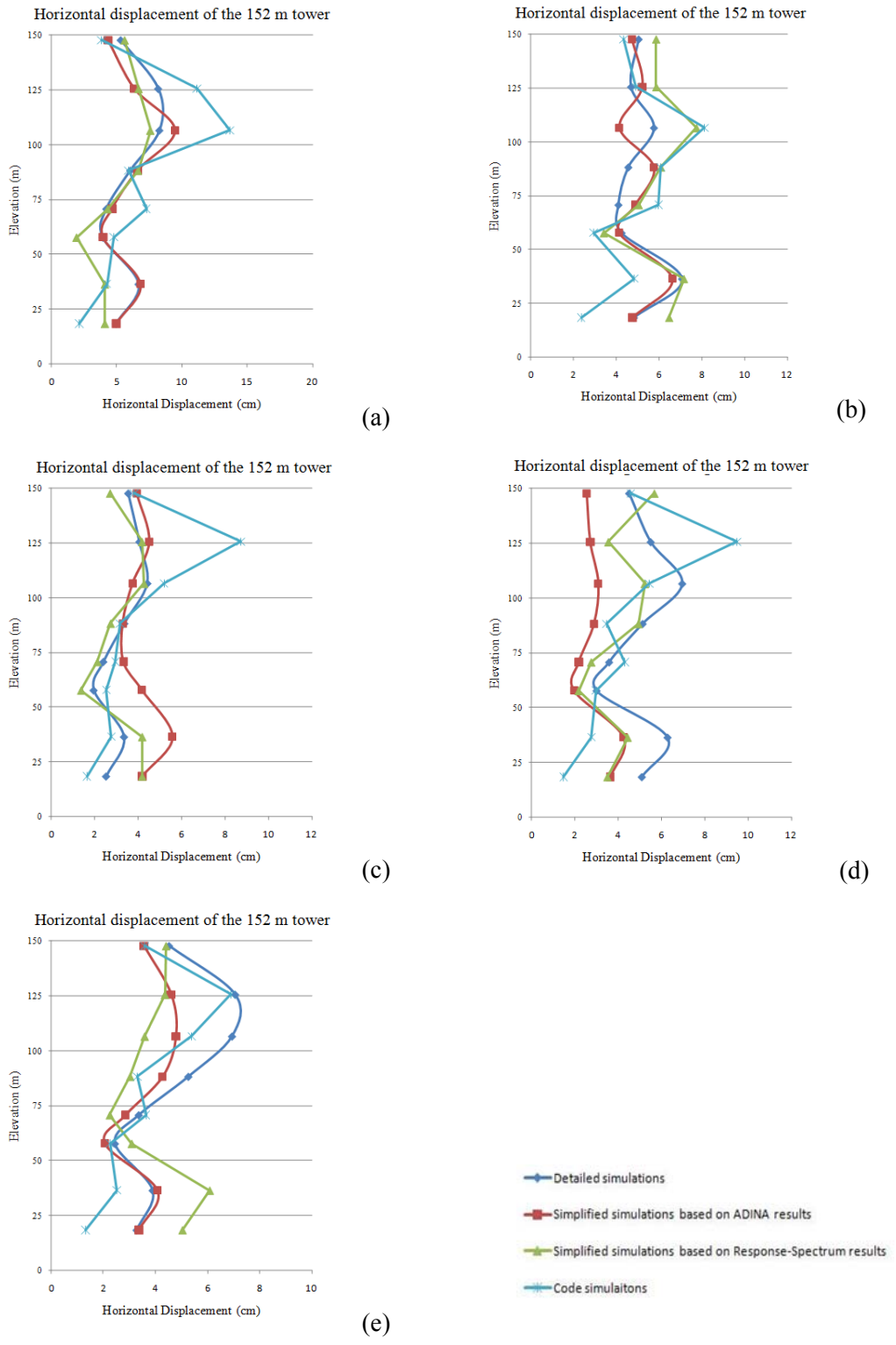

Figure D.3. Maximum horizontal mast displacement of the 152 m tower under different earthquakes: (a) ElCentro, (b) Parkfield, (c) Taft, (d) Montreal and (e) Synthetic Earthquakes.

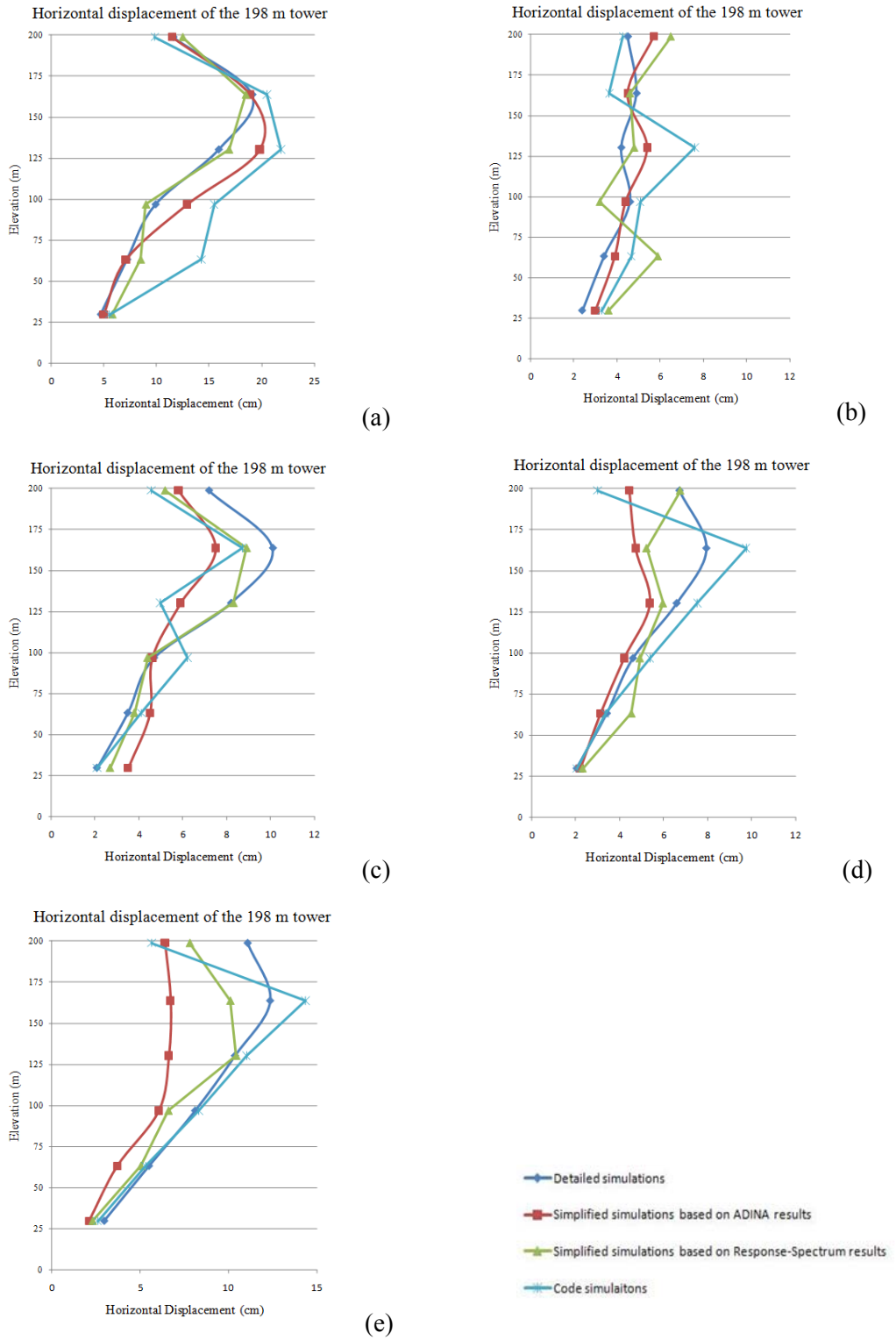

Figure D.4. Maximum horizontal mast displacement of the 198 m tower under different earthquakes: (a) ElCentro, (b) Parkfield, (c) Taft, (d) Montreal and (e) Synthetic Earthquakes.

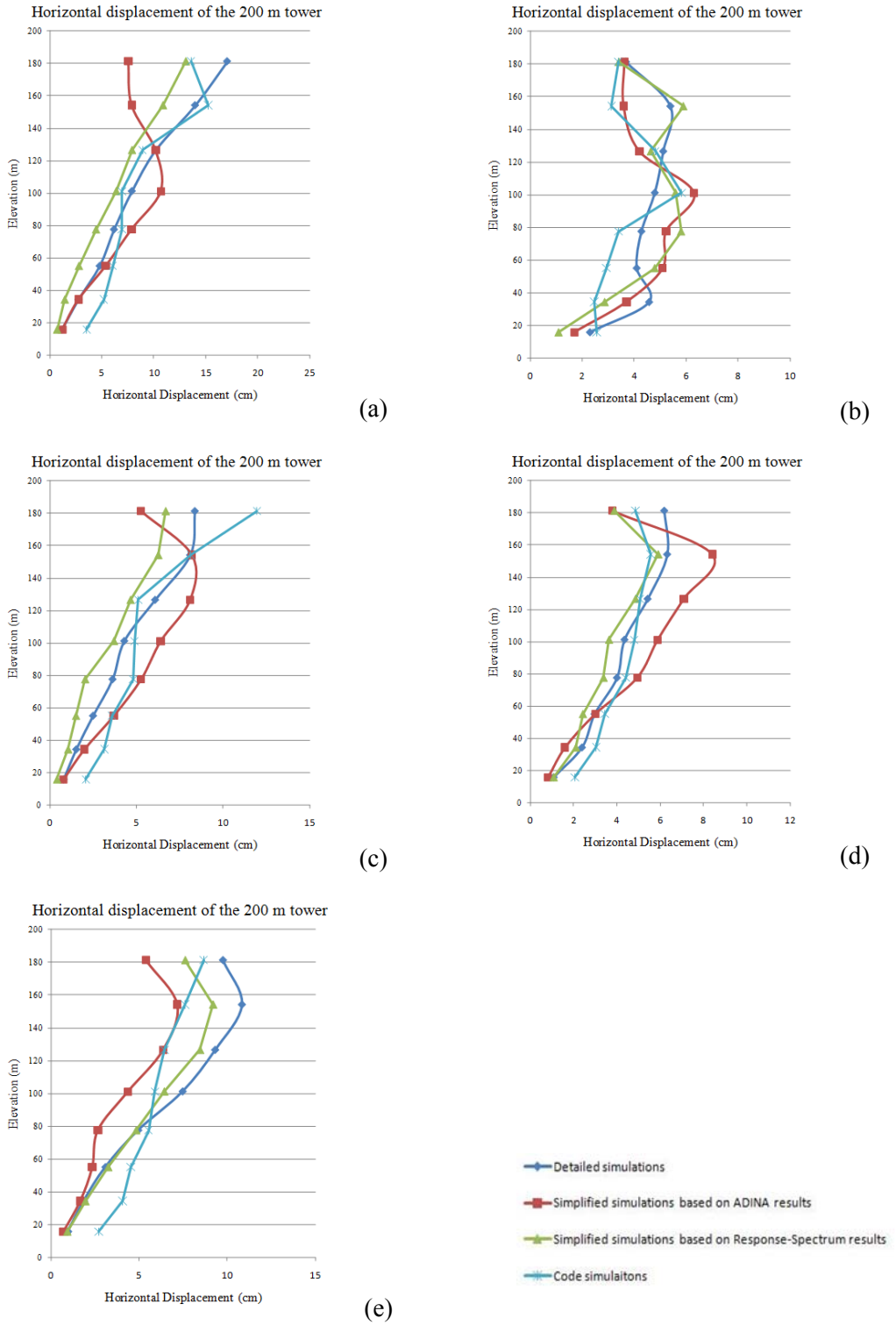

Figure D.5. Maximum horizontal mast displacement of the 200 m tower under different earthquakes: (a) ElCentro, (b) Parkfield, (c) Taft, (d) Montreal and (e) Synthetic Earthquakes.

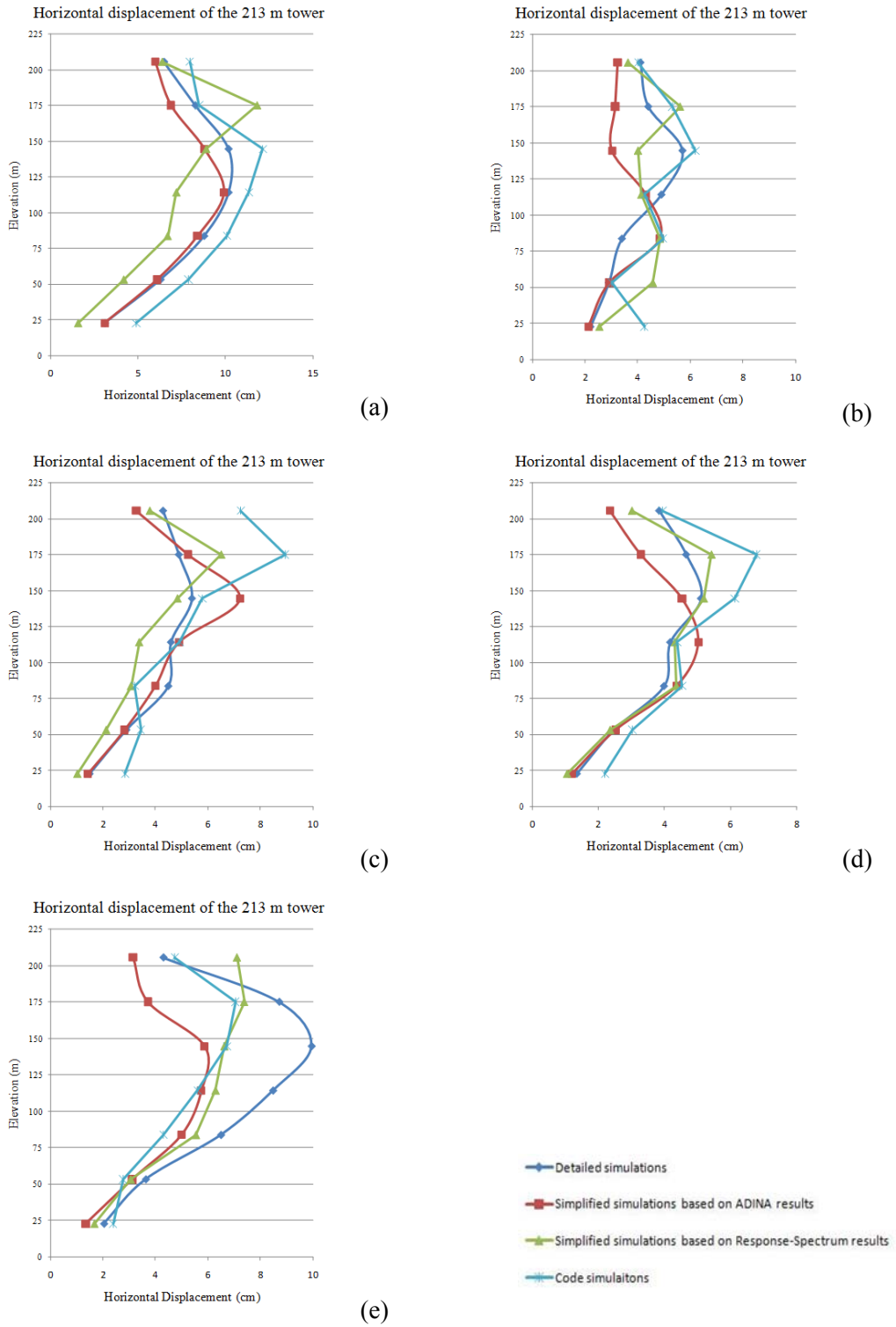

Figure D.6. Maximum horizontal mast displacement of the 213 m tower under different earthquakes: (a) ElCentro, (b) Parkfield, (c) Taft, (d) Montreal and (e) Synthetic Earthquakes.

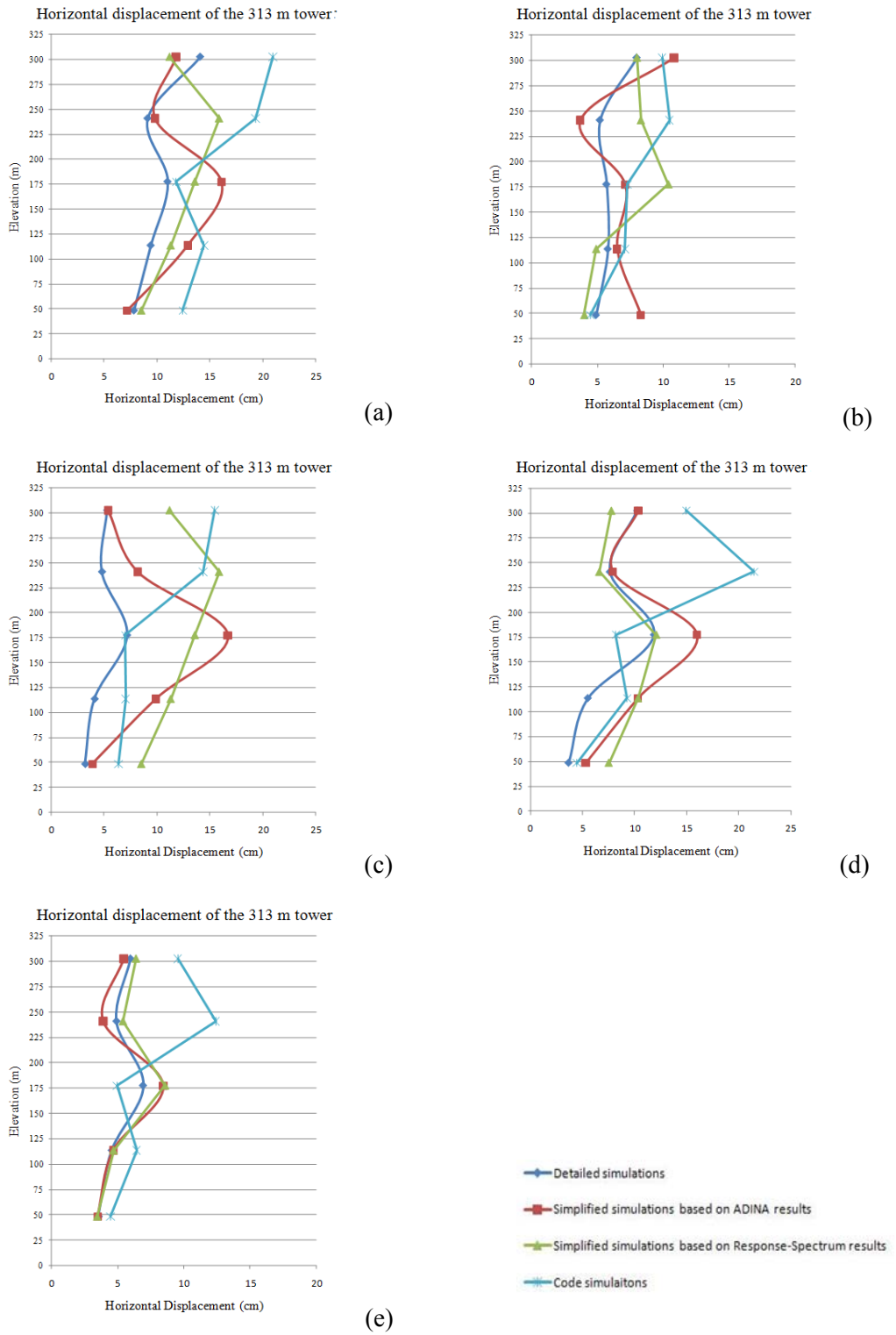

Figure D.7. Maximum horizontal mast displacement of the 313 m tower under different earthquakes: (a) ElCentro, (b) Parkfield, (c) Taft, (d) Montreal and (e) Synthetic Earthquakes.

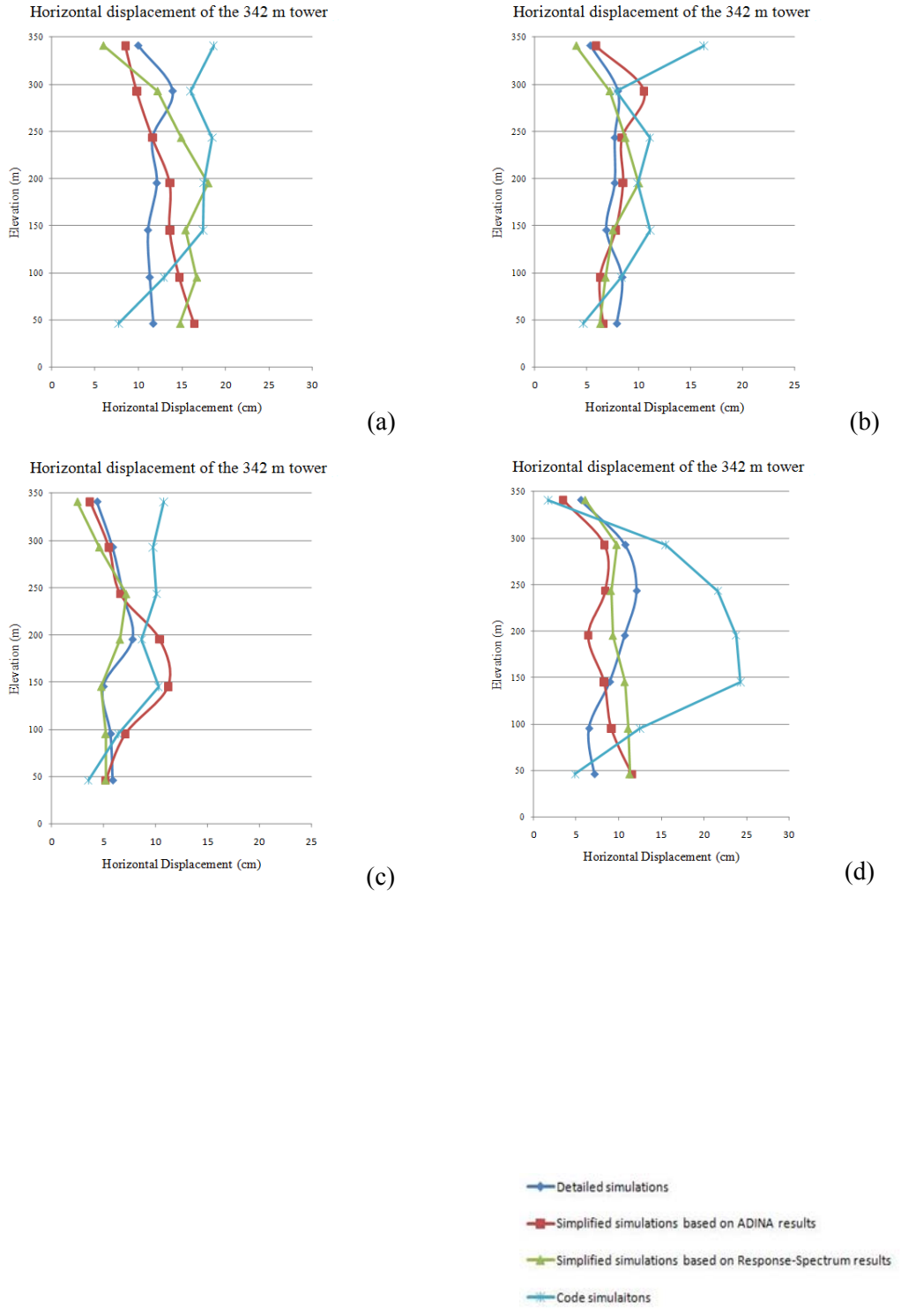

Figure D.8. Maximum horizontal mast displacement of the 342 m tower under different earthquakes: (a) ElCentro, (b) Parkfield, (c) Taft and (d) Montreal Earthquakes.

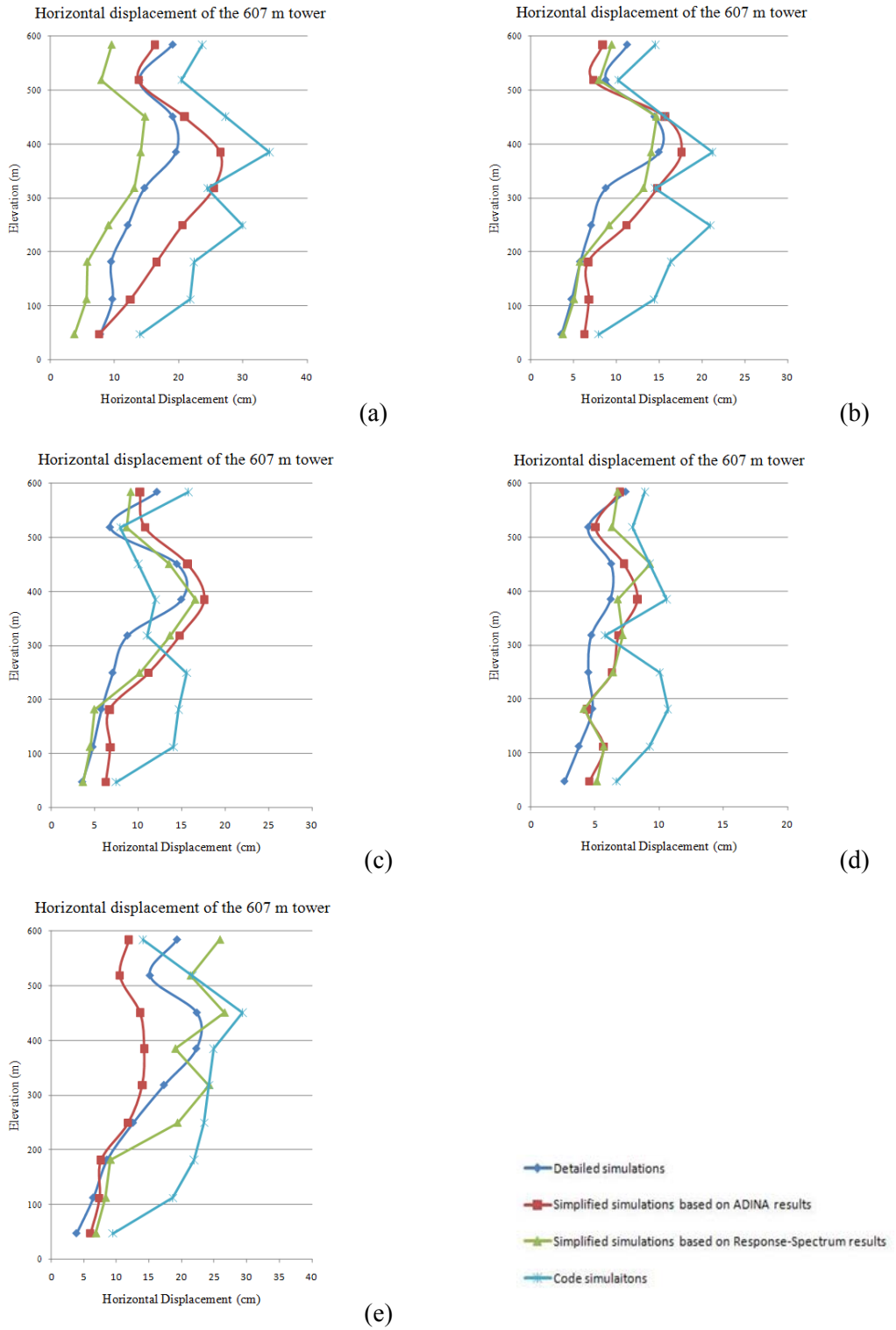

Figure D.9. Maximum horizontal mast displacement of the 607 m tower under different earthquakes: (a) ElCentro, (b) Parkfield, (c) Taft, (d) Montreal and (e) Synthetic Earthquakes.

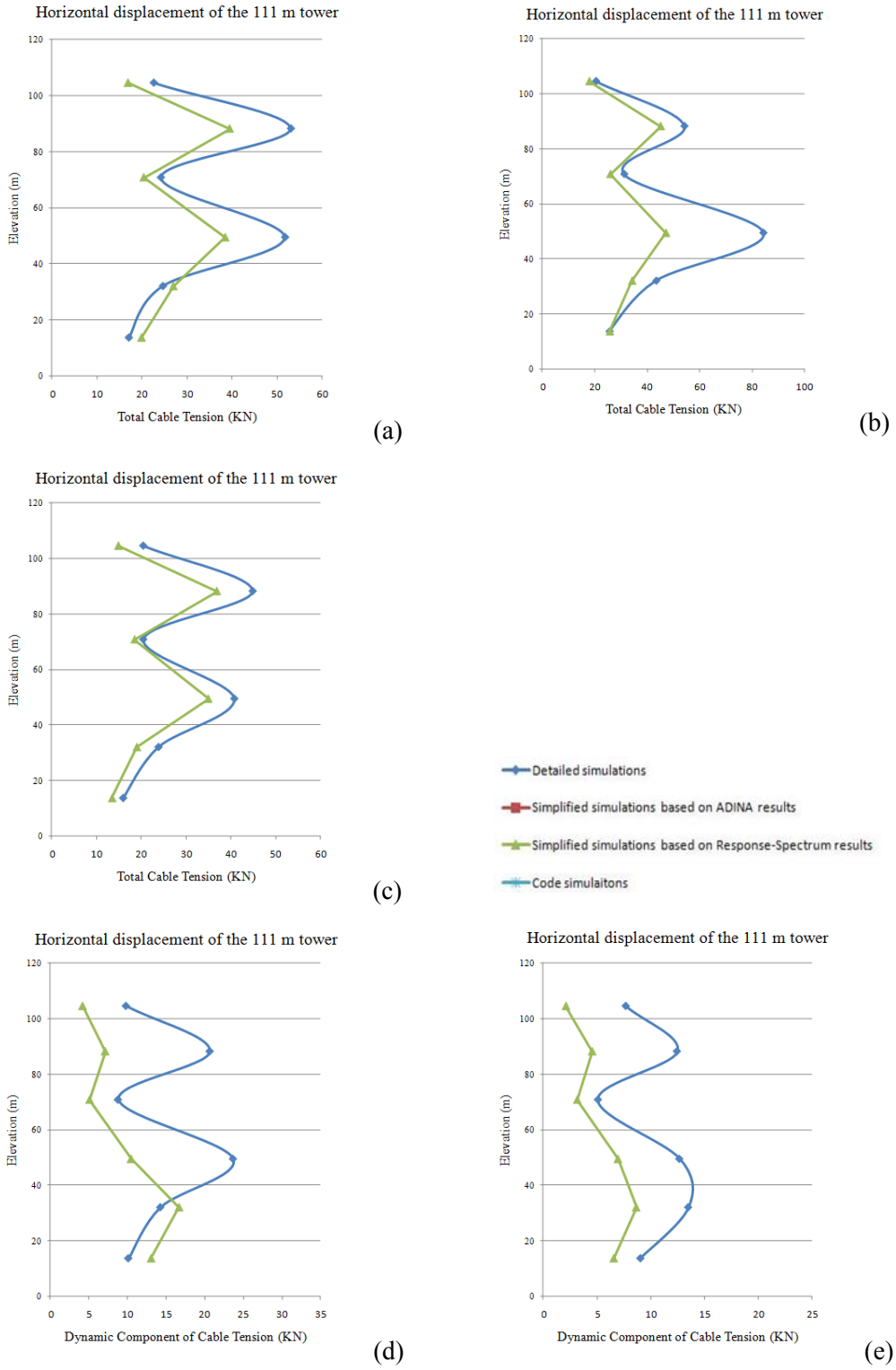

Figure D.10. Total average cable tensions of the 111 m tower under: (a) ElCentro, (b) Parkfield and (c) Taft, and the average cable tensions under: (d) ElCentro, and (e) Taft earthquakes.

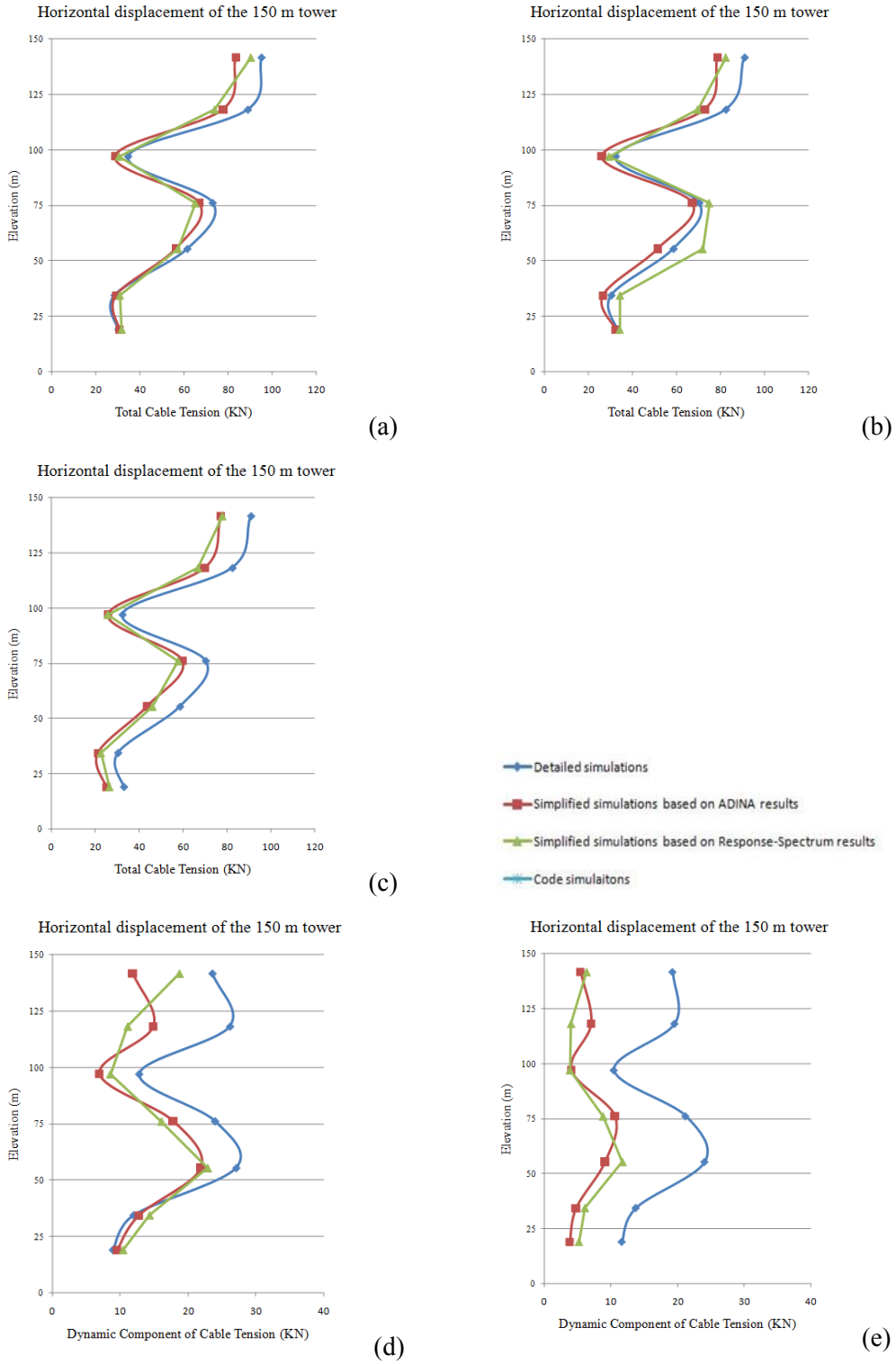

Figure D.11. Total average cable tensions of the 150 m tower under: (a) ElCentro, (b) Parkfield and (c) Taft, and the average cable tensions under: (d) ElCentro, and (e) Taft earthquakes.

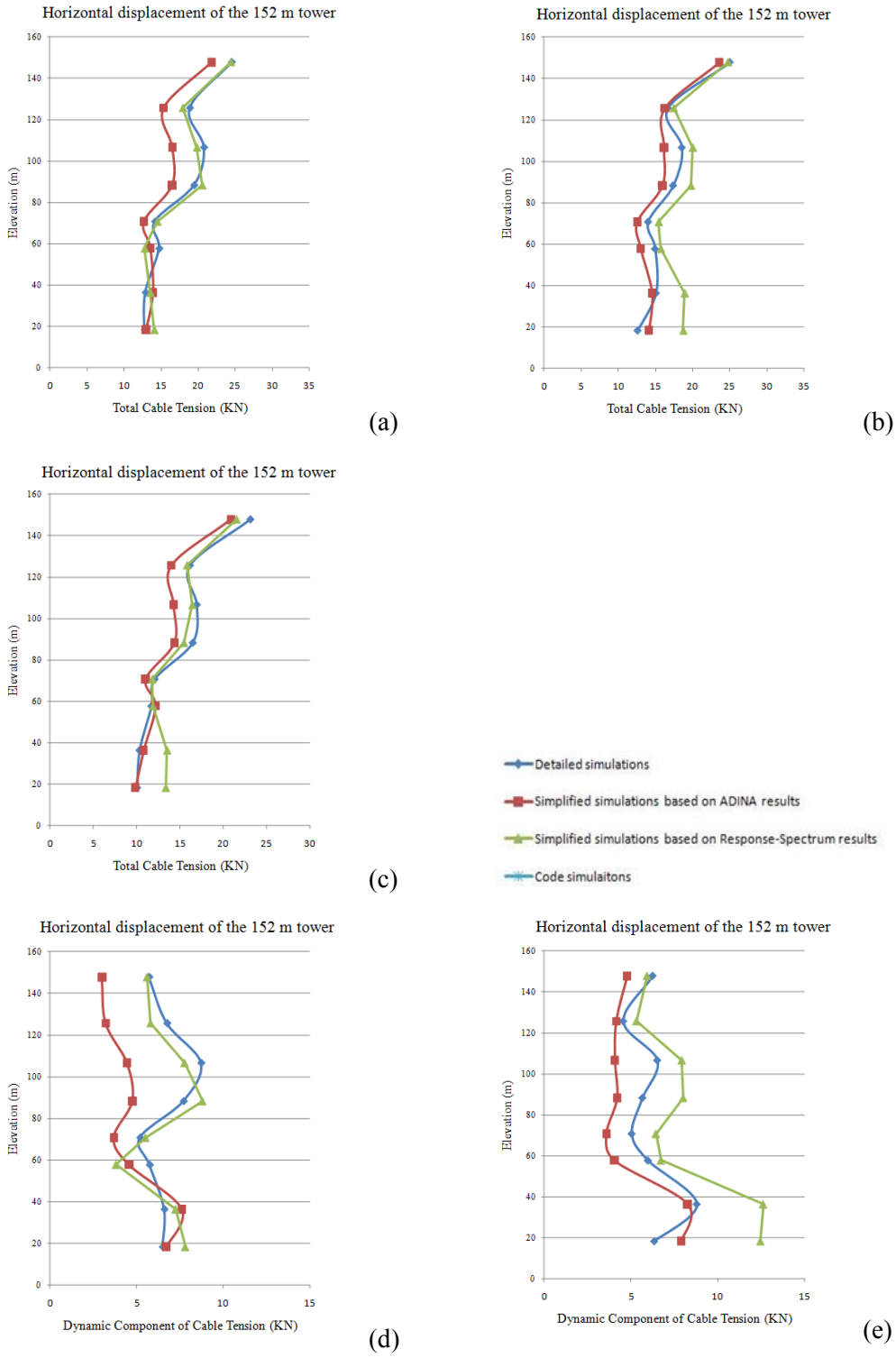

Figure D.12. Total average cable tensions of the 152 m tower under: (a) ElCentro, (b) Parkfield and (c) Taft, and the average cable tensions under: (d) ElCentro, and (e) Parkfield earthquakes.

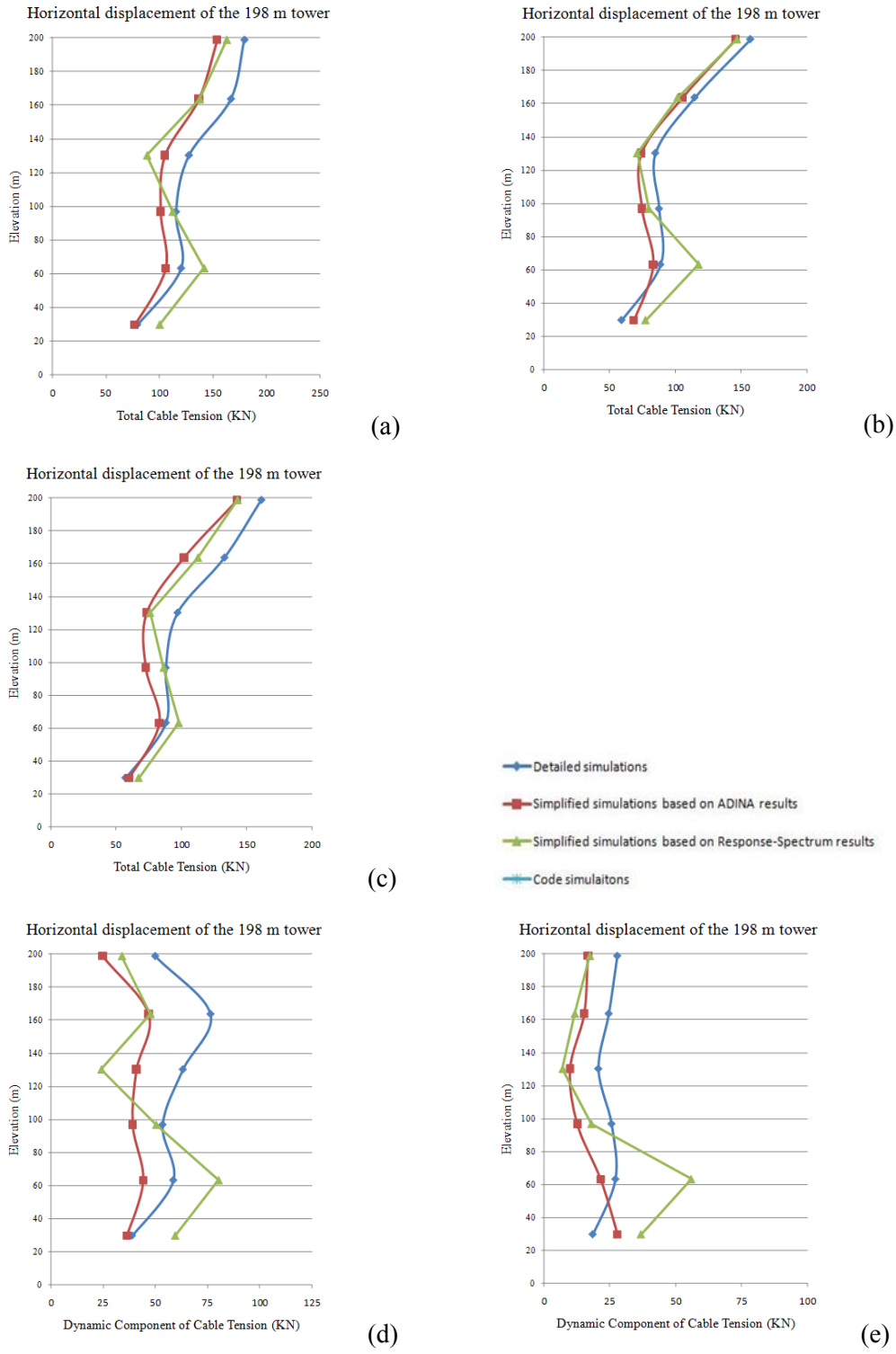

Figure D.13. Total average cable tensions of the 198 m tower under: (a) ElCentro, (b) Parkfield and (c) Taft, and the average cable tensions under: (d) ElCentro, and (e) Parkfield earthquakes.

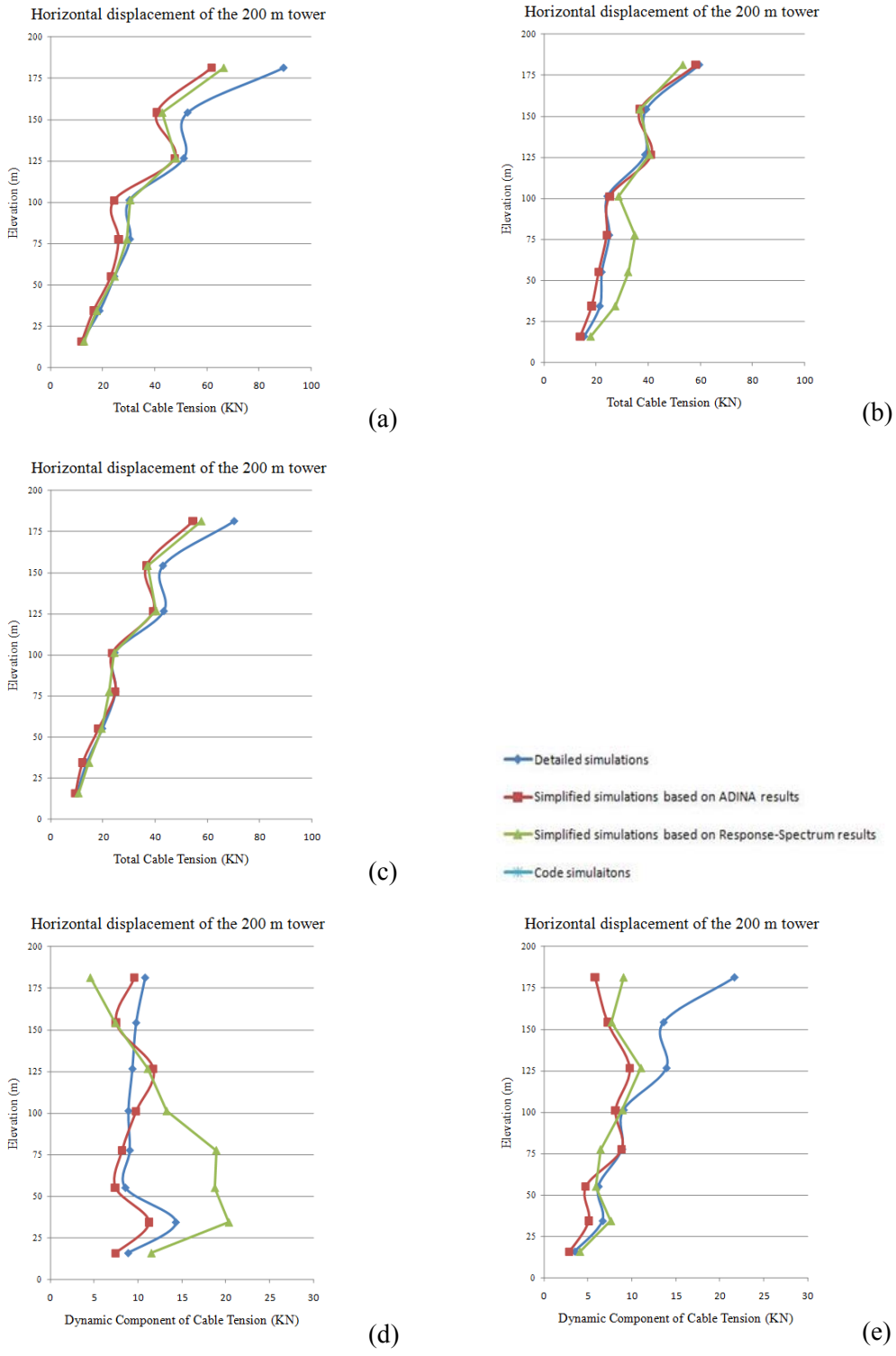

Figure D.14. Total average cable tensions of the 200 m tower under: (a) ElCentro, (b) Parkfield and (c) Taft, and the average cable tensions under: (d) Parkfield, and (e) Taft earthquakes.

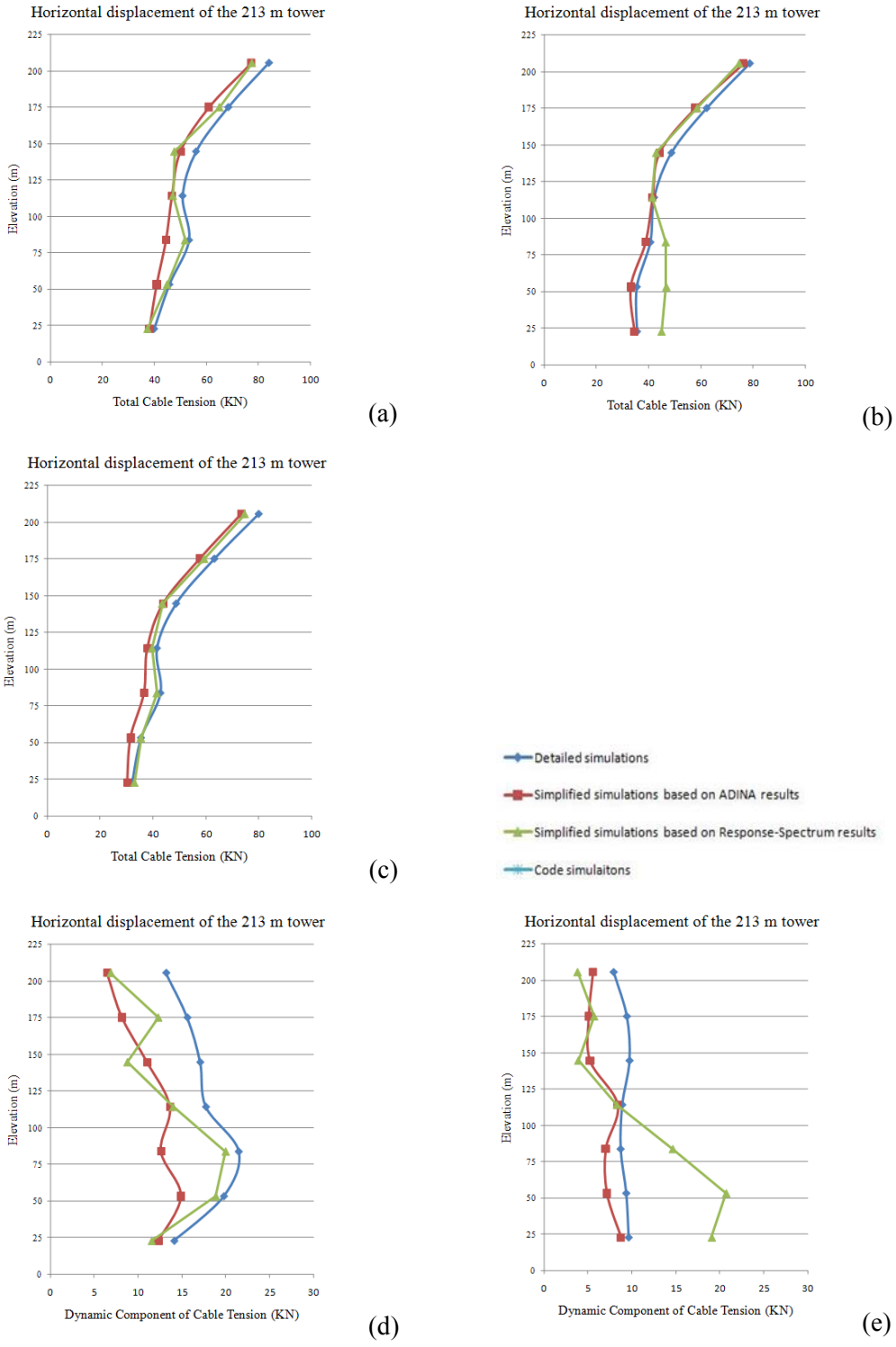

Figure D.15. Total average cable tensions of the 213 m tower under: (a) ElCentro, (b) Parkfield and (c) Taft, and the average cable tensions under: (d) ElCentro, and (e) Parkfield earthquakes.

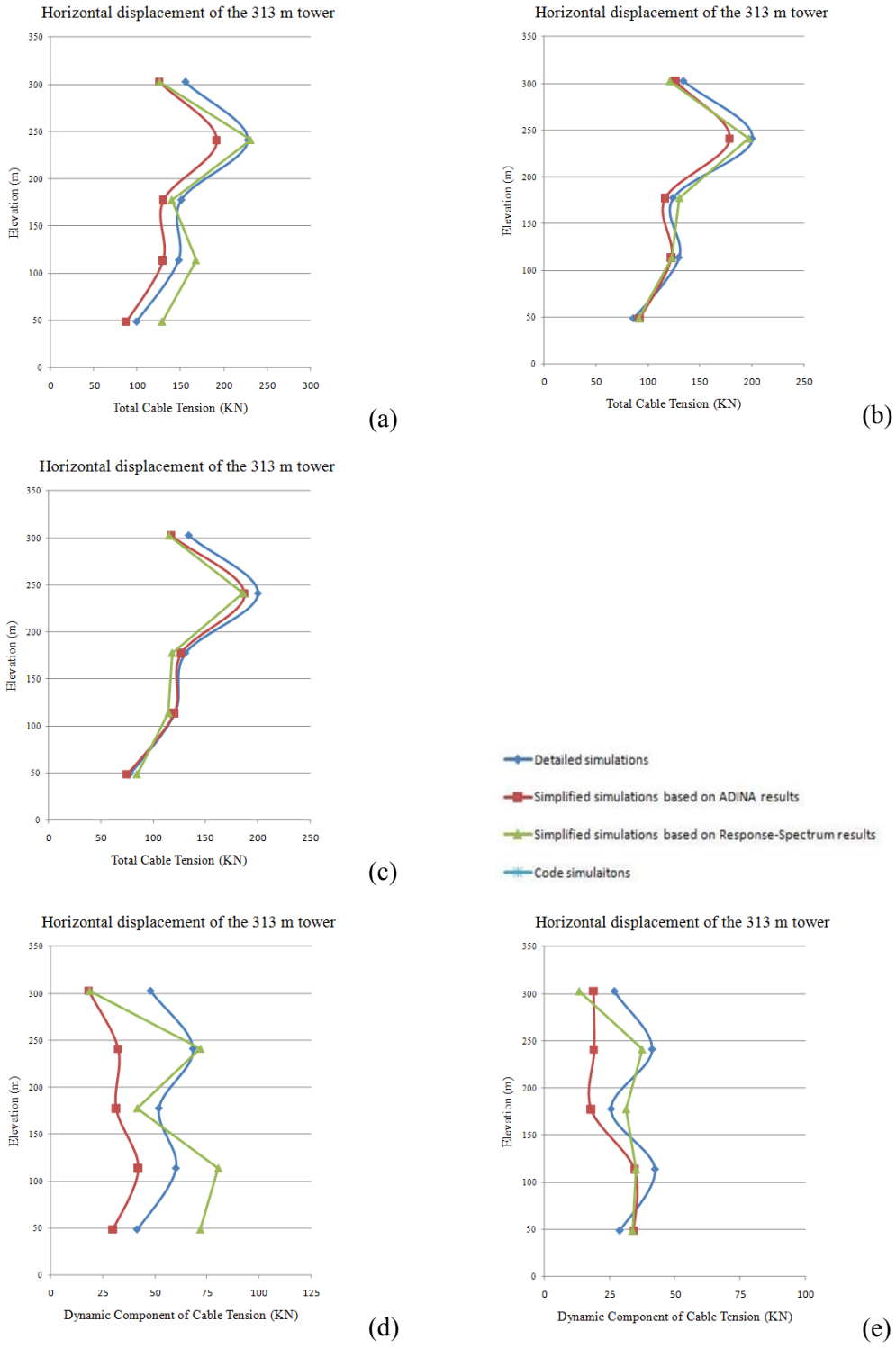

Figure D.16. Total average cable tensions of the 313 m tower under: (a) ElCentro, (b) Parkfield and (c) Taft, and the average cable tensions under: (d) ElCentro, and (e) Parkfield earthquakes.

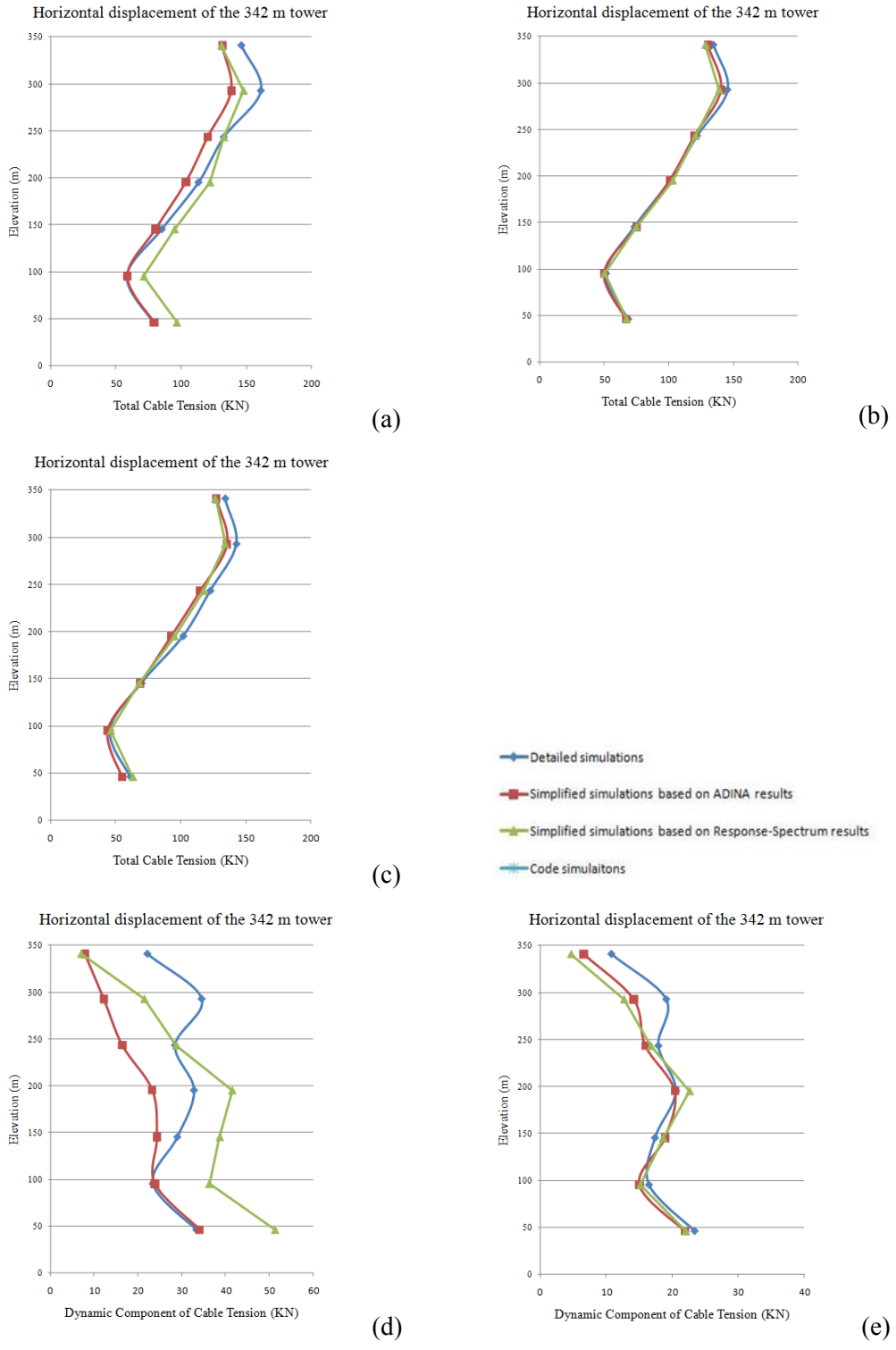

Figure D.17. Total average cable tensions of the 342 m tower under: (a) ElCentro, (b) Parkfield and (c) Taft, and the average cable tensions under: (d) ElCentro, and (e) Parkfield earthquakes.

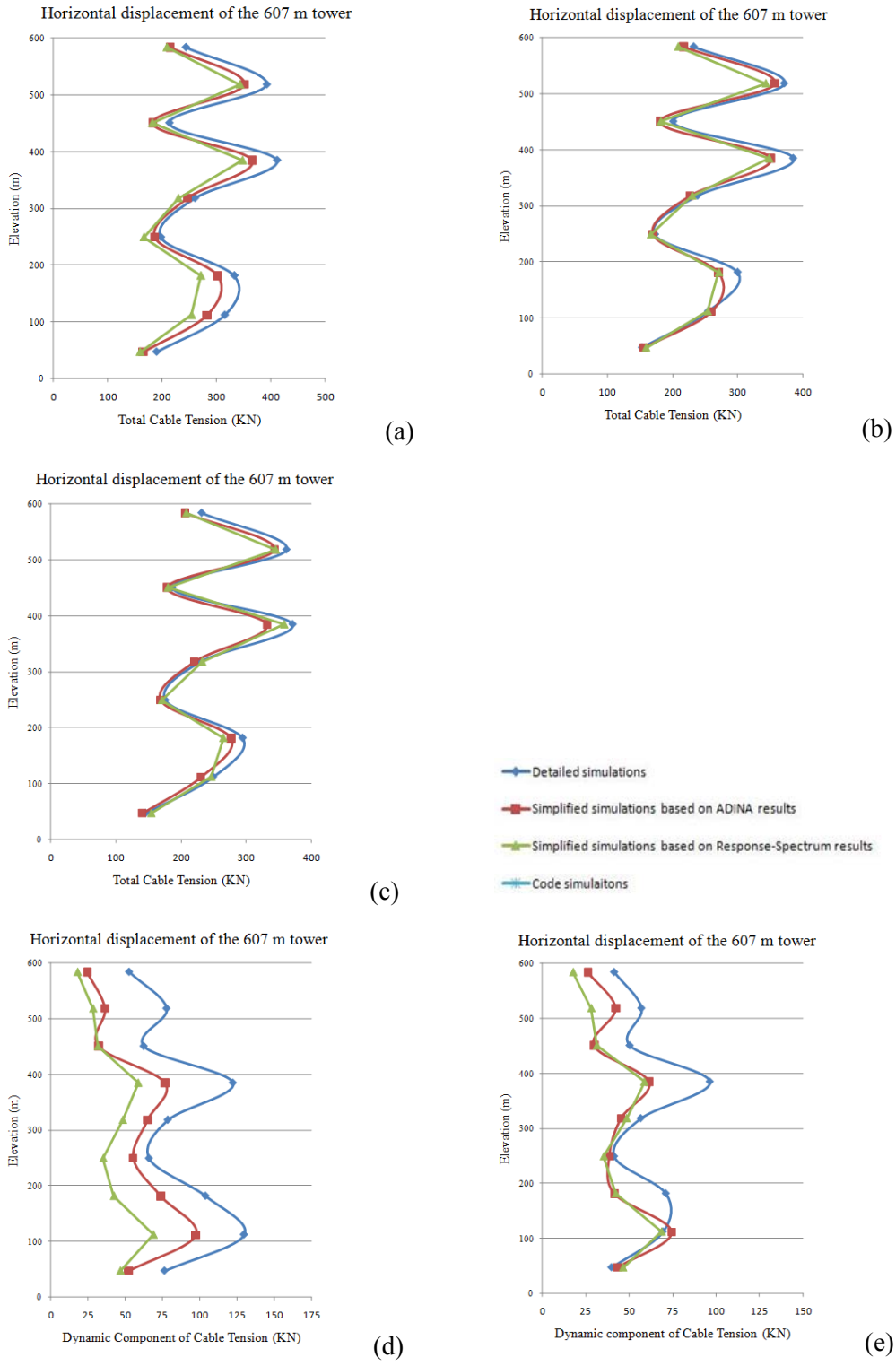

Figure D.18. Total average cable tensions of the 607 m tower under: (a) ElCentro, (b) Parkfield and (c) Taft, and the average cable tensions under: (d) ElCentro, and (e) Parkfield earthquakes.

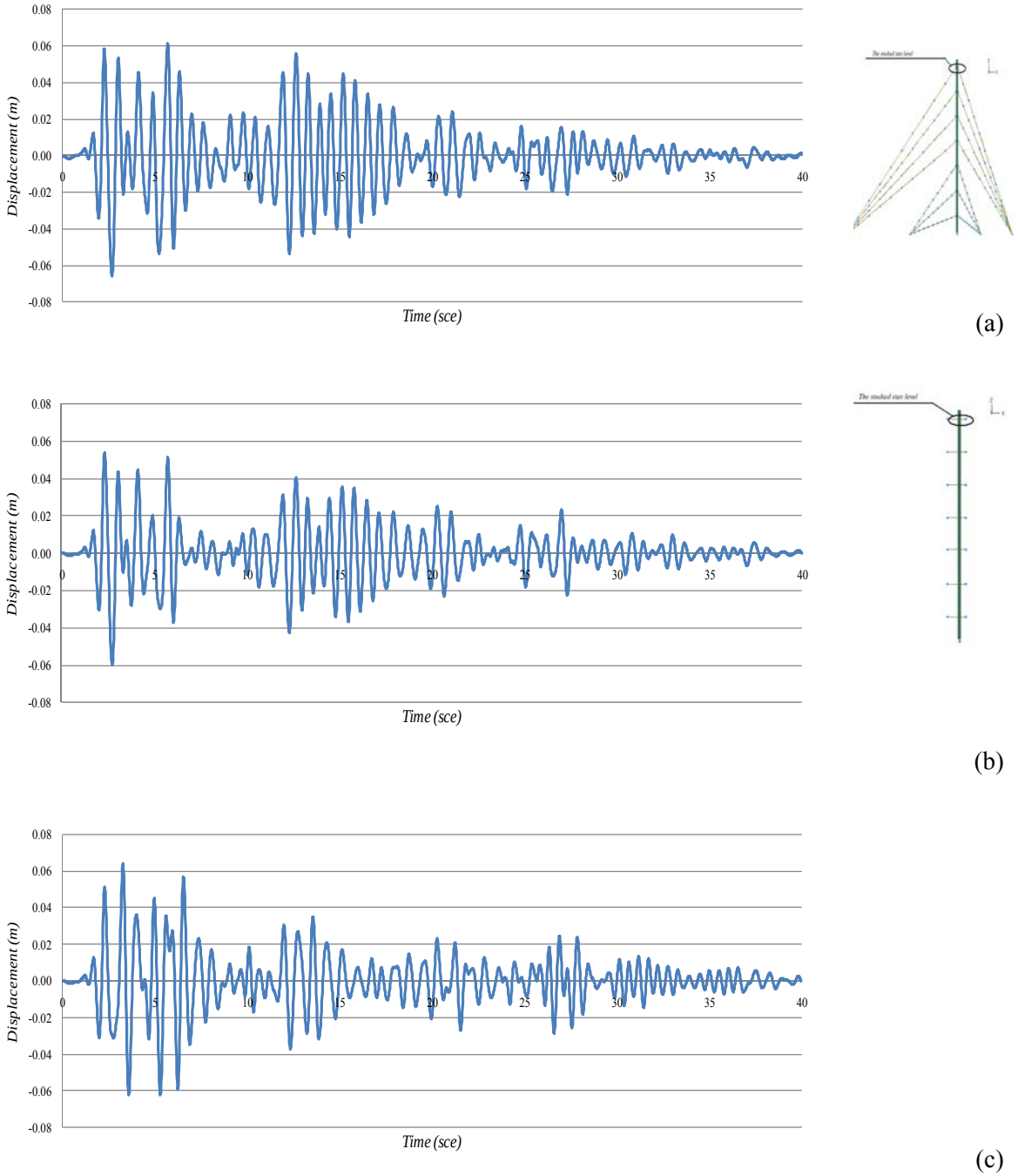

Figure D.19. Horizontal displacement time history of the 213 m mast at the 7th cluster level under ElCentro earthquake, (a) detailed nonlinear model, (b) simplified model based on the spring linearized stiffness obtained from ADINA simulations, (c) simplified model based on the spring stiffness obtained from the proposed response spectral method.

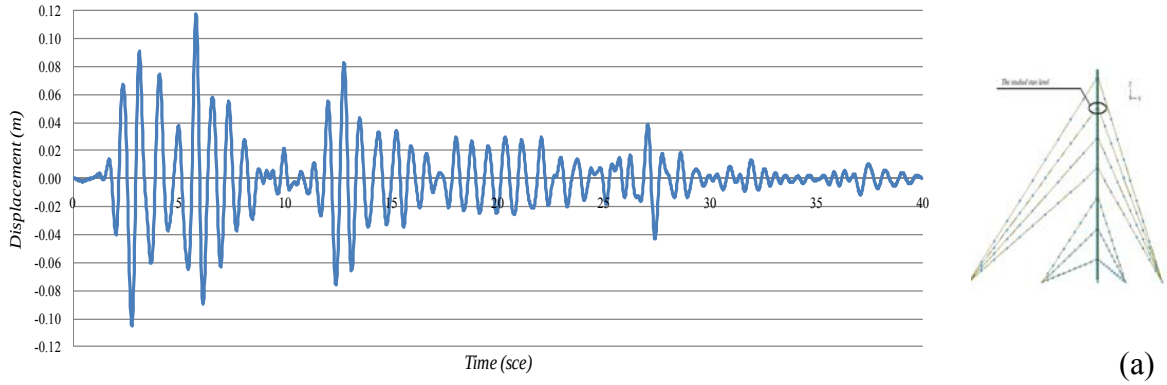

(a)

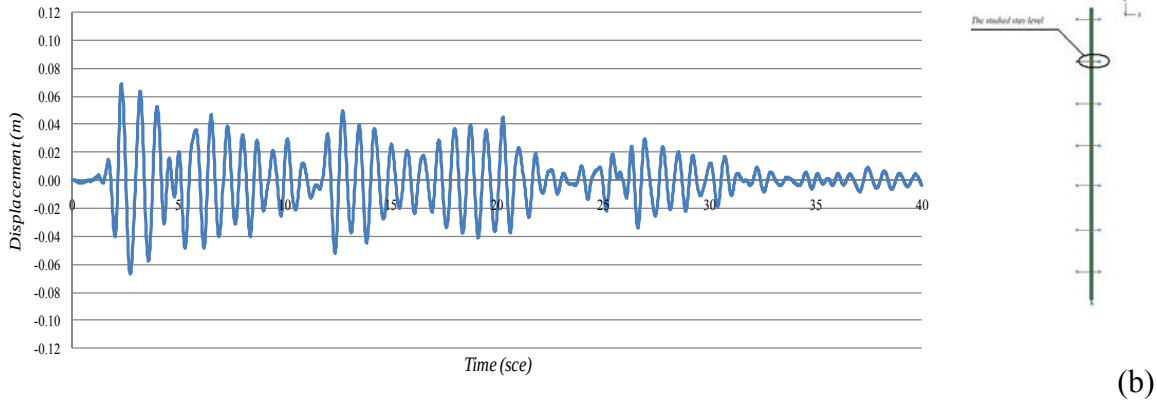

(b)

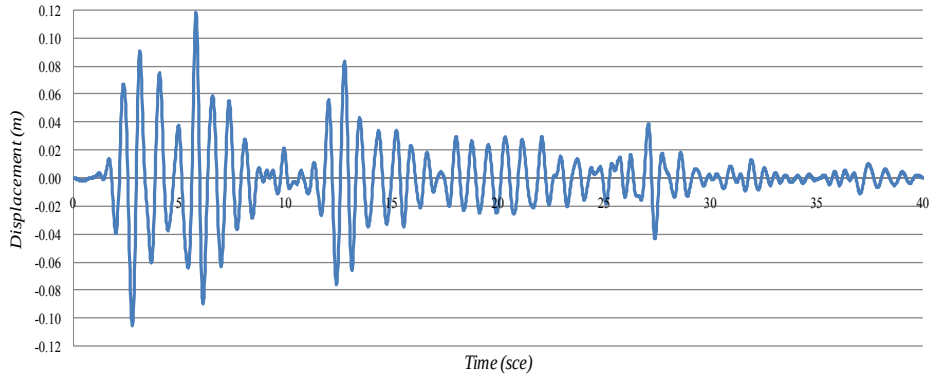

(c)

Figure D.20. Horizontal displacement time history of the 213 m mast at the 6th cluster level under ElCentro earthquake, (a) detailed nonlinear model, (b) simplified model based on the spring linearized stiffness obtained from ADINA simulations, (c) simplified model based on the spring stiffness obtained from the proposed response spectral method.

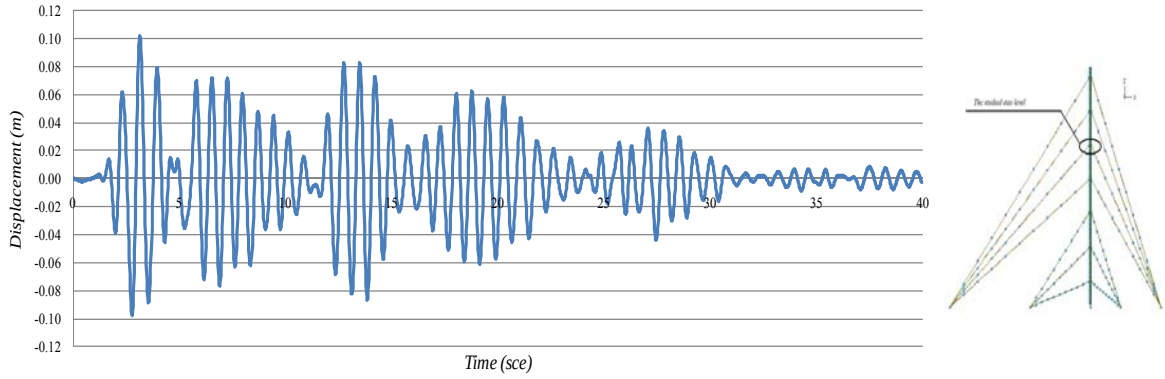

(a)

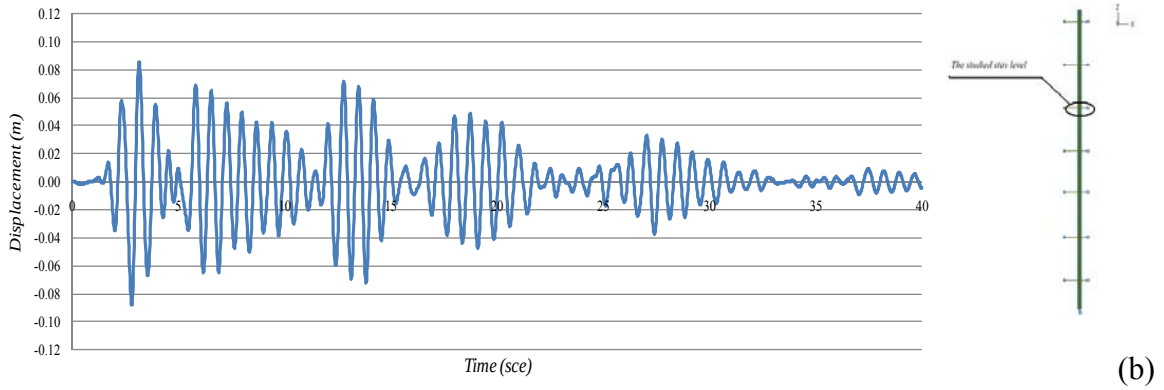

(b)

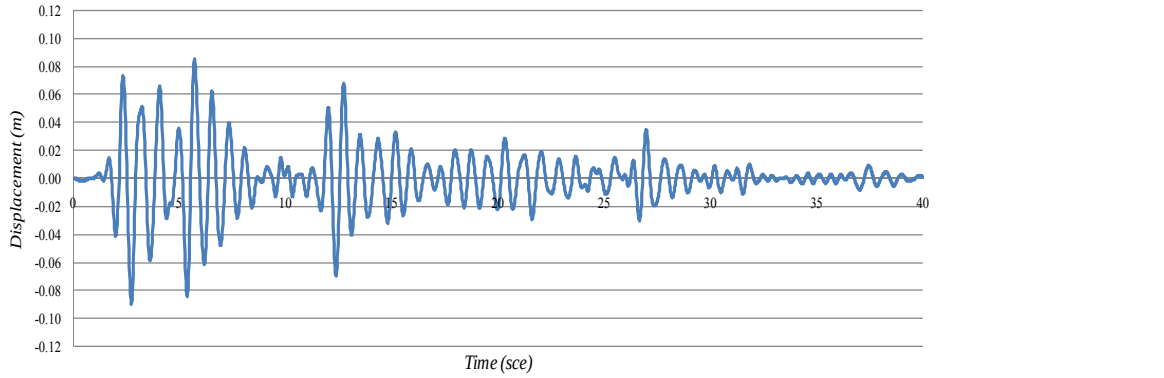

(c)

Figure D.21. Horizontal displacement time history of the 213 m mast at the 5th cluster level under ElCentro earthquake, (a) detailed nonlinear model, (b) simplified model based on the spring linearized stiffness obtained from ADINA simulations, (c) simplified model based on the spring stiffness obtained from the proposed response spectral method.

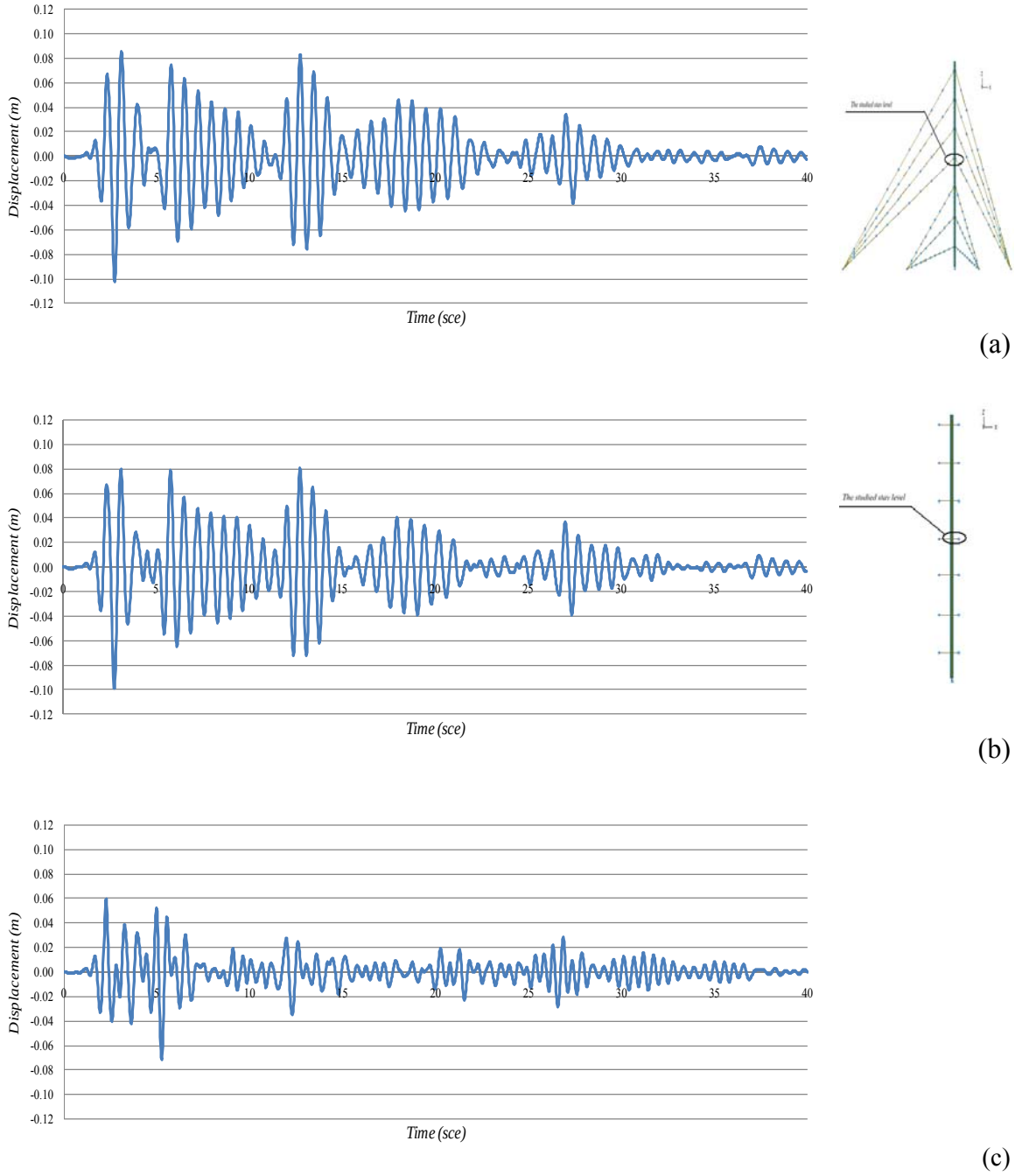

Figure D.22. Horizontal displacement time history of the 213 m mast at the 4th cluster level under ElCentro earthquake, (a) detailed nonlinear model, (b) simplified model based on the spring linearized stiffness obtained from ADINA simulations, (c) simplified model based on the spring stiffness obtained from the proposed response spectral method.

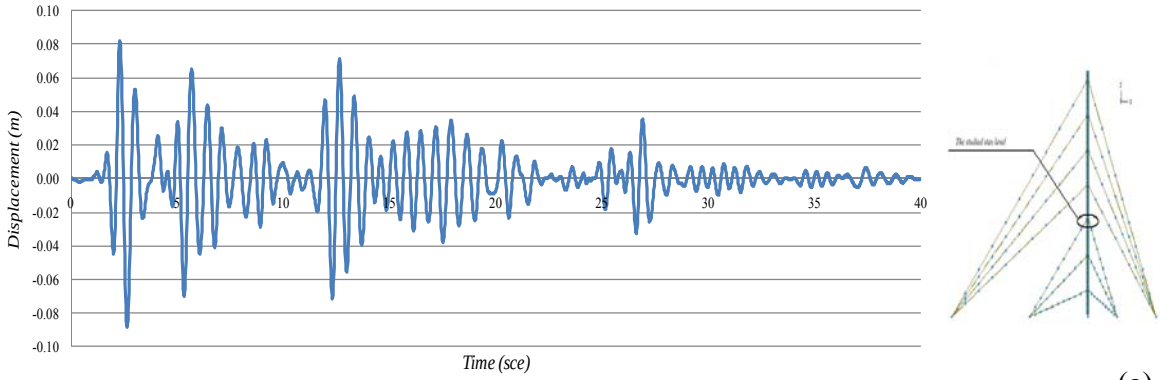

(a)

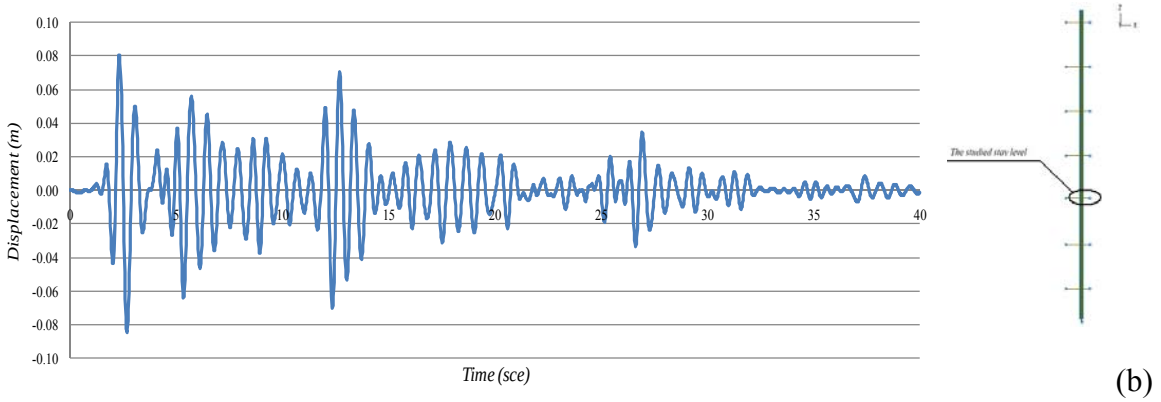

(b)

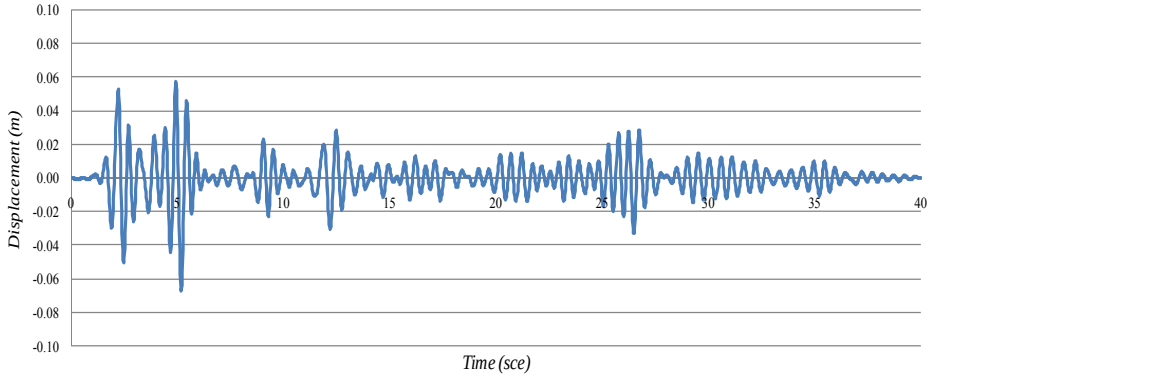

(c)

Figure D.23. Horizontal displacement time history of the 213 m mast at the 3rd cluster level under ElCentro earthquake, (a) detailed nonlinear model, (b) simplified model based on the spring linearized stiffness obtained from ADINA simulations, (c) simplified model based on the spring stiffness obtained from the proposed response spectral method.

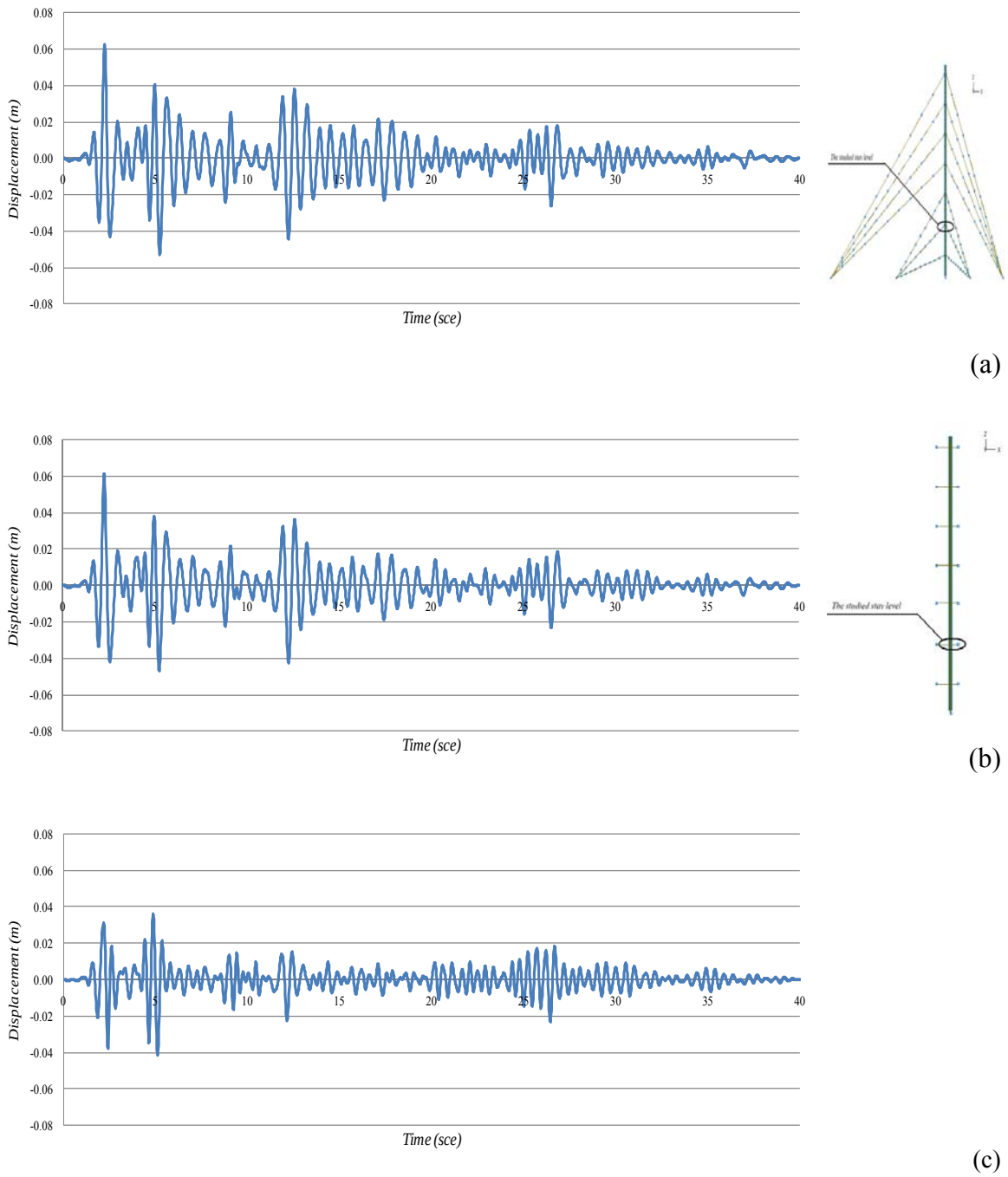

Figure D.24. Horizontal displacement time history of the 213 m mast at the 2nd cluster level under ElCentro earthquake, (a) detailed nonlinear model, (b) simplified model based on the spring linearized stiffness obtained from ADINA simulations, (c) simplified model based on the spring stiffness obtained from the proposed response spectral method.

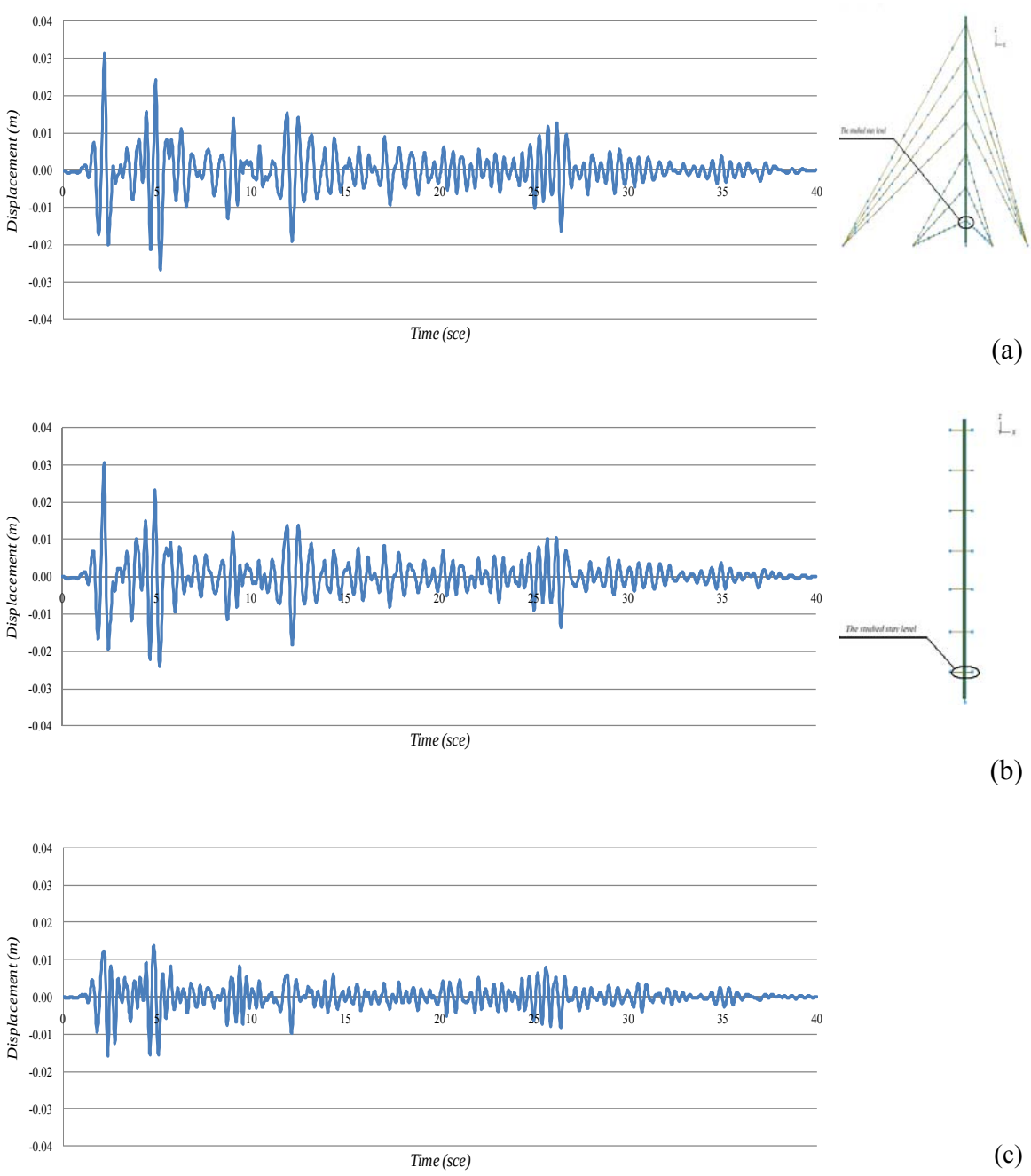

Figure D.25. Horizontal displacement time history of the 213 m mast at the 1st cluster level under ElCentro earthquake, (a) detailed nonlinear model, (b) simplified model based on the spring linearized stiffness obtained from ADINA simulations, (c) simplified model based on the spring stiffness obtained from the proposed response spectral method.

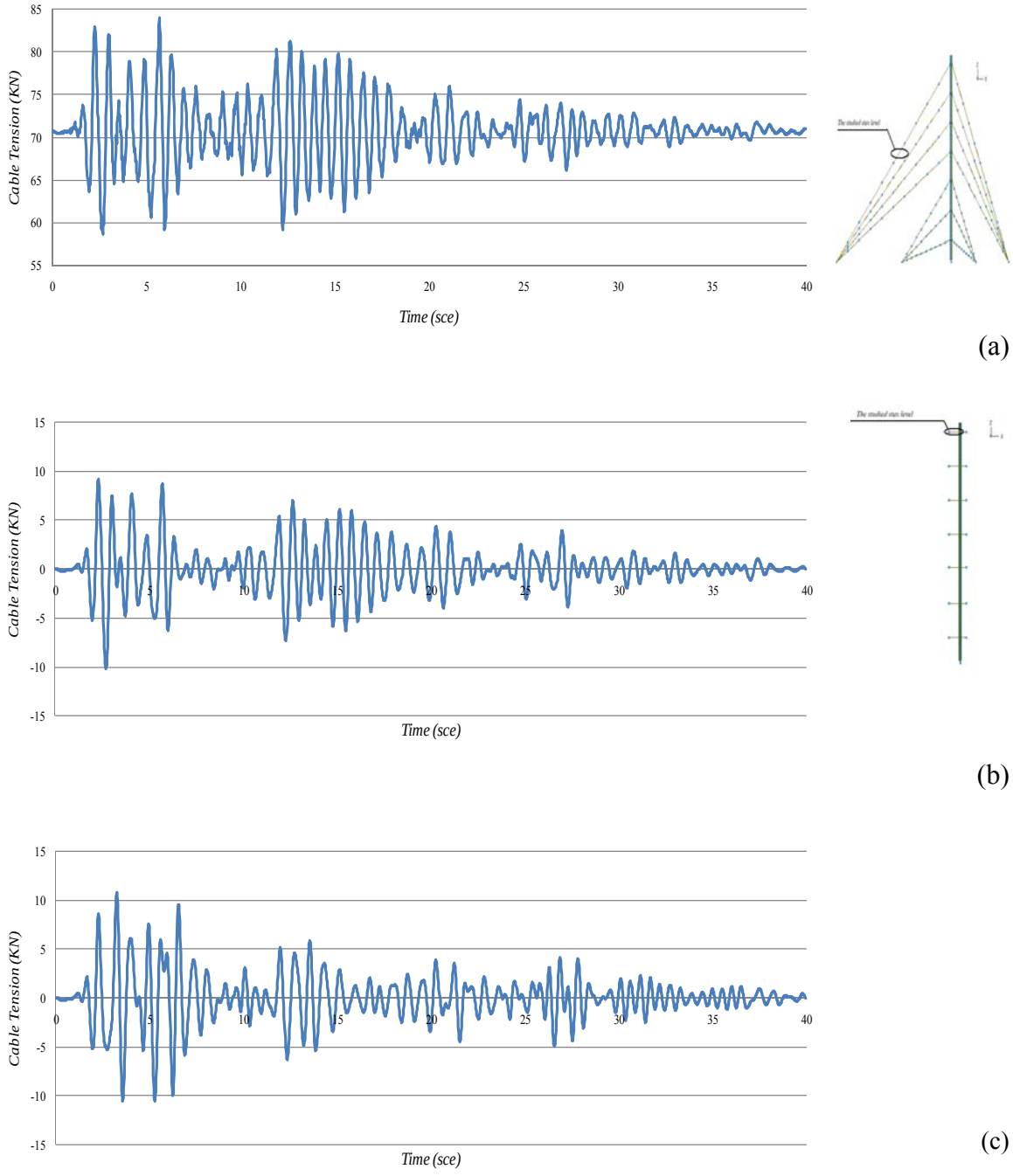

Figure D.26. Total average cable tensions force of the 213 m mast at the 7th cluster level under ElCentro earthquake, (a) detailed nonlinear model, (b) simplified model based on the spring linearized stiffness obtained from ADINA simulations, (c) simplified model based on the spring stiffness obtained from the proposed response spectral method.

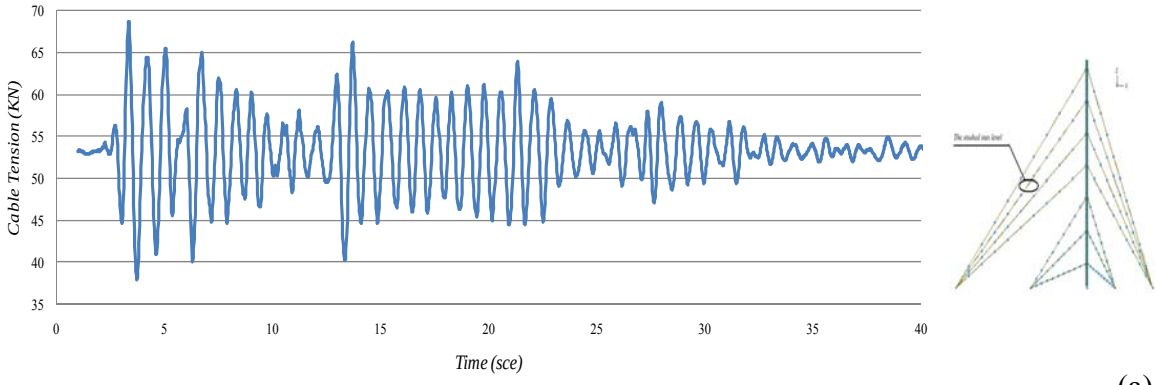

(a)

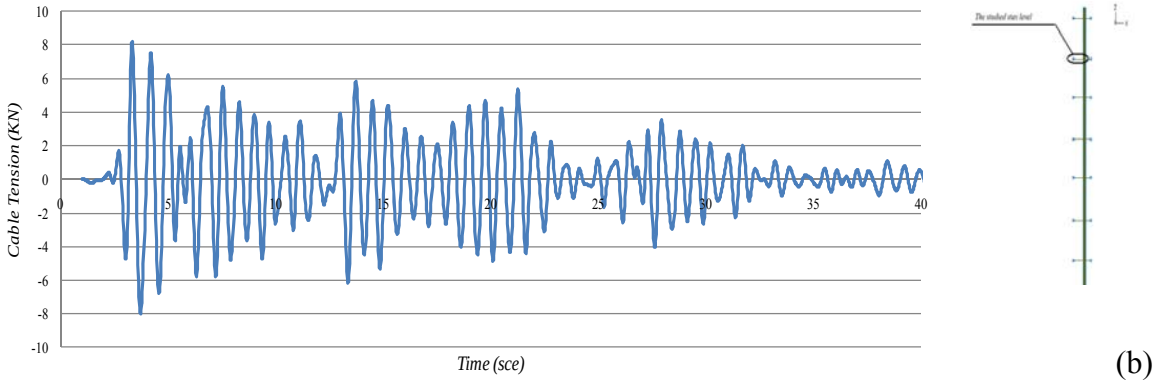

(b)

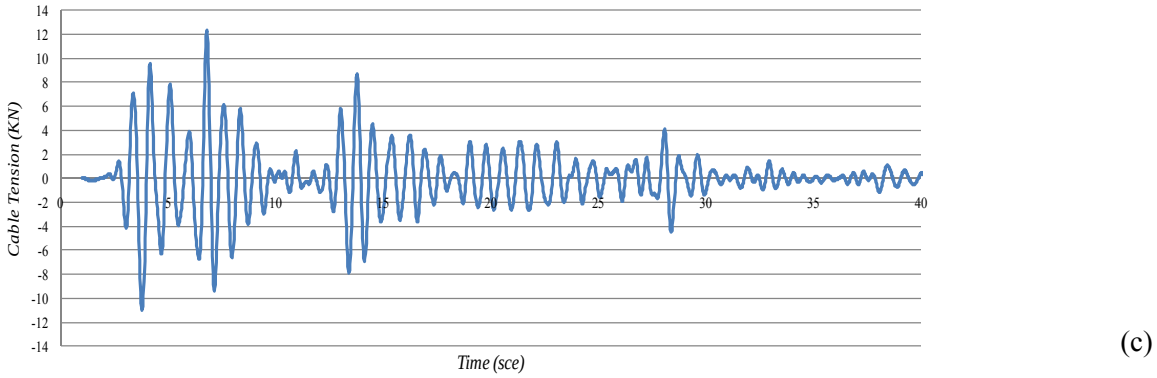

(c)

Figure D.27. Total average cable tensions force of the 213 m mast at the 6th cluster level under ElCentro earthquake, (a) detailed nonlinear model, (b) simplified model based on the spring linearized stiffness obtained from ADINA simulations, (c) simplified model based on the spring stiffness obtained from the proposed response spectral method.

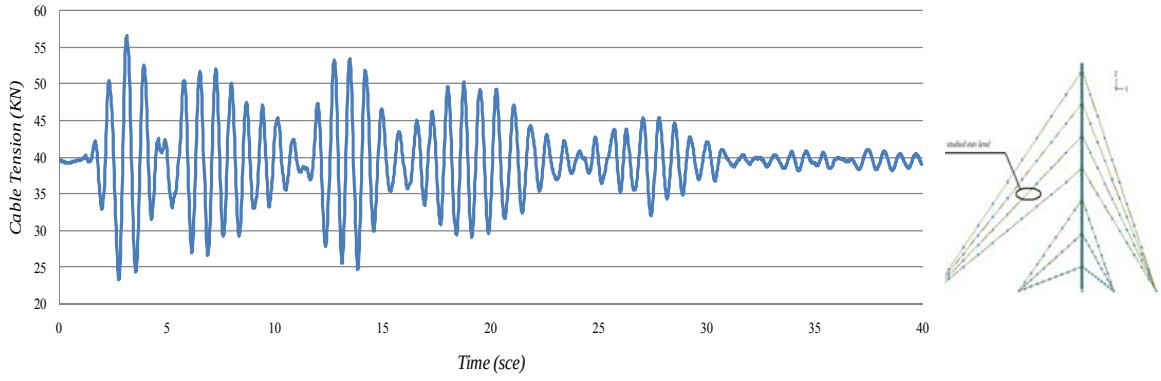

(a)

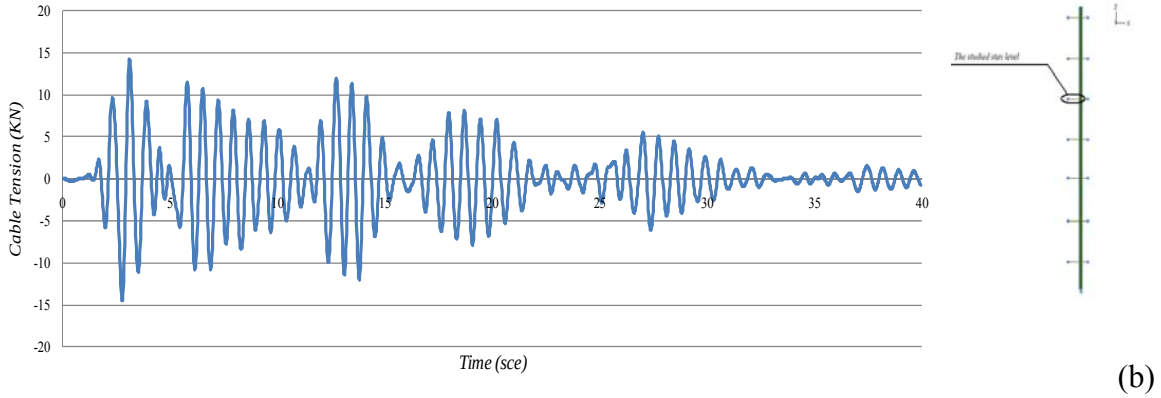

(b)

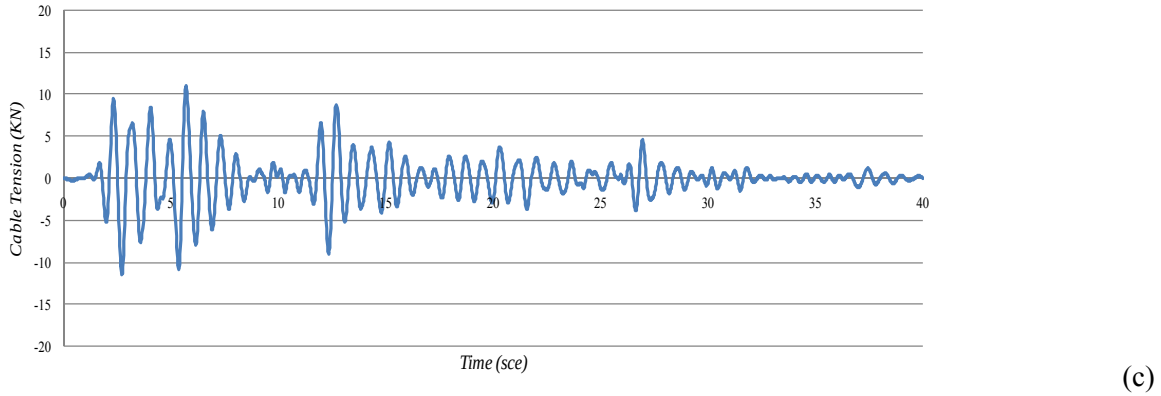

(c)

Figure D.28. Total average cable tensions force of the 213 m mast at the 5th cluster level under ElCentro earthquake, (a) detailed nonlinear model, (b) simplified model based on the spring linearized stiffness obtained from ADINA simulations, (c) simplified model based on the spring stiffness obtained from the proposed response spectral method.

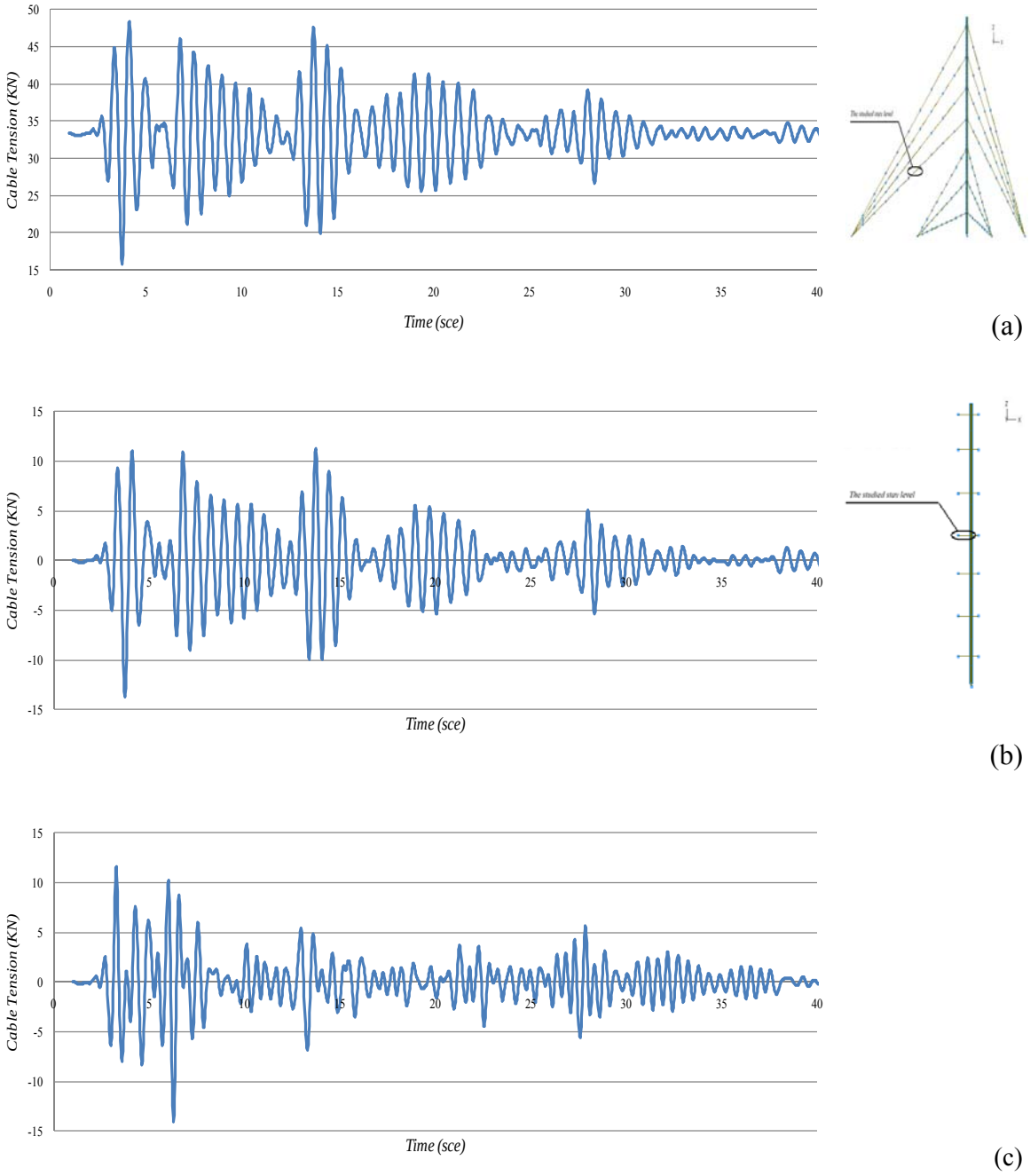

Figure D.29. Total average cable tensions force of the 213 m mast at the 4th cluster level under ElCentro earthquake, (a) detailed nonlinear model, (b) simplified model based on the spring linearized stiffness obtained from ADINA simulations, (c) simplified model based on the spring stiffness obtained from the proposed response spectral method.

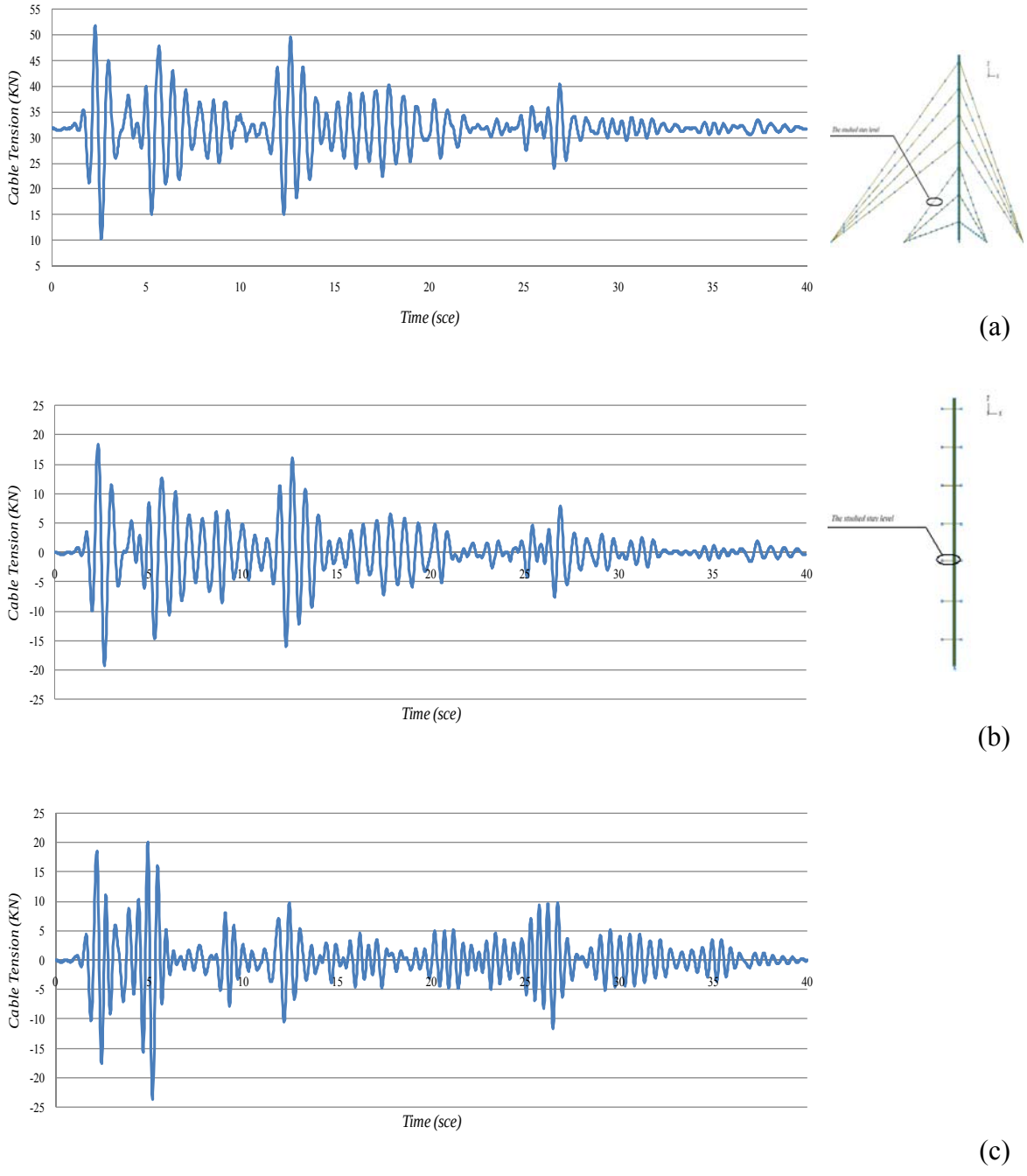

Figure D.30. Total average cable tensions force of the 213 m mast at the 3rd cluster level under ElCentro earthquake, (a) detailed nonlinear model, (b) simplified model based on the spring linearized stiffness obtained from ADINA simulations, (c) simplified model based on the spring stiffness obtained from the proposed response spectral method.

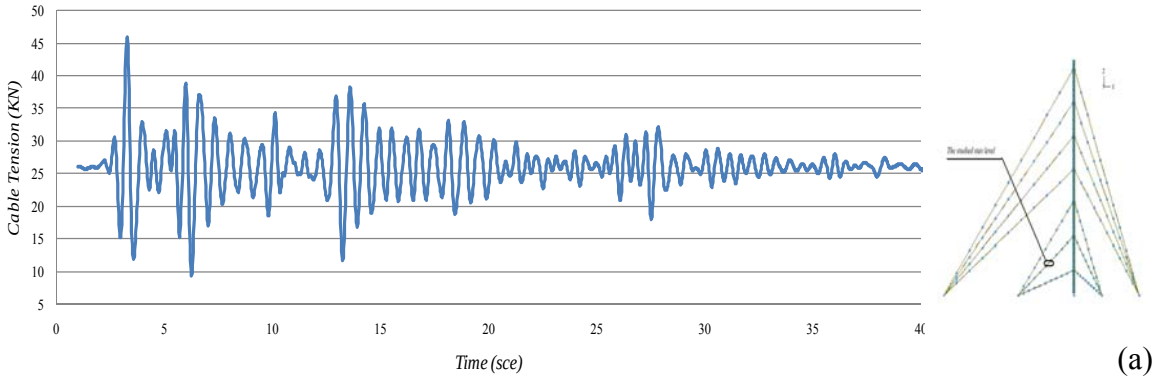

(a)

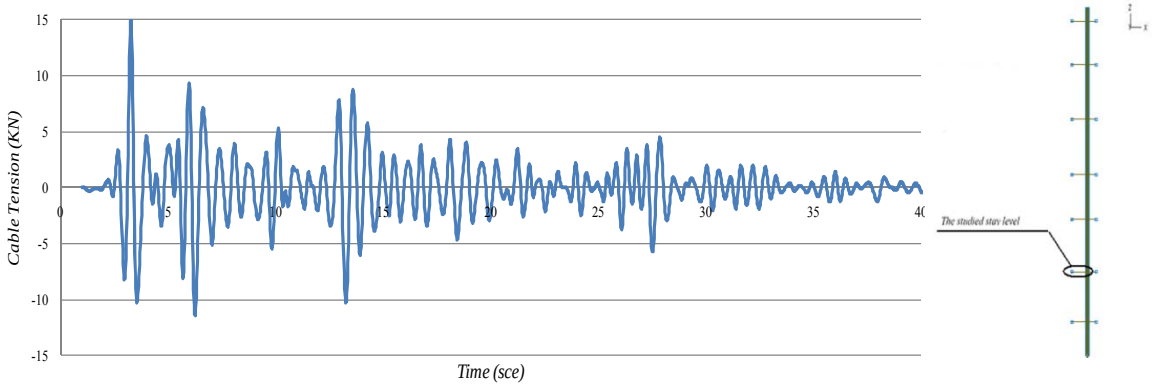

(b)

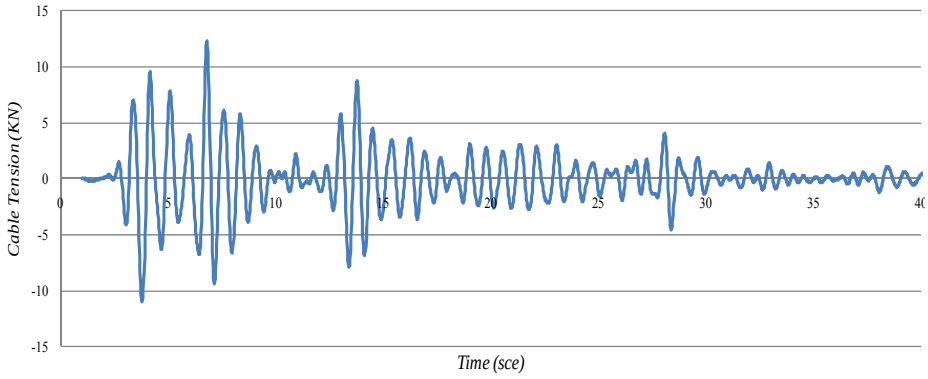

(c)

Figure D.31. Total average cable tensions force of the 213 m mast at the 2nd cluster level under ElCentro earthquake, (a) detailed nonlinear model, (b) simplified model based on the spring linearized stiffness obtained from ADINA simulations, (c) simplified model based on the spring stiffness obtained from the proposed response spectral method.

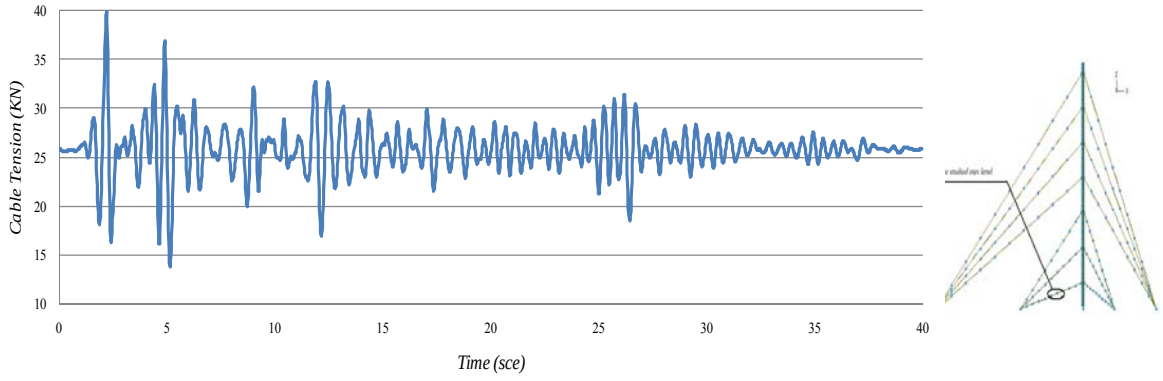

(a)

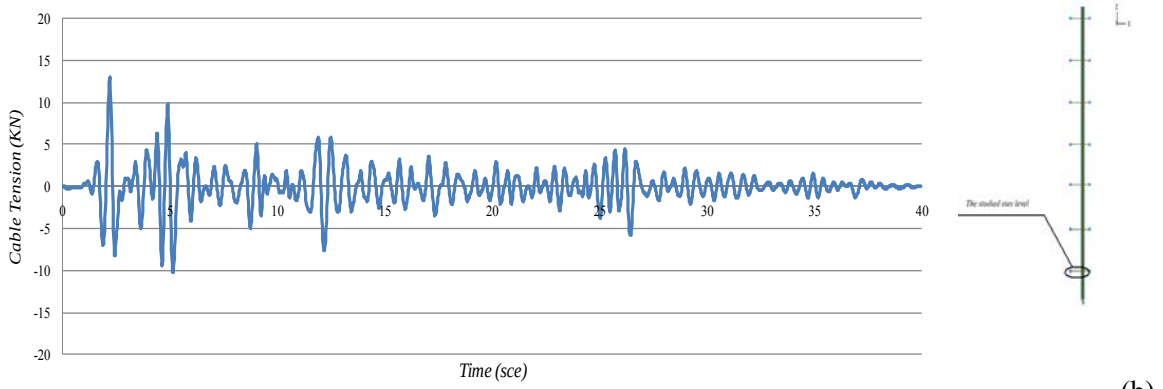

(b)

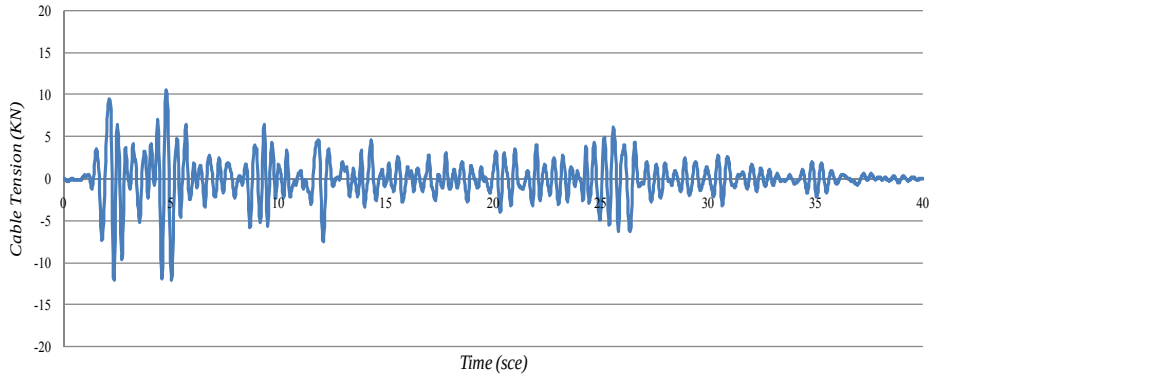

(c)

Figure D.32. Total average cable tensions force of the 213 m mast at the 1st cluster level under ElCentro earthquake, (a) detailed nonlinear model, (b) simplified model based on the spring linearized stiffness obtained from ADINA simulations, (c) simplified model based on the spring stiffness obtained from the proposed response spectral method.

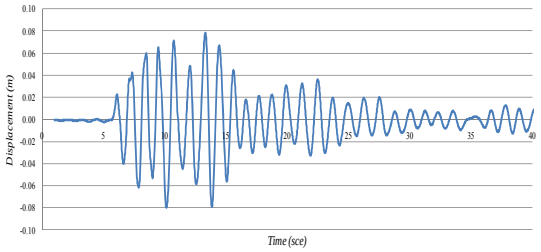

(a)

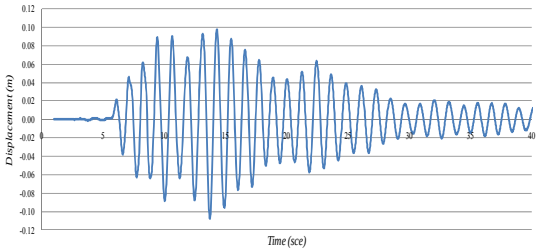

(b)

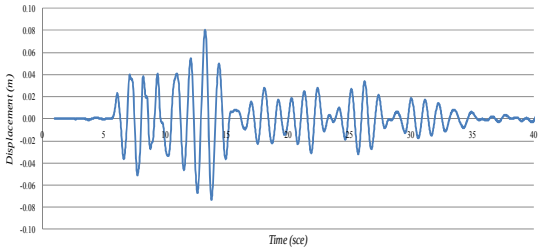

(c)

Figure D.33. Horizontal displacement of the 313 m mast at the 5th cluster level under Parkfield earthquake, (a) detailed nonlinear model, (b) simplified model based on ADINA spring, (c) simplified model based on proposed response spectral method spring.

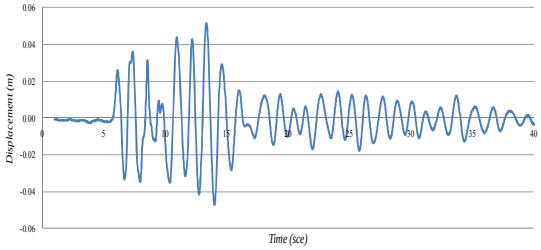

(a)

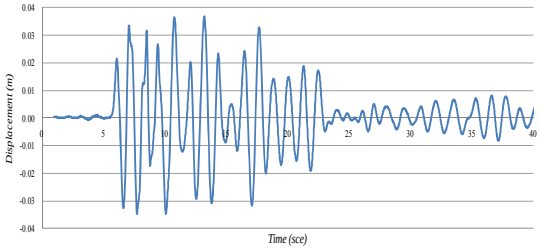

(b)

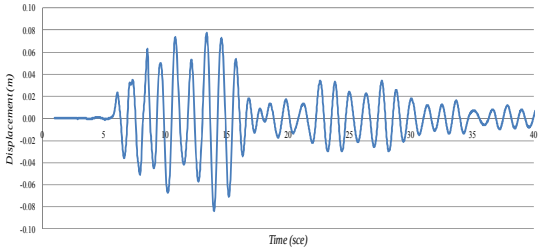

(c)

Figure D.34. Horizontal displacement of the 313 m mast at the 4th cluster level under Parkfield earthquake, (a) detailed nonlinear model, (b) simplified model based on ADINA spring, (c) simplified model based on proposed response spectral method spring.

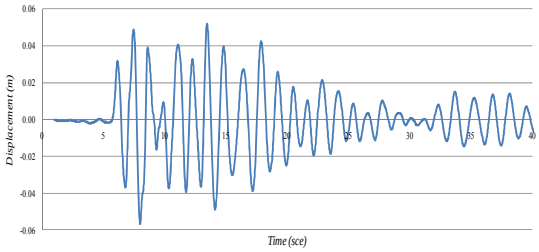

(a)

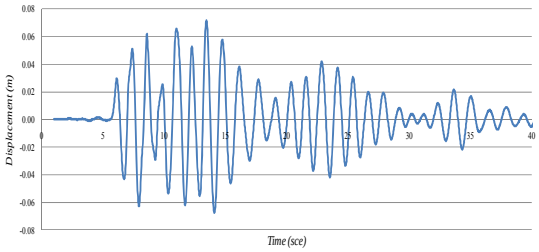

(b)

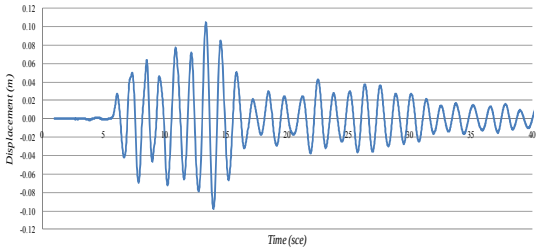

(c)

Figure D.35. Horizontal displacement of the 313 m mast at the 3th cluster level under Parkfield earthquake, (a) detailed nonlinear model, (b) simplified model based on ADINA spring, (c) simplified model based on proposed response spectral method spring.

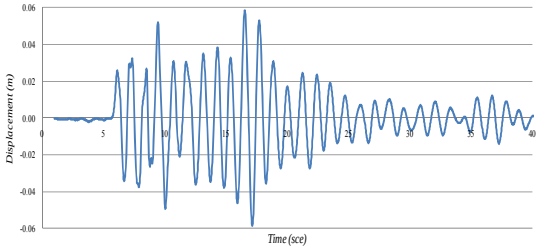

(a)

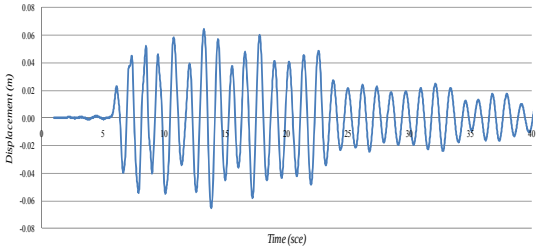

(b)

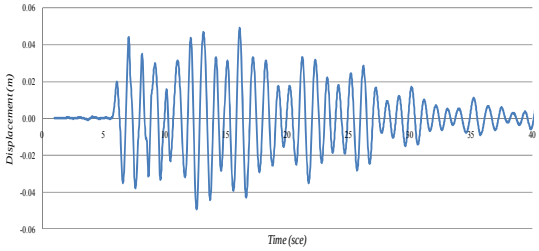

(c)

Figure D.36. Horizontal displacement of the 313 m mast at the 2nd cluster level under Parkfield earthquake, (a) detailed nonlinear model, (b) simplified model based on ADINA spring, (c) simplified model based on proposed response spectral method spring.

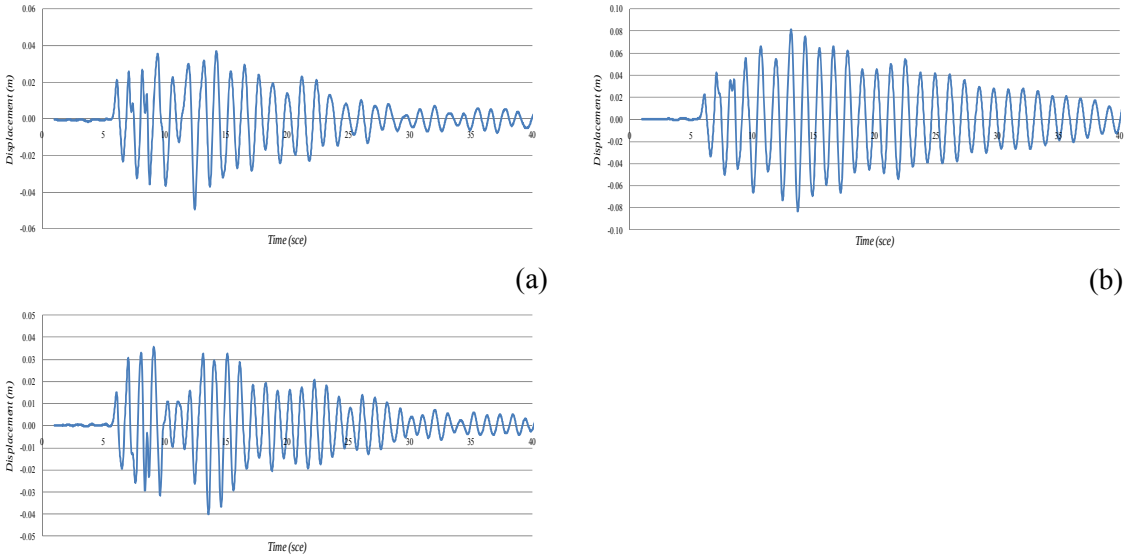

Figure D.37. Horizontal displacement of the 313 m mast at the 1st cluster level under Parkfield earthquake, (a) detailed nonlinear model, (b) simplified model based on ADINA spring, (c) simplified model based on proposed response spectral method spring.

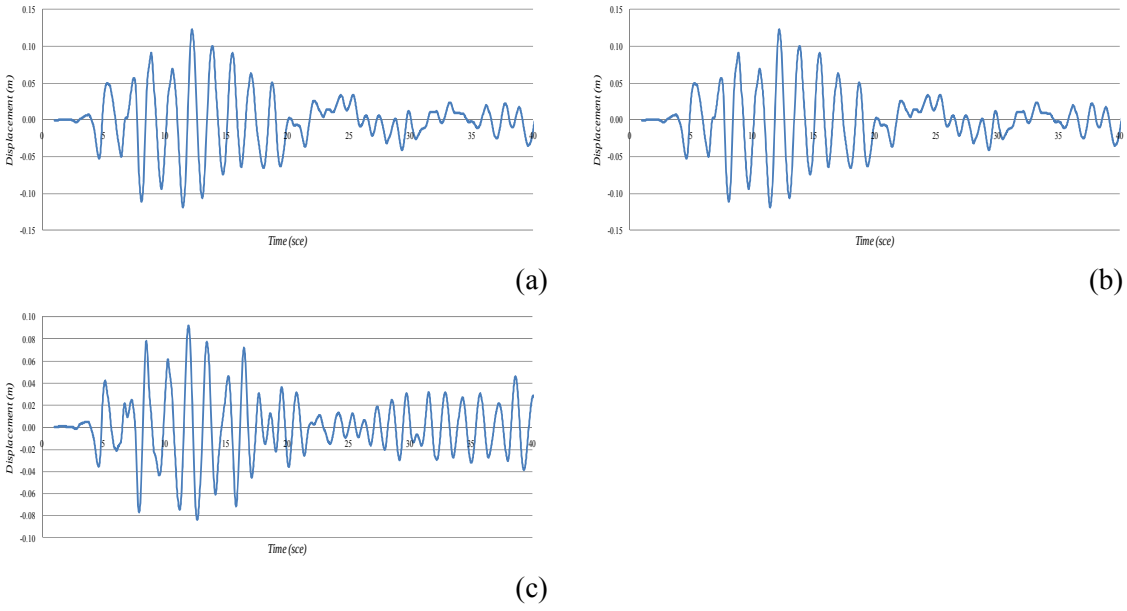

Figure D.38. Horizontal displacement of the 607 m mast at the 9th cluster level under Taft earthquake, (a) detailed nonlinear model, (b) simplified model based on ADINA spring, (c) simplified model based on proposed response spectral method spring.

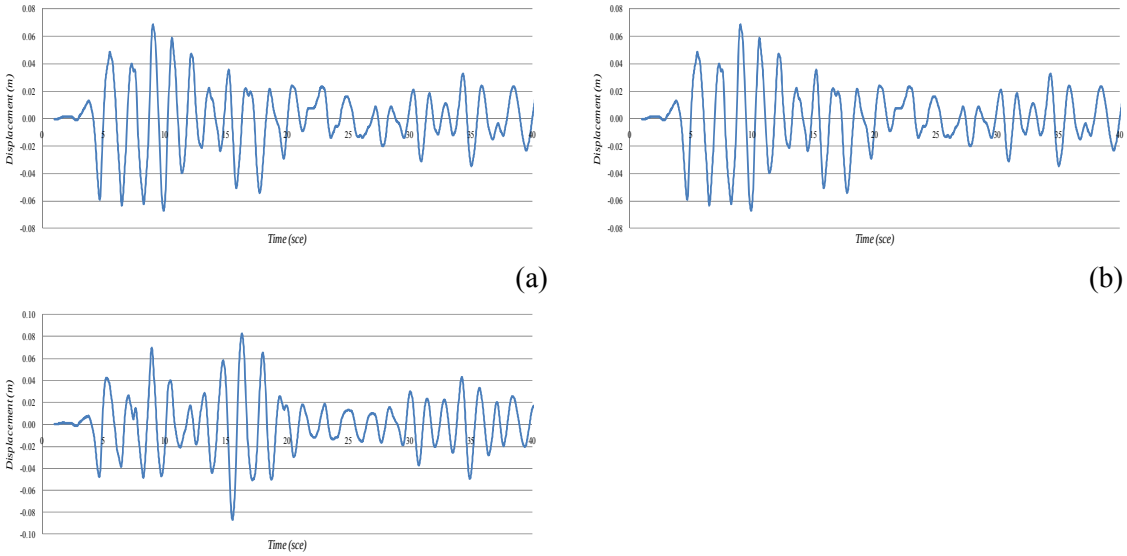

(a) (b)

(c)

Figure D.39. Horizontal displacement of the 607 m mast at the 8th cluster level under Taft earthquake, (a) detailed nonlinear model, (b) simplified model based on ADINA spring, (c) simplified model based on proposed response spectral method spring.

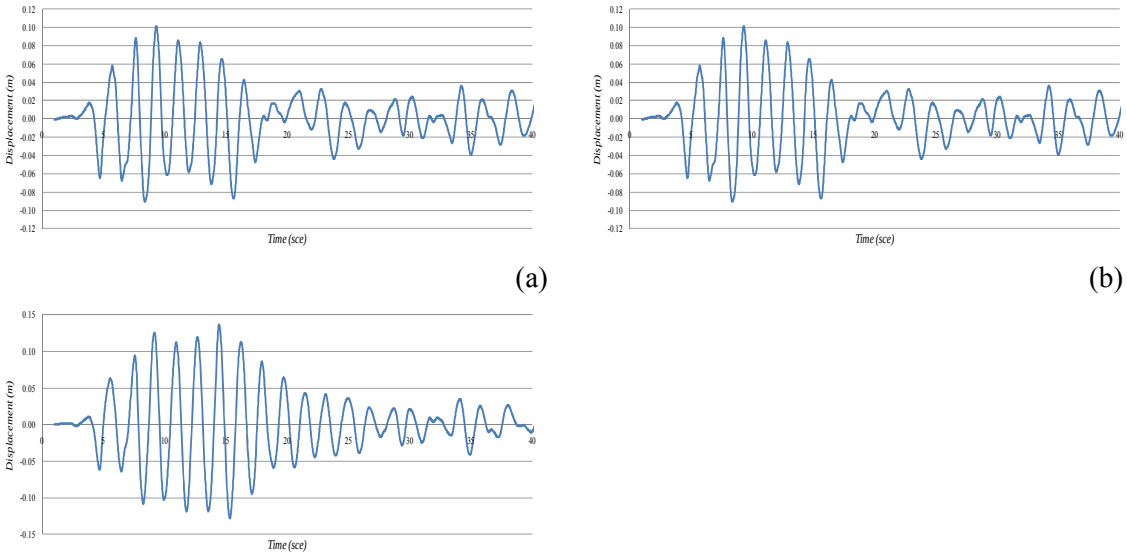

(a) (b)

(c)

Figure D.40. Horizontal displacement of the 607 m mast at the 7th cluster level under Taft earthquake, (a) detailed nonlinear model, (b) simplified model based on ADINA spring, (c) simplified model based on proposed response spectral method spring.

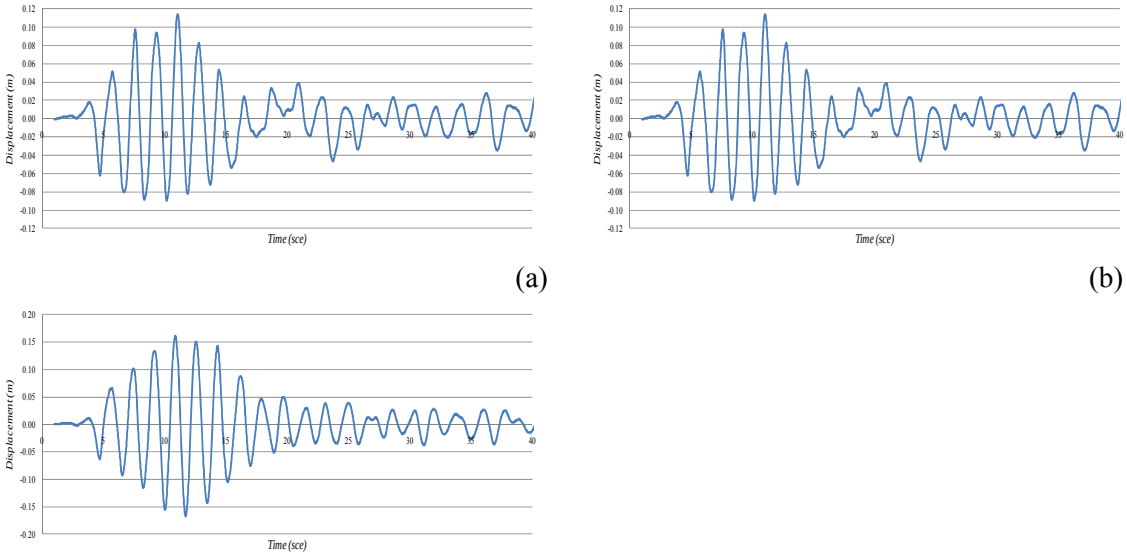

Figure D.41. Horizontal displacement of the 607 m mast at the 6th cluster level under Taft earthquake, (a) detailed nonlinear model, (b) simplified model based on ADINA spring, (c) simplified model based on proposed response spectral method spring.

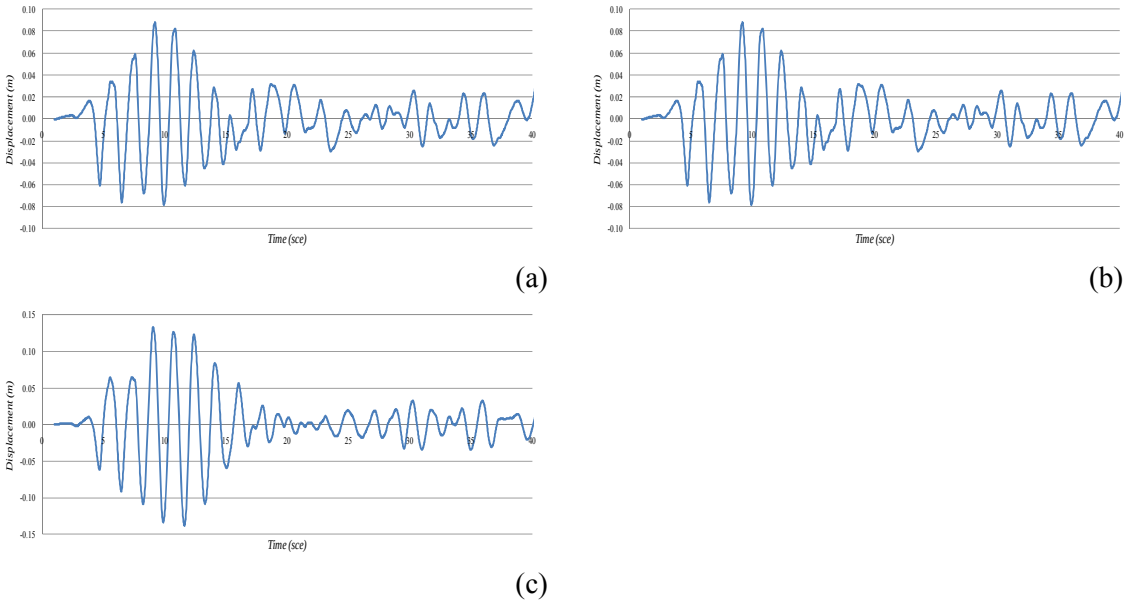

Figure D.42. Horizontal displacement of the 607 m mast at the 5th cluster level under Taft earthquake, (a) detailed nonlinear model, (b) simplified model based on ADINA spring, (c) simplified model based on proposed response spectral method spring.

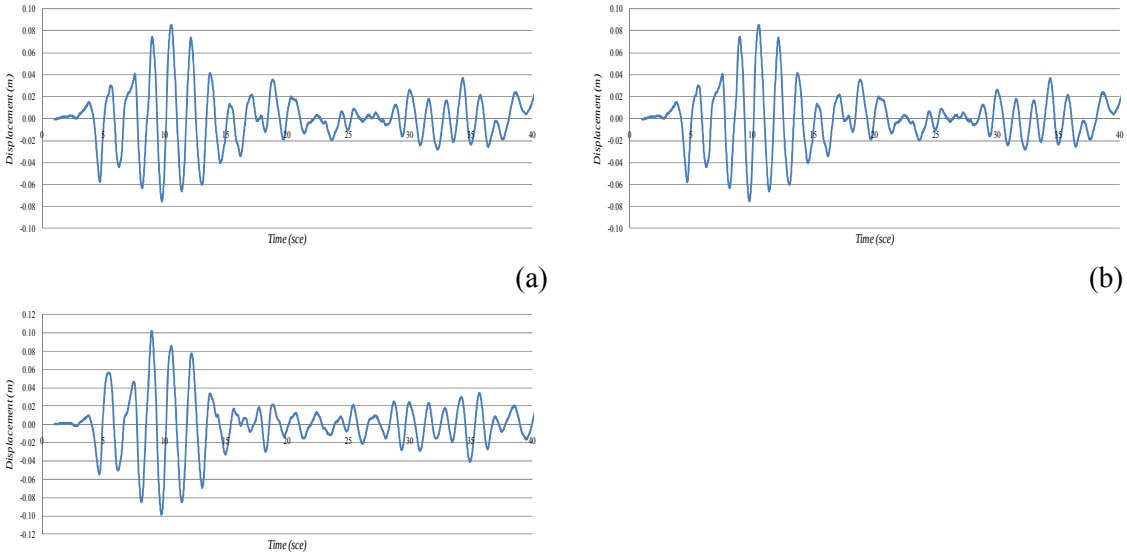

(a) (b)

(c)

Figure D.43. Horizontal displacement of the 607 m mast at the 4th cluster level under Taft earthquake, (a) detailed nonlinear model, (b) simplified model based on ADINA spring, (c) simplified model based on proposed response spectral method spring.

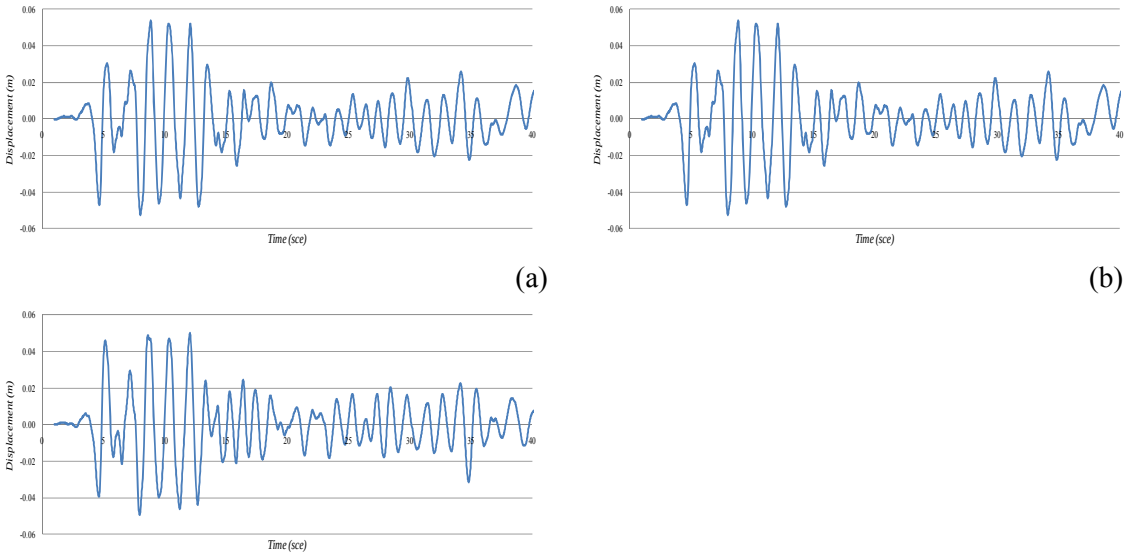

(a) (b)

(c)

Figure D.44. Horizontal displacement of the 607 m mast at the 3rd cluster level under Taft earthquake, (a) detailed nonlinear model, (b) simplified model based on ADINA spring, (c) simplified model based on proposed response spectral method spring.

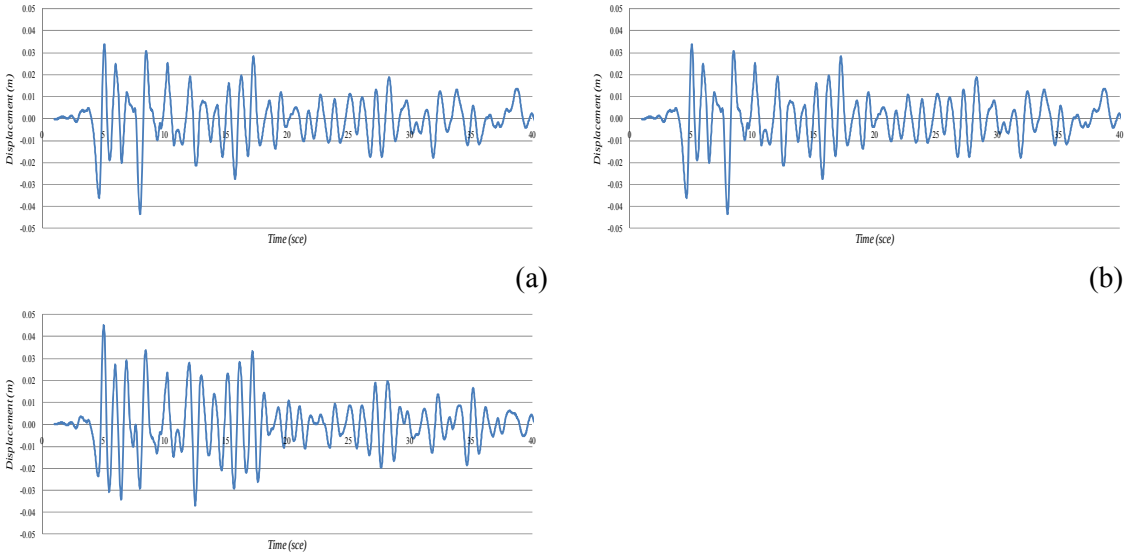

(a) (b)

(c)

Figure D.45. Horizontal displacement of the 607 m mast at the 2nd cluster level under Taft earthquake, (a) detailed nonlinear model, (b) simplified model based on ADINA spring, (c) simplified model based on proposed response spectral method spring.

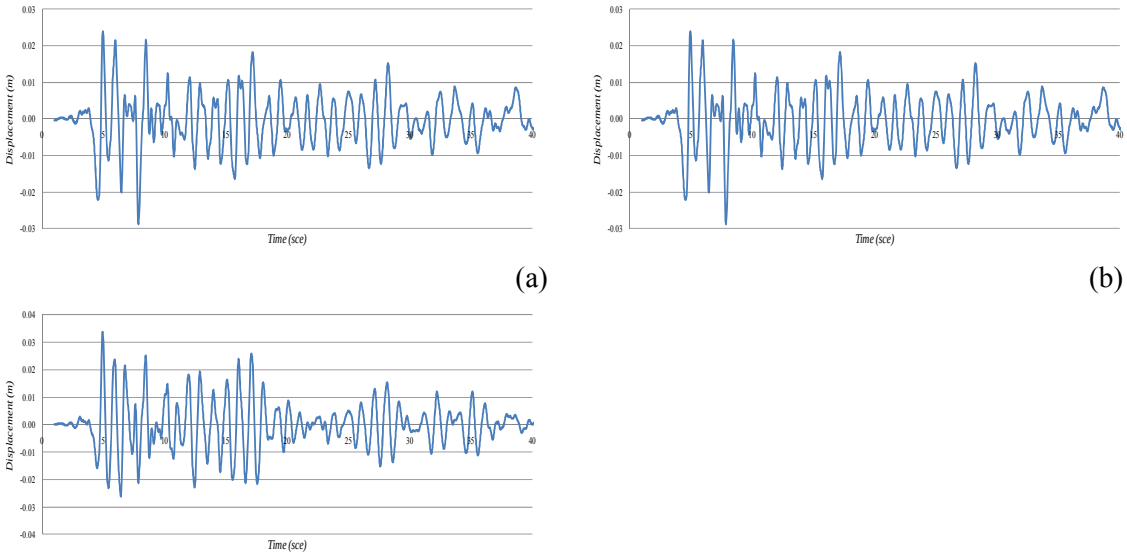

(a) (b)

(c)

Figure D.46. Horizontal displacement of the 607 m mast at the 1st cluster level under Taft earthquake, (a) detailed nonlinear model, (b) simplified model based on ADINA spring, (c) simplified model based on proposed response spectral method spring.

Appendix E: Field measurement planning for St-Hyacinthe tower

The 111.2-m guyed telecommunication mast owned by Hydro-Québec in St. Hyacinthe, Québec is selected for some field validation measurements. It consists of six stay levels arranged at two anchor groups with outriggers located at the fourth and the sixth stay levels from the bottom. The panel width and the height of the mast are 1.116 m and 1.02 m, respectively. Figure 4.1 illustrates the general layout and some structural details of this mast. The tower is among the most heavily equipped masts of the region. Some electrical and telecommunication equipment are shown in Figure E.1.

The first step to validate the dynamic characteristics of the St. Hyacinthe mast is to perform ambient vibration monitoring and measure the natural frequencies and structural

Figure E.1. *The electrical and telecommunication equipment installed on 111.2 m guyed mast located in St. Hyacinthe, Québec, Canada.*

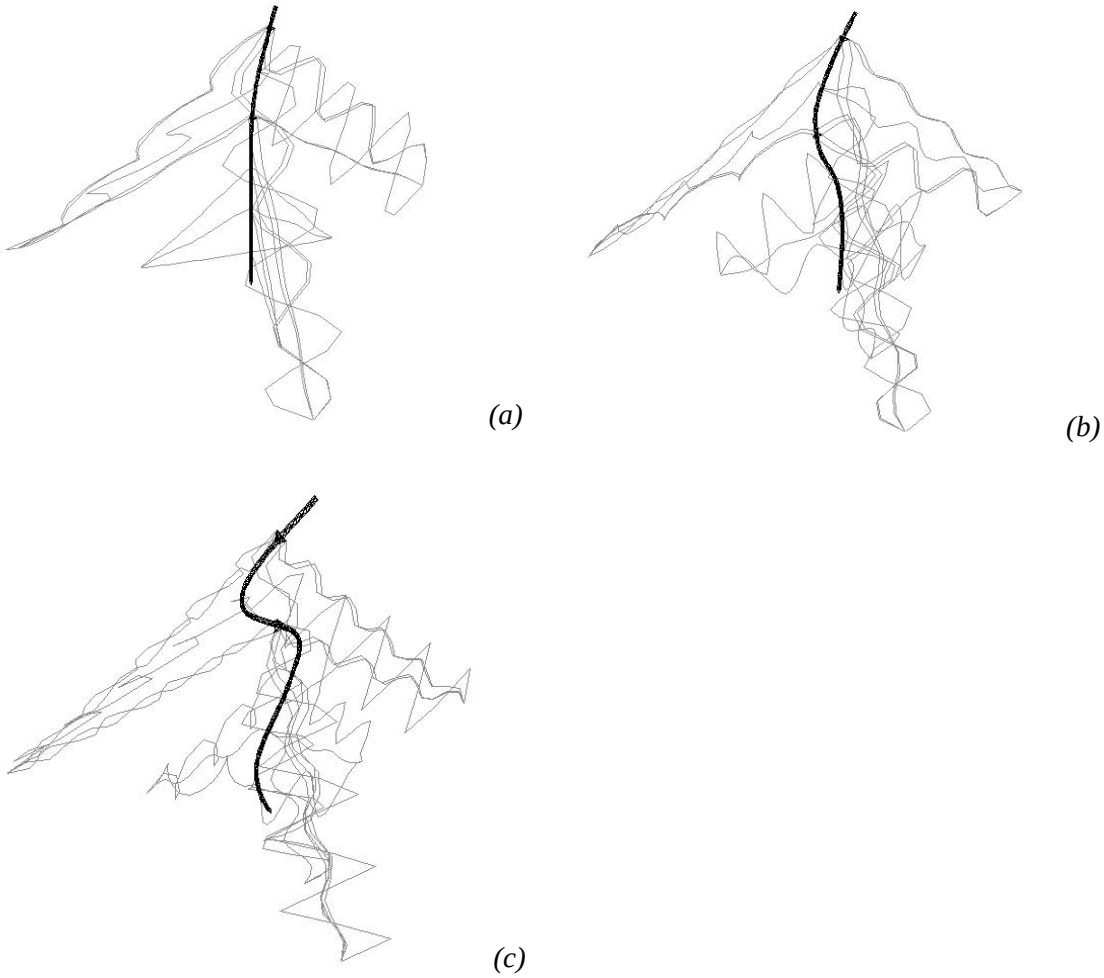

Figure E.2. *The first three fundamental mast/cable coupled mode shapes of the St. Hyacinthe tower. (a) $f_1 = 2.26\ Hz$, (b) $f_2 = 2.77\ Hz$, and (c) $f_3 = 3.70\ Hz$.*

damping of the structure. Special attention should be paid on the mast/cable coupled modes and the individual cable modes (each cable will be tested). According to the detailed numerical simulations of the idealized mast, the first mast/cable mode is at the natural frequency $f_1 = 2.26\ Hz$ ($T = 0.44$ sec). The corresponding mode shape is illustrated in Figure E.2 which indicates that mast vibrations are strongly coupled with higher modes of the guy cables. The second mast/cable mode frequency is $f_2 = 2.77\ Hz$ ($T = 0.36$ sce). These values should be verified through ambient vibration measurements on the mast.

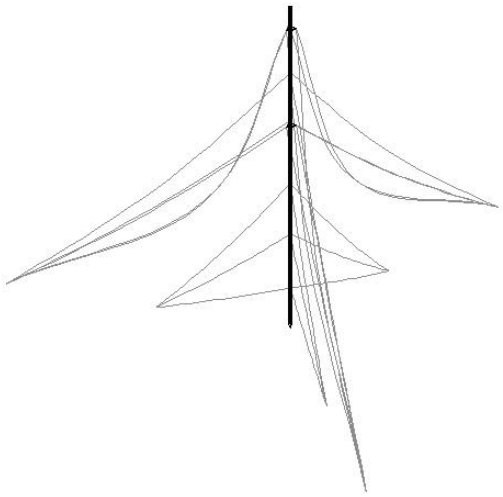

Figure E.3 *The fundamental mode shapes associated with cable vibrations of the St. Hyacinthe tower (at $f = 0.56\,Hz$)*

The next step should be devoted to the measurement the natural frequency of individual cables. Figure E.3 shows the fundamental mode associated with the longest cables (top cluster) of the tower, while the other guy cables and the mast remain at rest. The fundamental frequency of this cable according to finite element model simulations is $f_1 = 0.56\,Hz$ ($T = 1.78\,sec$). During the tests, the cables will be instrumented with accelerometers and fundamental frequencies and internal damping will be extracted from the ambient vibration and twang test (release from displaced position) records. Load cells will be installed to measure guy wire tensions so the numerical models can be reset with the actual values of cable tension.

Further experimental measurements are planned at Hydro-Québec's research institute (IREQ) to measure the dynamic characteristics of guy cables under forced periodic excitations. Such tests are not allowed on the St. Hyacinthe tower to prevent any interference with the normal communication operations at the site. Typical response spectra of stay cables under harmonic excitations, as illustrated in Figure 3.10, are of high interest.

References

ADINA R&D, Inc. *Theory and modeling guide, Volume 1: ADINA*. Report ARD 04-7, Watertown, MA, 2004.

Amiri, G.G. (1997): Seismic sensitivity of tall guyed telecommunication towers. *Ph.D. Thesis, Department of Civil Engineering and Applied Mechanics, McGill University, Montréal, Canada*, 243 pp.

Amiri, G.G. (2002): Seismic sensitivity indicators for tall guyed telecommunication towers. *Computers and Structures,* Vol. 80, pp. 349-364.

Amiri, G.G., Zahedi M., and Jalali R. S. (2004): Multiple-support seismic excitation of tall guyed telecommunication towers. *13th World Conference on Earthquake Engineering, Vancouver, Canada.*

ANSI/TIA/EIA-222-G (2005): Structural standards for steel antenna towers and antenna supporting structures. *TIA/222G Telecommunication Industry Standard*, US.

Bathe, K. J. (1996): *Finite Element Procedures*, Prentice Hall, Englewood Cliffs, NJ.

Ben Kahla, N. (1994): "Dynamic analysis of guyed towers." *Engineering Structures,* 16(4), 293-301.

British Standard (1994); *Lattice Towers and Masts, Part 4, Code of Practice for Lattice Masts. BS 8100 Part.* British Standard Institution, London, UK.

California Department of Water Recourses (CDWR) (2009): "The Strong Motion Program." CDWR, Sacramento, Calif., < http://www.oandm.water.ca.gov/earthquake/> (Dec 2009).

California Geological Survey, formerly California Division of Mines & Geology (CDMG) (2009): "Center for Engineering Strong Motion." CESMD, Sacramento, Calif., <http://www.conservation.ca.gov/cgs/> (Dec 2009).

CEN (1998): Eurocode 3 – Design of steel structures – part 3.1: Towers, masts, and chimneys – Towers and masts. *European prestandard (ENV 1993 – 3 - 1), Comité Européen de Normalisation, Brussels.*

Chopra, A. K. *Dynamics of Structures: Theory and Applications to Earthquake Engineering*, Second Edition. Prentice Hall, Upper Saddle River, New Jersey, 2000, 844 pp.

CSA Standard S37-01 (2001): Antennas, Towers, and Antenna-Supporting Structures, Appendix M: Earthquake-Resistant Design of Towers. *Canadian Standards Association,* Canada, pp. 106-113.

Desai, Y. M., and Punde, S. (2001). "Simple model for dynamic analysis of cable supported structures." *Engineering Structures*, 23(3), 271-279.

Dietrich, R. (1999): Three-Dimensional Dynamic Response of a 150-m Tall Guyed Mast under Displacement-Controlled Ground Motion. *Master's Thesis, Technische Universität München, Germany.*

Dumanoglu, A. A., Severn, R. T., (1989): Seismic response of modern suspension bridges to asynchronous longitudinal and lateral ground motion. *Structural engineering group, Proc. Instn Civ. Engrs, Part 2, Paper 9389, 73-86.*

Fantozzi, M.W. (2006): Seismic design of communication towers. Proceedings of the 2006 ASCE Structures Congress: Structural Engineering and Public Safety.

Faridafshin, F. (2006): Seismic investigation of tall guyed telecommunication towers. *Master's Thesis, Department of Applied Mechanics, Division of Dynamics, Chalmers University of Technology*, Göteborg, Sweden.

Faridafshin, F., and McClure, G. (2008): Seismic response of tall guyed masts to asynchronous multi-support and vertical ground motions. *ASCE Journal of Structural Engineering, 134(8), 1374-1382.*

Faridafshin, F., Ghafari Oskoei, S.A., McClure, G., (2007): Response of tall telecommunication masts to seismic wave propagation. *Meeting of IASS Working Group 4: Towers and Masts, Montréal, Québec, Canada.*

Faridafshin, F., Ghafari Oskoei, S.A., McClure, G., (2008): Response of tall guyed telecommunication masts to seismic wave propagation. 14th World Conference on Earthquake Engineering (14WCEE), Beijing, China, 12-17 Oct., Paper No. 06-0089, 8p.

Galvez, C. (1995): Static method for seismic design of self-supporting towers. *Master engineering project report, Department of Civil Engineering and Applied Mechanics, McGill University*, Montreal, Canada.

Galvez, C., and McClure, G. (1995): A simplified method for a seismic design of self-supporting lattice telecommunication towers. *Proceeding of 7th Canadian Conference on Earthquake Engineering*, pp. 541-548.

Georgakis, C. T., and Taylor, C. A. (2005a). "Nonlinear dynamics of cable stays. Part 1: sinusoidal cable support excitation." *Journal of Sound and Vibration*, 281(3-5), 537-564.

Georgakis, C. T., and Taylor, C. A. (2005b). "Nonlinear dynamics of cable stays. Part 2: stochastic cable support excitation." *Journal of Sound and Vibration,* 281(3-5), 565-591.

Ghafari Oskoei, S.A. (2008): Simplified seismic analysis methods for guyed telecommunication masts. *Structural Engineering Series Report. 2008-1*. Available at: http://www.mcgill.ca/library-findinfo/escholarship/

Ghafari Oskoei, S.A., McClure, G., (2008): Dynamic Analysis of Cable Roof Networks under Transient Wind. *Proceedings of the 6th International Conference on Computation of Shell and Spatial Structures (IASS-IACM 2008) – Spanning Nano to Mega*, 28-31 May, Cornell University, Ithaca, NY, USA, JF Abel and JR Cooke (eds.). Session T-4-B, Paper No. 2. (Book of Abstracts p. 170) – 4 p.

Ghafari Oskoei, S.A., McClure, G., (2008): Dynamic analysis of cable roofs under transient wind; a comparison between time domain and frequency domain approaches. *Journal of Tsinghua University – Science and Technology. Vol 13, Number S1, 53-57.*

Ghafari Oskoei, S.A., McClure, G., (2008): Dynamic analysis of cable roofs under transient wind; a comparison between time domain and frequency domain approaches. *12th International Conferences on Computing in Civil and Building Engineering & 2008 International Conference on Information Technology in Construction*, Beijing, China, 16-18 Oct, Paper no. 025, 6p.

Ghafari Oskoei, S. A., and McClure, G. (2009). "Simplified dynamic analysis methods for guyed telecommunication masts under seismic excitation." *ASCE Structures Congress' 09, April 30-May 2*, 2009, Austin, Texas, 1020-1029.

Ghafari Oskoei, S. A., and McClure, G. "A novel frequency domain algorithm to evaluate the dynamic stiffness of guy cables used in tall masts under earthquakes." *Journal of Structural Engineering, Manuscript STENG-742, submitted Aug 2009.*

Ghafari Oskoei, S. A., and McClure, G. "A robust linearized seismic analysis method for guyed telecommunication masts." *Journal of Structural Engineering, Manuscript STENG-1145, submitted June 2010.*

Ghafari Oskoei, S. A., and McClure, G. "Validation of a linearized seismic analysis method for tall guyed telecommunication masts", Technical note submitted to *Journal of Structural Engineering, Manuscript STENG-1200, submitted July 2010.*

Ghafari Oskoei, S. A. (2010): "Validation of a linearized seismic analysis method for tall guyed telecommunication masts" eScholarship@McGill, Montréal, Canada, < http://www.mcgill.ca/library-findinfo/escholarship/>.

Ghafari Oskoei, S.A., McClure, G., Mahmoudzadeh Kani, I. 2010, “Dynamic analysis of cable roofs under transient wind using a simplified frequency domain approach” *the*

Tenth International Conference on Computational Structures Technology, Valencia, Spain, Sep. 14-17.

Guevara, E.L. (1993): Nonlinear seismic analysis of antenna-supporting structures. Master Eng. Project Report. Department of Civil Engineering and Applied Mechanics, McGill University, Canada.

Guevara, E.L., McClure, G. (1993): Nonlinear response of antenna-supporting structures. *Computers and Structures*, Vol. 47, No. 4/5, pp. 711-724.

Haroun, A., M., Abdel-Hafez, E., (1987): Seismic response analysis of earth dams under differential ground motion. *Bulletin of the seismological society of America, Vol. 77, No. 5, 1514-1529.*

Hensley, G. M. (2005): Finite element analysis of the seismic behavior of guyed masts. *Master Thesis, Virginia Polytechnic Institute and State University*, USA.

Hensley, G. M., and Plaut, R. H. (2007). "Three-dimensional analysis of the seismic response of guyed masts." *Engineering Structures*, 29(9), 2254-2261.

Iannuzzi, A., and Spinelli, P. (1989). "Response of a guyed mast to real and simulated wind." *Journal of the International Association for Shell and Spatial Structures*, 30-1(99), 38-45.

IASS (1981): Recommendations for Guyed Masts. *IASS-WG4 (International Association for Shell and Spatial Structures Working Group No. 4),* Madrid, Spain, 107 pp.

Irvine, H. M. (1981): *Cable Structures. The MIT Press, Cambridge, Massachusetts.*

Kahla, N. B. (1994). "Dynamic analysis of guyed towers." *Engineering Structures*, 16(4), 293-301.

Khedr, M.A. (1998): Seismic analysis of lattice towers. *Ph.D. Thesis, Department of Civil Engineering and Applied Mechanics, McGill University, Montreal, Canada.*

Lai, P. S., (1983): Seismic response of a 4-span bridge system subjected to multiple-support ground motion. *Proceedings - 4th Canadian Conference on Earthquake Engineering, 561-570.*

Lilien, J. L., and Pinto Da Costa, A. (1994). "Vibration amplitudes caused by parametric excitation of cable stayed structures." *Journal of Sound and Vibration*, 174(1), 69-90.

Madugula, M.K.S., (2002): Dynamic response of lattice towers and guyed masts. *American Society of Civil Engineers (ASCE), Reston, Virginia, USA.*

Madugula, M.K.S., Kennedy, B.K., (2007): Recent research on guyed communication towers at the University of Windsor. *Meeting of IASS Working Group 4: Towers and Masts*, Montréal, Québec, Canada.

McClure, G., (1999): Earthquake-resistance design of towers. *Meeting of IASS Working Group 4: Towers and Masts*, Krakow, Poland.

McClure, G., and Lin, N. (1994). "Transient response of guyed telecommunication towers subjected to cable ice-shedding." *Proceedings of the IASS-ASCE International Symposium, April 24-28, 1994, Atlanta, Ga.,*801-809.

McClure, G., and Guevara, E.L. (1994): Seismic Behaviour of Tall Guyed Telecommunication Towers. *Proceedings of the IASS-ASCE International Symposium 1994, ASCE Structure Congress XII, April 24-28, Atlanta, Georgia, 259-268.*

Meshmesha, H.M. (2005): Dynamic analysis of guyed antenna towers for seismic loads. *Ph.D. Thesis, University of western Ontario*, London, Canada.

Meshmesha, H., Sennah, K., Kennedy, J.B. (2006): Simple methods for static and dynamic analysis of guyed towers. *Structural Engineering and Mechanics*, Vol. 23, No. 6, page 635-649.

Moossavi Nejad, S.E. (1996): Dynamic response of guyed masts to strong motion earthquake. *Proceedings of the 11th World Conference on Earthquake Engineering*, Acapulco, Mexico, Paper No. 289.

National Research Council of Canada (2005): National Building Code of Canada 2005. Ottawa, ON, Canada.

O'Rourke, J. M., Hmadit, K., (1988): Analysis of continuous buried pipelines for seismic wave effects. *Earthquake engineering and structural dynamics, Vol. 16, 917-929.*

O'Rourke, J. M., Castro, G., Centola, N., (1980): Effects of seismic wave propagation upon buried pipelines. *Earthquake engineering and structural dynamics, Vol. 8, 455-467.*

Pacific Earthquake Engineering Research Center (PEER). (2005). "PEER strong motion database." PEER, Berkeley, Calif., <http://peer.berkeley.edu/smcat/index.html> (Sept. 10 2005).

Peil, U., Nolle, H., and Wang, Z. H. (1996). "Dynamic behaviour of guys under turbulent wind load." *Journal of Wind Engineering and Industrial Aerodynamics*, 65(1-3), 43-54.

Sackmann, V. (1996): Prediction of natural frequencies and mode shapes of self-supporting lattice telecommunication towers. *Master engineering project report, Department of Civil Engineering and Applied Mechanics, McGill University, Montreal, Canada.*

Smith, W.B. (2007): *Communication Structures*. Thomas Telford, London, UK.

Southern California Earthquake Center (SCEC). (2009). "Southern California Earthquake Center Databases and Resources." Los Angeles, Calif., <http://www.data.scec.org> (Dec 2009).

Sparling, B.F. (1995): The dynamic behaviour of guys and guyed masts. *Ph.D. Thesis, University of western Ontario, London, Canada.*

Sparling, B.F., (2007): Dynamic response of cantilevered antennas on guyed masts. *Meeting of IASS Working Group 4: Towers and Masts*, Montréal, Québec, Canada.

Sparling, B.F., Davenport, A.G., (1999): The nonlinear behaviour of guy cables in turbulent winds.

Sparling, B.F., Smith, B.W., Davenport, A.G., (1996): Simplified dynamic analysis methods for guyed masts in turbulent winds. *Journal of IASS*, Vol. 37.

Standards Australia (1994): Design of steel lattice towers and masts. *As 3995 – 1994, Sydney, Australia.*

US National Earthquake Information Center (USGS). (2009). "Earthquake Hazards Program." Pasadena, Southern Calif., <http://earthquake.usgs.gov/regional/neic/> (Dec 2009).

Wahba, Y.M.F. (1999): Static and dynamic analysis of guyed communication tower. *Ph.D. Thesis, University of western Ontario, London, Canada.*

Wilson, E. L. (2000): Static and dynamic analysis of structures. *Computers and Structures, Inc., Berkeley, California, USA.*

Xie, X., Zhang, H., and Zhang, Z. (2008). "Nonlinear dynamic response of stay cables under axial harmonic excitation." *Journal of Zhejiang University SCIENCE A*, 9(9), 1193-1200.

Zhang, Q.L., Peil, U. (1996): Stability behaviors of guyed towers under earthquake conditions. *Proceedings of the1st International Conference on Earthquake Resistant Engineering Structures, ERES 96*, Thessaloniki, Greece.

(2006) *MATLAB User's Guide.* The MathWorks, Inc., Natick, Mass. <http://www.mathworks.com>

(2010) SeismoSignal, User's Guide. Earthquake Engineering Software Solutions. Messina, Italy. Free download available from: http://www.seismosoft.com/